USARTL-TR-78-15

LEVEL

ENGINE/AIRFRAME/DRIVE TRAIN
DYNAMIC INTERFACE DOCUMENTATION

H. W. Hanson, R. W. Balke, B. D. Edwards,
W. W. Riley, B. D. Downs
Bell Helicopter Textron
P.O. Box 482
Fort Worth, Texas 76101

204 p.

October 1978

Final Report, for period September 1977 — August 1978,

DAAJ02-77-C-0045

1L262.001 AH 76

00

Prepared for

APPLIED TECHNOLOGY LABORATORY
U. S. ARMY RESEARCH AND TECHNOLOGY LABORATORIES (AVRADCOM)
Fort Eustis, Va. 23604

79 01 15 056

APPLIED TECHNOLOGY LABORATORY POSITION STATEMENT

This report provides the details of a program that is part of a larger effort designed to provide a complete report of past and present engine/airframe/drive train dynamic interface problems. The problems of vibration-related interface compatibility in engine/drive system installations are usually complicated by the inherent coupling of the three major multi-degree-of-freedom systems: engine, airframe, and drive train. The result of this effort is a report documenting dynamic interface problems associated with the OH-4A, Model 206, Model 309, the YAH-63, and the 214B. The ultimate benefit will be the accumulation of data that will eventually lead to a solution of generic problems of this type.

This report is one of five reports resulting from engine/airframe/drive train dynamic interface documentation efforts funded by the Applied Technology Laboratory, U. S. Army Research and Technology Laboratories (AVRADCOM). The related reports and their final report numbers are: Boeing Vertol, USARTL-TR-78-11; Hughes Helicopters, USARTL-78-12; Kaman Aerospace, USARTL-78-14; Sikorski Aircraft, USARTL-TR-78-13; and Bell Helicopter, USARTL-78-15.

Mr. Allen C. Royal, Propulsion Technical Area, Technology Applications Division, Applied Technology Laboratory, served as Project Engineer for this effort.

REPORT DOCUMENTATION PAGE		READ INSTRUCTIONS BEFORE COMPLETING FORM
1. REPORT NUMBER USARTL-TR-78-15	2. GOVT ACCESSION NO.	3. RECIPIENT'S CATALOG NUMBER
4. TITLE (and Subtitle) ENGINE/AIRFRAME/DRIVE TRAIN DYNAMIC INTERFACE DOCUMENTATION		5. TYPE OF REPORT & PERIOD COVERED Final Report Sep 1977 - August 1978
		6. PERFORMING ORG REPORT NUMBER
7. AUTHOR(s) H. W. Hanson W. W. Riley R. W. Balke B. D. Downs B. D. Edwards		8. CONTRACT OR GRANT NUMBER(s) DAAJ02-77-C-0045
9. PERFORMING ORGANIZATION NAME AND ADDRESS BELL HELICOPTER TEXTRON P. O. Box 482 Fort Worth, Texas 76101		10. PROGRAM ELEMENT, PROJECT, TASK AREA & WORK UNIT NUMBERS 62209A 1L262209AH76 00 206 EK
11. CONTROLLING OFFICE NAME AND ADDRESS APPLIED TECHNOLOGY LABORATORY U. S. Army Research and Technology Lab (AVRADCOM), Ft. Eustis, VA 23604		12. REPORT DATE October 1978
		13. NUMBER OF PAGES 214
14. MONITORING AGENCY NAME & ADDRESS(if different from Controlling Office)		15. SECURITY CLASS. (of this report) Unclassified
		15a. DECLASSIFICATION/DOWNGRADING SCHEDULE

16. DISTRIBUTION STATEMENT (of this Report)

Approved for public release; distribution unlimited.

17. DISTRIBUTION STATEMENT (of the abstract entered in Block 20, if different from Report)

18. SUPPLEMENTARY NOTES

19. KEY WORDS (Continue on reverse side if necessary and identify by block number)

Helicopters	Torsional Stability	Rotor Droop
Compatibility	Engine Vibration	Driveshaft Critical Frequency
Dynamic	Engine Governing	Driveshaft Coupling Loads
Interface	Engine Overspeed	Gearbox Mount Failure
Drive Train	Engine Noise	Hydraulic System Noise

20. ABSTRACT (Continue on reverse side if necessary and identify by block number)

The purpose of this program was to survey Bell Helicopter Textron past and present experiences as related to gas-turbine-powered helicopter engine/airframe/drive train dynamic interface problems as part of an overall Government effort to define specific areas in which future research funding should be placed to develop improved design, analytical

DD FORM 1473 EDITION OF 1 NOV 65 IS OBSOLETE

79 01 15 056

Block 20.   Continued

and test methods to ensure helicopter dynamic compatibility.

Thirteen dynamic interface problems have been documented with
a detailed discussion, solutions considered and/or applied,
and identifiable shortcomings.   Recommendations are made for
future research funding in five specific areas.   The appendixes
provide the detailed documentation for each of the dynamic
interface problems.

PREFACE

The work presented in this report was performed by Bell Helicopter Textron (BHT) under Contract DAAJ02-77-C-0045 for the Applied Technology Laboratory, U. S. Army Research and Technology Laboratories (AVRADCOM), Fort Eustis, Virginia.

This is an extension of previous efforts to define the specific areas in which research funding should be placed in order to develop improved design, analytical, and test methods to ensure dynamic compatibility of the engine, drive system, and airframe. Previous efforts are found, in part, in USAAMRDL TR's 74-47[1], 74-85[2], and 74-87[3].

The study was conducted in two stages. First, a review of previous experience related to past and present gas-turbine-powered helicopter engine/airframe/drive system dynamic interface problems, including internal and external noise, was conducted. Second, coordination with the engine manufacturers was then conducted to ensure completeness of detail for the specific problems selected for documentation.

The program was implemented under the technical direction of Mr. Allen C. Royal of the Technology Applications Division, ATL. Principal Bell Helicopter Textron personnel associated with this contract were Messrs. B. D. Downs (Propulsion), W. W. Riley (Drive Train), E. D. Edwards (Acoustics), and R. W. Balke (Dynamics). Mr. H. W. Hanson was the BHT Project Engineer.

---

1. White, James A., Bell Helicopter Company; OH-58A PROPULSION SYSTEM VIBRATION INVESTIGATION, USAAMRDL Technical Report 74-47, Eustis Directorate, U. S. Army Air Mobility Research and Development Laboratory, Fort Eustis, Virginia, August 1974, AD A002672.

2. Sullivan, R. J., et al., Hughes Helicopters; OH-6A PROPULSION SYSTEM VIBRATION INVESTIGATION, USAAMRDL Technical Report 74-85, Eustis Directorate, U. S. Army Air Mobility Research and Development Laboratory, Fort Eustis, Virginia, January 1975, AD A007225.

3. Parker, W. H., Detroit Diesel Allison; T63 ENGINE CHARACTERISTICS ANALYSIS, USAAMRDL Technical Report 74-87, Eustis Directorate, U. S. Army Air Mobility Research and Development Laboratory, Fort Eustis, Virginia, January 1975, AD A007243.

TABLE OF CONTENTS

TABLE OF CONTENTS -- Concluded

LIST OF ILLUSTRATIONS

8

9

LIST OF TABLES

INTRODUCTION

Previously, the development schedule of a new helicopter often
encountered delays due to both anticipated and unexpected
dynamic compatibility problems associated with vibration,
oscillatory loading, and/or stability. Although progress has
been made in both the prediction and the solution of many of
these problems, development programs of present-day helicop-
ters continue to incur significant schedule delays - and thus
unacceptable cost increases - due to dynamic problems. Addi-
tionally, dynamic problems sometimes develop in the field,
possibly due to an accumulation of flight time on the compo-
nents, or due to a design change that has been introduced.

Vibration and oscillatory loading problems are largely related
to rotor harmonic excitations, the magnitude thereof, their
proximity to the system natural frequencies, and the associat-
ed damping characteristics. Stability problems may occur due
to numerous and varied reasons. Particular attention must be
given to the coupling associated with the combining of two or
more components or systems, each having its own set of un-
coupled natural frequencies and response characteristics.
When combined, the inertial and geometric coupling effects may
cause frequency shifts resulting in significant changes in
vibratory response or reductions in damping which could lead
to instabilities.

One area wherein the dynamic interface problems are of concern
is that of the engine/airframe/drive train. This problem is
somewhat compounded by the fact that both the engine and air-
frame manufacturer have a detailed familiarization with the
characteristics and requirements of their own design, but
inadequate knowledge and appreciation for the characteristics
and requirements of the other design or the characteristics
of the coupled system. It is further compounded by the fact
that the types of analyses used are often unique in assump-
tions, methodology content, and format of presentation.

Additionally, there is sometimes a lack of test techniques
wherein the data can be compared directly to that of the
system analysis.

It is therefore desirable to identify the specific areas in
which research funding should be applied in order to develop
improved and compatible design, analytical, and test methods
to ensure dynamic compatibility of the engine/airframe/drive
train.

11

The objectives of this study were:

1. To identify helicopter engine/airframe/drive train dynamic interface problems.

2. To coordinate with engine manufacturers to ensure completeness of detail.

The general problem areas which were investigated are categorized as:

1. Steady state dynamic loading

2. Transient dynamic loading

3. Component installation resonances

4. Stability

   a. Supercritical shafting

   b. Classical torsional stability

5. Engine governing accuracy

   a. Transient power excursions

   b. Transient speed excursions

6. Noise

For selection of problems to be presented, most emphasis has been placed on recent problems (documentation material more readily available), and those of a generic nature (problems of an inherent nature normally associated with engine/airframe/ drive train applications, as opposed to those problems dealing with a new type of interface situation).

The body of the report summarizes the problems, solutions, and shortcomings. Recommendations are made for future research funding. The appendixes describe each individual problem.

It is endeavored in each appendix to define the problem, describe the solutions considered and/or applied, and define the final solution or, alternately, the adjustments made to accommodate the problem. Additionally, each appendix defines, where appropriate, the shortcomings in design guides, analytical capability, and test methodology.

12

SUMMARY OF PROBLEMS

Previous BHT experience related to gas-turbine-powered helicopter engine/airframe/drive train dynamic interface problems was reviewed.

Thirteen problems were selected for documentation as summarized in Table 1. These are presented in chronological order by year, identified by helicopter model and type of aircraft (whether military or commercial), generically classified, and briefly described.

The first column of Table 1 assigns a problem identification code which is used throughout the report. A separate appendix having the same letter designation code provides the detailed discussion of each problem.

TABLE 1. SUMMARY OF DOCUMENTED ENGINE/AIRFRAME/DRIVE TRAIN INTERFACE PROBLEMS

Appendix	Date	Model	Type	Classification	Problem description
A	1962	OH-4A	Mil Obs/ Prototype	Generic	Classical drive system torsional instability
B	1963	OH-4A	Mil Obs/ Prototype	Generic	Excessive engine and fuse-lage vibration at engine-to-transmission shaft speed
C	1967	206	Commercial/ Production	Nongeneric	High-frequency engine noise in aft cabin area
D	Early 1972	309	Mil Attack/ Prototype	Generic	Engine installation resonance
E	Mid—1972	309	Mil Attack/ Prototype	Generic	High transient drive system loads following engine throttle chops
F	Mid—1974	YAH-63	Mil Attack/ Prototype	Generic	Shaft dynamic loading on engine
G	Mid—1974	YAH-63	Mil Attack/ Prototype	Generic	Installed vibration in excess of engine limits
H	Late 1974	YAH-63	Mil Attack/ Prototype	Generic	Destructive shaft whirl of 20,000 rpm engine-to-trans-mission driveshaft
I	Mid—1975	YAH-63	Mil Attack/ Prototype	Military only	IR blower driveshaft failure

14

TABLE 1. - Concluded

Appendix	Date	Model	Type	Classification	Problem description
J	Mid-1975	YAH-63	Mil Attack/Prototype	Nongeneric	Failure of tail rotor and accessory drive gearbox mounts
K	Mid-1975	YAH-63	Mil Attack/Prototype	Generic	Poor governing and excessive transient rotor droop
L	Late 1975	YAH-63	Mil Attack/Prototype	Generic	Excessive torsional loading of the drive system during engine overspeed trips
M	Early 1976	214B	Commercial/Production	Nongeneric	Hydraulic system noise

SUMMARY OF SOLUTIONS

A brief summary of the solutions considered, designed, analyzed, and/or tested for each problem is provided in Table 2.   In some cases solutions were adopted into the design; in other instances program development was discontinued before alternate solutions could be fully evaluated and no solution was achieved.

The letter designation code in the first column of Table 2 refers to the problem identification code previously assigned in Table 1.

TABLE 2. SUMMARY OF SOLUTIONS CONSIDERED AND APPLICABILITY

Item	Problem/Solution	Extent of application				
		Consideration only	Design	Analysis	Test	Adopted
A	Torsional stability:					
	– Signal deadband		x	x	x	x
	– Signal hysteresis		x	x	x	x
	– N$_2$ flyball coupling			x.		
	– T/R driveshaft damping		x	x	x	
B	Engine vibration at shaft 1/rev:					
	– Soft mount engine		x		x	
	– Balance shaft		x		x	
	– Redesign shaft support		x		x	x
C	Excessive cabin noise:					
	– Soundproofing		x		x	x
	– Engine change-out				x	x
	– Soft mount engine		x		x	*
	– Modify engine gearbox		x		x	**

* Awaiting certification
** Awaiting engine manufacturer test results

TABLE 2. – Continued

		Extent of application				
Item	Problem/Solution	Consideration only	Design	Analysis	Test	Adopted
D	Engine mounting resonance:					
	– Add lateral dampers to engine mounting		x		x	
E	High transient drive system loads:					
	– Soft tail rotor drive-shaft coupling	x				
	– Overrunning clutch in tail rotor drive system	x				
F	Shaft dynamic loading on engine:					
	– Analyze coupling forces			x		
	– Evaluate calculated forces			x		
G	Installed vibration in excess of engine limits:					
	– Revise engine mountings		x	x	x	
	– Change pylon geometry			x		
	– Change main rotor mast length			x		

18

TABLE 2. - Continued

Item	Problem/Solution	Extent of application				
		Consideration only	Design	Analysis	Test	Adopted
H	Destructive shaft whirl:					
	– Change coupling material		X		X	X
	– Hoop stress determination	X				
	– Change centering spring design		X		X	X
	– Improve coupling balance		X		X	X
	– Stiffen coupling support cone		X	X	X	X
	– Preload bearings		X	X	X	
	– Reverse coupling design		X	X	X	
	– Change type of coupling		X	X	X	
	– Change shafting inter-face clamp-up		X		X	X
	– Redesign to subcritical system			X		
	– Change coupling tooth profile		X	X	X	
	– Add external shaft damper (elastomeric)				X	
	– Incorporate squeeze-film damper in input quill support bearings		X	X	X	X

19

TABLE 2. - Continued

Item	Problem/Solution	Extent of application				
		Consideration only	Design	Analysis	Test	Adopted
H (Cont)	Destructive shaft whirl:					
	- Change shaft support bearing to triplex		x		x	x
	- Lubricate threaded joints				x	x
	- Add double pilots to spline joints		x	x	x	x
	- Stiffen shafting		x	x	x	x
	- Change design to add nose reduction gearbox		x	x		
	- Change coupling grease seal design		x		x	x
	- Change coupling radial clearance		x		x	x
	- Index components		x		x	x
	- Tighten tolerances		x		x	x
	- Dynamically balance components		x		x	x
I	IR blower shaft failure:					
	- Revise pilot rotor brake release procedure				x	x
	- Add accumulator to brake actuation hydraulics	x				

20

TABLE 2. - Continued

Item	Problem/Solution	Extent of application				
		Consideration only	Design	Analysis	Test	Adopted
J	90° gearbox support failure:					
	- Add soft mount under one support				x	
	- Add braces				x	x
	Accessory gearbox support failure:					
	- Revise strut mount location				x	
	- Change mounting stiffness				x	
K	Poor governing; excessive transient droop:					
	- Modify fuel control/governor		x	x	x	x
	- Reduce control linkage hysteresis	x				
L	Excessive torsional loading due to over-speed trip:					
	- Revise over-speed trip system checkout procedure				x	x

TABLE 2. – Concluded

		Extent of application				
Item	Problem/Solution	Consideration only	Design	Analysis	Test	Adopted
M	Hydraulic system noise:					
	– Soundproofing		x		x	x
	– Vibration isolation	x				
	– Change to different pump design	x				
	– Reduce pressure oscillations		x		x	x

22

IDENTIFICATION OF SHORTCOMINGS

In the conduct of this study, a number of shortcomings have been identified. These may be deficiencies in:

1. Design guidelines

2. Design details

3. Analytical procedures and methods

4. Test procedures and methods

or a combination thereof. These shortcomings are briefly summarized in Table 3.

The shortcomings listed are consistent with the time period in which the individual problem was encountered. Significant advances have been made over the past years in many of these areas. Where appropriate, additional information has been provided in the comment column.

The letter designation code in the first column of Table 3 refers to the problem identification code previously assigned in Table 1; the dash number is a counter to indicate the number of shortcomings identifiable to each specific problem.

TABLE 3. SUMMARY OF SHORTCOMINGS IDENTIFIED IN
ENGINE/AIRFRAME/DRIVE TRAIN TECHNOLOGY

Item	Description	Comment
A-1	Lack of a nonlinear analysis with which to evaluate trade-offs between stability, governing accuracy, and transient response	Significant improvements have been made in this area.
A-2	Lack of acceptance criteria for helicopter drive system stability and oscillatory amplitudes	
B-1	Lack of knowledge of the spring rate effect of ball bearings and the probability of the spring rates of the free-wheeling and output shaft support bearings controlling the engine-to-transmission shaft natural frequencies	Shaft critical frequencies were calculated from the classical equations for shaft bending of a rigidly supported shaft.
B-2	Lack of knowledge and availability of analytical methods and/or computer programs with which to calculate the bearing spring rates	Significant improvements have been made in this area, but confidence is lacking for low bearing load conditions.
B-3	Lack of knowledge and availability of balancing techniques for a 6000 rpm floating shaft	Significant improvements in dynamic balancing techniques have been made since this time.
C-1	Lack of knowledge of elastomeric properties for the proper combination of noise reduction/dynamic stiffness characteristics	Methodology often results in trial-and-error procedures.

24

TABLE 3. - Continued

Item	Description	Comment
C-2	Lack of analytical methods and/or of measured data to accurately determine exact source of noise generation in a geared drive train	Propagation of noise through aircraft structure can be reduced to some extent.
D-1	Failure to analyze the engine mounting system to account for the effects of localized airframe flexibility	Dampers were added as an interim fix but were not considered acceptable for a production configuration.
E-1	Lack of available analysis and/or computer program with which to compute the transient loading of the drive train	Significant improvements have been made in this area.
E-2	Lack of design procedures which would require that the system be designed and stressed for discrete transient drive system loadings, in general, or at least for a high-speed throttle chop	BHT general design factor of 1.5 for dynamic loads is not sufficient.
E-3	Initial lack of experience relating to which parameters control the dynamic loading: e.g., backlash, spring rate, frequency, torque decay rate, magnitude of initial torque	

25

TABLE 3. — Continued

Item	Description	Comment
F-1	Lack of measured data and/or analytical methods with which to accurately predict the shaft chucking forces and misalignment moments - particularly for the shaft torques, misalignment angles, chucking angles, and frequency thereof related to a 20,000 rpm design	Data extrapolated from UH-1 coupling data obtained in early 1960's at 6000 rpm; no unbalance data available.
F-2	Lack of definition on the engine installation drawing of the dynamic or oscillatory loading limits and the effect of these oscillatory loads upon the mean limits	Engine manufacturer evaluated BHT data and acknowledged acceptance.
G-1	Inability to accurately predict the main rotor induced dynamic loads at the engine mounts, and/or the input drive-shaft dynamic loads on the engine	Significant improvements in the prediction of rotor excitations have been made in the last 1½ years.
G-2	Lack of an efficient ground vibration test methodology which was directly relatable to the analytical methods used (in this case NASTRAN)	Rigorous analytical/test correlation of the engine mounting system was not performed.
H-1	Inadequate design guides and design criteria for high-speed and super-critical shafting	AMCP 706-201[4] was not released until after the initial design was completed.

4. ENGINEERING DESIGN HANDBOOK, HELICOPTER ENGINEERING, PART ONE: PRELIMINARY DESIGN, AMC Pamphlet No. 706-201, Headquarters, U.S. Army Material Command, Alexandria, Virginia, 30 August 1974.

TABLE 3. - Continued

Item	Description	Comment
H-2	Lack of driveshaft coupling design capable of transmitting the required torque and accommodating the required misalignment and chucking	Repeated discussions with Bendix, Lord, Kaman, and others indicate no couplings of practical size, weight, and cost other than crown tooth adequate for requirements.
H-3	Lack of definition of crown tooth coupling chucking forces and misalignment moments at the design, torque, speed misalignment angles, and chucking amplitudes and of how the magnitude changes with shaft unbalance	Data extrapolated for UH-1 coupling data obtained in early 1960's at 6000 rpm; no un-balance data available.
H-4	Lack of balance criteria for high-speed shafting	Range of potential unbalance with minimum and maximum tolerances was accomplished; no definition of design requirement available.
H-5	Lack of test data and correlation with analysis of bearing spring rates as a function of rotational speed, radial load due to gear loading, and/or shaft unbalance	Analysis available to compute spring rates, but confidence in correlation at low radial loads is lacking.
H-6	Lack of adequate experience/criteria for joint stability of high-speed shafting	Experience factors apparently available in engine industry; needed by AVM's.

27

TABLE 3. - Continued

Item	Description	Comment
H-7	Lack of data on lubricated threads versus dry threads for joint stability	Experience factors apparently available in engine industry; needed by AVM's.
H-9	Lack of coupling grease seal for 20,000 rpm shaft with high misalignment and chucking requirements	Grease dam was used as interim measure, but new seal needed for production.
H-9	Lack of centering device design for crown tooth coupling operating at 20,000 rpm with high chucking requirements	Centering device eliminated as interim measure; no problems encountered.
H-10	Lack of data on 'internal' or rotating system damping produced by greased crown tooth coupling for the applicable operational parameters	Internal damping is mechanism of supercritical nonsynchronous shaft whirl instability; need more test data.
I-1	Lack of design criteria requiring that the drive system, or at least the accessories, be designed and analyzed for specific transient loading conditions	BHT uses a design factor of 1.5 to cover dynamic loading.
I-2	Lack of an accumulator in the brake hydraulic system which would slow down the rotor brake release rate	
I-3	Lack of prescribed pilot operating procedures for rotor brake release	Revised procedures to a prescribed slow rate of release of rotor brake.

TABLE 3. - Continued

Item	Description	Comment
J-1	Failure to analyze the installation to include the effects of local stiffness distribution of the airframe	
J-2	Lack of design procedures which require that the mounting of the gearboxes be designed and analyzed for specific dynamic loading conditions	Ballistic vulnerability redundant mounting criteria are in direct opposition to optimum design for reducing stress loads.
K-1	Inability of nonlinear torsional stability analysis to accurately predict drive system transient response characteristics for certain specific critical maneuvers	
K-2	Analysis does not account for range of permissible pilot techniques to accomplish the same maneuver	Need information on probable control input limitations (displacements and rates).
L-1	Engine overspeed trip switching frequency not compatible with drive system torsional natural frequencies	Possibility of incurring damaging drive system loads during an overspeed trip cyclic condition.
L-2	Lack of proper pilot operating procedures for functional checkout of overspeed trip system	Overspeed trip checkout procedures were revised to keep torsional oscillations at a minimum.

29

TABLE 3. - Concluded

Item	Description	Comment
M-1	Inadequacy of soundproofing materials to provide efficient noise reduction without prohibitive weight penalties	
M-2	Noise generated from high-frequency pressure pulsations in hydraulic lines not considered in design criteria of hydraulic system	Installed pulsation damper in high pressure hydraulic line from pressure pump.

RECOMMENDATIONS

Future Army research funding should be provided to accomplish
the following:

1. Continued development of both analytical and test
    methodology to predict and verify the sources of
    transmission gearbox vibration and noise, including
    transmissibility and control to the fuselage
    structure. This program should be directed
    at application of the latest state-of-the-art
    methods, such as finite-element representation for
    gear and gearbox analyses, and rapid modal transfer
    function test techniques. Further, the study should
    evaluate problems associated with a specific design,
    analytically predicted improvements, test verification
    of the modifications, and, ultimately, flight-measured
    noise and vibration data to demonstrate the level of
    improvement actually attained.

2. Test verification of analytically predicted bearing
    spring rates as a function of bearing preload, reac-
    tion load, and shaft/rotor unbalance. This program
    should provide static and dynamic test data in a
    carefully controlled laboratory test setup which can
    be used for comparative correlation with existing
    analytical bearing spring rate programs. The results
    of this study should identify specific areas where
    analytical improvements are indicated, if any. After
    acceptable correlation is attained, the study should
    yield guidelines for design and analysis of future
    drive systems.

3. Development of a general-purpose program for the
    analysis of torsional stability, transient response,
    engine governing accuracy, and drive train dynamic
    loading to include flexible rotor effects.

4. Development of test methodology for rapid and accurate
    measurement of component (particularly engine)
    installation natural frequencies, mode shapes, and
    frequency response characteristics. This methodology
    should be compatible in data output format with analy-
    tical procedures (NASTRAN).

31

5. Analyses and tests on high-speed driveshaft applications to include evaluation of coupling designs, especially where coupling chucking amplitudes and/or misalignment angles are significant. This is of particular importance with the advent of the Advanced Technology Engine (ATE) which has power turbine shaft speeds of 30,000 rpm wherein supercritical shafting is likely to become a realistically unavoidable design criteria.

REFERENCES

1. White, James A., Bell Helicopter Company; OH-58A PROPUL-
    SION SYSTEM VIBRATION INVESTIGATION, USAAMRDL Technical
    Report 74-47, Eustis Directorate, U. S. Army Air Mobility
    Research and Development Laboratory, Fort Eustis, Virginia,
    August 1974, AD A002672.

2. Sullivan, R. J., et al., Hughes Helicopters; OH-6A PROPUL-
    SION SYSTEM INVESTIGATION, USAAMRDL Te

2. Sullivan, R. J., et al., Hughes Helicopters; OH-6A PROPUL-
    SION SYSTEM VIBRATION INVESTIGATION, USAAMRDL Technical Re-
    port 74-85, Eustis Directorate, U. S. Army Air Mobility
    Research and Development Laboratory, Fort Eustis, Virginia,
    January 1975, AD A007225.

3. Parker, W. H., Detroit Diesel Allison; T63 ENGINE CHARAC-
    TERISTICS ANALYSIS, USAAMRDL Technical Report 74-87, Eustis
    Directorate, U. S. Army Air Mobility Research and Develop-
    ment Laboratory, Fort Eustis, Virginia, January 1975,
    AD A007243.

4. ENGINEERING DESIGN HANDBOOK, HELICOPTER ENGINEERING, PART
    ONE: PRELIMINARY DESIGN, AMC Pamphlet No. 706-201, Head-
    quarters, U. S. Army Material Command, Alexandria, Virginia,
    30 August 1974.

5. Oradat, F. R., Hanson, H. W., and Alexander, R. M.,
    DEVELOPMENT OF SUPER-CRITICAL SHAFTING USING CROWN-TOOTH
    GEAR COUPLINGS, Bell Helicopter Textron Report
    299-909-004, Fort Worth, Texas, 15 January 1976.

6. Puckett, J. D., RESULTS OF INPUT DRIVESHAFT CHUCKING FORCE
    INVESTIGATION ON UH-1 DRIVESHAFT, Bell Helicopter Textron
    Report 55865M-12, Fort Worth, Texas, 15 December 1965.

7. Hanson, H. W., and Oradat, F. R., DRIVE SYSTEM ANALYSIS,
    ADDENDUM A: 409-140-025 INPUT DRIVESHAFT INSTALLATION
    CRITICAL SPEED ANALYSIS, Bell Helicopter Textron Report
    409-940-001, Fort Worth, Texas, 17 November 1975.

8. ADVANCED ATTACK HELICOPTER SYSTEM, SUBSTANTIATING TECHNI-
    CAL DATA: STRUCTURE AND DYNAMICS, Bell Helicopter Textron
    Report 409-199-006, Fort Worth, Texas, 15 February 1973.

REFERENCES - Concluded

9. Cronkhite, J. D., and Hanson, H. W., PRELIMINARY AIR
   VEHICLE VIBRATION REPORT FOR THE MODEL YAH-63 HELICOPTER,
   Bell Helicopter Textron Report 409-930-003, Fort Worth,
   Texas, November 1974.

10. Brunken, J. E., PROTOTYPE AIR VEHICLE VIBRATION ANALYSIS FOR
    THE MODEL YAH-63 HELICOPTER, Bell Helicopter Textron Report
    409-930-019, Fort Worth, Texas, February 1976.

11. Killion, S. W., and White, J. A., TOTAL SYSTEM VIBRATION
    SURVEY FOR THE YAH-63 ADVANCED ATTACK HELICOPTER, Bell
    Helicopter Textron Report 409-909-009A, Fort Worth, Texas,
    28 June 1976.

12. Killion, S. W., ENGINE VIBRATION AND STRESS SURVEY AND
    ENGINE VIBRATION DEMONSTRATION FOR THE YAH-63 ADVANCED
    ATTACK HELICOPTER, Bell Helicopter Textron Report
    409-909-008B, Fort Worth, Texas, 25 June 1976.

13. Shipman, D. P., PRELIMINARY TRANSIENT RESPONSE AND TOR-
    SIONAL COMPATIBILITY ANALYSIS OF THE MODEL 240/220 ENGINE,
    GOVERNOR, ROTORS, AND DRIVE SYSTEM, Bell Helicopter
    Textron Report 240-909-001, Fort Worth, Texas, April 1972.

14. Killion, S. W., MODEL 409 ENGINE/ROTOR TORSIONAL COM-
    PATIBILITY, Bell Helicopter Textron Report 409-909-007,
    Fort Worth, Texas, 30 July 1974.

15. Giesen, G. L., ENGINE/AIRFRAME COMPATIBILITY SURVEY AND
    DEMONSTRATION FOR THE YAH-63 ADVANCED ATTACK HELICOPTER,
    Bell Helicopter Textron Report 409-993-008B, Fort Worth,
    Texas, 28 June 1976.

16. Kamat, H. V., YAH-63/T700/G09 ECU TORSIONAL STABILITY
    AND TRANSIENT RESPONSE ANALYSIS, Bell Helicopter Textron
    Report presented to U. S. Army Source Selection Evalua-
    tion Board (SSEB), Fort Worth, Texas, 4 November 1976.

34

APPENDIX A

CLASSICAL DRIVE SYSTEM TORSIONAL INSTABILITY

The OH-4A was the BHT entry into the Army's Light Observation Helicopter (LOH) competition cf the early 1960's. This ship was powered by a single Allison (250 series) turbine engine.

During the design phase of the OH-4A helicopter, BHT obtained data from the engine manufacturer defining the engine and fuel control parameters suitable for a linear perturbation analysis about specified power conditions. The perturbation analysis conducted by BHT showed some potential drive system torsional instability problems. BHT then discussed this with the engine manufacturer and the fuel control manufacturer. BHT recommended several approaches to modification of the pneumatic governor/fuel control system and conducted studies on selected options. Considerations included: (1) the introduction of a dead band in the output governor pressure (P_G) signal; (2) hysteresis in the P_G signal; (3) a flexible, damped coupling to drive the governor N_2 flyball; and (4) a flexible, damped coupling in the tail rotor drive system.

Prior to the first ground run, no basic changes were made to the design. However, as a result of the analytical studies, alternate hardware was available.

During the initial ground run, the system exhibited a torsional instability when going onto the governor schedule. A number of fixes were attempted without success. Finally, sufficient accumulator volumetric damping was achieved by installing 72 inches of #10 flexible hose in the P_G line and the system became stable. The initial flight was made in this configuration.

Subsequent to the first flight, BHT and the engine and fuel control manufacturers pursued modifications to achieve acceptable stability without undue sacrifice of governing accuracy and/or transient response. On two occasions, approximately 3 months and 6 months after the initial ground run, a series of ground run tests were made to evaluate numerous control configurations. These configurations included P_G accumulators (hysteresis), P_G double check valves (dead band), governor input servo pressure (Py) accumulators (hysteresis), governor gain, and combinations thereof.

Additionally, BHT analyzed the flexible flyball coupling (Figure A-1) and the flexible tail rotor driveshaft coupling. Both of these concepts were found to be analytically attractive

for drive system torsional stability improvement. However, incorporation of a flexible flyball coupling would necessitate requalification of the fuel control/governor system which was an unpopular option with the engine and fuel control manufacturers; therefore, the flexible tail rotor driveshaft coupling was selected as the better approach to pursue.

BHT designed, fabricated, installed, and tested an elastomeric coupling (Figure A-2) in the tail rotor drive system. Three coupling spring rates were evaluated. The nominal spring rate provided satisfactory frequency placement of the torsional modes and sufficient damping to stabilize a fuel control configuration that was otherwise unstable. These results correlated well with the stability analysis.

An important element in this area was that the analysis showed the baseline fuel control/governor system to be unstable when the tail rotor driveshaft was disconnected. A test was conducted on ground runs which verified this analytical prediction. Thus, the flexible coupling was designed such that, should the elastomer fail, the internal stops would permit the coupling to continue to transmit full torque.

Although the flexible tail rotor drive system coupling provided a satisfactory interim solution, there still existed such design deficiencies in this approach as elastomer fatigue life, temperature effects, and nonlinearity of the stiffness and damping characteristics.

Finally, the engine and fuel control manufacturers developed a set of back-to-back check valves which effected a ±0.25 psi dead band in the P_G signal. This, along with accumulator volumes before and after the check valves, became the selected configuration.

The engines were delivered to three air vehicle manufacturers (AVM's), each having distinctly different rotor and drive system configurations. During the period of competitive evaluation this system was used successfully on all three aircraft.
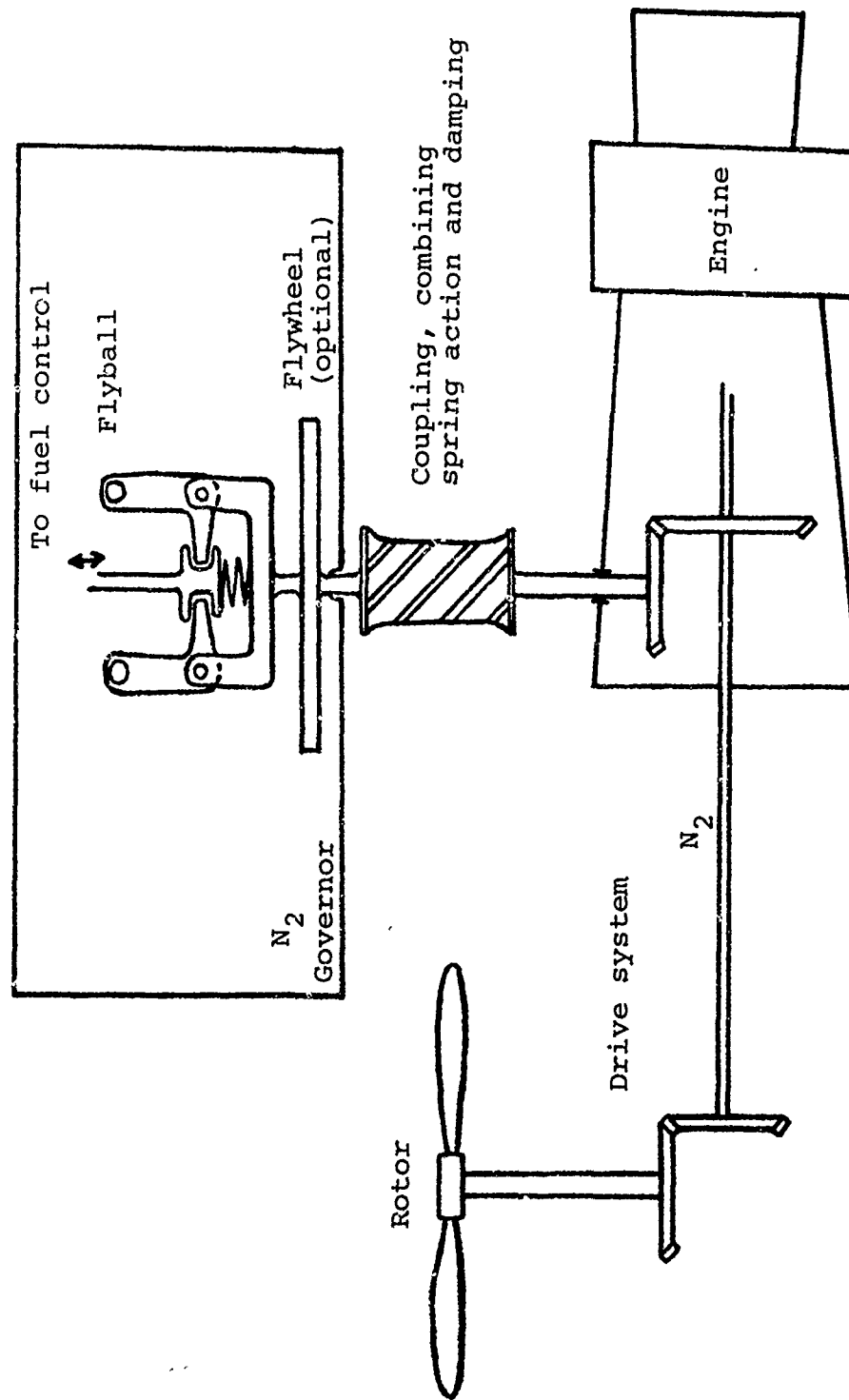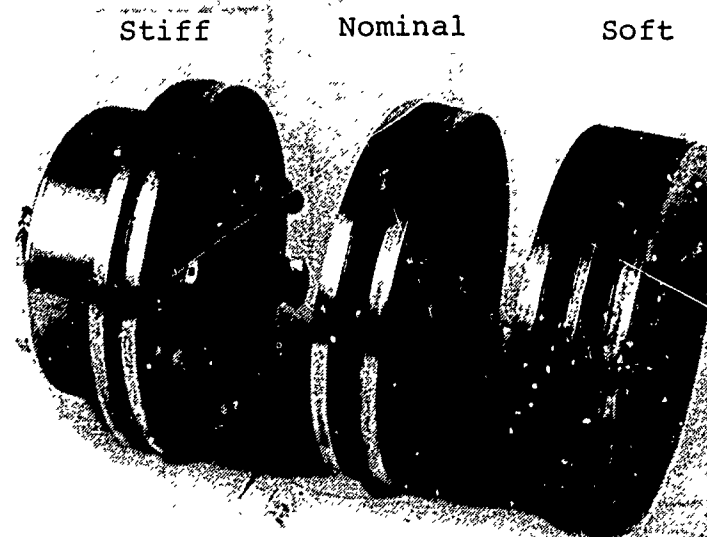
To fuel control

Flyball

Flywheel
(optional)

Coupling, combining
spring action and damping

Engine

N_2 Governor

Drive system

N_2

Rotor

Figure A-1. A flexible, damped coupling for the governor
N_2 flyball.

Stiff   Nominal   Soft
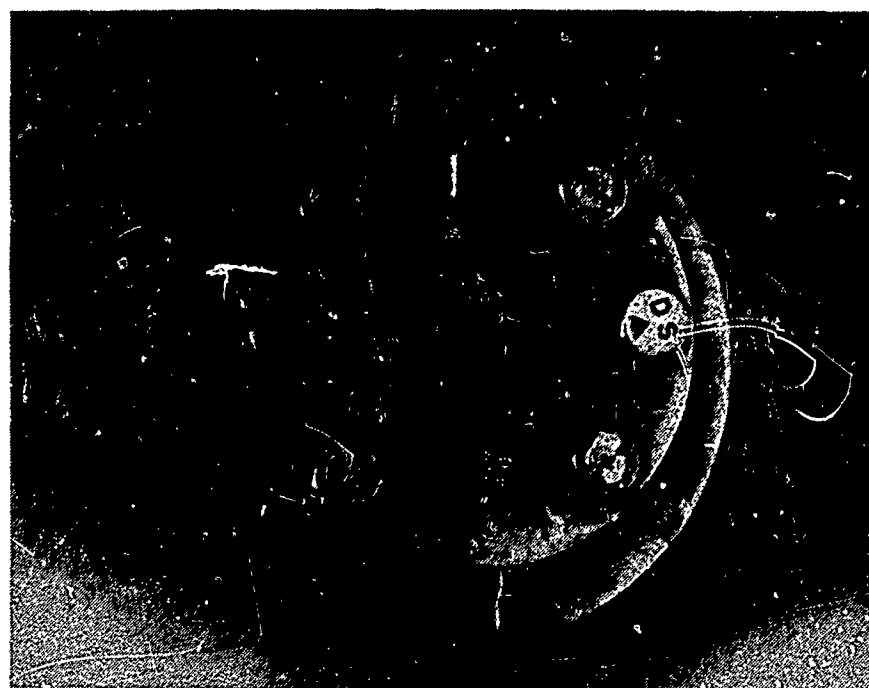
(Three spring rate configurations shown)

Figure A-2. Elastomeric tail rotor driveshaft coupling.

APPENDIX B

EXCESSIVE ENGINE AND FUSELAGE VIBRATION
AT ENGINE-TO-TRANSMISSION SHAFT SPEED

BHT developed the OH-4A helicopter as an entry into the Army's Light Observation Helicopter (LOH) competition. The OH-4A was powered by a single Allison (250 series) turbine engine with an output shaft speed of 6000 rpm. The engine was mounted on three bipods as shown in Figure B-1.

During ground run development tests, excessive high-frequency vibration was encountered. The frequency was determined to be 100 Hz or 1/rev of the input driveshaft. Magnitudes of 0.5 g were measured in the cockpit and were high enough to cause severe tingling of the facial tissues of the crew after only a few minutes of exposure.

Attempts at reducing this level included: (1) soft mounting the engine, (2) shaft balancing, and (3) redesigning the freewheeling unit and output shaft support at the engine takeoff.

Soft mounting of the engine was accomplished through the use of three Lord Kinematics rubber isolators, Part No. LM-405-1, modified by drilling out holes to soften the radial spring rates as shown in Figure B-2. These isolators were installed in the engine mounting system as shown in Figure B-3. This design modification did not satisfactorily alter the magnitudes or frequencies of the vibration.

Attempts to refine shaft balancing may have been ineffective because zero indexing of the shaft could not be maintained from one balance move to the next. This condition is indicative of shaft whirling due to bearing radial clearances.

Both the original and revised freewheeling unit and output shaft support designs are shown in Figure B-4. The revised design extended the gearbox case and provided substantially more bearing support, which precluded shaft whirling. This was found to be an acceptable modification to effectively reduce input driveshaft 1/rev vibrations to acceptable levels.
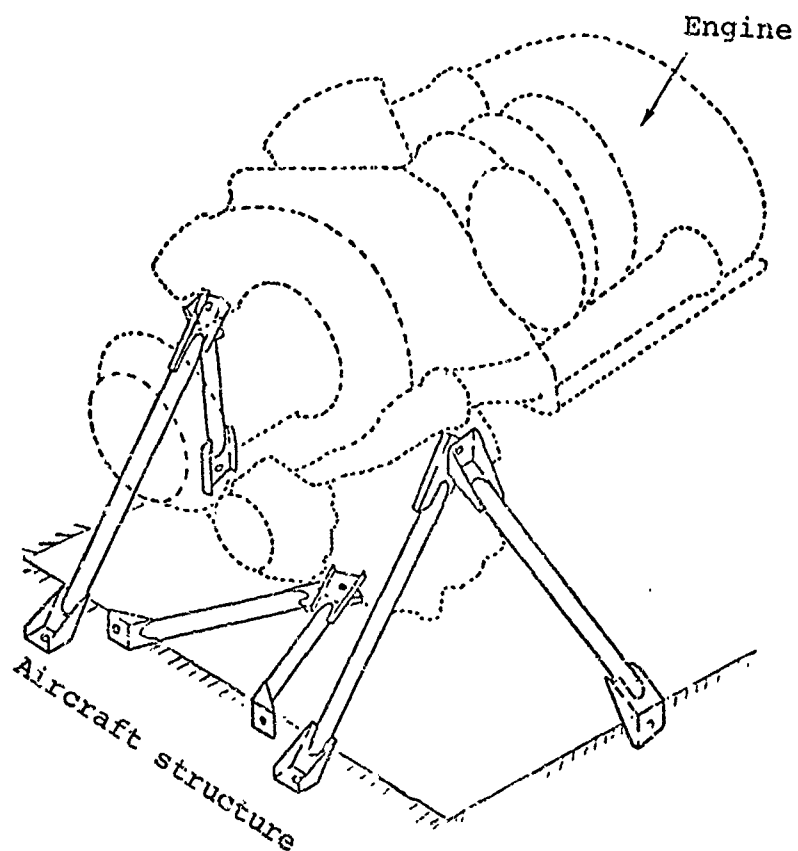
Engine

Aircraft structure

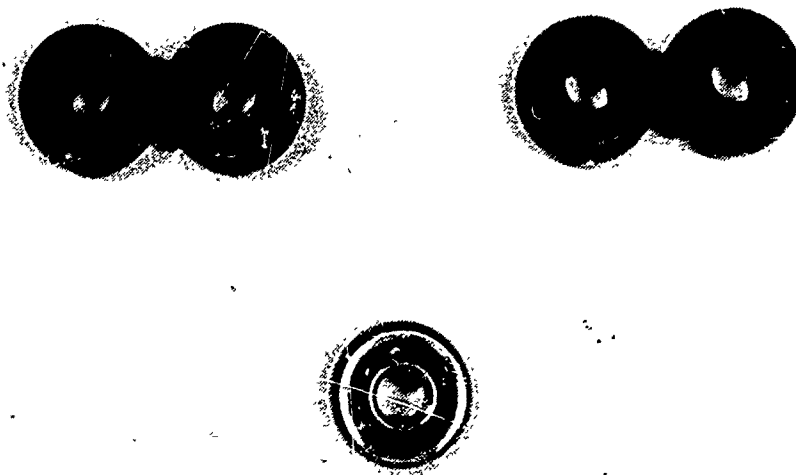Figure B-1. OH-4A engine mount installation.

Figure B-2. Lord isolation mounts.

(Typical - three places)
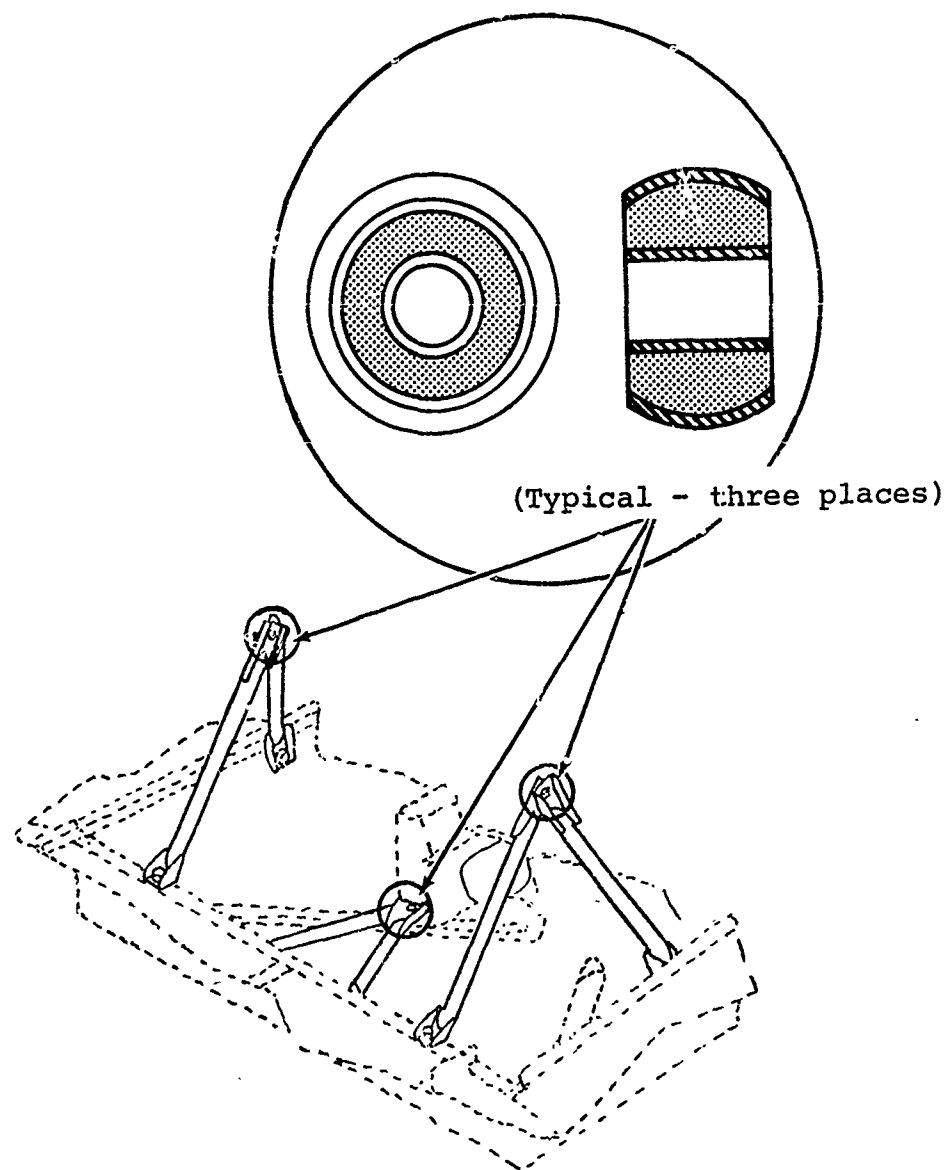
Figure B-3.   Soft engine mount installation.

Support bearings

Case

Output shaft

Clutch

Engine gearshaft

Clutch outer race

(Original design)

Outer bearing case

Support bearings

Case

Output shaft

Clutch

Engine gearshaft

Clutch outer race

(Revised design)
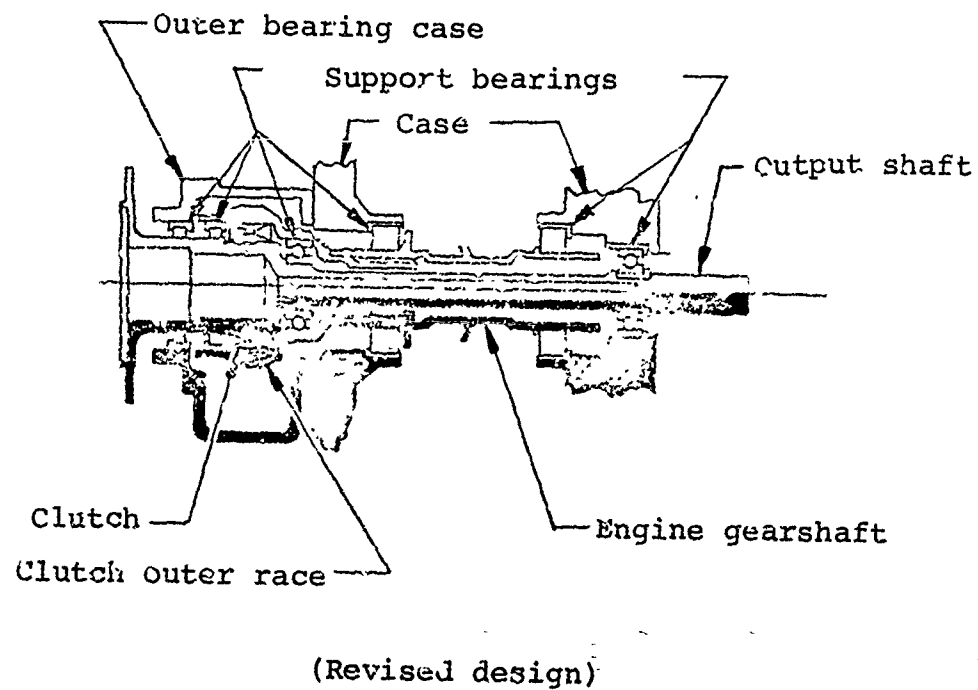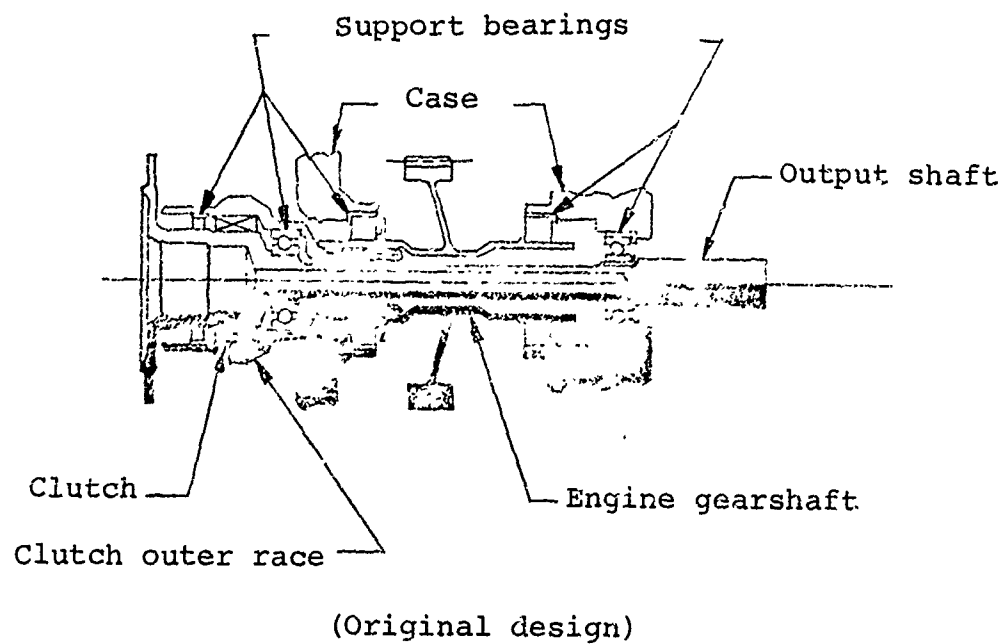
Figure B-4. Freewheeling unit and output shaft support installation.

APPENDIX C

HIGH-FREQUENCY ENGINE NOISE IN AFT CABIN AREA

Description of Problem

Cabin noise of the 206A, 206B, and 206L helicopters is charac-
terized by a high amplitude pure tone at 5000 Hz. Since its
frequency is within the most sensitive range of human hearing,
this tone is highly annoying to passengers in the cabin. The
spectral content of the 206B cabin noise is shown in Figure
C-1. The dominant noise sources in the 206B are the engine
and transmission, the relative locations of which are shown in
Figure C-2. The noise is produced by vibrations set up in the
engine output gearbox by a gear mesh of the output drive train.
The engine is supported at three mounting points as shown in
Figure C-3. Tests have shown that vibrations set up in the
gearbox are transmitted through the engine mounting points,
into the support legs, and into the aircraft structure. These
vibrations then radiate into the cabin as noise.

Solutions Considered

Several approaches were taken to reduce this high-frequency
noise, including standard soundproofing techniques, isolation
of the engine from the airframe, and modification of the gear-
box.

Soundproofing: Initial attempts at reducing this 5000-Hz tone
involved the installation of extra soundproofing to the aft
cabin walls, primarily in the hatbin bulkhead as shown in Figure
C-4. This proved to have little effect even though a consider-
able amount of soundproofing was used. The standard sound-
proofing installed in these helicopters had reduced the ampli-
tude of this noise spike as much as practical using sound-
proofing alone.

Engine Changeout: For specific customer complaints, the high-
frequency noise was reduced by exchanging a high-noise engine
with a normal one. Even though the 5000-Hz tone was associated
with the engine output gearbox, the complete engine/gearbox
assembly had to be replaced, since these two units were mated
together at the engine manufacturer. The replacement engine
was usually selected at random. Since the original engine gen-
erated higher-than-average cabin noise, the engine replacement
usually resulted in a noise reduction. This was an effective
solution, but it was obviously limited to specific complaints
and did nothing to improve overall 206B cabin noise. It was
also quite costly in terms of man-hours.

44

Elastomeric Engine Mounts: Since the 5000-Hz tone was caused by vibrations transmitting through the engine mounts and into the airframe structure vibration, isolation was introduced by incorporating an elastomer within the engine mounting assembly.

Two basic isolation concepts were considered. The first involved a replacement of each of the six engine support legs with a new leg made up of two concentric tubes separated by an elastomer. Each leg was built up as shown in Figure C-5, with no metal-to-metal contact between the inner and outer tubes but with through-bolts in oversized holes to provide a fail-safe feature in case of elastomer failure. The legs were installed on the aircraft as shown in Figure C-6. These mounts were installed in a flight test 206B helicopter, but no final evaluation was ever made regarding the noise-reducing capability of these mounts because they allowed excessive motion of the engine during initial ground tests. The engine went into a pitching motion at 70-80% N_2 RPM, producing excessive vertical motion to the pilot compartment. These mounts were not evaluated further. The concept itself may or may not be feasible, but the specific tube-in-tube mounts tested were not practical. The problem might not have occurred if a different elastomer were selected for use in these mounts.

A second concept of elastomeric engine mount was evaluated and was more successful. This second concept consisted of a steel/elastomer washer assembly placed at each of the three engine mounting points. Details are in Figure C-7(a). The washer assembly was installed as shown in Figure C-7(b), so that the engine gearbox vibrations imposed on the inner metal sleeve are separated from the airframe support legs which attach to the outer metal sleeve. Because the frequency of interest was so high (5000 Hz), only a small thickness of elastomer was needed to produce effective isolation. Flight test measurements were made with these elastomeric mounts installed to show the effects upon cabin noise. These tests show reductions in the 5000-Hz tone of as much as 10 decibels. Since this is a significant noise reduction, and since these types of elastomeric mounts involve relatively minor changes to existing hardware, the mounts are now undergoing qualification testing to allow them to be installed on a production basis.

Modification of Gearbox: Detroit Diesel Allison (DDA), the manufacturer of the C18, C20, and C20B engines, is aware of the noise problem associated with their gear train and is conducting studies to find the cause of the 5000-Hz vibration. These tests are currently in progress, with the following modifications being evaluated on an experimental basis:

1. Changing geartooth profile
2. Adding mass to gear webs to change natural frequency

45

3. Changing number of teeth on gears
4. Adding stiffness to gearbox case

Joint Program: BHT and DDA are working cooperatively on this problem, exchanging data on gearbox noise and vibration as measured on the installed engine and in the test cell to reduce this engine noise problem. It is felt that this effort will result in an improved cabin noise signature in the 206-series helicopters.
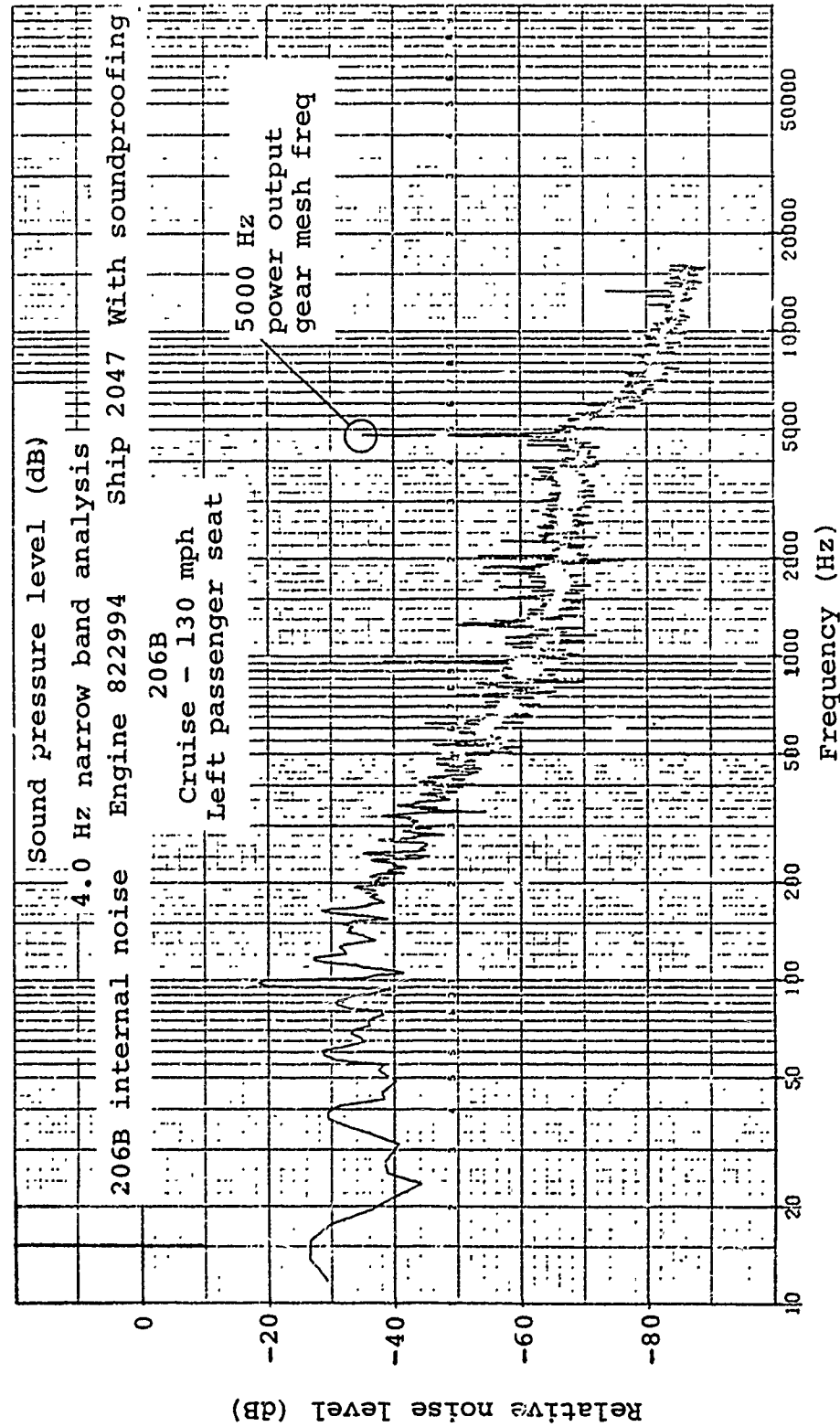
46

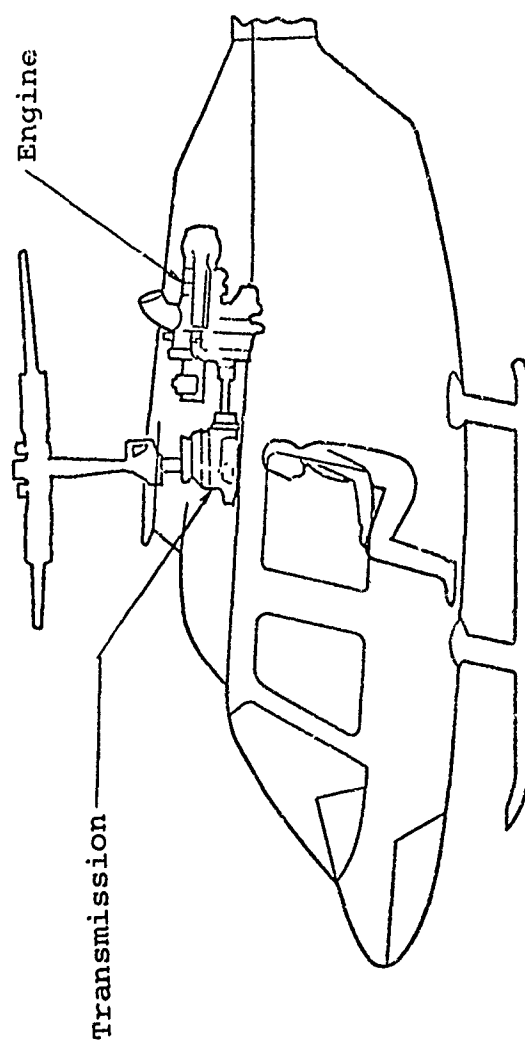Figure C-1. Cabin noise spectrum of 206B helicopter.

47

Engine

Transmission

Figure C-2. Relative location of noise sources.
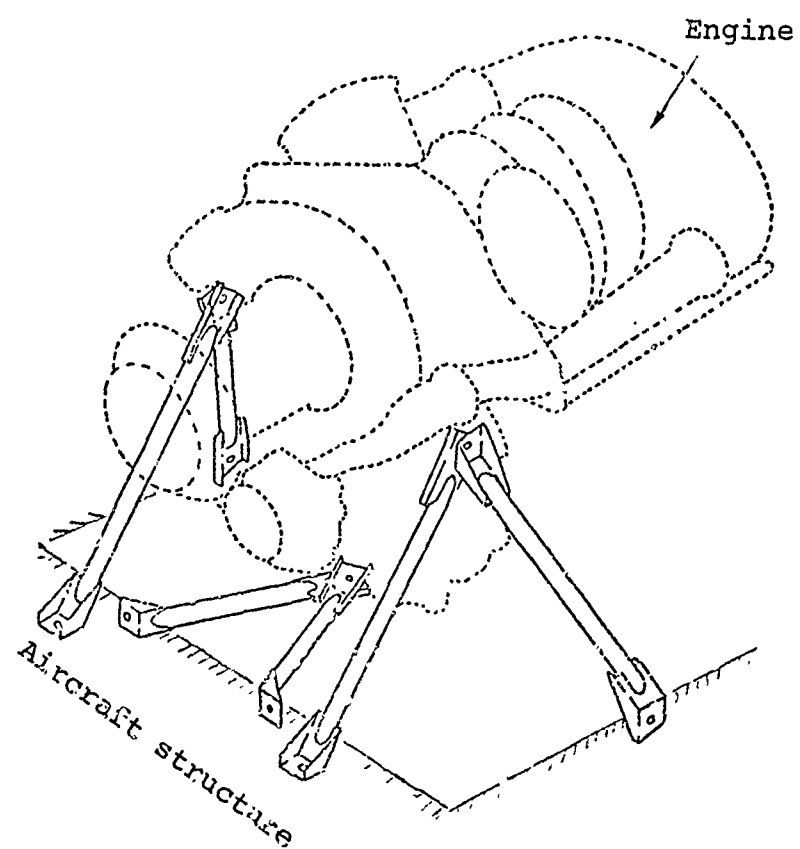
Figure C-3.   206B engine mount assembly.
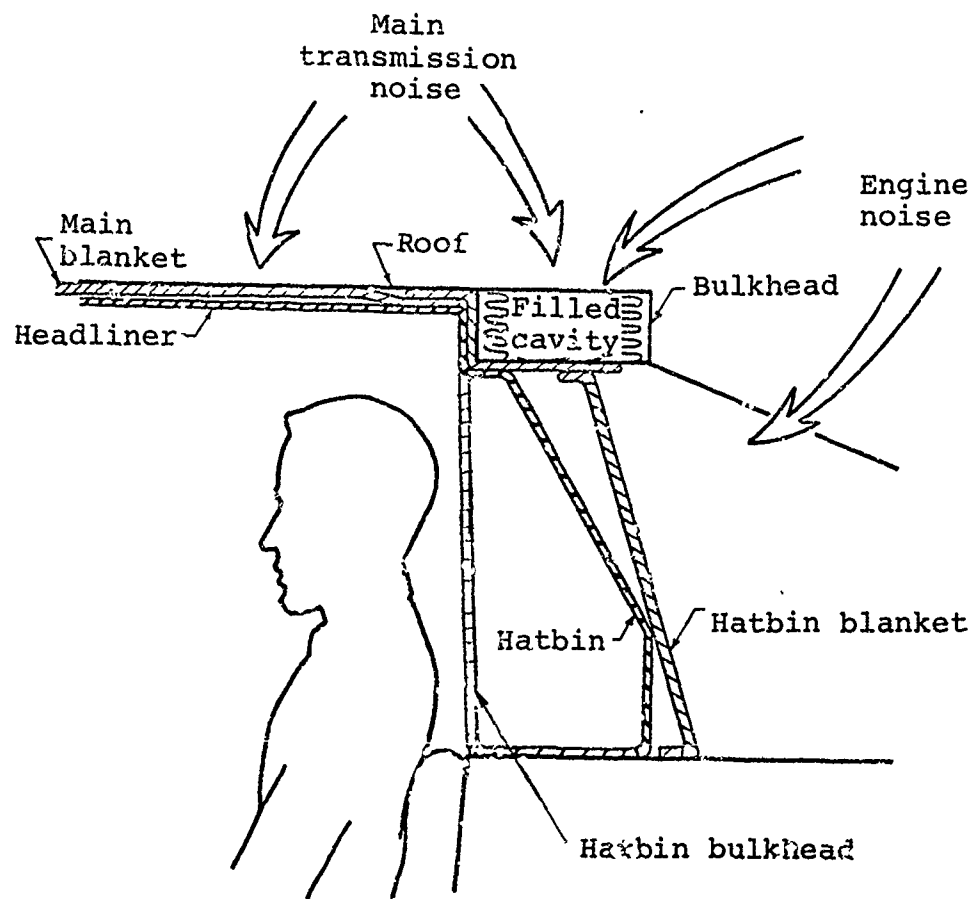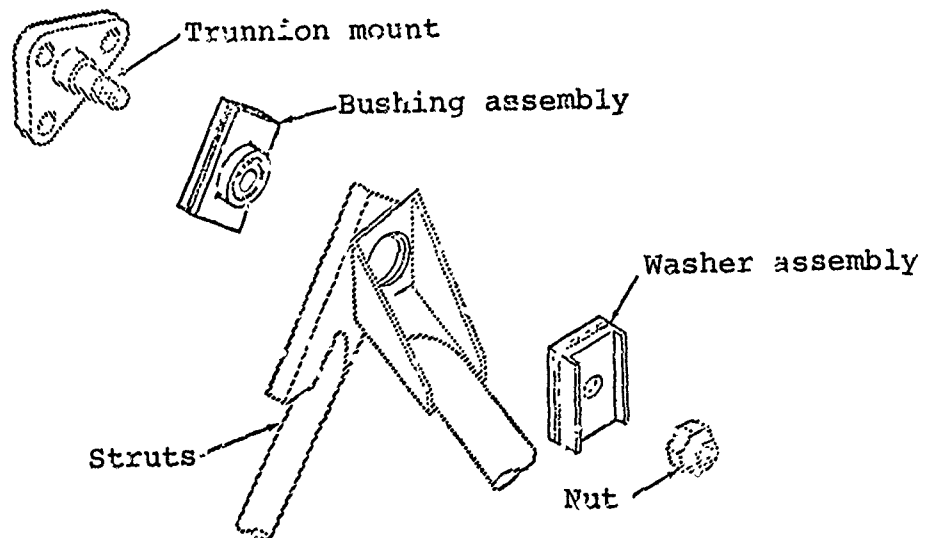
Figure C-4. Schematic of 206B soundproofing treatment.
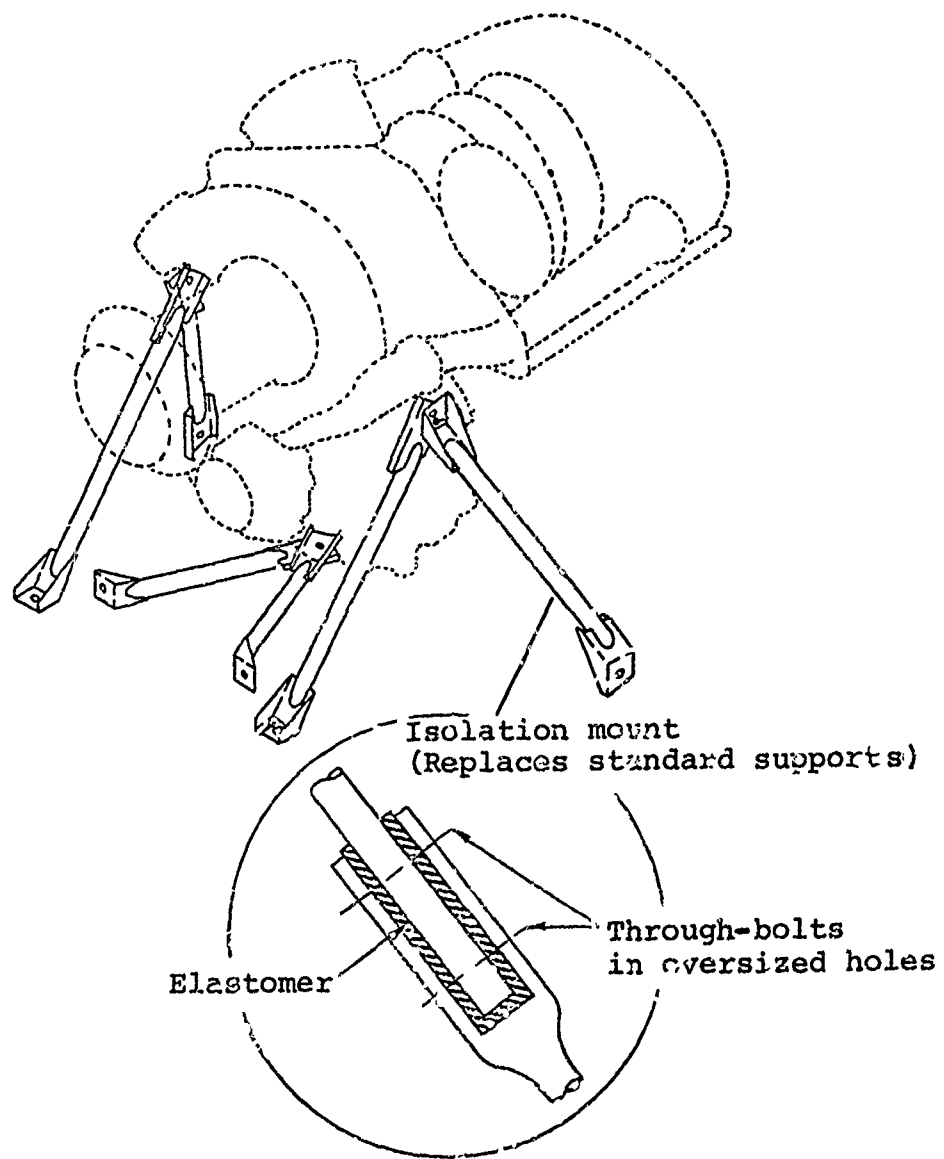
Figure C-5. Tube-in-tube engine support legs for vibration
            isolation.

Engine

Engine mounting stud

Airframe

Airframe

Figure C-6. Installation of tube-in-tube engine support legs.
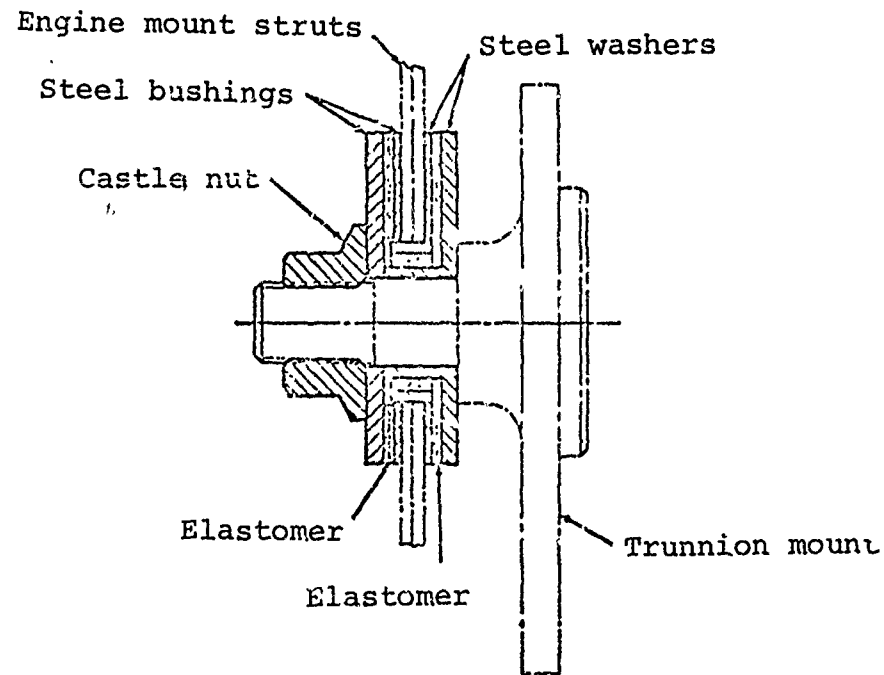
(a)   Cross section of elastomer engine mount as installed.

(b)   Exploded view of assembly.

Figure C-7.   206B elastomeric engine mounts for
noise reduction.

APPENDIX D

ENGINE INSTALLATION RESONANCE

In 1971 BHT, under company funding, developed the Model 309 King Cobra helicopter as an advanced version of the AH-1G gunship. Two ships were built. The power plant for the initial design was a Lycoming T55 engine. One ship was later converted to a twin-engine configuration employing the Pratt and Whitney T400 engines and combining gearbox.

During initial ground runs of the ship with the original single Lycoming T55 engine, the aft end of the engine was observed to have abusive lateral vibration occurring at the main rotor 2/rev frequency.

In order to conform to the engine manufacturer's requirement for a nonredundant engine mounting system, the engine mounting arrangement consisted of a forward tripod on the left side of the engine, a forward bipod on the right side of the engine, and an aft vertical monopod.

In an effort to correct the lateral vibration problem, two viscous dampers were added to the engine. The left engine damper installation is shown in Figure D-1. Lycoming was consulted to determine the maximum permissible load which could be transmitted to the engine at the aft combustor flange damper attachment point. The damper links were then instrumented with strain gages and the level of damping was adjusted to maintain the loads below the designated limits.

Subsequent ground runs indicated that the dampers reduced the lateral vibration of the engine to an acceptable level to permit flight test of the air vehicle to proceed. This configuration was utilized throughout the remainder of the developmental flight test program.

Although the damper arrangement was satisfactory for the prototype air vehicle, Lycoming did not consider this a desirable engine mounting design for a production configuration.

During the latter stages of the Model 309 program, the decision was made by BHT to incorporate the Pratt and Whitney T400 twin-engine arrangement as a more attractive power plant configuration for the AEFA* testing and fly-off evaluation. Consequently, no further work was performed on the single-engine Lycoming installation.

---

*U. S. Army Aviation Engineering Flight Activity (AEFA), Edwards Air Force Base, California.
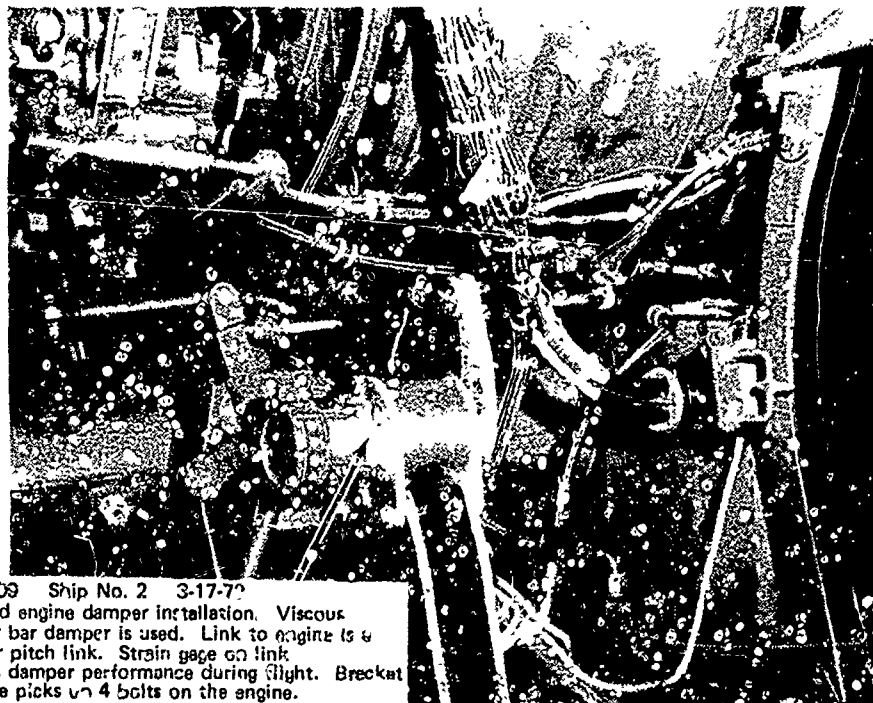
Model 309   Ship No. 2   3-17-72
Left hand engine damper installation. Viscous
stabilizer bar damper is used. Link to engine is a
tail rotor pitch link. Strain gage on link
measures damper performance during flight. Bracket
on engine picks up 4 bolts on the engine.
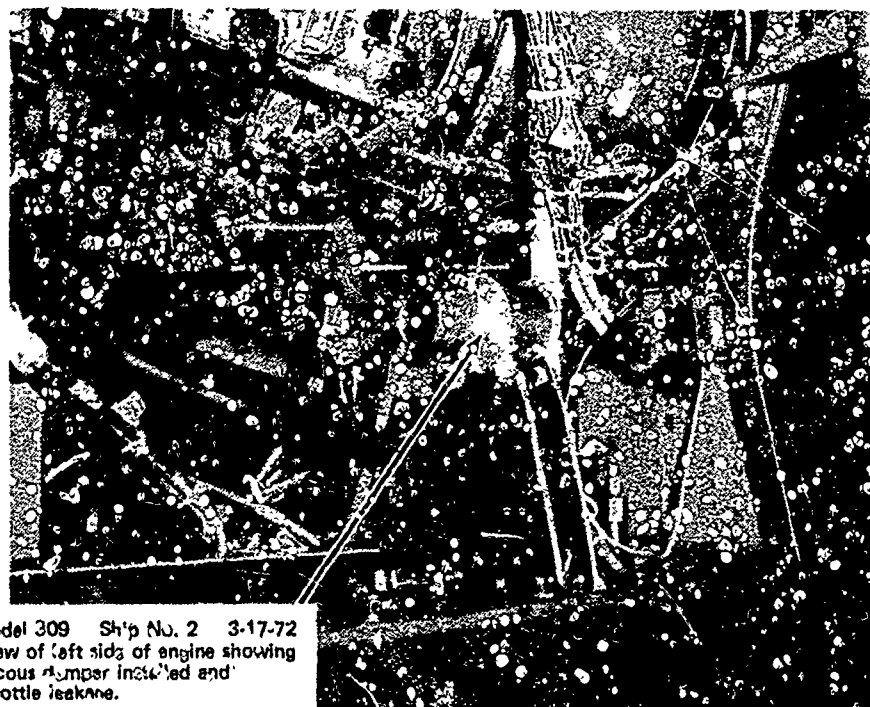
Model 309   Ship No. 2   3-17-72
View of left side of engine showing
viscous damper installed and
throttle leakage.

Figure D-1. Left engine damper installation.

APPENDIX E

HIGH TRANSIENT DRIVE SYSTEM LOADS FOLLOWING
ENGINE THROTTLE CHOPS

The BHT Model 309 King Cobra helicopter was developed in 1971
under company funding as an advanced version of the AH-1G
gunship.

Preparatory to AEFA testing and a fly-off evaluation with the
Sikorsky Blackhawk, BHT flight tests were conducted to obtain
quantitative data. The Army had specifically requested that
high-speed throttle chops be evaluated. BHT tests were con-
ducted in a buildup fashion, gradually increasing speed.
Measurement of the tail rotor drive system during these
throttle chops showed excessive torsional loading. It became
evident that high transient loads - in excess of the basic
design capability - would be encountered at high speed and power.

Additionally, BHT conducted analyses of the drive system in
an effort to better understand the cause of the high loads
and to evaluate possible design changes which would minimize
or eliminate the problem. The initial study established
acceptable correlation between calculated and measured data
as shown in Figure E-1. The analysis showed that the high
torsional loads were closely related to the decay charac-
teristics (initial to final torque, rate of decay, etc.)
of the engine output torque. More detailed documentation of
the analytical approach is provided in Attachment 1 to this
appendix.

Several drive train design changes were considered in an
effort to make the drive train more tolerant of engine
torque oscillations.

A method of providing torsional damping was considered which
involved installing a torsionally soft elastomeric coupling
in the tail rotor drive train. The objective was to provide
a means of absorbing torsional shock which would substantially
reduce the torque excursions to well within the drive train
capability.

Also considered was a torsional decoupling concept which
involved installing an overrunning clutch in the tail rotor
drive train. It was anticipated that the torque oscillations
would be reduced to acceptable levels if the negative torque
excursions could be eliminated.

The Model 309 program was subsequently terminated before
any design modification hardware was produced.   However,
the analytical procedures developed under this program were
later used in the initial design stages of the drive system
for the Model YAH-63 prototype Advanced Attack Helicopter
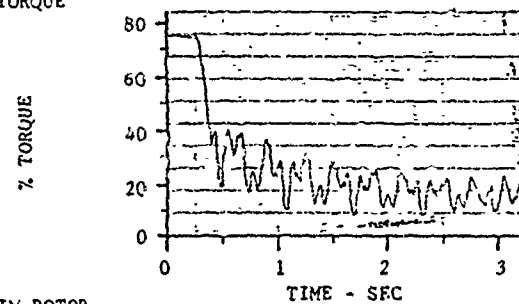(see Appendix K of this report).

FLIGHT TEST DATA

Counter Number: 93
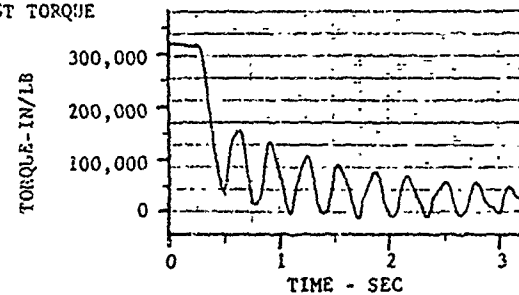Flight Number: 103A
Ship Number: 2503
Date: 5-27-72
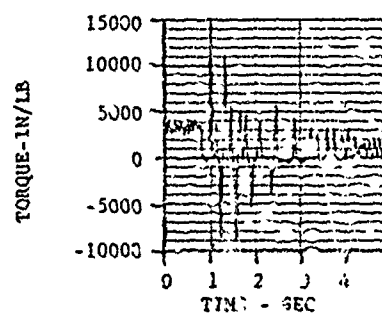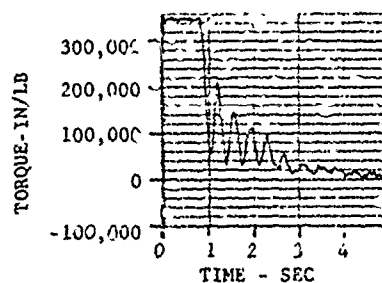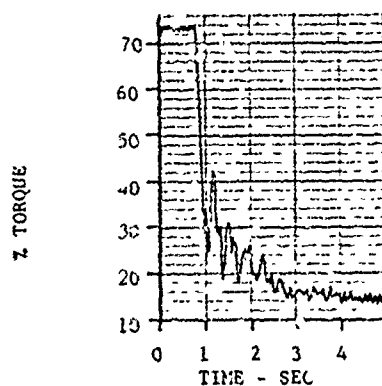
POWER TURBINE
TORQUE DECAY

ENGINE DELTA
TORQUE

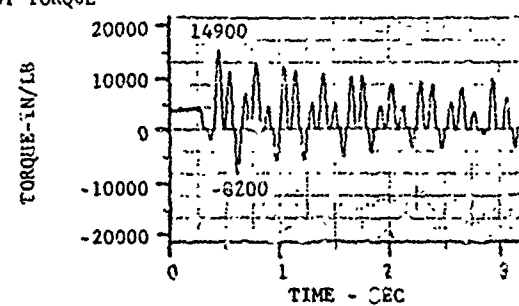MAIN ROTOR
MAST TORQUE

TAIL ROTOR
MAST TORQUE

HYBRID DATA
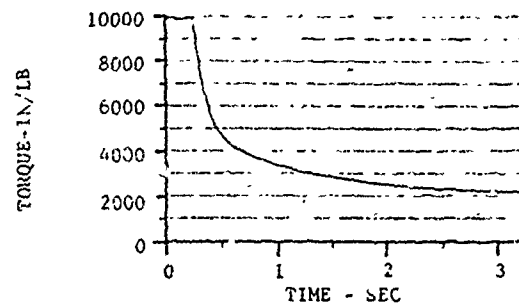
Figure E-1.   Analytical correlation of measured data.

ATTACHMENT 1 TO APPENDIX E

BELL HELICOPTER COMPANY
INTER-OFFICE MEMO

81:DB:jl-771
12 November 1973

MEMO TO: Mr. . . Hall*

COPIES TO: Messrs. J. Drecs*, W. Jennings*, D. Kidd, L. Kingston*, R. Lynn*,
             C. Moore*, E. Roseler*, C. Seibel*, Dynamics File,
             ₂CF

SUBJECT: MODEL 309 TORSIONAL STUDIES

SUMMARY

Experience at BHC shows that the peak load in the tail rotor drive system usually
occurs following a throttle chop and that these chops produce the highest loads
when initiated from high power conditions. To investigate this phenomenon an
analytical model of the Model 309 drive system was developed and programmed on the
hybrid computer. Throttle chops were simulated and correlated to actual flight
test results of the Model 309 helicopter.

ANALYTICAL MODEL

For this study, the drive system is considered as a series of lumped rotational
inertias connected by torsional springs as shown in Figure 1. The principal
inertias are the main rotor, main transmission, engine, and tail rotor. The
principal springs are the main rotor mast, transmission input shaft, and tail rotor
driveshaft. Engine aerodynamic torque was used as a driving function and decay
characteristics thereof were varied.

The main rotor and tail rotor torques required were calculated as a function of main
rotor collective pitch. The logic used to set the tail rotor pitch is shown
schematically in Figure 2. The basic equation and the constants used are given in
Table I. The values for the constants are derived in Enclosure 1. The Model 309
flow diagram used for implementation on the hybrid computer is shown in Figure 3.
The results are presented herein. Studies are continuing in order to determine
practical means of reducing the peak torque loads. The resulting loads were
found to be dependent on the power setting prior to the throttle chop, the amount
of backlash in the drive system, and the rate at which the engine torque decreased.
A 1000 in-lb torque loss was assumed for accessory load.

PROGRAM INPUTS

For each correlation case, the main rotor and tail rotor collective settings were
adjusted so that the steady state torque approximated the flight test steady state
values. Both of these settings were held constant during the throttle chop. The
engine mast torque decay rate was adjusted to give an engine torque decay rate close
to that shown in the flight test data.

*w/o enclosures

ATTACHMENT 1 TO APPENDIX E

The amount of backlash in the gears was set equal to 160 percent of the nominal (print callout) value. This setting yielded the best correlation for both trace character and peak values. Table II lists the calculated parameters (both raw and engine output speed referenced) and the values actually used in the analysis if the two differ. One of the parameters altered is the tail rotor driveshaft spring rate, KTR. It was lowered 25 percent from the calculated value so that the torsional frequency of the tail rotor would be closer to the measured value. This modification brought the character of the hybrid tail rotor torque curves more in line with those of the flight test data.

RESULTS

Table III shows the steady state values for main rotor, tail rotor, and engine torques from the hybrid analysis compared with test data.

Table IV gives the measured torsional frequencies and the hybrid frequencies. The higher main rotor frequency for the calculated case is probably due to the coupling effects of the main transmission torque restraint and lateral pylon rocking mode which were not considered in the analysis.

Figures 4 to 9 show the compared data. Figure 10 shows the actual and calculated positive and negative tail rotor torque peaks for each power setting.

CONCLUSION

The analytical model and technique are adequate to predict the peak load characteristics provided the engine decay rate is well defined. For future designs, the possibility of obtaining these decay characteristics data from engine test cell work should be explored.

$\mathcal{D7.K.}$

Doug Brister
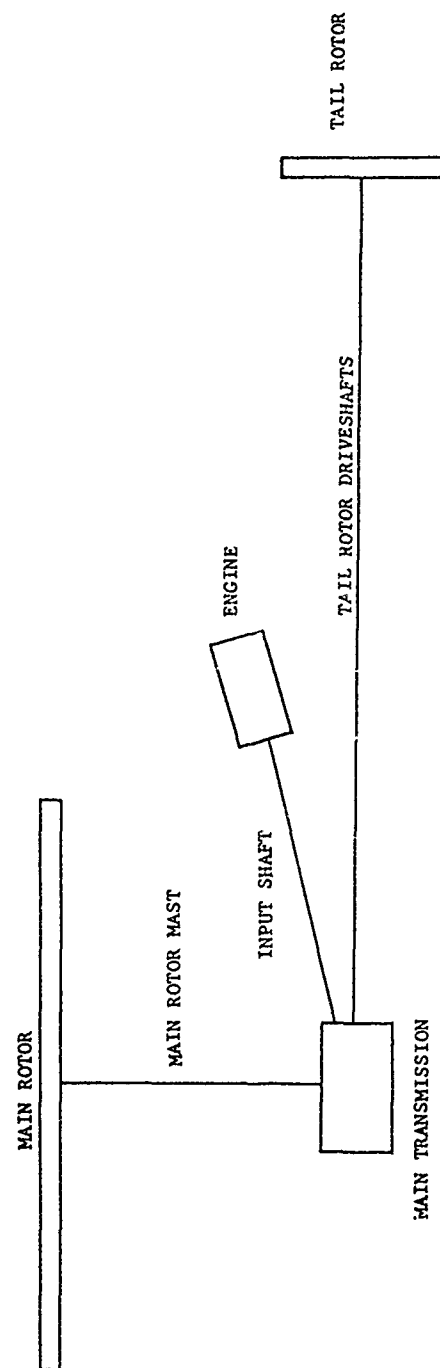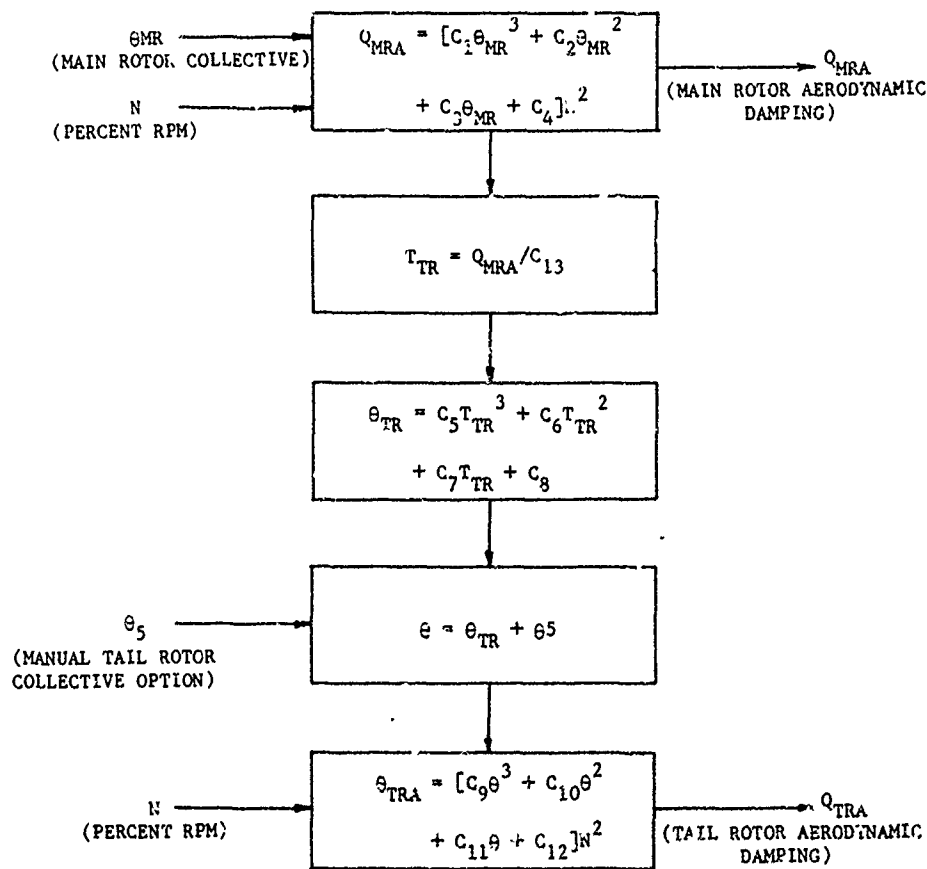Dynamics Group
Ext. 2886/2889

ATTACHMENT 1 TO APPENDIX E

Figure 1. Lumped Drive System Representation

INPUTS   OUTPUTS

$$Q_{MRA} = [C_1 \theta_{MR}^3 + C_2 \theta_{MR}^2$$

θMR ————→
(MAIN ROTOR COLLECTIVE)

$$+ C_3 \theta_{MR} + C_4]N^2$$

N ————→
(PERCENT RPM)

→ Q_{MRA}
(MAIN ROTOR AERODYNAMIC DAMPING)

$$T_{TR} = Q_{MRA}/C_{13}$$

$$\theta_{TR} = C_5 T_{TR}^3 + C_6 T_{TR}^2$$

$$+ C_7 T_{TR} + C_8$$

θ_5 ————→
(MANUAL TAIL ROTOR COLLECTIVE OPTION)

$$\theta = \theta_{TR} + \theta_5$$

$$\theta_{TRA} = [C_9 \theta^3 + C_{10} \theta^2$$

N ————→
(PERCENT RPM)

$$+ C_{11} \theta + C_{12}]N^2$$

→ Q_{TRA}
(TAIL ROTOR AERODYNAMIC DAMPING)

*Constants C_1 through C_{13} are listed in Table II, and defined in Er⸱.osure 1.

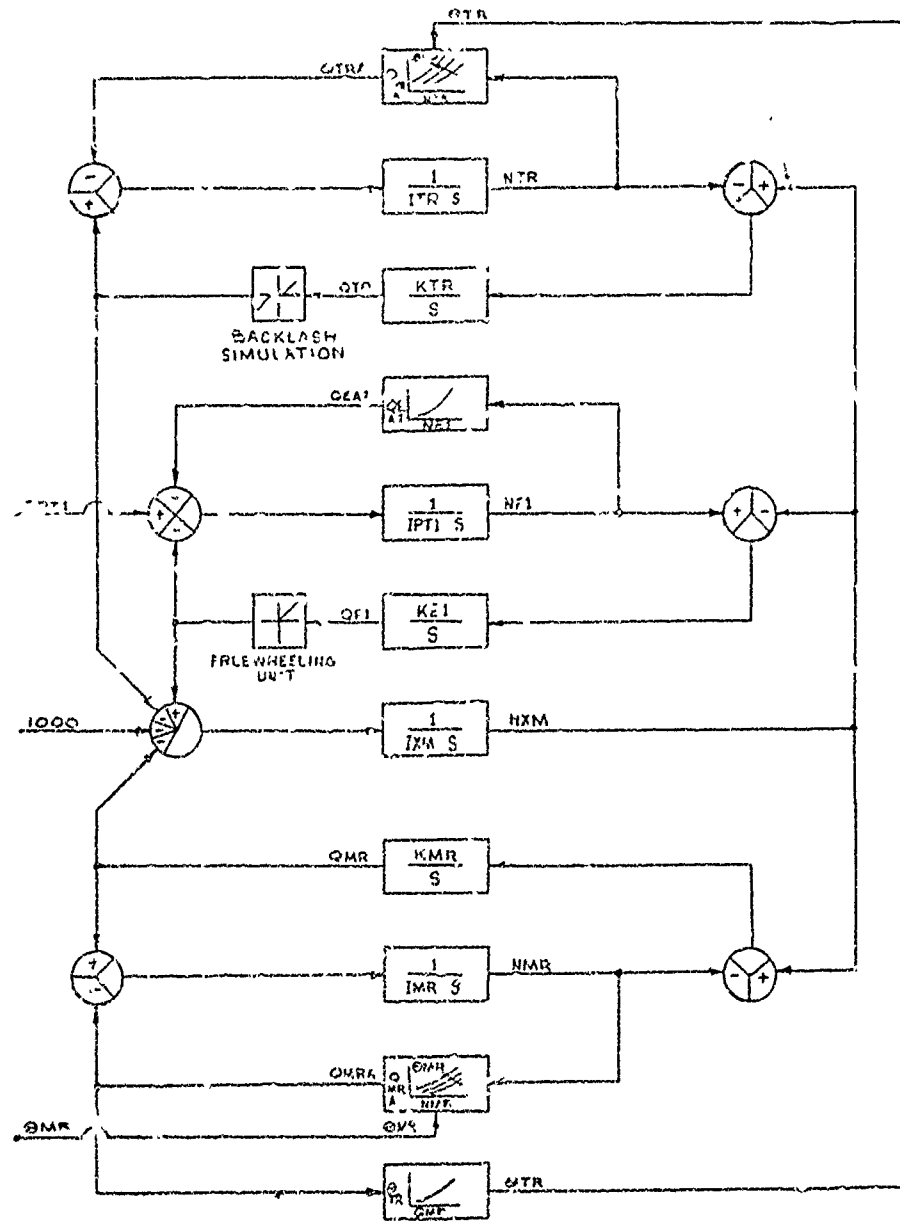Figure 2. Tail Rotor Collective Setting Logic Schematic.

Figure 3. Model 309 Hybrid F'ow Diagram.

TABLE I

Equation	Constant	
Main Rotor Aerodynamic Damping		
$QMRA = [C_1 \theta_{MR}^3 + C_2 \theta_{MR}^2$		
$+ C_3 \theta_{MR} + C_4]N^2$	C_1	1.0314 E -3
	C_2	- 4.4915 E -2
	C_3	7.7408 E -1
	C_4	- 4.3620 E 0
Tail Rotor Collective Setting		
$\theta_{TR} = C_5 T_{TR}^3 + C_6 T_{TR}^2$		
$+ C_7 T_{TR} + C_8$	C_5	1.2329 E -4
	C_6	- 5.5716 E -6
	C_7	1.3496 E -2
	C_8	1.2331 E 0
Tail Rotor Aerodynamic Damping		
$Q_{TRA} = [C_9 \theta_{TR}^3 + C_{10} \theta_{TR}^2$		
$+ C_{11} \theta_{TR} + C_{12}]N^2$	C_9	9.5203 E -6
	C_{10}	6.1796 E -4
	C_{11}	- 1.5726 E -3
	C_{12}	1.3626 E -2
Tail Rotor Thrust Required		
$T_{TR} = Q_{MRA}/C_{13}$	C_{13}	8.3
Power Turbine Aerodynamic Damping		
$Q_{EA} = C_{14}N^2$	C_{14}	0.09589

NOTE: N is percent rpm

ATTACHMENT 1 TO APPENDIX E

TABLE II

Parameter INERTIAS	Raw Value $(in\text{-}lb\text{-}sec^2)$	Actual Effective Value $(in\text{-}lb\text{-}sec^2)$	Modified Effective Value $(in\text{-}lb\text{-}sec^2)$	Percent Of Original Value (%)
I_{MR} (Main Rotor)	72886	39.22	Same	100
I_{XM} (Transmission)	1	.2425	Same	100
I_{PT} (Power Turbine)	8.037	1.949	San ›	100
I_{TR} (Drive Train)	55.6	.8049	Same	100
Torsional Springs	$(in\text{-}lb/rad)$ $\times 10^6$	$(in\text{-}lb/rad)$	$(in\text{-}lb/rad)$	
K_{MR} (Main Rotor Mast)	2.02	1089	1250	115
K_E (Engine)	2.0	2,000,000	Same	100
K_{TR} (Drive Train)	.0196	2740	2060	75
Other	(rad)	(rad)	(rad)	
C_{15} (Backlash)	.0856	.23	.368	160

65

ATTACHMENT 1 TO APPENDIX E

TABLE III

DATA POINT	ENGINE DELTA TORQUE		MAIN ROTOR MAST TORQUE		TAIL ROTOR MAST TORQUE	
	MEASURED (%)	CALCULATED (%)	MEASURED (in-lb)	CALCULATED (in-lb)	MEASURED (in-lb)	CALCULATED (in-lb)
124 Knot	54	52	229,000	224,000	2000	2060
141.5 Knot	62	60	269,000	260,000	2300	2480
146.5 Knot	67	67	300,000	300,000	2600	2800
150 Knot	68	70	319,000	310,000	3120	3300
153 Knot	73	74	340,000	334,000	3500	3700
155.5 Knot	77	77	369,000	370,000	3720	4000

TABLE IV

TORSIONAL NATURAL FREQUENCY

	FLIGHT TEST	HYBRID MODEL (modified effective values)
Main Rotor	2.68	3.22
Tail Rotor	9.1	7.5

66

ATTACHMENT 1 TO APPENDIX E

FLIGHT TEST DATA

POWER TURBINE
TORQUE DECAY

HYBRID DATA

Counter Number: 83
Flight Number: 107D
Ship Number: 2503
Date: 5-27-72
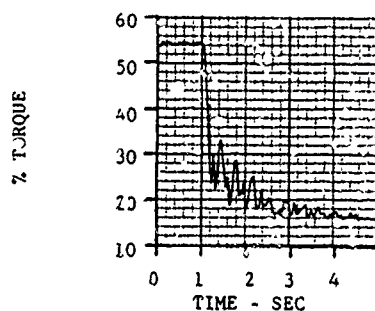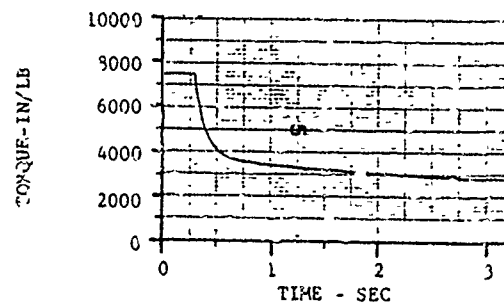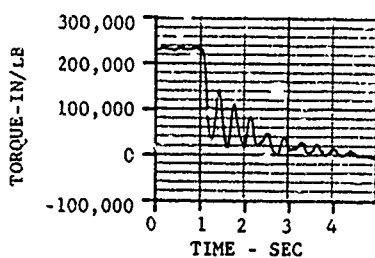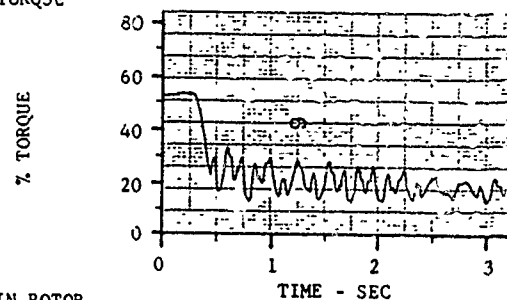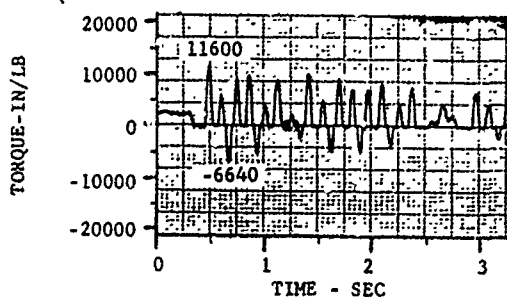
Figure 4. Data Set I - 124-Knot Power Setting.

FLIGHT TEST DATA

POWER TURBINE
TORQUE DECAY

HYBRID DATA
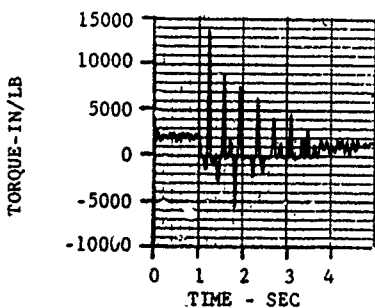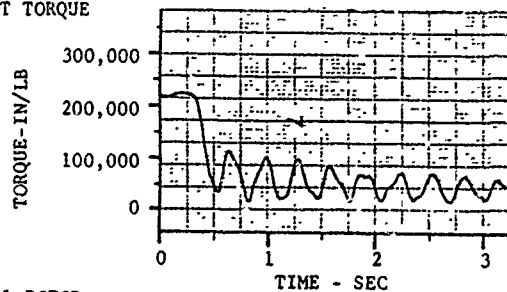
Counter Number: 84
Flight Number: 107D
Ship Number: 2503
Date: 5-27-72
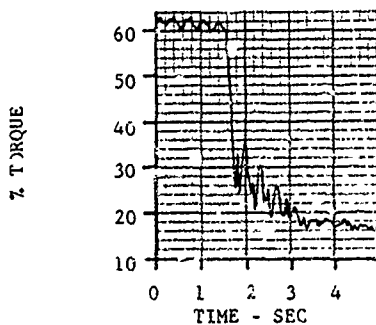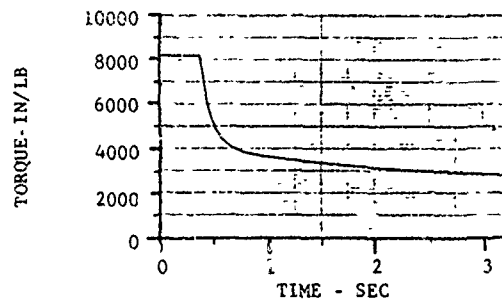
ENGINE DELTA
TORQUE
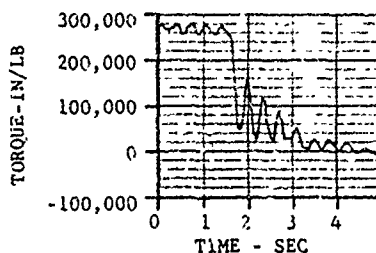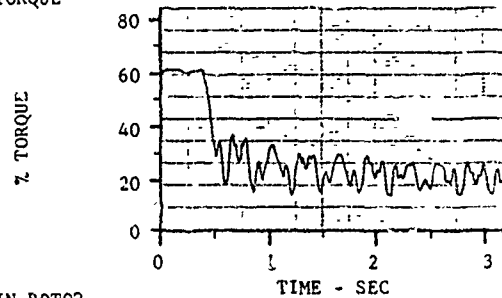
MAIN ROTOR
MAST TORQUE

TAIL ROTOR
MAST TORQUE

Figure 5. Data Set II - 141.5-Knot Power Setting.

FLIGHT TEST DATA

POWER TURBINE
TORQUE DECAY

HYBRID DATA

Counter Number: 85
Flight Number: 107D
Ship Number: 2503
Date: 5-27-72
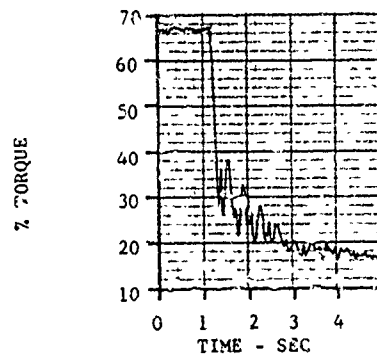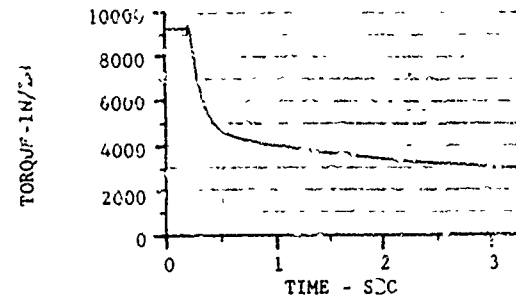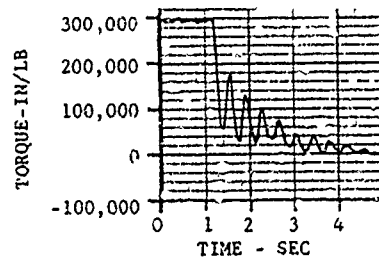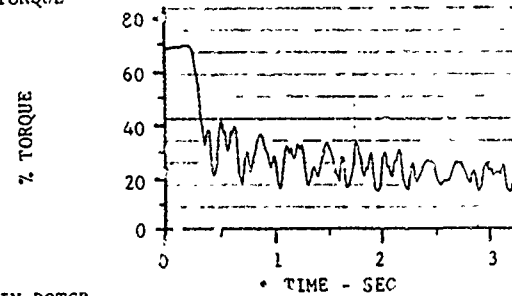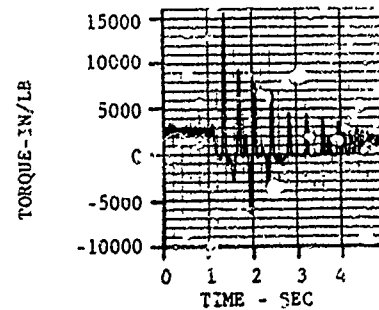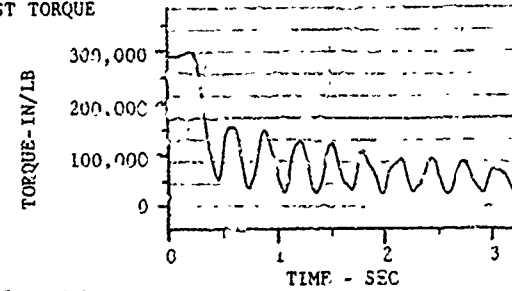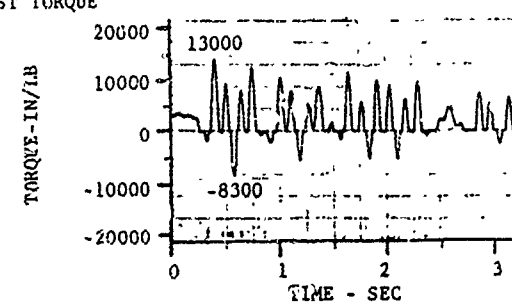
Figure 6.   Data Set III – 146.5-Knot Power Setting.

FLIGHT TEST DATA

POWER TURBINE
TORQUE DECAY

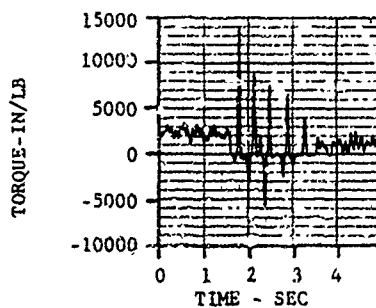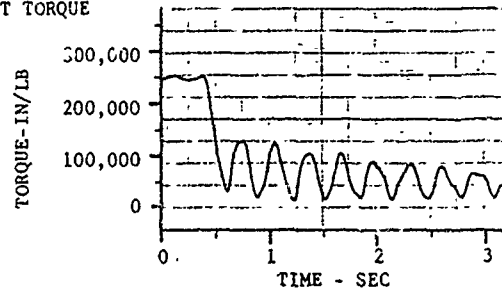HYBRID DATA

Counter Number: 92
Flight Number: 108A
Ship Number: 2503
Date: 5-27-72

ENGINE DELTA
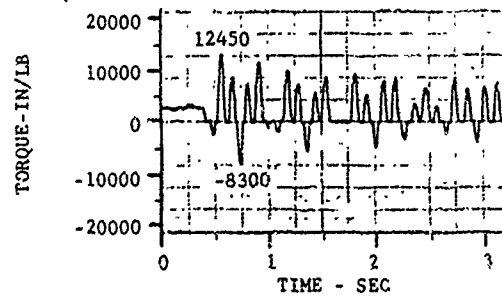TORQUE

MAIN ROTOR
MAST TORQUE
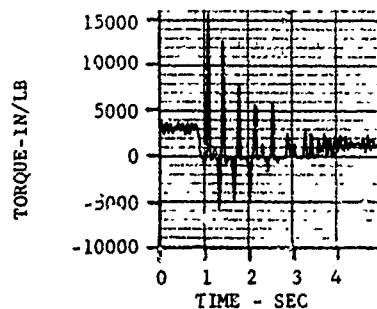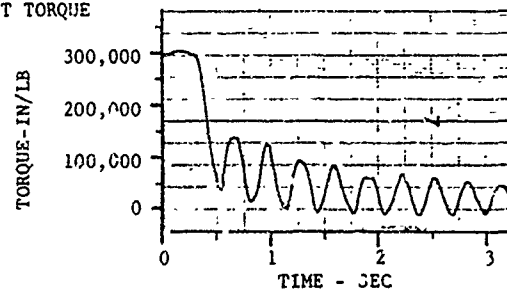
TAIL ROTOR
MAST TORQUE

Figure 7. Data Set IV - 150-Kpot Power Setting.

70

ATTACHMENT 1 TO APPENDIX E

FLIGHT TEST DATA

POWER TURBINE
TORQUE DECAY

HYBRID DATA

Counter Number: 93
Flight Number: 108A
Ship Number: 2503
Date: 5-27-72
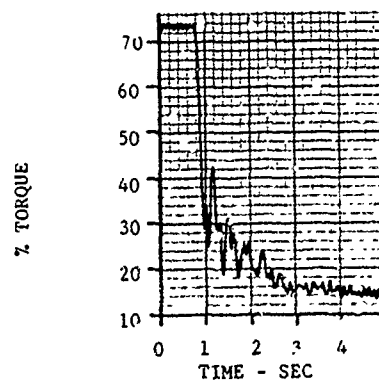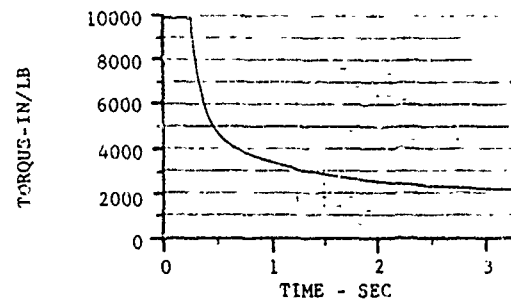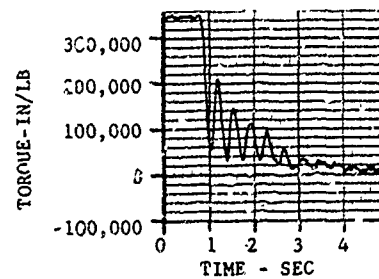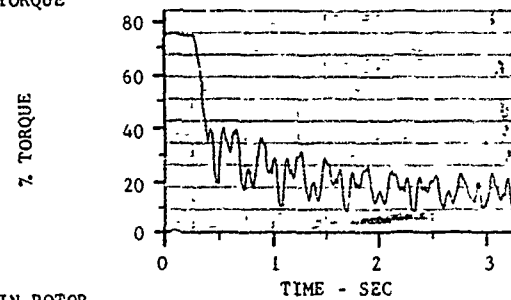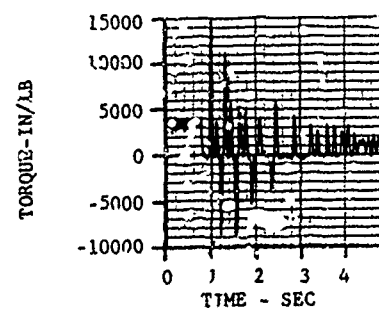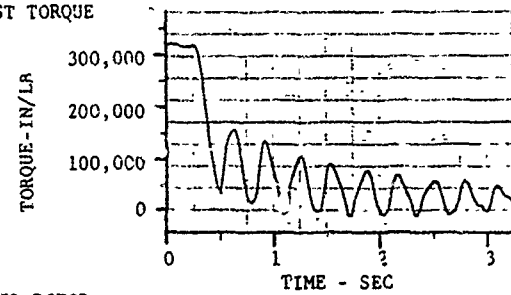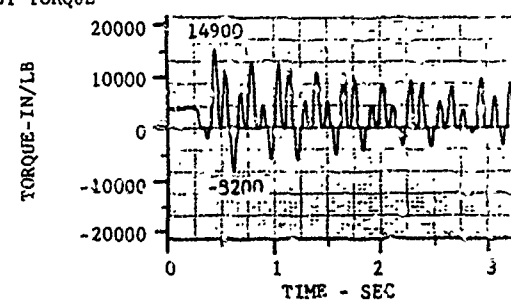
Figure 8. Data Set V — 153-Knot Power Setting.

FLIGHT TEST DATA

Counter Number: 94
Flight Number: 108A
Ship Number: 2503
Date: 5-27-72
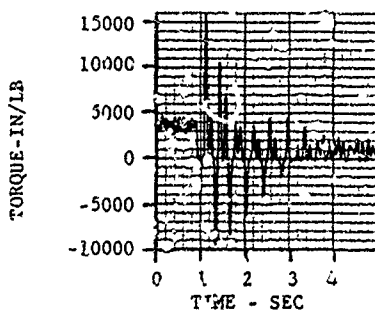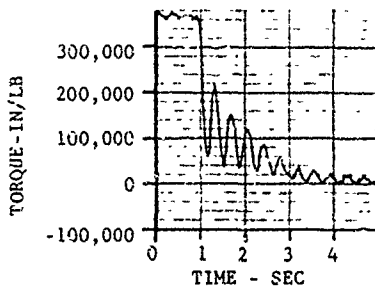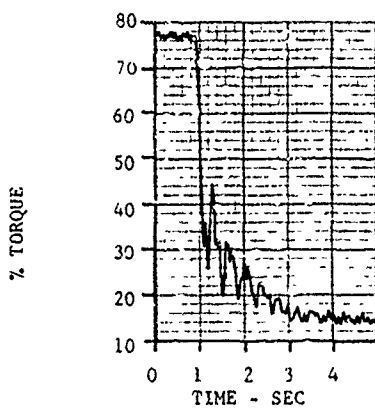
% TORQUE

TORQUE-IN/LB

TORQUE-IN/LB

POWER TURBINE
TORQUE DECAY

HYBRID DATA

TORQUE-IN/LB

ENGINE DELTA
TORQUE

% TORQUE

MAIN ROTOR
MAST TORQUE

TORQUE-IN/LB

TAIL ROTOR
MAST TORQUE

TORQUE-IN/LB
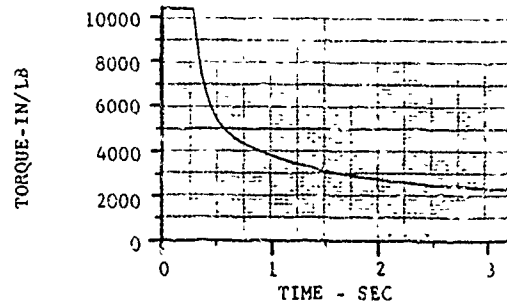
Figure 9. Data Set VI - 155.5-Knot Power Setting.

72

ATTACHMENT 1 TO APPENDIX E
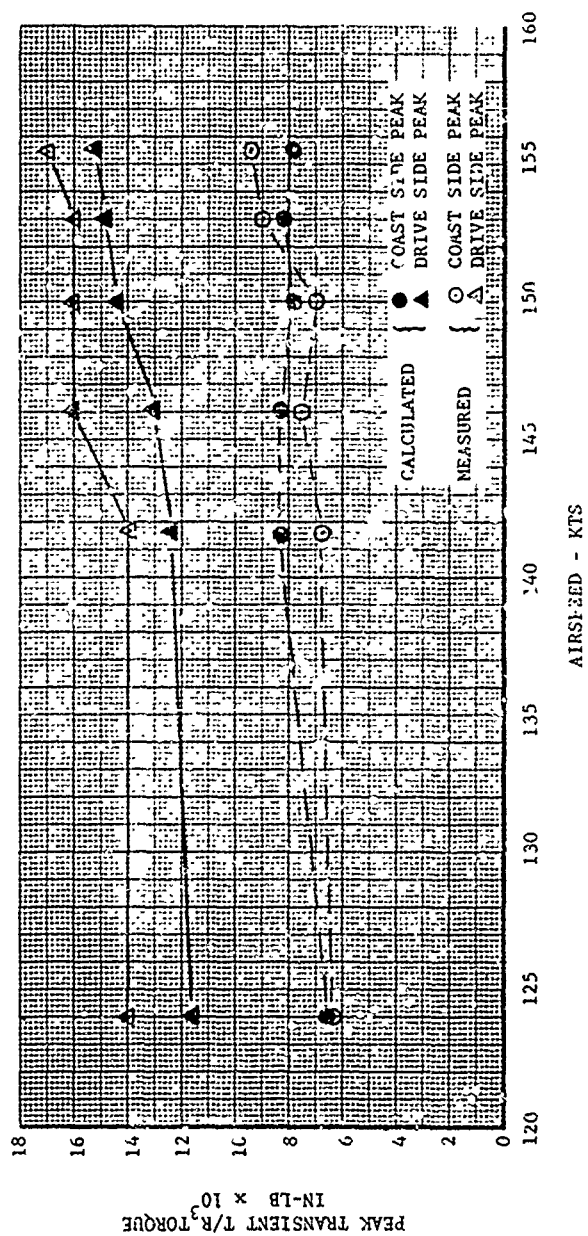
Figure 10. Comparison of Measured and Flight Test
Tail Rotor Torque Peaks

ATTACHMENT 1 TO APPENDIX E

ENCLOSURE 1 - DERIVATION OF CONSTANTS

I   Engine Aerodynamic Damping Equation
II   Main Rotor Aerodynamic Damping Equation
III   Tail Rotor Aerodynamic Damping Equation
IV   Tail Rotor Thrust Required Equation
V   Tail Rotor Collective versus Thrust Required Equation

I. Engine Aerodynamic Damping Estimation

The aerodynamic damping associated with the Model 309 was assumed to take the
form of

$$Q_{EA} = C_{14}N^2$$

where the terms are defined as

Q_{EA} =   the engine aerodynamic damping in in-lb torque

N =   the percent rpm

C_{14} =   a constant term

The constant C_{14} is derived by assuming the aerodynamic damping of the engines to be
equal to 10 percent of the engine torque at 100 percent rpm setting. Since at 100
percent rpm

Model 309

Engine HP = 2000
      RPM = 13148

$$Q_E = \frac{(63025)(2000)}{13148} = 9589.1 \text{ in-lb}$$

Since the damping is assumed = 10 percent

$Q_{EN} = 958.9$ in-lb @ 100% RPM

So, the constant C_{14} term can be found by

$$Q_{EA} = C_{14}N^2$$
$$C_{14} = Q_{EA}/N^2$$

$$C_{14} = \frac{958.9}{(100)(100)} = 0.09589 \text{ in-lb/%}$$

74

ATTACHMENT 1 TO APPENDIX E

II. Main Rotor Aerodynamic Damping

As with the engine, the main rotor aerodynamic damping was assumed to be a function of the percent rpm squared.

$$Q_{MRA} = C_{MR} N^2$$

where the terms are defined as

Q_{MRA} =   the main rotor aerodynamic damping

N =   the percent rpm

C_{MR} =   a constant term that varies with main rotor collective setting

At any particular main rotor setting, a corresponding value for C_{MR} can be found if the Q_{MRA} for 100 percent rpm is known.

$$C_{MRA} = \frac{Q_{MRA}}{(100)^2} = 1 \times 10^{-4} Q_{MRA}$$

This data is available from flight tests for the 309. Table E1 contains this data, along with the C_{MR} value for each data point.

In order to convert from HP to C_{MR} values, note that

$$Q_{MR'} = \frac{(63025)(HP)}{N_{MR}}$$

and

$$N_{MR} = \frac{N_{MR}}{100} N$$

But, referencing to engine system,

$$Q_{MR} = \frac{N_{MR}}{N_E} Q_{MR'}$$

then since

$$C_{MR} = \frac{Q_{MR}}{N^2}$$

$$= \frac{N_{MR}}{N_E} \frac{(63025)(HP)}{\left[\frac{N_{MR}}{100} N\right] N^2} = \frac{6302500 \ HP}{(NE)(N^3)}$$

75

where

N_E = RPM of engine

HP = horsepower absorbed by the rotor

Using this equation and the 309 parameters yields

Model 309

N_E = 13148

N = 100% (for data used)

$$C_{MR} = \frac{(6302500)(HP)}{(NE)(N)^3}$$

$$= \frac{6302500}{(13148)(1 \times 10^6)}(HP)$$

$$= (0.47935 \times 10^{-3})(HP)$$

The C_{MR} and collective setting values for each model were curve fit to the third degree equation

$$C_{MR} = C_1 \theta_{MR}^3 + C_2 \theta_{MR}^2 + C_3 \theta_{MR} + C_4$$

The constants are listed in Table I in the memo.

TABLE E1

Model 309

Collective Setting θ_o	Power HP	C_{MR}
14	1050	0.50299
15	1300	0.62280
16	1560	0.7474
17	1850	0.8863
18	2170	1.0396
19	2500	1.1979
20	2950	1.4074

ATTACHMENT 1 TO APPENDIX E

III. Tail Rotor Aerodynamic Damping

Again, the damping was assumed to be of the form

$$Q_{TRA} = C_{TR} N^2$$

where

Q_{TRA} = the tail rotor aerodynamic damping

N = the % rpm

C_{TR} = a constant term that varies with tail rotor collective setting

As with the main rotor, a value for C_{TR} corresponds to a fixed collective (tail rotor) setting. Model 309 data is available from flight tests. This data is given in Table E2, along with the calculated C_{TR}.

As with the main rotor, the data is in terms of absorbed HP and is converted to C_{TR} value as follows:

$$Q_{TR}' = \frac{(63025)(HP)}{N_{TR}}$$

and

$$N_{TR} = \frac{N_{TR}}{100} N$$

Referencing to the engine system

$$Q_{TR} = \frac{N_{TR}}{N_c} Q'_{TR}$$

Then with

$$C_{MF} = \frac{Q_{TR}}{N^2}$$

$$= \frac{N_{TR}}{N_E} \frac{(63025)(HP)}{\left[\frac{N_{TR}}{100} N\right] N^2} = \frac{(6302500)(HP)}{(N_E)(N^3)}$$

where

N_E = RPM of engine

HP = horsepower absorbed by the tail rotor

Again using the 309 parameters yields

77

ATTACHMENT 1 TO APPENDIX E

Model 309

N_E = 13148

N = 100%

C_{TR} = $\dfrac{(6302500)(HP)}{N_E \, N^3}$

= $(0.47935 \times 10^{-3})(HP)$

The C_{TR} and collective setting values for each model were curve fit to the third degree equation

$$C_{TR} = C_9 \theta_{TR}^3 + C_{10} \theta_{TR}^2 + C_{11} \theta_{TR} + C_{12}$$

The constants are listed in Table 1 in the memo.

TABLE E2

Model 309

Collective Setting ϵ_o	Power HP	C_{TR}
- 4	60	0.0297
- 2	36	0.0179
0	28	0.0140
2	28	0.0140
4	36	0.0174
6	54	0.0272
8	86	0.0461
10	138	0.0691
12	206	0.1004
14	288	0.1385

ATTACHMENT 1 TO APPENDIX E

IV. Tail Rotor Thrust Required

The inclusion of the tail rotor collective logic makes necessary the calculation of the tail rotor thrust required to counterbalance the main rotor torque. This is found by

$$T_{TR} = \frac{Q_{MRA}}{L}$$

where

T_{TR} = thrust of tail rotor

Q_{MRA} = main rotor torque

L = length from main rotor to tail rotor

Also, since Q_{MRA} is an engine referenced value and T_{TR} is non-referenced the equation is modified to be

$$T_{TR} = \frac{Q_{MRA}}{L} \cdot \frac{N_E}{N_{MR}}$$

so that

Model 309

$$T_{TR} = \frac{Q_{MRA}}{346.75} \frac{13148}{306}$$

$$= \frac{Q_{MRA}}{8.09}$$

*In memo, the constant in each of the above equations is referred to as C_{13} where

$$T_{TR} = \frac{Q_{MRA}}{C13}$$

79

V. Tail Rotor Collective versus Thrust Required

In order to complete the logic sequence, the tail rotor collective setting for a given required tail rotor thrust was necessary. The data, collective versus thrust, for the Model 309 is derived from flight tests. This information is in Table E3. The equation was of the form

$$\theta_{TR} = C_5 \, T_{TR}^3 + C_6 \, T_{TR}^2 + C_7 \, T_{TR} + C_8$$

where

$$\theta_{TR} \quad = \quad \text{tail rotor collective setting}$$

$$T_{TR} \quad = \quad \text{tail rotor thrust}$$

$$C_N \quad = \quad \text{constant terms}$$

*The constants are given in Table I in the body of the memo.

ATTACHMENT 1 TO APPENDIX E

TABLE E3

Model 309

Thrust Lb	Collective Setting
-400	-4.0
-300	-3.5
-200	-2.5
-100	-1.5
0	0.6
100	2.0
200	4.4
300	5.4
400	6.3
500	7.0
600	7.8
700	8.2
800	8.8
900	9.6
1000	10.2
1100	10.8
1200	11.4
1300	12.0
1400	12.6
1500	13.2
1600	13.8
1700	14.2
1800	14.6

APPENDIX F

SHAFT DYNAMIC LOADING ON ENGINE

BHT, under Contract DAAJ01-73-C-0741(P40), developed a proto-
type Advanced Attack Helicopter, the YAH-63, powered by twin
General Electric 700-GE-T700 engines with 20,000 rpm output
shaft speeds. The air vehicle vibration criteria dictated a
high degree of rotor force attenuation, which for the BHT two-
bladed main rotor design necessitated use of the focal pylon/
nodal beam isolation systems resulting in relatively high pylon
pitch, roll, and vertical oscillatory motions. To accommodate
these pylon motions required an input driveshaft coupling
design capable of relatively large misalignment and chucking
motions.

BHT has evaluated many coupling designs over the years, in-
cluding a Bendix diaphragm coupling and the Kaman Kaflex
coupling. For the YAH-63 program BHT investigated several
other coupling designs as described in Reference 5 (also see
Appendix H of this report). The combined requirements in
this application of rotational speed, torque, misalignment,
and chucking apparently exceed the capability of most coup-
lings. Thus, the BHT design employed crown tooth gear
couplings like those currently used on all BHT helicopters
in the field today.

During the proposal effort and prototype design stage of the
YAH-63, BHT and General Electric engineering personnel dis-
cussed the various interface considerations. One area of
particular concern, identified by both parties, was the steady
state and transient loading of the engine through the engine-
to-transmission shaft.

One problem encountered was that the initial engine installa-
tion drawing defined only static load limitations at the power
takeoff pad. There were not specifications to define the
oscillatory loading or the combinations of steady and oscilla-
tory loading allowed.

The second problem was that no data were available to BHT to
define the chucking forces and misalignment moments for crown
tooth gear couplings operating at 20,000 rpm. BHT had only

---

5.   Oradat, F. R., Hanson, H. W., and Alexander, R. M.,
     DEVELOPMENT OF SUPER-CRITICAL SHAFTING USING CROWN-TOOTH
     GEAR COUPLINGS, Bell Helicopter Textron Report 299-909-004,
     Fort Worth, Texas, 15 January 1976.

limited data on shaft chucking forces as a function of mis-
alignment angle, torque, and chucking amplitudes at speeds
up to 6000 rpm (Reference 6) but no data on shaft moments
generated by coupling misalignment.

An empirical relationship utilizing available data extrapolated
to the torques, speeds, and coupling diameter was formulated
to estimate the forces and moments occurring on the 20,000 rpm
YAH-63 floating driveshaft. Based on these empirical data,
BHT supplied GE with the maximum values expected for output
shaft chucking loads. Testing of driveshaft load actions and
coupling reactions during the YAH-63 development program
provided further empirical data refinements, somewhat reducing
the required output shaft loading envelope. Table F-1, taken
from Reference 7, shows an example of the coupling force and
moment data which was transmitted to GE. GE in return re-
viewed these data, evaluating the effect on the output pad
thrust bearing and the engine case, and ultimately accepted
the BHT values as compatible with the T700 engine design.
No design changes were made and no further action was taken.

Appendix G of this report describes the YAH-63 T700 engine
installation vibration characteristics and notes that the
fore-and-aft engine accelerations at the main rotor 2/rev
frequency may be due to the driveshaft axial chucking forces.

During this study, it became evident that such factors as
coupling radial clearance, tooth profile, shaft unbalance.
type and amount of grease, and high centrifugal field (rpm
and diameter) would have very significant effects on these
forces and moments. Thus, for future designs with stringent
vibration requirements, further research is needed to define
these parametric effects.

---

6. Puckett, J. D., RESULTS OF INPUT DRIVESHAFT CHUCKING
   FORCE INVESTIGATION ON UH-1 DRIVESHAFT, Bell Helicopter
   Textron Report 55865M-12, Fort Worth, Texas,
   15 December 1965.

7. Hanson, H. W., and Oradat, F. R., DRIVE SYSTEM ANALYSIS,
   ADDENDUM A: 409-140-025 INPUT DRIVESHAFT INSTALLATION
   CRITICAL SPEED ANALYSIS, Bell Helicopter Textron Report
   409-940-001, Fort Worth, Texas, 17 November 1975.

The effects of these forces and moments impact upon:

1. The engine output pad thrust bearing capacity and other engine components.

2. Engine mount loading.

3. Vibratory engine environment relative to the installation limits (Appendix G).

4. The transmission input quill design.

5. The capability of the rotor/pylon isolation system to function as designed, thus impacting on crew comfort and component reliability.

TABLE F-1. 20,000 RPM OUTPUT SHAFT COUPLING MISALIGNMENT AND CHUCKING REACTION CAPABILITY AT THE MAIN ROTOR PYLON 2/REV (9.6 HZ) FREQUENCY

G's	Speed %V_H	Amp ± IN.	Misalign, deg Min	Misalign, deg Max	Time Percent	Shaft HP	Axial Force lb Mean	Axial Force lb ± Osc	Radial Force lb Mean	Radial Force lb ± Osc	Moment lb-in. Mean	Moment lb-in. ± Osc	Friction Coeff.
ENGINE COUPLING													
1	0	.106	.467	.615	33.00	725	26	11	3	3	45	3	.018
1	0.6	.246	0	.503	4.95	500	119	116	7	4	93	93	.195
1	0.7	.219	.351	.844	14.12	594	29	31	5	1	64	18	.040
1.25	0.7	.275	.478	1.011	3.69	594	33	31	4	1	57	13	.032
1	0.8	.173	0	1.273	10.25	850	187	190	10	7	151	151	.194
1.50	0.8	.361	.622	1.831	2.84	350	35	49	4	2	61	29	.029
2	0.9	.288	.687	1.298	10.69	1200	45	36	6	2	80	20	.023
1.75	0.9	.507	.966	2.733	8.68	1200	41	70	5	3	73	47	.028
1	1.0	.317	.897	1.639	8.80	1355	45	41	5	2	79	24	.021
1	1.2	.409	.971	2.100	2.98	1355	45	56	5	3	80	36	.024
1.8	0.6	.362	0	1.331	0	1000	202	205	14	14	165	165	.181
1.8	0.6	.393	0	1.354	0	1150	257	253	20	15	209	209	.201
2.12	0.9	.043	0	2.954	0	1355	100	100	8	7	86	86	.071
TRANSMISSION COUPLING													
1	0	.106	.700	1.016	33.00	725	20	12	3	0	35	5	.015
1	0.6	.246	.451	1.355	4.95	500	27	31	7	4	46	17	.033
1	0.7	.219	.517	1.267	14.12	594	27	27	5	1	47	15	.027
1.25	0.7	.275	.678	1.641	3.69	594	24	33	4	1	42	17	.027
1	0.8	.173	.703	2.013	10.25	850	31	48	10	7	54	28	.026
1.5	0.8	.301	1.035	3.762	2.84	850	22	47	4	2	38	24	.020
1	0.9	.288	1.017	2.133	10.69	1200	30	38	6	2	52	33	.017
1.75	0.9	.507	1.601	4.106	8.68	1200	22	61	5	3	38	31	.025
1	1.0	.317	1.589	2.740	8.80	1355	25	41	5	2	45	23	.014
1	1.2	.409	1.535	3.432	2.98	1355	24	51	5	3	43	29	.015
1.8	0.6	.342	0	1.329	0	1600	195	196	11	14	159	159	.174
1.8	0.6	.372	0	1.354	0	1150	247	243	17	17	201	201	.194
2.12	0.9	.798	0	2.856	0	1355	648	689	47	47	558	558	.458

APPENDIX G

INSTALLED VIBRATION IN EXCESS OF ENGINE LIMITS

BHT, under Contract DAAJ01-73-C-0711 (P40), developed a proto-
type Advanced Attack Helicopter, the YAH-63. The RFP required
a twin-engine installation using 700-GE-T700 engines, GFE-
supplied. An isometric view of the engine installation is
shown in Figure G-1.

To evaluate the coupled interaction between engine mounting
frequencies and elastic engine bending modes, combined with
both rigid and flexible input driveshaft modes, BHT conducted
a NASTRAN analysis of the engine installation during the propo-
sal effort of the program (Reference 8). Bending and torsional
stiffness distributions for the T700 case, as well as the
weight distribution for the basic engine, were provided by GE.
The analytical model is shown in Figure G-2.

Later, during the contract development program, the analytical
model was refined to include influence coefficient type infor-
mation provided by GE, which defined engine case localized
structure stiffness from the engine centerline to the mount
attachment points, and for the engine output shaft bearing
support.

Engine mounting frequency parametric studies were initially
conducted by simultaneously varying the spring rates of the
fuselage mounting points to determine the minimum acceptable
values for fuselage structure design requirements. Later,
mounting spring rates were determined from the fuselage 3-D
NASTRAN model (References 9 and 10) and used in the engine
simulation.

---

8. ADVANCED ATTACK HELICOPTER SYSTEM, SUBSTANTIATING TECHNICAL
   DATA: STRUCTURE AND DYNAMICS, Bell Helicopter Textron
   Report 409-199-006, Fort Worth, Texas, 15 February 1973.

9. Cronkhite, J. D., and Hanson, H. W., PRELIMINARY AIR
   VEHICLE VIBRATION REPORT FOR THE MODEL YAH-63 HELICOPTER,
   Bell Helicopter Textron Report 409-930-003, Fort Worth,
   Texas, November 1974.

10. Brunken. J. E., PROTOTYPE AIR VEHICLE VIBRATION ANALYSIS
    FOR THE MODEL YAH-63 HELICOPTER, Bell Helicopter Textron
    Report 409-930-019, Fort Worth, Texas, February 1976.

Paralleling this effort, GE obtained mounting data from BHT and conducted a similar analysis using the VAST structural analysis computer program.

Both the BHT and the GE analyses predicted no serious problems except for two rigid body engine mounting modes near the main rotor 4/rev frequency at 18.4 Hz. The BHT and GE analytical results are compared in Table G-1.

Further parametric studies conducted by BHT indicated that stiffening of the aft engine mount outboard support structure would improve the frequency margin relative to 4/rev and would require approximately 1 pound of added weight.

The concern and the available fixes were discussed by BHT and GE engineering teams. It wa decided that no structural changes would be made prior to acquiring flight test data, but that GE would monitor engine vibrations during developmental testing at BHT.

Subsequently, as a part of the joint engine interface document, a preliminary shake test was conducted by GE on the T700 installation in the YAH-63. The purpose of the test was two-fold· to define the natural frequencies of engine-mounted accessories, and to define the engine installation mounting frequencies.

Toward the end of the YAH-63 development program, BHT conducted a total system vibration test (Reference 11) which further documented the measured engine installation mounting frequencies.

Both the GE and the BHT vibration tests showed no significant problems related to engine-mounted accessories. The measured engine mounting frequencies are compared in Table G-2.

As a further requirement of the YAH-63 contract, an engine vibration and stress survey and an engine vibration demonstration (Reference 12) were conducted by BHT to define the induced engine vibration and stress environment for all speeds and power conditions of the helicopter operational envelope. The results of the tests showed the predominant engine vibrations

11. Killion, S. W., and White, J. A., TOTAL SYSTEM VIBRATION SURVEY FOR THE YAH-63 ADVANCED ATTACK HELICOPTER, Bell Helicopter Textron Report 409-909-009A, Fort Worth, Texas, 28 June 1976.

12. Killion, S. W., ENGINE VIBRATION AND STRESS SURVEY AND ENGINE VIBRATION DEMONSTRATION FOR THE YAH-63 ADVANCED ATTACK HELICOPTER, Bell Helicopter Textron Report 409-909-008B, Fort Worth, Texas, 25 June 1976.

to be, in general, in the 2/rev axial and 4/rev lateral direc-
tions. Although some vibration levels exceeded the GE speci-
fied engine installation limits (exceedances were less than
8% of the design flight spectrum), the corresponding stress
levels were low. Thus, the engine installation was considered
acceptable for the GCT air vehicle configuration and flight
envelope for AEFA testing and fly-off competition.

As a result of the engine vibration analysis and tests con-
ducted by both GE and BHT, GE proposed new engine installation
vibration limits as summarized in Table G-3. None of the
measured engine vibration levels exceeded the proposed limits.
These new proposed engine vibration limits were submitted
to the Army SSEB* for approval as an acceptable contractual
deviation.

Just prior to the fly-off competition, BHT conducted static
tests on the aft engine mount outboard support structure,
then added a strut brace (Figure G-3) and repeated the test.
The load-deflection results (Figure G-4) showed that the
addition of the strut increased the mount vertical stiffness
by a factor of approximately four. Although some improvement
was made, this change did not bring the engine vibration
levels within the current installation limits. However,
this failure to achieve acceptable levels may have been (to
a significant degree) caused by a combination of main rotor
induced 4/rev of nominal to moderately high levels combined
with a strong main rotor mast lateral bending mode near 4/rev.
Frahm absorbers mounted on the pylon were used to partially
absorb these vibrations, thus reducing the transmissibility
to the fuselage and ultimately to the engines. Stress levels
in the engine mounts were significantly reduced by these
methods to obtain the desired mount life characteristics
such that additional efforts to further reduce engine vibra-
tory levels were curtailed. The AEFA flight tests conducted
by the Army were flown with this revised mount support
structure.

Meanwhile, during the proposal evaluation, the Army rejected
the proposed change in engine vibratory limits, presumably on
the basis that this would give BHT an unfair advantage in the
overall competition evaluation.

For the production aircraft, BHT plans called for improved
pylon isolation characteristics, accomplished by changes in
main rotor pylon geometry and mast height, resulting in

---

*U. S. Army Source Selection Evaluation Board (SSEB).

reduced 2/rev and 4/rev engine excitation amplitudes. The aft engine mount was also to be redesigned (Figure G-5), combined with additional airframe backup structure stiffness increases, to provide the additional dynamic stiffness requirements in both the lateral and vertical directions necessary to raise the first natural frequency of the engine installation significantly above the main rotor 4/rev frequency to preclude excessive induced engine vibration.

The YAH-63 program was subsequently contractually terminated and the anticipated results due to proposed design changes were never confirmed.

89

Aft engine mts (Ref)

RH engine

Trunnion fitting

Aft

Fwd

LH engine

Tube assembly

Aft

Engine mount fitting

LH edge of work deck

Trunnion fitting

Fwd

Engine mount fitting installation

RH edge of work deck
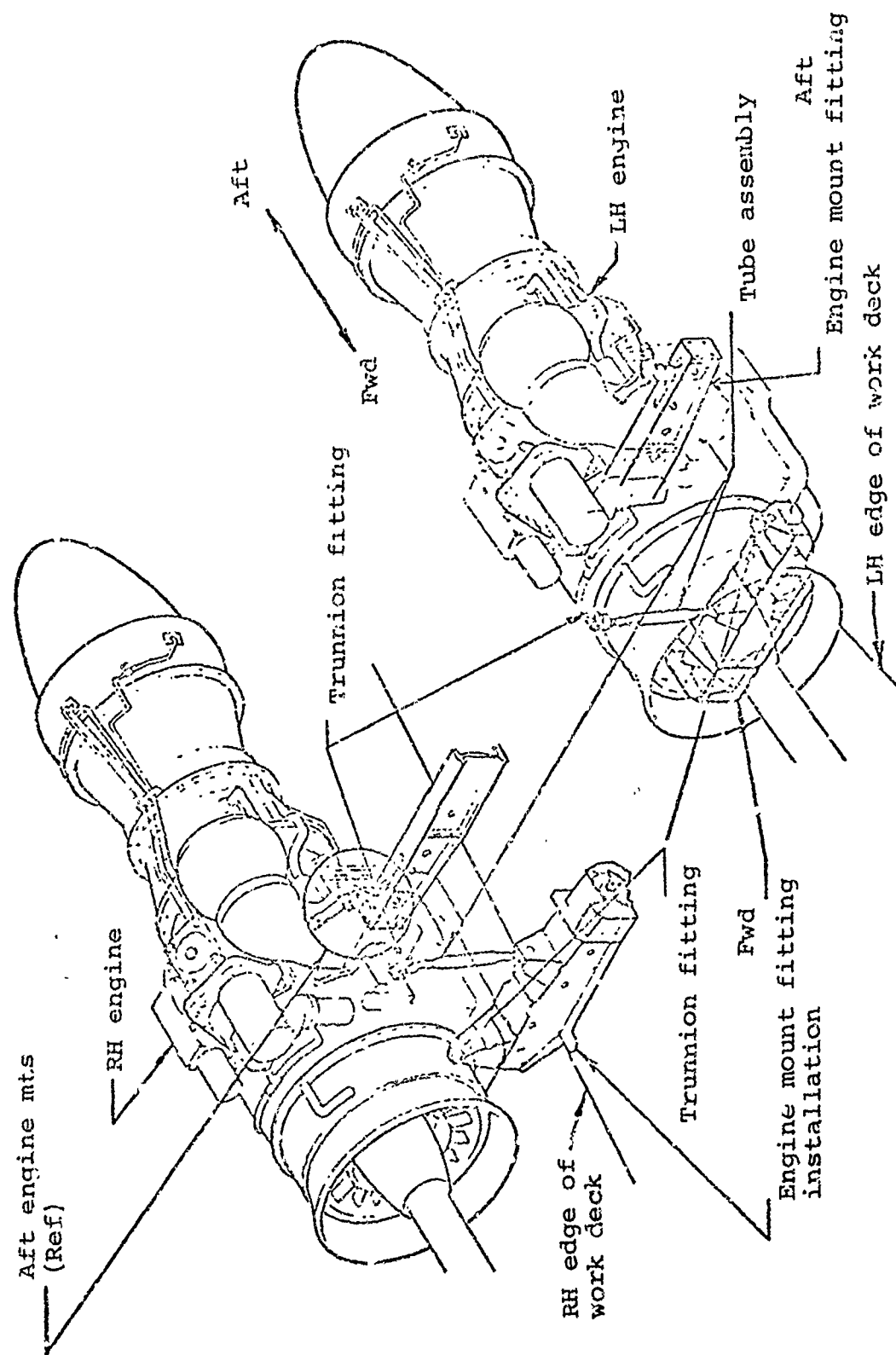
Figure G-1. YAH-63 engine installation.

90
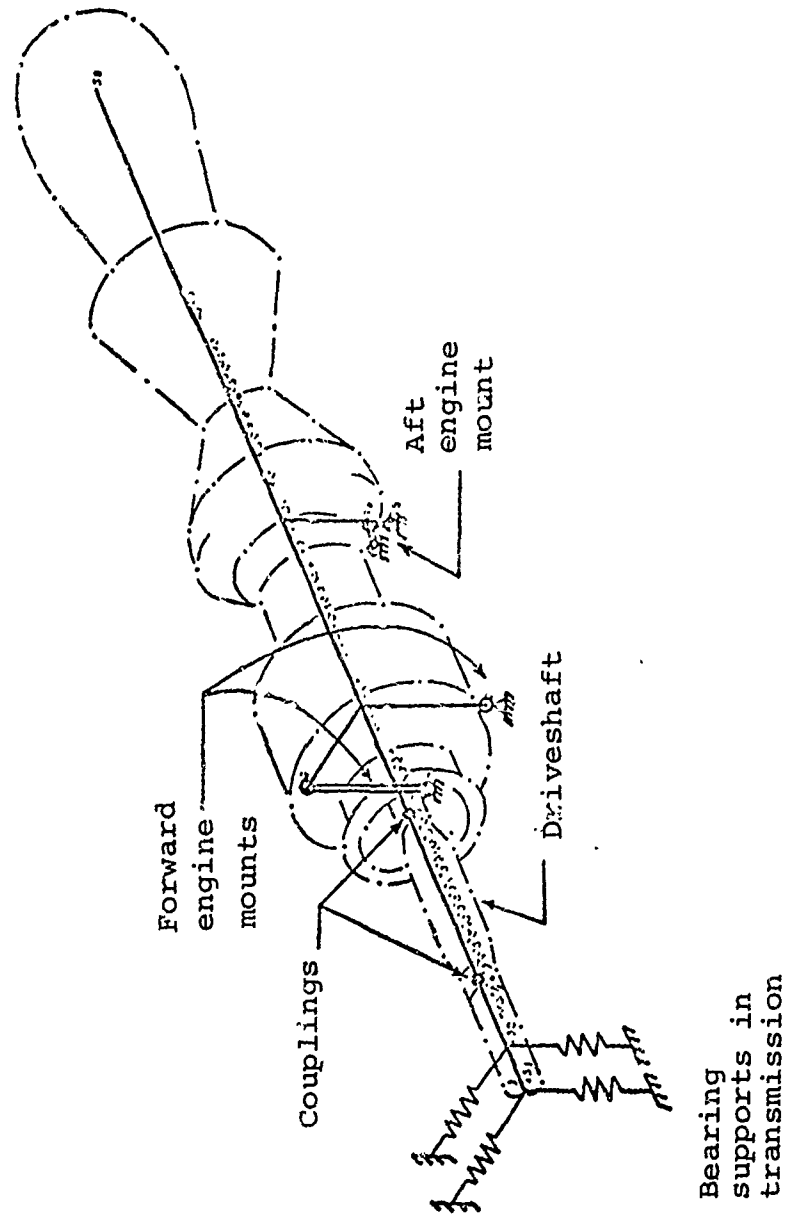
Figure G-2. NASTRAN model of engine and engine mounting.

IR suppressor

Aft
engine
mount

Forward
engine
mounts

Driveshaft

Couplings

Bearing
supports in
transmission

TABLE G-1. COMPARISON OF BHT AND GE ANALYTICALLY PREDICTED ENGINE INSTALLATION NATURAL FREQUENCIES

	BHT analysis	GE analysis	GE analysis	BHT analysis
	Elastic engine on mount springs	Elastic engine on mount springs	Rigid engine on mount springs	Rigid engine on elastic airframe
First Engine Installation Mode	19.2 Hz	17.5 Hz	19.1 Hz	17.0 Hz
Second Engine Installation Mode	21.5 Hz	19.7 Hz	21.3 Hz	18.6 Hz

TABLE G-2. COMPARISON OF BHT AND GE MEASURED ENGINE INSTALLATION NATURAL FREQUENCIES

	GE Preliminary shake test	BHT Total system vibration survey
First Engine Installation Mode	15.9 Hz	17.5 Hz
Second Engine Installation Mode	19.1 Hz	---

TABLE G-3. CURRENT AND PROPOSED ENGINE VIBRATION LIMITS

| Measured parameter (direction) | Vibration limits (in/sec) frequency band | | | | | | Steady state exceedance time limit (sec) |
| | (0-50 Hz) | | (25-50 Hz) | | (50-800 Hz) | | |
	Steady state	Tran- sient	Steady state	Tran- sient	Steady state	Tran- sient	
Current vibration limits							
Vertical/Lateral	5.0	7.0	N.A.	N.A.	2.5	3.5	5.0
Axial	2.5	5.0	N.A.	N.A.	N.A.	N.A.	5.0
Proposed vibration limits							
Vertical/Lateral	7.0	14.0	3.5	7.0	2.5	3.5	10.0
Axial	3.5	6.0	N.A.	N.A.	N.A.	N.A.	10.0

N.A. - Not Applicable

93

Phase 1 engine mount
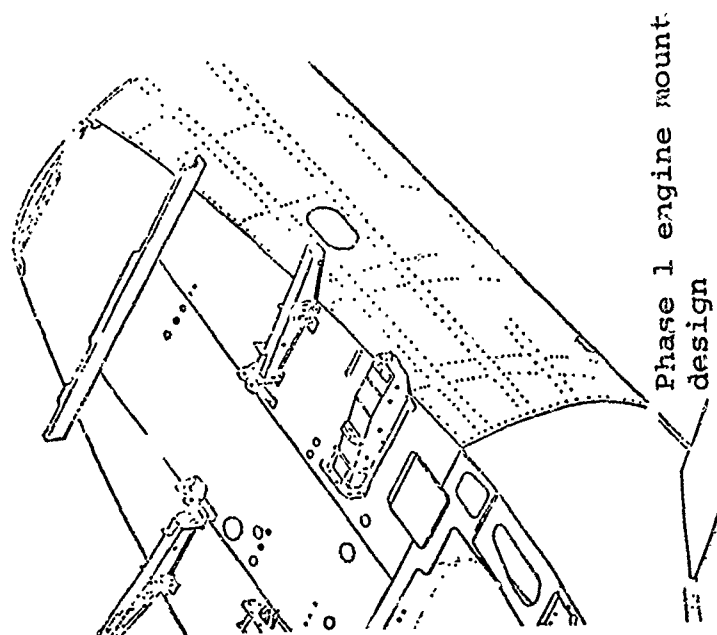design with aft
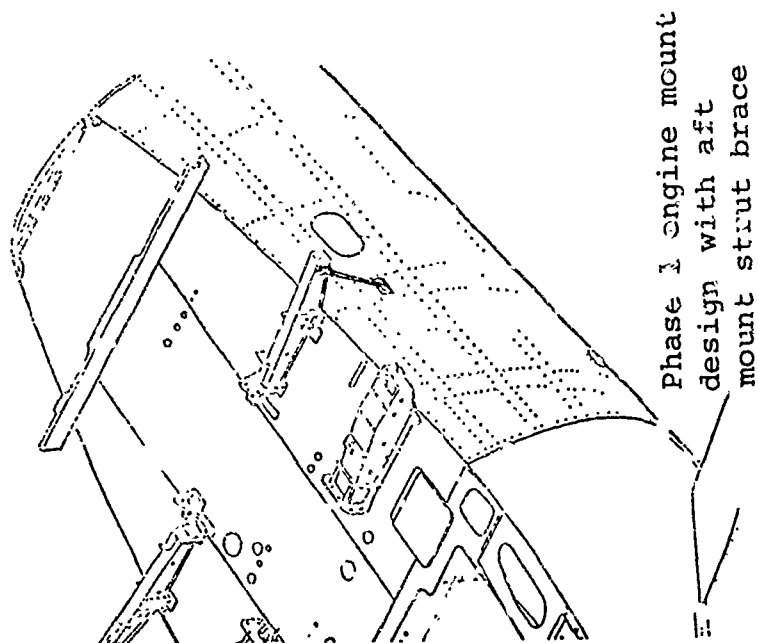mount strut brace

Phase 1 engine mount
design

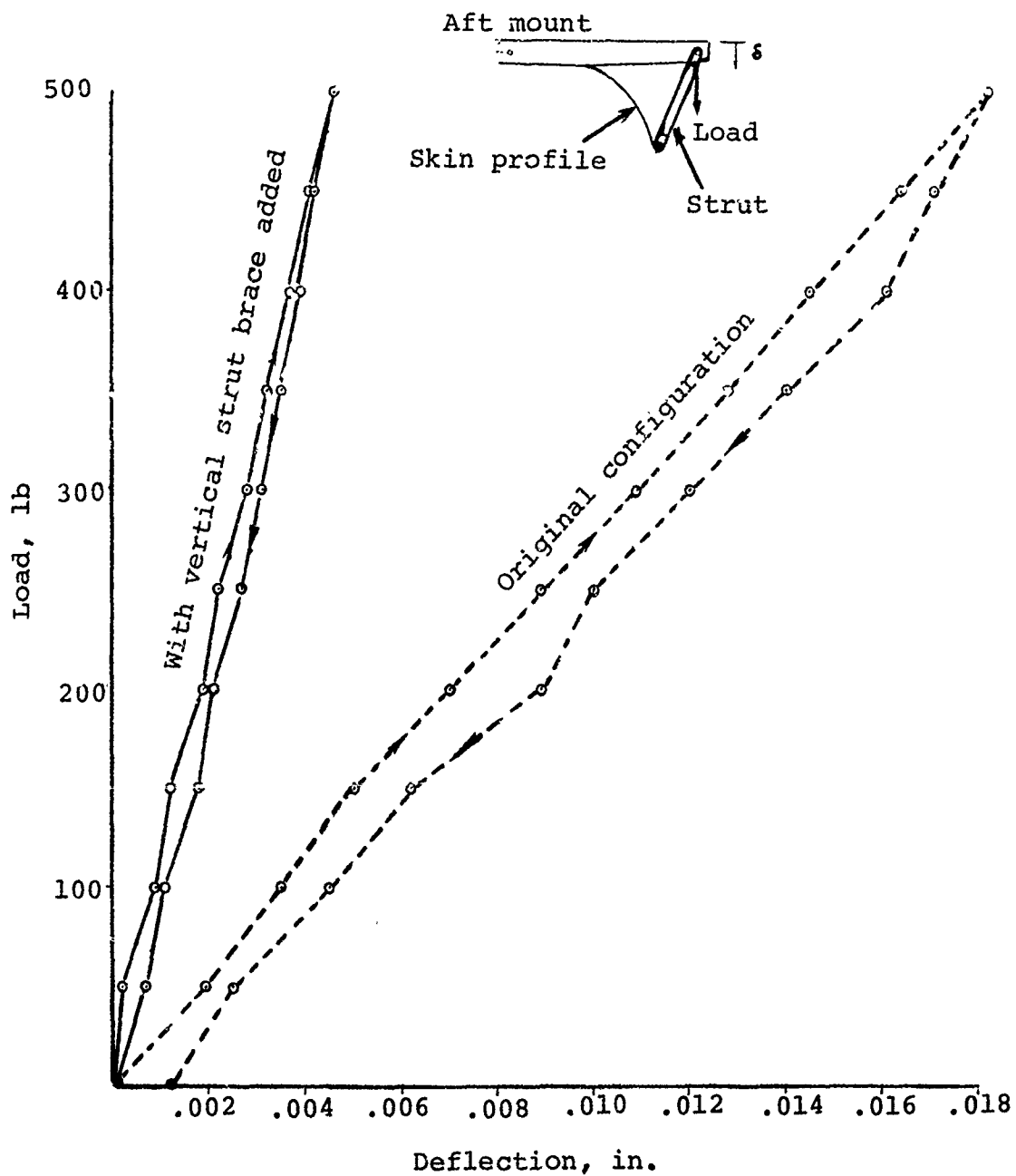Figure G-3. Aft engine mount strut brace modification.
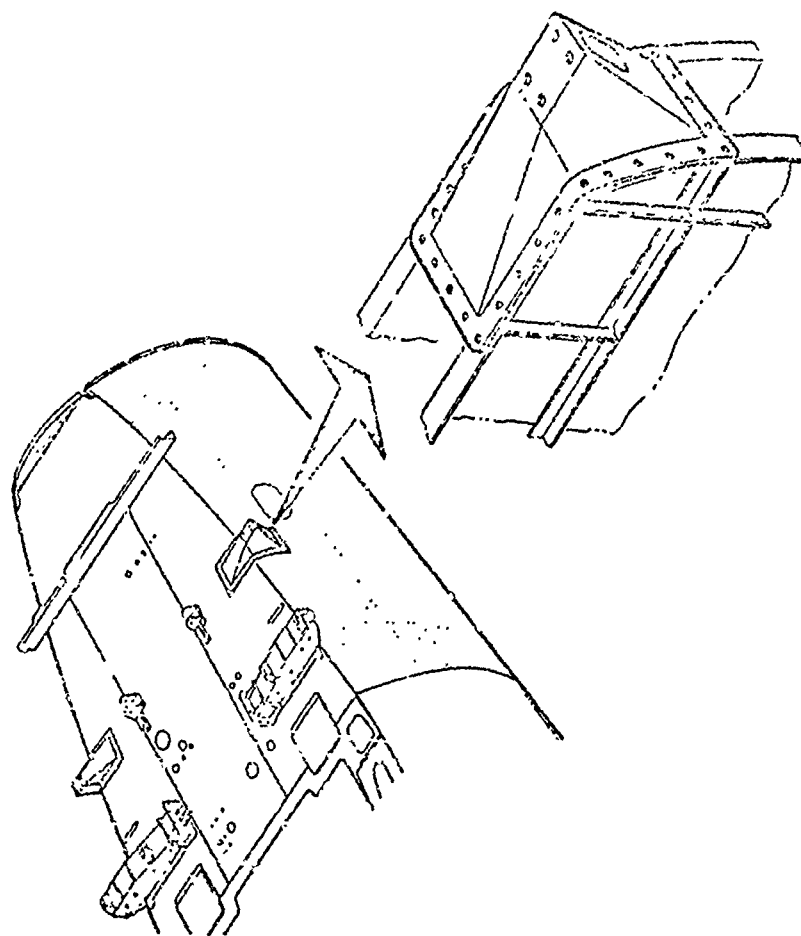
94

Figure G-4. Aft engine mount load-deflection data.

Figure G-5. Proposed design modification of aft engine mount.

APPENDIX H

DESTRUCTIVE SHAFT WHIRL OF 20,000 RPM
ENGINE-TO-TRANSMISSION DRIVESHAFT

Advancements in the state of the art of turbine engine tech-
nology led to the development of the 1500 shp Advanced Tech-
nology Engine (ATE) for helicopters: the General Electric
700-GE-T700 engine. During the preliminary design phase of
this program, the competing engine manufacturers obtained in-
puts from the various AVM's. One question was with regard to
the desired output speed. The majority of the requests were
for high output speed on the order of 20,000 rpm. One ratio-
nale for the choice of a high-speed output was that of deliver-
ing power from the engine at high speed and combining all speed
reduction into a single gearbox for weight and cost savings.
Unfortunately, these recommendations were not fully evaluated
in terms of dynamic considerations of vibration and stability.

In early 1973, BHT submitted a proposal to the Army as an
entry into the Advanced Attack Helicopter (AAH) competition
and was awarded a contract for the development program.

The approach of a high-speed output, coupled with the AAH vi-
bratory limits for crew comfort and component reliability, and
the selected vibration isolation system, resulted in a floating
shaft employing crown tooth couplings (see Appendix F).

The combination of these requirements compounded some design
deficiencies and resulted in destructive shaft whirl. A sig-
nificant slippage of the development program schedule - and,
no doubt, a significant impact on cost - resulted.

Attachment 1 to this appendix traces the shaft development
program from initial design, design changes contemplated,
design modifications explored by analysis, design, fabrica-
tion and testing, and finally to the final configuration.
The significant highlights of the program are presented in
the following paragraphs.

For the proposal (Reference 8) BHT conducted a NASTRAN analysis
to evaluate the coupled interaction between engine mounting
frequencies and elastic engine bending modes, combined with
both rigid and flexible modes of the engine-to-transmission
input driveshaft.

97

After receipt of the Phase 1 contract, BHT refined the analysis
to include detailed design parameters and engine bearing spring
rate data provided by GE. Similarly, GE obtained shaft dynamic
parameters from BHT and conducted a parallel analysis which was
submitted to BHT. Both analyses showed two rigid body drive-
shaft modes, one at the engine end in the proximity of 10,000
rpm and one on the transmission end near 15,000 rpm. Both
analyses also showed the transmission end mode to have signi-
ficant deflection occurring on the support bearings and
within the input quill shafting.

Shortly after the completion of these analyses the input shaft
coupling test was initiated on the 409-140-033 driveshaft design.
The first shaft failure occurred at approximately 14,000 rpm
during the first run-up. Subsequent development tests resulted
in five additional failures of the shaft assembly.

The first failure, wherein the female coupling disintegrated,
initiated an intense investigation and development program to
develop a satisfactory shaft design.

Perhaps one of the most significant outcomes of this development
program for BHT was the investigation into the mechanism of
nonsynchronous shaft whirl instability. Since the shaft
bending modes showed acceptable margins above the shaft operating
speed, whirl instabilities of the rigid body shaft modes
had not been considered previously in terms of a supercritical
installation.

Many references were studied to gain an insight into the non-
synchronous whirl phenomenon. All references concurred that
the mechanism of nonsynchronous whirl instability comes about
due to the internal friction in a supercritical rotating system.
With a floating shaft/spline tooth coupling design, the rigid
body shaft modes can produce this internal sliding friction
which can become quite high and, in fact, nonlinear with higher
friction at higher coupling misalignment angles. Another poten-
tial source of internal friction in the shaft design is clamped
joints and shrink fits.

With the supercritical shaft instability mechanism thus iden-
tified, it was important to achieve a balance in the amount
of external damping to control the shaft displacement and trans-
mitted force. A squeeze-film damper was found to be an effec-
tive method of supplying significant external damping in the
fixed system. It serves both the purposes of reducing one-per-
rev response to shaft unbalance when traversing system natural
frequencies and damping nonsynchronous whirl for supercritical
shaft operation.

BHT engineers developed a prototype squeeze-film damper design which was laboratory tested to evaluate and establish the final design parameters necessary for the particular requirements of the YAH-63 driveshaft installation. The success of these tests led to a squeeze-film damper design which could be integrated directly into the bearing support of the transmission input quills. Only the transmission end was developed since there was already a squeeze-film damper for the engine end power turbine shaft in the nose of the T700 engine. Concurrent with the squeeze-film damper development was a concentrated effort to improve the stability of the driveshaft assembly clamped joints and shrink fits. Significant design considerations are summarized in Table H-1.

The final shaft design, designated the 409-140-025-1, was then submitted to excessive endurance laboratory testing before installation into the air vehicle. After installation, the displacement response of the couplings was monitored in real time during ground runs and flight tests using a real-time spectral analyzer. No indication of shaft nonsynchronous whirl was noted.

In conclusion, the supercritical 20,000 rpm input shaft operating under fairly large coupling misalignment and chucking criteria produced a severe design environment, both from vibration and stability viewpoints. The failures encountered during the shaft development program pointed out the need for very fine balance control in tolerances and assembly procedures, stable clamp-up joints, and sufficient external damping for vibration and stability control. It is questionable from the data whether the damper was needed once the balance control and joint stability features were refined. However, it is unquestionable that the damper helped reduce vibration levels due to transiting rotating system resonances, instilled confidence in the design, and made the supercritical input shaft a viable design option for helicopters. More detailed documentation of the BHT supercritical driveshaft development program can be found in Reference 5.

Experience with the YAH-63 20,000 rpm shaft demonstrated acceptable performance and the system completed all Army tests successfully.

TABLE H-1. SUMMARY OF DESIGN CHANGES CONSIDERED

Item	Design change/rationale	Action				
		Consideration only	Design	Analysis	Test	Adopted
1	Change female coupling to more ductile material; may be too brittle		x		x	x
2	Conduct detailed analysis of Hoope's stresses in female coupling	x				
3	Redesign or eliminate centering spring; may be unstable when compressed under centrifugal force		x		x	x
4	Remove scallops around flange of female coupling; improve balance		x		x	x
5	Stiffen cone adapter and increase cone angle; flexibility is contributing to low shaft critical speed		x	x	x	x
6	Preload duplex bearing supporting transmission input quill		x	x	x	
7	Change shaft design; invert to put female coupling on floating shaft and male coupling on quill shaft		x	x	x^1	

100

TABLE H-1. - Continued

Item	Design change/rationale	Consideration only	Design	Analysis	Test	Adopted
8	Change coupling design; eliminate crown tooth coupling		x	x	x^2	
9	Change method of clamping cone adapter to shaft; failure mode indicates flanged nut to be inadequate		x	x	x	x
10	Place shaft mode above 26,000 rpm by stiffening shafts and bearings; eliminate supercritical operation with low damping			x		
11	Change tooth profile and or tooth design of crown tooth coupling		x	x	x	
12	Add external damper using elastomeric shear pad; added damping would permit transition through critical speed				x^3	

101

TABLE H-1. - Continued

Item	Design change/rationale	Consideration only	Action Design	Analysis	Test	Adopted
13	Add squeeze-film damper (SFD) behind duplex bearing supporting transmission input quill; SFD on engine end does good job of controlling response of first mode		x	x	x	x
14	Change duplex bearing supporting input quill to triplex bearing with light preload; stiffens support and reduces radial run-out		x	x	x	x
15	Lubricate threads of bolt clamping cone adapter to shaft; attempt to get best clamp-up possible				x	x
16	Add double piloted splines at cone adapter/quill shaft interface; provide improved stability, reduce radial run-out		x	x	x	x
17	Beef-up input quill shaft; stiffens adapter support		x	x	x	x

102

TABLE H-1. - Concluded

Item	Design change/rationale	Consideration only	Action			
			Design	Analysis	Test	Adopted
18	Add nose reduction gearbox, reduce shaft speed tc 8000 to 10,000 rpm; eliminate supercritical operation relative to second mode		x	x		
19	Change guillotine seal to grease dam seal; eliminate possible nonsynchronous whirl of seal		x		x	x
20	Change radial clearance between male and female coupling; reduce radial run-out		x		x	x
21	Index components; reduce radial run-out		x		x	x
22	Tighten manufacturing tolerances; reduce potential unbalance, reduce radial run-out		x		x	x
23	Dynamically balance components; reduce unbalance forces		x		x	x

[1]Shake test only
[2]Nonrotating static test only for evaluation of misalignment/torque capability
[3]Small-scale lab model only

103

ATTACHMENT 1 TO APPENDIX H

HIGH-SPEED SHAFT DEVELOPMENT
FOR HELICOPTERS

R. W. Balke, Group Engineer, and
J. M. Bilger, Senior Engineer
Structural ·Dynamics
Bell Helicopter Textron
Fort Worth, Texas

Abstract

Advancements in the state of the art of turbine-engine technology led to the development of the 1500 shp Advanced Technology Engine (ATE) for helicopters. One objective, that of delivering power from the engine at high speed and combining all speed reduction into a single gearbox resulted in an output shaft speed of 20,000 rpm. This approach, coupled with the current helicopter specification vibratory limits for crew comfort and component reliability, and the selected vibration isolation system, resulted in a floating shaft employing crown tooth couplings on a recent Bell Helicopter Textron (BHT) helicopter design.

This paper describes initial design and testing of the floating shaft, which resulted in coupling failures. Development of the final design configuration included critical speed and nonsynchronous whirl stability analyses, system nonrotating vibration tests, tightening of manufacturing and assembly tolerances, and the development of a squeeze film damper for the transmission input quill. Data from high-speed full-scale bench testing, laboratory testing of squeeze film dampers, NASTRAN frequency analysis, and a discussion of nonsynchronous whirl are presented. Actual operational experience with a developmental design is also described. This development program illustrated the importance of considering the effects of shaft rigid-body critical speeds as well as the classical shaft-bending critical speeds on response to unbalance and nonsynchronous whirl stability.

Introduction

During the preliminary design stages of the 1500 horsepower advanced technology engine, a survey of air vehicle manufacturers reflected a preference for a relatively high-speed power output shaft compared with that of the then existing helicopter engines. One strong rationale for this choice was to combine all or at least the majority of the gear reduction in one gearbox, thus permitting a weight and power

savings in the shafting, gearing, and gearboxes. This development led to the first production ATE: the 700-GE-T700 engine, with an output shaft speed of 20,000 rpm.

The first two helicopter design competitions using this engine, the Utility Tactical Transport Aircraft System (UTTAS), and the Advanced Attack Helicopter (AAH), reflected a requirement that the dominant harmonic vibrations of crew and equipment areas must be less than ±0.05g up to cruise velocity (V_{CR}).

The Bell Helicopter Textron (BHT) entry in the AAH competition utilized a two-bladed semi-rigid rotor. To isolate the rotor forces from the fuselage in order to meet the vibration requirements, the BHT-developed NODAMATIC system, Reference 1, which combines a focal pylon for isolation of inplane forces and a nodal beam for isolation of vertical forces, was chosen. The isolation system configuration is shown in Figure 1. The use of an isolation system between the main transmission and the airframe, and the selected location and geometry of the dual engine inputs combined with the prescribed motions of the transmission, dictated a shafting design which could accommodate large steady state misalignments -- up to 4 degrees for the forward coupling, and 2.5 degrees for the aft coupling -- combined with large axial chucking up to ±1.13 inches.
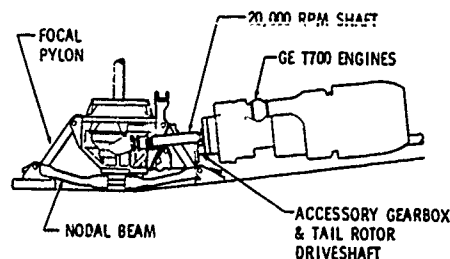

Figure 1. YAH-63 Installation and Isolation System

Presented at the 33rd Annual National Forum of the American Helicopter Society, Washington, D.C., May 1977.

1

Initial Shaft Design

The initial design, Figure 2, features a direct drive from engine to transmission using a 20,000 rpm floating shaft, and crown tooth geared couplings at each end to accommodate the required misalignment.
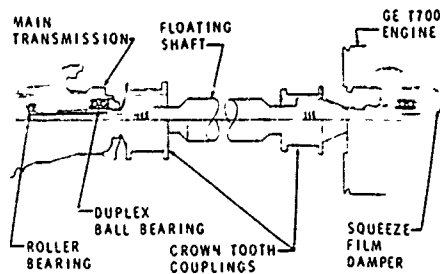

Figure 2. 20,000 RPM Shaft - Initial Design

The shaft was supported at the forward end by a female coupling supported by a flat-angle coned adaptor mounted to the quill shaft. The quill shaft in turn rotated on a set of duplex ball bearings and a roller bearing. At the aft end, the shaft was supported by the engine output module which incorporated a squeeze film damper.

The coupling and quill shaft details, Figure 3, included a centering spring and a guillotine grease seal. The cone adaptor was attached to the quill shaft through a single-piloted spline and a bolt clamp-up. The female coupling was made of nitrided M50 steel, and approximately .001-inch radial clearance was provided between the male and female couplings in order to permit the desired misalignment. Lubrication of the duplex ball bearings in the transmission was provided by centrifuging oil from inside the quill shaft, through a passage to the bearings. Static balance of the shaft was permitted.
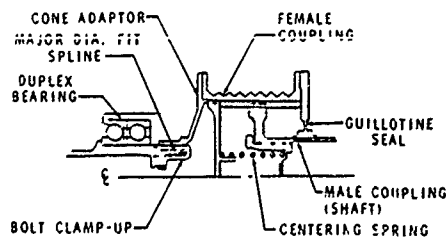

Figure 3. Quill and Coupling Detail - Initial Design

Although most of these design features are used for 6000 rpm shafts, when operating at the same horsepower at 20,000 rpm, the centrifugal force (CF) is increased by a factor of 11.1 and the torque is decreased by 0.3 resulting in an increase in the CF/torque ratio by a factor of 37. This increases the possibility that the male coupling may not rotate concentrically within the female coupling.

Initial critical speed analyses by BHT and GE were in good agreement. The BHT analysis showed the first mode at 169 Hz to be a rigid body shaft mode with deflections at the engine support shaft and bearings.

The second mode, at 263 Hz, consisted of rigid body shaft motion and bending in the transmission quill shaft with deflections in the quill support bearings. The third mode, at 724 Hz, involved classical shaft bending but placement was such as to provide satisfactory margins above the overspeed limits. These mode shapes are shown in Figure 4.
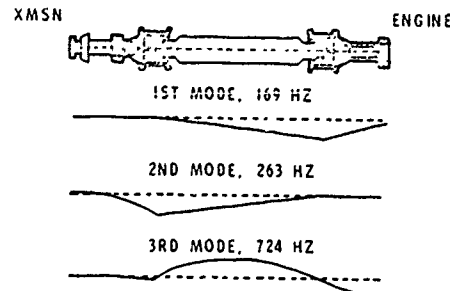

Figure 4. Natural Frequencies, Mode Shapes - Initial Design

Drive System Test Rigs

To develop the drive system, BHT built two regenerative rigs. The first, a coupling test rig, was designed to develop the input shaft male and female couplings. It had the capability to provide steady shaft misalignment, and oscillatory shaft misalignment and chucking at approximately 5 Hz, while applying up to full torque and operating up to 26,000 rpm.

The second, a bench test rig, included two power input shafts driven through individual gear speedup boxes into the main transmission, a main rotor shaft loaded through the regenerative loop, and accessory and tail rotor drive shafting loaded by a dynamometer.

2

Shaft Failures Encountered

During the initial run-up to the coupling test rig, while increasing the shaft speed to approximately 14,000 rpm, the first shaft failure was encountered. Subsequent development tests resulted in five additional failures of the shaft assembly, four on the coupling development rig and one on the bench test rig.

The first failure, wherein the female coupling disintegrated, initiated an intense investigation and development program to develop a satisfactory shaft design.

Investigative Actions

Early attempts to determine the cause of failure, including monitoring of subsequent tests, were thwarted due to insufficient instrumentation to measure shaft motions and gearbox accelerations. Also, initial static shake tests failed to confirm the analyses.

Therefore, the investigations following the first two failures centered primarily on coupling material defects, improper material application, column buckling of the centering spring, and load distribution of the female coupling. Additionally, the critical frequency calculations were refined to include the engine and engine support structure and to better represent the cone adaptors.

Parametric studies were made to determine the controlling parameters and the design changes required to place the first mode above 26,000 rpm. Typical results, shown in Figure 5, indicate the bearing spring rates and the cone adaptor stiffness required. However, because of the military requirement for both long component life and for 30-minute run-dry capability, the preload necessary to obtain the desired bearing stiffness could not be obtained.

Alternate design approaches were developed and some were fabricated and tested. An inverted coupling design, Figure 6, was fabricated and subjected to shake tests. The first mode frequency was significantly increased but did not place it above operating speed.

A nose reduction gearbox, Figure 7, was designed to provide a 10,000 rpm shaft. However, the reduction in shaft length resulted in unacceptable coupling misalignments while difficulty was encountered in getting the first mode involving the reduction gearbox above operating speed.
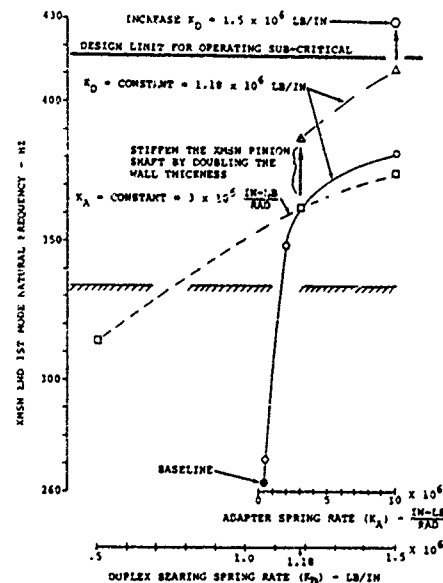

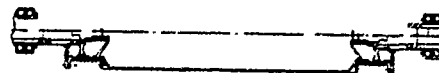Figure 5. Component Stiffness Requirements for a Subcritical Shaft Design

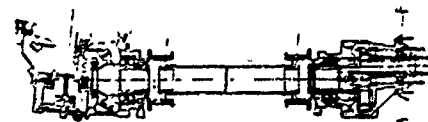Figure 6. Inverted Coupling Design Driveshaft Installation

Figure 7. Nose Reduction Gear Box Driveshaft Installation

3

A number of coupling designs involving leaf springs or multiple plates in a cruciform arrangement as shown in Figure 8 were studied These required a centering device which could also react the chucking forces which were to be taken on a sliding ball spline. Tests were conducted which demonstrated that the leaves could withstand the steady and oscillatory misalignment and withstand the static torque without excessive stresses. However, no acceptable centering device was found, and the ball spline failed to perform as required.

DETAIL A
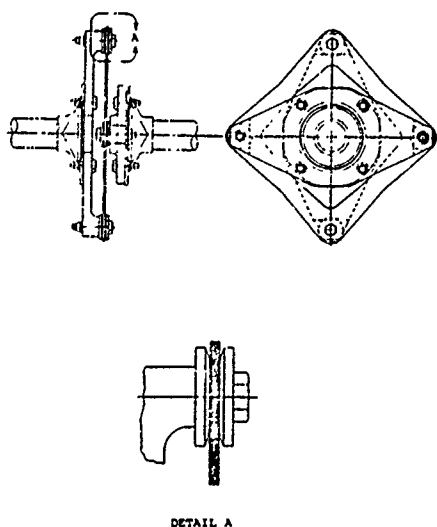
Figure 8. Thomas Type Single and Multiple Leaf Coupling

The forces due to permissible unbalance were determined which led to dynamic balancing of all components or subassemblies.

Shake tests were repeated with torque applied and correlation with analyses were significantly improved. Apparently, the clearance in the coupling and bearings resulted in impact damping until light torque was applied. As torque was increased to higher values, a corresponding increase in natural frequency was obtained. Thus, the effect of bearing loading on bearing spring rates was carefully evaluated and discussed with bearing experts.

One failure apparently occurred due to the failure of the bolt head which provides clamp-up of the cone adaptor to the supporting shaft.

Finally, one failure was recorded using accelerometers on the bearing supports and proximity probes on the shaft. These data, Figure 9, clearly showed the occurrence of a subharmonic whirl. With these new results, studies were now directed to the mechanism of nonsynchronous whirl instability. Since the shaft bending mode showed an acceptable margin, whirl instabilities of the rigid body shaft modes had not been considered previously.
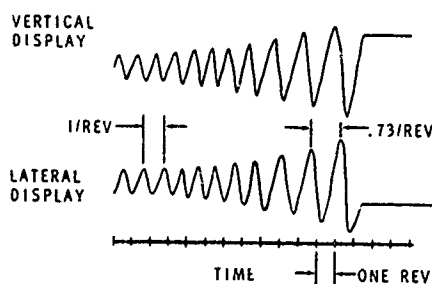

Figure 9. Traces of Bench Test Shaft Failure

Whirl Instability Investigations

Many references, such as 2, 3 and 4, on the phenomenon of nonsynchronous whirl were studied to gain an insight into this problem. These references all conclude that the mechanism of nonsynchronous whirl instability comes about due to the internal friction in a rotating system. The rigid body shaft modes of this development design can produce the "hysteretic" type of internal friction, described in Reference 5, at the crown tooth couplings. The mode shapes presented in Figure 4 show the relative angular misalignment of the shaft and input quill portions of the coupling. This relative motion is what produces the internal friction. Another potential source of internal friction in the design is clamped joints and shrink fits.

Shaft Dynamics

The dynamics of a shaft spinning on an axis has been treated extensively in many texts and papers, but shaft vibrations due to unbalance and the mechanism of shaft whirl instability are repeated briefly here to clarify the particular problems encountered during this development program. Unbalance in a shaft causes the shaft to respond at the rotational frequency and introduces a one-per-rev vibration into the fixed system and a steady load in the rotating system. The control of the amount

4

of unbalance, the external damping in the fixed system, and the location of the natural frequency with respect to the rotational frequency determine the level of this response. For a single-degree-of-freedom system, the response is shown in Figure 10. The important aspects are to keep the shaft response within geometrical and stress limits and minimize the force transmitted to the structure.
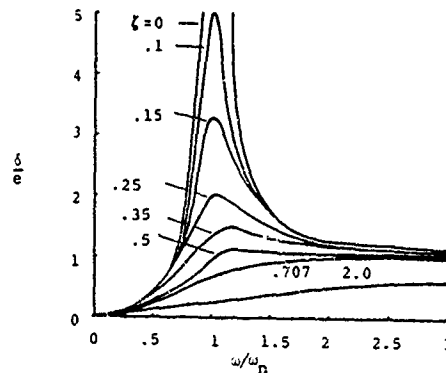

Figure 10. Amplitude Ratio Versus Speed Ratio for Various Amounts of Viscous Damping for an Inertial Driving Force

The vibratory forces transmitted to the support structure are the sum of the spring forces due to shaft displacement and damper forces due to shaft velocity. This force transmissibility is shown in Figure 11, which shows the transmitted force to increase with damping in the supercritical region. For supercritical operation, it is therefore important to achieve a balance in the amount of external damping to control the shaft displacement and transmitted force.
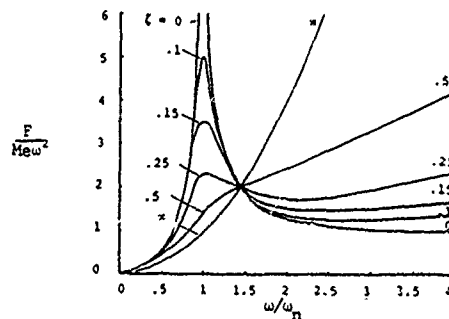

Figure 11. Transmissibility Ratio Versus Speed Ratio for Various Amounts of Viscous Damping for an Inertial Driving Force

Internal damping is the cause of potential shaft whirl instabilities. The direction of the internal friction force, whether it is a driving or damping force, is dependent on the magnitude and direction of the whirl or precession frequency relative to the shaft rotational frequency. Four cases can be considered: (1) forward precession and supercritical, (2) forward precession and subcritical, (3) backward precession and supercritical, and (4) backward precession and subcritical. Considering a shaft with splined crown tooth couplings, the relative frequency in the rotating system is that at which the shaft appears to wobble in the coupling. This is expressed as:

$$f_\omega = \omega - \Omega \qquad (1)$$

where:

f_ω is wobble frequency, positive in direction of Ω

ω is whirl frequency, positive in direction of Ω

Ω is shaft rotational frequency

Figure 12 shows how this relative wobbling frequency produces relative velocity between the shaft coupling and support quill spline teeth resulting in a friction force couple about an axis in the plane of the rotating mode shape. For the condition of forward precession and supercritical operation, the relative wobble frequency, according to equation 1, is opposite the shaft rotational frequency. Therefore, with forward whirl the splines on the leading side of the coupling, referenced to the whirl direction, are sliding together while those on the trailing side are sliding apart. This then produces a moment which is in the direction to increase the tangential whirl velocity of the shaft, thus providing the mechanism for whirl instability.
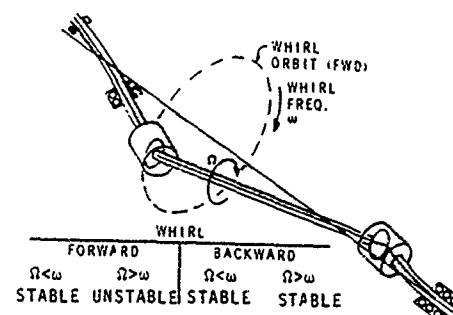

Figure 12. Mechanism of Instability

5

108

The other three combinations of precession direction and subcritical or supercritical operation produce relative wobble frequencies which result in the spline teeth sliding together on the trailing side of the coupling referenced to whirl direction. This results in a damping or stabilizing force. References 2 and 4 give good treatments of this whirl phenomenon.

With a floating shaft/spline tooth coupling design to allow for shaft misalignment and chucking, this internal sliding friction due to modal displacements can become quite high and in fact nonlinear with higher friction at higher coupling angles.

Supercritical (Squeeze Film Damper) Design

A squeeze film damper (SFD) is an effective method of supplying significant external damping in the fixed system. It serves both the purposes of reducing one-per-rev response to unbalance when traversing system natural frequencies and damping nonsynchronous forward precession whirl for supercritical operation. References such as 6 through 8 give detailed information on SFD theory. Basically, when a portion of a thin film of oil between two cylinders, one attached to the fixed system and one to the rotating system, is displaced, the hydrodynamic pressure is increased to move the oil to the portion of the journal now having more volume. As shown in Figure 13, this is very similar to an orifice-type damper as oil is forced through the portion of the journal having minimum radial clearance. This 'orifice' moves around the circumference as the rotating system whirls. This increase in pressure exerts a force back on the inner cylinder out of phase with the radial velocity thus becoming a damping force.
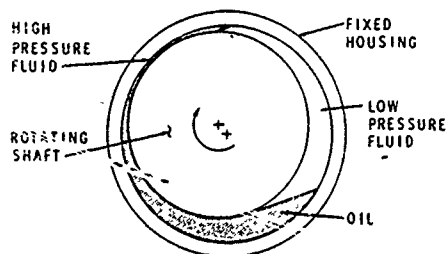

Figure 13. Principle of Squeeze Film Damper

This thin journal of oil can be under pressure to increase its effectivity and can be used in conjunction with retainer (cage) springs between the cylinders. One of the cylinders can be rotating (squirrel-cage type) or with fixed with a set of bearings isolating the rotating and nonrotating parts.

Due to the chucking forces associated with frictional forces within the coupling and pylon motion, squirrel-cage or finger-type damper cages could not be used. Therefore, Bell engineers developed a design using a flanged cylinder concept, as shown in Figure 14, which provided adequate column strength and a section of reduced thickness adjacent to the flange to provide the necessary flexibility.
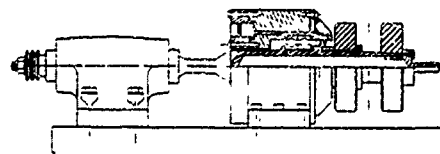

Figure 14. SFD Research Test Rig

Laboratory tests of the SFD were conducted in the rig, shown in Figure 14, which was designed to simulate the shaft and coupling stiffness and mass characteristics. Tests of this prototype damper, although conducted with minimal instrumentation, were successful, showing a high degree of damping when oil was introduced. Additionally, tests with coupling mass unbalance simulated did not significantly increase the whirl motion. The results of these tests are shown in Figures 15, 16 and 17 for various oil film thicknesses.

The success of these tests led to a design which could be integrated directly into the bearing support of the transmission input quills as shown in Figure 18. A spin test rig was developed as shown in Figure 19 to evaluate and establish final design parameters in terms of damper cage spring rate, diametral clearance, and oil pressure, and to compare the effects of duplex and triplex bearings. Only the transmission end was developed since there was already a squeeze film damper for the engine power turbine shaft in the nose of the T700 engine. Figure 20 shows the deflection of the damper cage due to applied load. These data are beneficial in establishing movement of the input quill shaft due to gear contact loads.
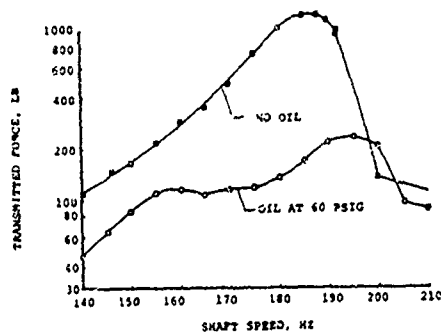
6

109

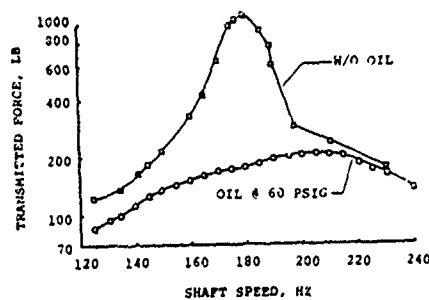Figure 15. SFD Test Data, Film Thickness 0.004 Inch, 4 GM-Inch Unbalance

Figure 16. SFD Test Data, Film Thickness 0.006 Inch, 6 GM-Inch Unbalance, Bearing Preload: 300 Lb
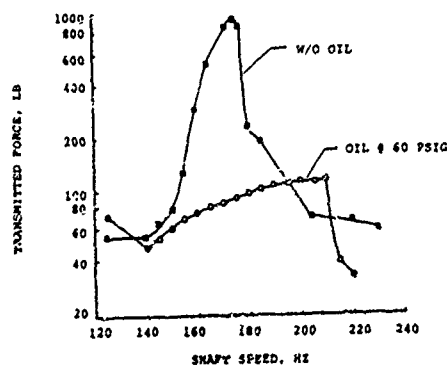

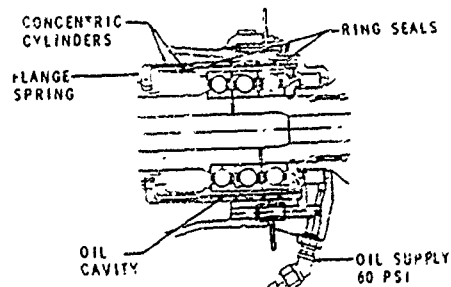Figure 17. SFD Test Data, Film Thickness 0.008 Inch, No Unbalance
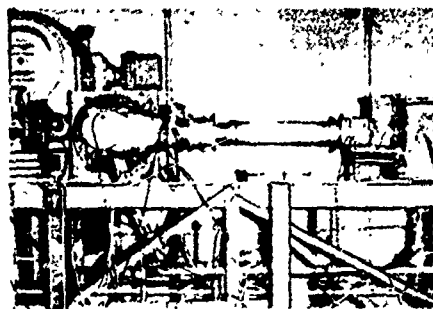

Figure 18. Squeeze Film Damper Design

Figure 19. Spin Test Rig

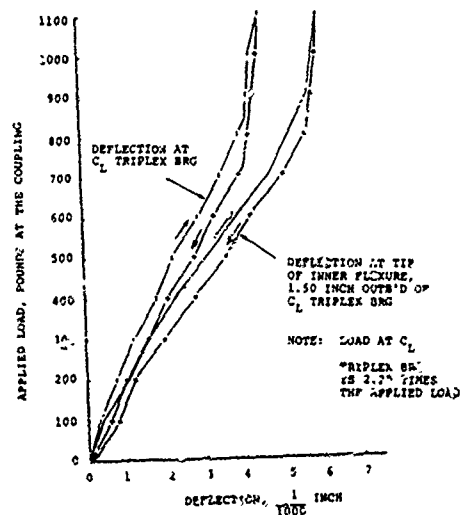Figure 20. Damper Static Deflection Test

7

There was some concern about gear contact wear patterns due to this floating input shaft, but no problems were encountered. The results of the spin test rig for various oil film thicknesses are shown in Figure 21, 22 and 23. The procedure was to install significant unbalance, more than expected in service, on the couplings and sweep shaft speed up to 20,000 rpm and back to zero with the oil pressure set at zero. The oil pressure was then applied and the rpm sweep repeated. The displacement response of the coupling was recorded and compared with and without oil pressure. The film thickness of .010 inch showed to be better than .006 inch or .012 and was therefore chosen as the design value. Oil pressures above approximately 30 psig showed no significant improvement in damping.
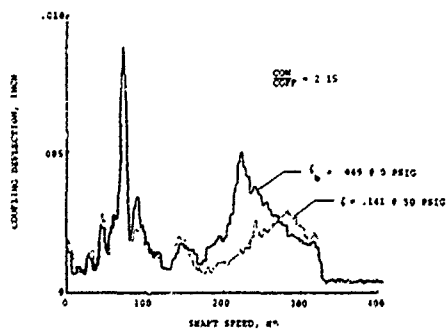

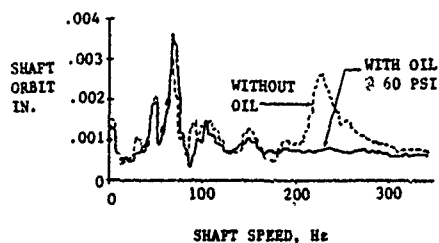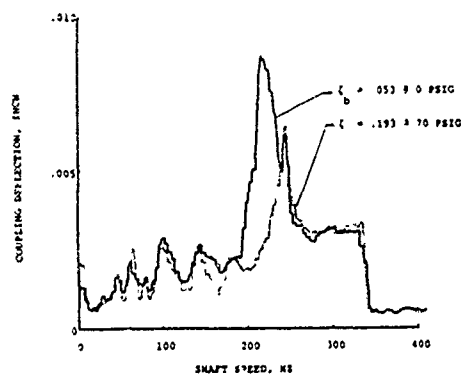Figure 23. Spin Test Rig Results, Film Thickness .012 Inch

Final Design

To diminish face and radial run-outs and joint instabilities, double piloted splines, a stiffened cone adapter, jam grease seals, improved clamp-up, indexed parts, and tightened manufacturing tolerances were incorporated into the final design as shown in Figures 24 and 25. Also each component was dynamically balanced.
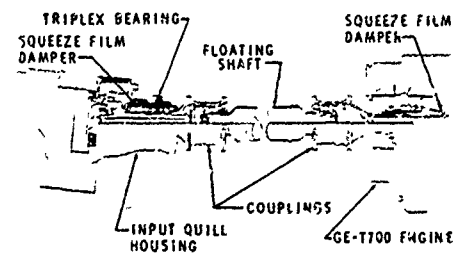

Figure 21. Spin Test Rig Results, Film Thickness .006 Inch

Figure 24. 20,000 RPM Shaft - Final Design
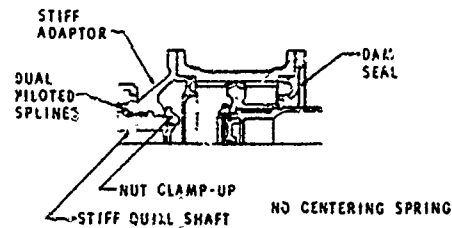

Figure 22. Spin Test Rig Results, Film Thickness .010 Inch

Figure 25. Coupling Detail - Final Design

8

Additionally, static tests on the adaptor clamp-up method, with and without lubricated threads were conducted. A typical plot of the deflection of the adaptor under radial shear load is presented in Figure 26 showing the joint instability of the early design. To check joint stability of the final design, a test was conducted at GE wherein the engine end adapter and output quill assembly were spun up to operating speed several times with unbalance added. Each time the assembly was disassembled and reassembled with the face and radial runout at each joint checked with no significant changes noted between runs. The natural frequencies for this final design are shown in Figure 27.
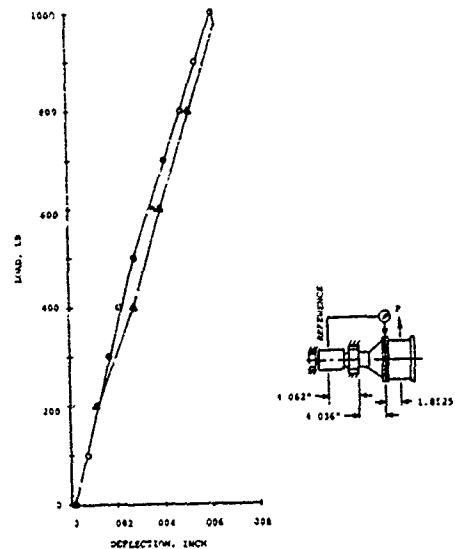

Figure 26. Load Deflection Curve Showing Joint Instability Under Simulated C.F. Loading
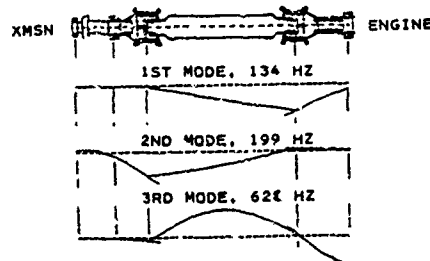

Figure 27. Natural Frequencies, Mode Shapes - Final Design

To continue transmission and bench test development, and ultimately flight tests with minimal schedule slippage, a back-up shaft design was provided. This shaft system used 3.1-inch pitch diameter couplings of the Model 206A/B helicopter which limited tests with this shaft to 1000 hp per shaft with 2.5 degrees of misalignment (steady state), and a maximum of ±.26 inches chucking. The use of this shaft was substantiated by extensive endurance testing in the coupling and bench test rigs.

To permit ground run and flight tests of the air vehicle to proceed, the nodal beam was clamped down, thus eliminating vertical isolation and oscillatory misalignment. It did successfully permit continued testing until the full-capability shaft was available. Although this shaft had supercritical rigid body modes also, no problems were encountered. This shaft did, however, have smaller diameter couplings and no joint instabilities, both of which reduced unbalance loads. Also, the lower horsepower and oscillatory misalignment reduced the internal friction which was the cause of nonsynchronous whirl instabilities.

The final design shafts were then installed and the nodal beam was unlocked for final flight testing. The production balance procedure and tolerance controls of the final shaft design, along with the SFD operation on the resonances, allowed engines and/or shafts to be changed with low vibration levels obtainable. Typical response plots for a full rpm sweep are shown in Figure 28. The amount of external damping added by the SFD did not create high vibration levels for supercritical operations.
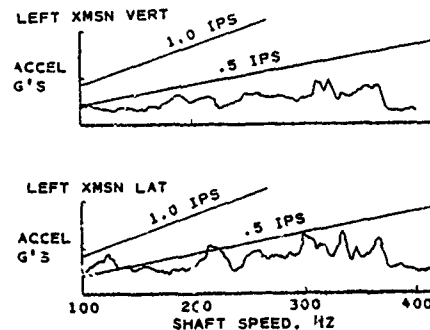

Figure 28. Air Vehicle Installed Vibration Levels

The displacement response of the couplings was monitored in real time during ground runs and flight tests using a real time spectral analyzer. The nodal beam

9

stops were gradually opened to their operational limits and no indication of the nonsynchronous whirl was noted.

Conclusions

The supercritical 20,000 rpm engine output shaft coupled with the NODAMATIC pylon isolation system produced a severe design environment both from a vibration and stability viewpoint. The illustrated test point failures obtained showed the need for very fine balance control in tolerances and assembly procedures, stable clamp-up joints, and sufficient external damping for vibration and stability control. It is questionable from the data whether the damper was needed once the balance control and joint stability features were refined. However, it is unquestionable that the damper helped reduce vibration levels due to transiting rotating system resonances, instilled confidence in the design, and made the supercritical input shaft a viable design option for helicopters. Experience with the YAH-63 20,000 rpm shaft demonstrated acceptable performance and the system completed all Army tests successfully.

Acknowledgements

The authors would like to thank the many designers, analysts, and technicians at BHT who have contributed to this paper through their work on this high-speed shaft development program. This paper is a summary of all their efforts.

References

1. D. P. Shipman, "Nodalization Applied to Helicopters," Society of Automotive Engineers, National Aerospace Engineering and Manufacturing Meeting, October, 1973.

2. E. J. Gunter, Jr., "Dynamic Stability of Rotor-Bearing Systems," NASA SP-113, U.S. Government Printing Office, Washington, D.C., 1966.

3. F. F. Ehrich, "Shaft Whirl Induced by Rotor Internal Damping," Journal of Applied Mechanics Paper No. 64-APM-7, ASME Applied Mechanics Division, April 15, 1963.

4. Rozell Williams, Jr. and Ronald Trent, "The Effects of Non-Linear Asymmetric Supports on Turbine Engine Rotor Stability," SAE Paper 700320, Society of Automotive Engineers National Air Transportation Meeting, 1970.

5. Cyril M. Harris and Charles E. Crede, "Shock and Vibration Handbook," McGraw-Hill Book Co., 1961.

6. J. Cooper, "Preliminary Investigation of Oil Films for the Control of Vibration," IME Paper 28, Institution of Mechanical Engineers, Lubrication and Wear Convention, 1963.

7. M. G. Jones, "An Experimental Investigation of Squeeze Film Hydrodynamics," N.G.T.E. Report No. R320, National Gas Turbine Establishment Proceedings, 1973.

8. S. Mohan and E. J. Hahn, "Design of Squeeze Film Damper Supports for Rigid Rotors," ASME Paper 73-DET-130, Design Engineering Technical Conference, 1973.

10

APPENDIX I

IR BLOWER DRIVESHAFT FAILURE

BHT, under Contract DAAJ01-73-C-0741(P40), developed a proto-
type Advanced Attack Helicopter, the YAH-63. The RFP required
an Air Management System (AMS) to provide an air supply
for an infrared radiation suppression system. The AMS
consisted of a ducting assembly charged by a high volume
axial flow blower (the IR blower). The power for the IR
blower was provided at a takeoff pad on the accessory drive
gearbox and transmitted to the blower by a driveshaft
assembly. A view of the installation is shown in Figure I-1.

The IR blower driveshaft assembly was designed so that a tor-
sional overload condition would fail the shaft in a manner
that was both predictable and controlled. The purpose of this
designed-in failure mode was to protect the remainder of
the accessory gearbox drive train from torsional overload in
the event of blower damage.

Tie-down testing of the prototype aircraft included evaluations
of various starting and stopping procedures. It was discovered
that a starting procedure involving a quick release of the
rotor brake could impose a transient torsional load into the
IR blower drive train that exceeds the driveshaft shear section
capacity. The shear section would fail due to simple shear
overload without the driveshaft inflicting additional damage
on the drive train or surrounding structure.

An investigation was conducted to define the dynamic properties
of the system.

The mass moment of inertia of the IR blower/driveshaft assembly
was determined. It was found that an acceleration from zero
to 100% speed in something less than 2 seconds would be
required, in addition to normal blower loads, to fail the
shear section. It was clear that simple drive train accelera-
tion could not have caused the failure.

The IR blower/driveshaft assembly torsional natural frequency
was determined to be approximately 30 Hz. No coincidences
were found to exist between the torsional natural frequency
and any normal operational frequencies. It was concluded
that torsional resonance, by itself, could not cause the failure.

The driveshaft was instrumented to measure torque and the
actual torque values were measured under various operating
conditions. Figures I-2, I-3, and I-4 are representative

IR blower torque versus time plots for three operating conditions: normal operation, rotor brake release, and rotor brake application.

In Figure I-2 (normal operation), it can be seen that the torque varies at the system torsional natural frequency, resulting in a low-amplitude beating resonance. Since no fatigue evidence or failures were observed, the conclusion was verified that simple torsional resonance did not cause the driveshaft failures.

Study of Figures I-3 and I-4 revealed the transient torsional loads resulting from rotor brake operation. Note that in both figures, a large amplitude torsional oscillation occurs at the system torsional natural frequency which lasts for several cycles when no failure occurs. Note also that the transient load oscillation due to rotor brake release at zero rpm (Figure I-3) lasts longer and exhibits larger amplitude excursions than the transient oscillation resulting from brake application at 30% speed (Figure I-4). The reduced response of the system to brake application at 30% speed was believed to be due to the inherent aerodynamic damping provided by the blower during operation.

It was concluded that the driveshaft shear section failures were due to a combination of events and conditions peculiar to the YAH-63 engines and drive train. The 700-GE-T700 engines, GFE supplied, could be started with the drive train locked using the rotor brake. The engines also utilize a torsionally soft power turbine shaft for torque measurement purposes. The combination of significant starting torque, mechanical windup through the drive train, and gear backlash resulted in a torsional impact type load being applied to the IR blower/driveshaft assembly. In the absence of aerodynamic damping, the torsional natural frequency of the IR blower/driveshaft assembly was impact excited every time the system bounced across the backlash while the drive train was accelerating. It was concluded that the shear section would fail when an additive combination of resonant and impact torques occurred. The resulting high instantaneous net torque would then fail the shear section.

Several methods were available to prevent this type of failure. The rate at which the pilot released the rotor brake was found to be significant. The chatter of the IR blower/driveshaft assembly could be reduced significantly by slowly releasing the brake pressure, as opposed to "dumping" the brake pressure. In order to reduce dependency on proper pilot technique, a modification to the brake hydraulic system was proposed that would provide a controlled release of the braking pressure.

The program subsequently was contractually terminated and the proposed modifications were never implemented.

View looking right

IR blower

Ducting assembly

Airframe structure

Shear section

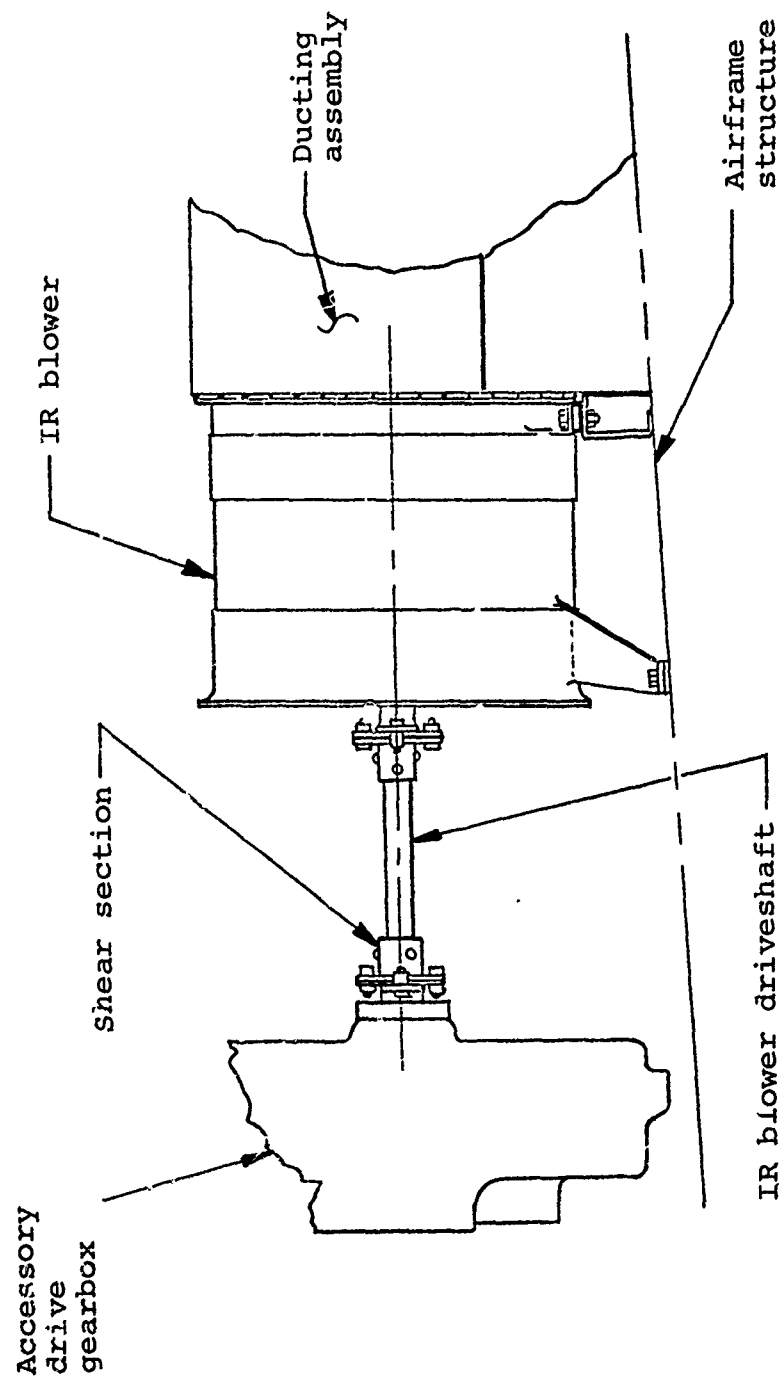IR blower driveshaft

Accessory drive gearbox

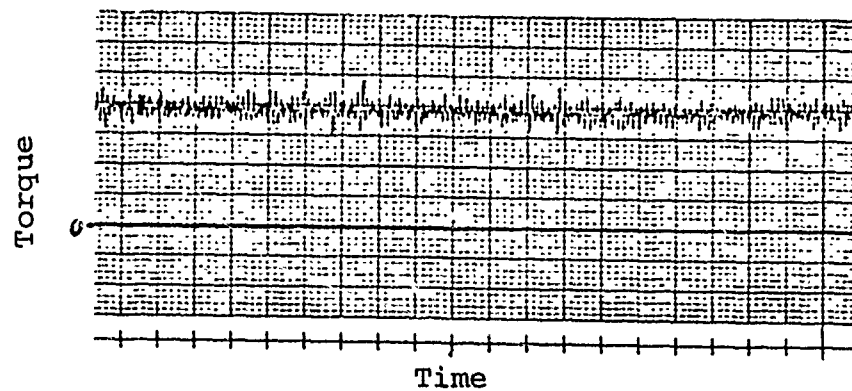Figure I-1. IR blower driveshaft installation.

Figure I-2. Time-history of IR driveshaft torsional loading during normal operation.
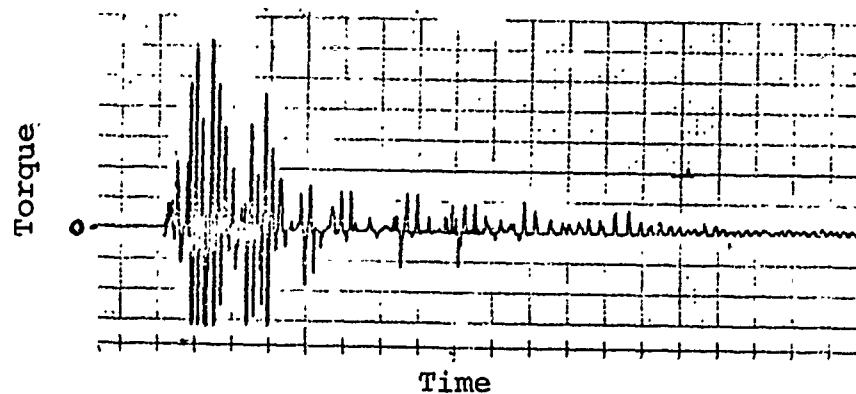

Figure I-3. Time-history of IR driveshaft torsional loading for a locked drive system rotor brake release with engines operational.
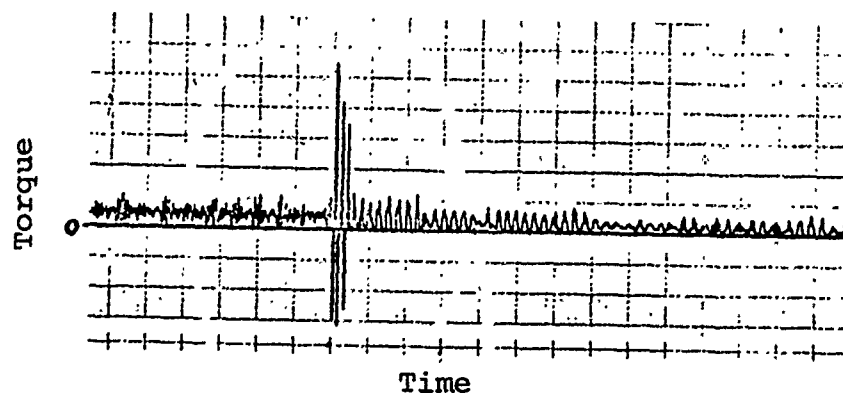

Figure I-4. Time-history of IR driveshaft torsional loading for a rotor brake application at 30% rpm.

117

APPENDIX J

FAILURE OF TAIL ROTOR AND ACCESSORY DRIVE GEARBOX MOUNTS

BHT, under Contract DAAJ01-73-C-0741(P40), developed a proto-type Advanced Attack Helicopter, the YAH-63. A tail rotor gearbox was created to turn the drive train 90 degrees and transmit the tail rotor loads to the airframe. An accessory drive gearbox was created as a mounting pad for the APU and to provide power takeoff pads for the aircraft accessory and auxiliary systems. Front and side views of the tail rotor gearbox installation are shown in Figure J-1. Front and side views of the accessory drive gearbox installation are shown in Figure J-2.

Both gearboxes were designed to be mounted on the airframe utilizing four attachment points (each) as shown in Figures J-1 and J-2. Four attachment points were used on the tail rotor gearbox to provide structural redundancy in the event of ordnance damage in compliance with RFP survivability requirements. The four attachment points used on the accessory drive gearbox were the minimum required to provide proper support.

For both gearboxes, the mounting schemes were analyzed under flight and crash loads to determine the load sharing distributions. Also, the tail rotor gearbox load sharing distribution was determined for the condition of one mount point missing and limit flight loads. All margins of safety were determined to be positive and acceptable.

Early in the YAH-63 Ground Test Program, both the tail rotor gearbox and the accessory drive gearbox suffered fatigue failures at mount points.

The tail rotor gearbox experienced failure of leg "A" (Figure J-1) due to bending fatigue. The failure consisted of a fatigue crack which started in the area of point "B" (Figure J-1) and propagated across the leg until visually detected by routine inspection. The crack origin was found to be in an area of transition from machined to as-cast surfaces. Strain gage instrumentation was installed and the actual dynamic load sharing distribution was determined. It was found that the actual load sharing distribution did not agree with the predicted distribution. The variance between the actual and the calculated distributions was believed to be a result of an unequal local stiffness distribution in the airframe and, to some extent, the flexibility

118

characteristics of the tailboom. This conclusion was supported by the fact that the actual load distribution was improved by the use of a soft mount (elastomer) assembly installed between the subject leg and the airframe. Due to installation envelope limitations, the soft mount stiffness could not be adjusted sufficiently to provide an optimum load distribution. It was decided that the best solution for the prototype aircraft would be to provide an additional load path in the form of a strut assembly (Figure J-1). The strut assembly served to share the loads imposed on leg "A," and acceptable stress levels were experienced for the duration of the prototype development program. Design changes for both the tail rotor gearbox and the tailboom structure were proposed for the pre-production phase of the aircraft development program. The design changes included relocation of machined surfaces, shortening and thickening of the gearbox legs, and redesign of the airframe structure to provide a more uniform stiffness distribution at the mount points. The program subsequently was contractually terminated and the anticipated results due to design changes were never confirmed.

The accessory drive gearbox experienced a fatigue crack type failure of the case wall immediately adjacent to boss "A" (Figure J-2). Only one such failure was experienced, during ground tie-down testing. It was determined that the stiffness characteristics of the airframe mounting hard points were not as anticipated. The firewall structure did not provide sufficient moment resistance and the elastomer bushings were too soft in the axial direction. Subsequent distortion of the load-sharing distribution resulted in excessive structural loads at the area of failure. A redesign effort, focused on the mounting scheme, resulted in the selection of a satisfactory hard point location on the airframe which could be tied by a strut to boss "A". Additionally, the elastomer bushings were replaced with much stiffer bushings. Upon reconfiguring the prototype aircraft, no additional failures or distress were observed. No further design changes were proposed for the pre-production development phase of the program.

It was apparent that the design analysis performed was in error. Factors contributing to the analysis inaccuracies included assumptions concerning actual airframe stiffness characteristics, and inaccurate prediction of both the tail rotor loads and the forces due to main rotor pylon motions as transmitted by the tail rotor driveshaft gear couplings (see Appendix F of this report for discussion of gear coupling chucking and misalignment loads). Additionally, the requirement for a redundant mounting system to reduce ballistic vulnerability conflicts with that of a design configuration for low mount attachment loads.
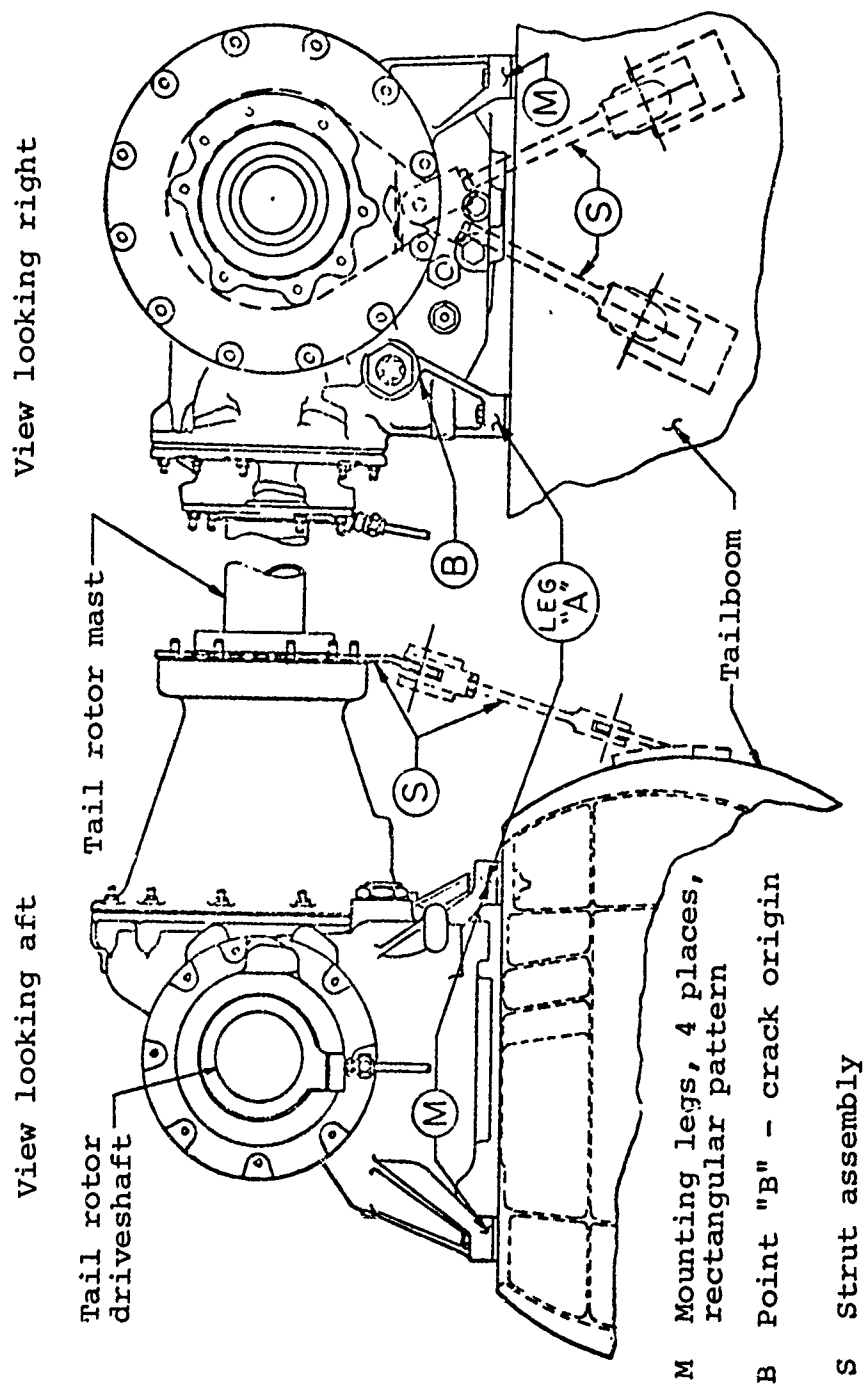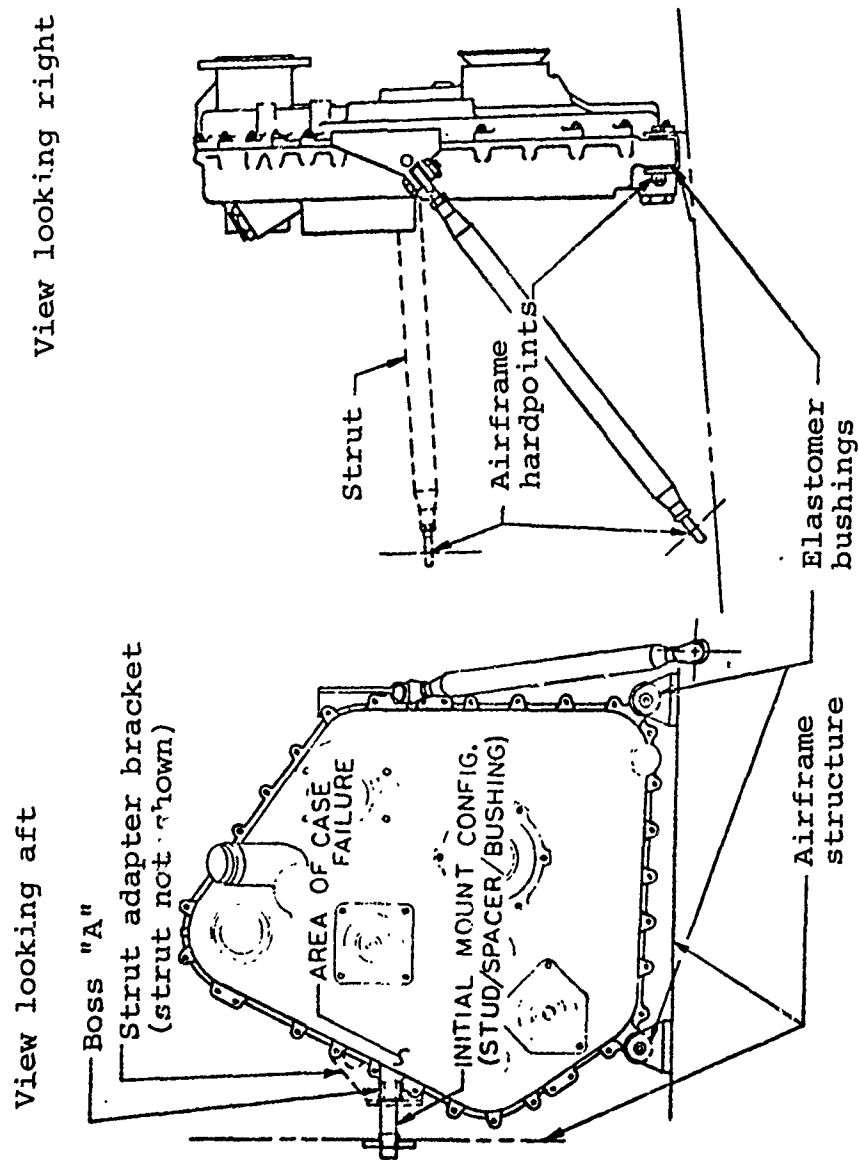
View looking right

View looking aft

Tail rotor mast

Tail rotor driveshaft

B

S

LEG "A"

M

S

M

B

Tailboom

M Mounting legs, 4 places, rectangular pattern

B Point "B" - crack origin

S Strut assembly

Figure J-1. Tail rotor gearbox installation.

View looking right

Strut

Airframe
hardpoints

Elastomer
bushings

View looking aft

Boss "A"

Strut adapter bracket
(strut not shown)

AREA OF CASE FAILURE

INITIAL MOUNT CONFIG.
(STUD/SPACER/BUSHING)

Airframe
structure

Figure J-2. Accessory drive gearbox installation.

121

APPENDIX K

POOR GOVERNING AND EXCESSIVE
TRANSIENT ROTOR DROOP

From the installation of the first turbine engine at BHT in
the mid-1950's to about 1969, torsional stability analyses
conducted at BHT were linear perturbation analyses about a
few selected power conditions. Although these analyses could
be used with reasonable accuracy to achieve stability, no
means other than actual helicopter ground and flight tests
were available to evaluate the effects of control parameter
changes upon governing accuracy and/or transient response.

It has been the procedure at BHT since about 1969 to conduct
transient nonlinear analyses on each new helicopter developed.
This type of analysis permits not only a check of torsional
stability, but also permits (with certain limitations) an
evaluation of governing accuracy and transient response.
Thus, a degree of optimization is achieved.

In early 1973, BHT entered a proposal into the Advanced Attack
Helicopter competition. During the proposal effort BHT con-
ducted a nonlinear transient analysis of its entry, the YAH-63
helicopter with the GE T700 engine installed, as documented in
Reference 8. This analysis was similar to one conducted for
the UTTAS proposal (Reference 13). It was conducted on the
Group 04 engine control configuration.

BHT was awarded a Phase 1 development contract and subsequently
requested that GE update the control configuration data. This
data was provided to BHT in November 1973, and another update
was received in February 1974. BHT then updated its nonlinear
analysis.

As required by contract, BHT submitted linear stability analysis
and concurrently conducted transient nonlinear analysis. Addi-
tionally, both BHT and AEFA testing was conducted. Further
amplification of the most significant details follow.

---

13. Shipman, D. P., PRELIMINARY TRANSIENT RESPONSE AND TOR-
     SIONAL COMPATIBILITY ANALYSIS OF THE MODEL 240/220 ENGINE,
     GOVERNOR, ROTORS, AND DRIVE SYSTEM, Bell Helicopter Textron
     Report 240-909-001, Fort Worth, Texas, April 1972.

To meet the contractual requirements, which were to provide a linear analytical model of the drive train, engine, and control in accordance with ADS-9, BHT requested linear data from GE. This data was received and a report (Reference 14) was then submitted by BHT to the Army in July 1974.

In January 1975 GE submitted data to BHT for control system transient performance. On June 10, 1975, GE submitted to BHT further slight changes in the then-current G07 electronic control unit (ECU) and P07 hydro mechanical unit (HMU) configuration released for production. These changes were made based on:

1. Initial field testing of current configuration ECU's and HMU's which revealed excessive transient power turbine speed changes during flight maneuvers involving load changes.

2. UTTAS test results wherein a small (less than 1% N_p), low-frequency (0.3 cps) oscillation during operation at low power was noted. This low frequency oscillation was traced to a slight opening/closing of the starting bleed valve which was corrected by a change to the valve.

To improve rotor "droop" out of autorotation, N_p overshoot, and slow N_p recovery, the ECU and HMU were thus modified. GE requested of BHT at this time that:

1. Additional ground test vehicle (GTV) running, with the prototype ECU's, be accomplished to further confirm system stability.

2. The BHT computer simulation be re-run, based on these latest modifications, to determine that the resulting changes appear satisfactory.

3. A meeting be established to review the results of the BHT and forthcoming GE stability and transient analyses to confirm that, "To the best of our abilities, no potential problems exist."

In July 1975 GE submitted an update of the control and rotor system transient and stability analysis based upon the then-current G07 and P07 control changes as transmitted in

---

14. Killion, S. W., MODEL 409 ENGINE/ROTOR TORSIONAL COMPATIBILITY, Bell Helicopter Textron Report 409-909-007, Fort Worth, Texas, 30 July 1974.

June 1975. Excerpts of this data are provided as Attachment 1 to this Appendix.

In September 1975 the configuration of the HMU increasing the acceleration fuel flow was re-identified as P08 HMU.

In December 1975 BHT submitted to the Army a test plan (Reference 15) for an engine/airframe compatibility survey and demonstration. This plan was subsequently revised at the request of the Army. The survey and demonstration were conducted and the results are presented in Part II of Reference 15.

The report concludes, in part: "The torsional stability characteristics demonstrated acceptable damping under all conditions tested. Significant N_2 droop occurred during rapid jump takeoffs and during recoveries from autorotation to power. This may be reduced somewhat by pilot control technique."

During this development stage GE was investigating a further modification to the control system allowing for a nonlinear control gain to improve the transient droop condition, later to be identified as the G09 control. However, this latest modification could not be fully qualified before the scheduled AVM fly-off competition. Both AVM's used the same T700 G07 controls during the AEFA evaluation.

At the completion of the AEFA testing, the Army forwarded to BHT test data regarding transient response characteristics for information and evaluation. Additionally, the SSEB required additional clarification/rationale relating to the AEFA testing pertaining to "poor rotor speed control during maneuvering flight" and "excessive transient rotor speed droop when rapid power application from minimum power conditions were conducted (i.e., quick stops)." Further, the SSEB requested a "torsional stability analysis per ADS-9A with T700 G09 ECU necessary for evaluation."

---

15. Giesen, G. L., ENGINE/AIRFRAME COMPATIBILITY SURVEY AND DEMONSTRATION FOR THE YAH-63 ADVANCED ATTACK HELICOPTER, Bell Helicopter Textron Report 409-993-008B, Fort Worth, Texas, 28 June 1976.

BHT responded with Reference 16, excerpts of which are found in Attachment 2 to this Appendix. The analysis evaluates stability with the G09 controls, shows correlation with AEFA test data, and evaluates the effects of hysteresis. One deficiency was identified, that of excessive hysteresis in the rotor control system. This was more pronounced on one particular ship and led to a correlation error between measured and analytical data. The analysis further demonstrated that the G09 control would substantially reduce the rotor speed droop to values well within the design objective limits for the YAH-63.

The YAH-63 program was subsequently contractually terminated before sufficient measured data could be evaluated to fully confirm the analytical predictions for the T700 G09 control performance.

In conclusion, both BHT and GE conducted transient nonlinear analyses and were in good agreement with each other. Each analysis gave slightly conservative results - as desired - with regard to measured stability data. However, there were shortcomings in the analyses in their ability to accurately predict transient response characteristics for some types of maneuvers. Those conditions include:

1. Transitions from autorotation to power

2. Transitions from power to autorotation

3. Stabilized autorotation

4. Jump takeoffs

5. Quick stops

6. S-turns

One problem in predicting transient maneuvers is that a wide variety of pilot techniques are used and the same pilot may execute the same maneuver twice in such a manner as to obtain significantly different results. This suggests that information is needed on the control inputs (displacements and rates) and the combination or sequence thereof which bound the probable limits so that the analyst has some tractable numbers of conditions which can be used to evaluate both the norm and the extremes.

---

16. Kamat, H. V., YAH-63/T700/G09 ECU TORSIONAL STABILITY AND TRANSIENT RESPONSE ANALYSIS, Bell Helicopter Textron Report presented to U. S. Army Source Selection Evaluation Board (SSEB), Fort Worth, Texas, 4 November 1976.

ATTACHMENT 1 TO APPENDIX K

On July 28, 1975, GE transmitted to BHT an updated T700
transient analysis. This update was based on UTTAS flight
testing and computer simulation which identified some areas
where improvements could be made. The transients were run
using then-current T700 engine and control simulation - the
(G07) ECU and the (P07) HMU LDS schedule changes, Figures 1
and 2, respectively - plus the latest aircraft simulation
available at GE.

A list of the thirteen transients evaluated are shown in
Table I. The simulation data for these transients are included
herein, Figures 3 through 15 of this attachment. Scaling on
these figures has been intentionally removed as information is
proprietary to the engine manufacturer.

The figures occur in pairs where "A" is engine one in a twin-
engine helicopter, and "B" is engine two. Generally, engine
one is a nominal engine, while engine two is purposely made
not nominal. This gives two unequal engines as would be
expected for a twin-engine installation. The N_p reference for
engine No. 2 is not set at 100% as part of the engine in-
equality. This is the reason that many of these transients
seem to want to run at 100.5% N_p. The figures titled "UEQ ENG"
were run with unequal engines.

Table II shows the key to the scales on the figures. The
timing of the load changes can be determined from the BETA
curve which appears on all of the figure "B"s.

Note: Figures 1 and 2 intentionally omitted. Information
       proprietary to engine manufacturer.

ATTACHMENT 1 TO APPENDIX K

TABLE I.   LIST OF TRANSIENTS

1. 2-second load burst and chop, 380 hp to 3072 hp to 380 hp

2. Twin-engine throttle burst - GI to fly at flat pitch

3. Single engine failure from 1500 hp

4. ECU failure at 1000 hp

5. ECU failure at flat pitch

6. 1-second load chop - 2500 hp to 1500 hp - without moving
    LDS and collective

7. 1-second load chop - 1000 hp to autorotation - without
    moving LDS and collective

8. 2-second load burst autorotation to 830 hp

9. 2-second load burst autorotation to 1500 hp

10. 2-second load chop,1500 hp to autorotation

11. 1-second load chop and burst, 2000 hp to 1500 hp to 2000 hp

12. N_p reference change:

    100% to 95% in 2 seconds

     95% to 100% in 1 second

13. Cyclic excitation at rotor resonance

TABLE II. ABBREVIATIONS

PCNT   % rotor speed as measured at the gearbox

PCNMR   % rotor speed as measured at the main rotor

PCNTR   % rotor speed as measured at the tail rotor

WFM   Fuel flow - pph

TRQP   Power turbine torque - ft-lb

T4.5 EL   Cockpit indication of T4.5 - °R

PCNP   % N_P

PCNG   % N_G

PASA   Power available spindle angle - deg

BETA   Load demand spindle angle and collective

NOTE:

PCNP1   % N_P engine #1 and

PCNP2   % N_P Engine #2, etc.

PCNT (or PNCMR) and PCNP1 will run superimposed until the
needle splits in autorotation. The needle split is noted
by a difference between PCNT (or PCNMR) and PCNP.

ATTACHMENT 1 TO APPENDIX K
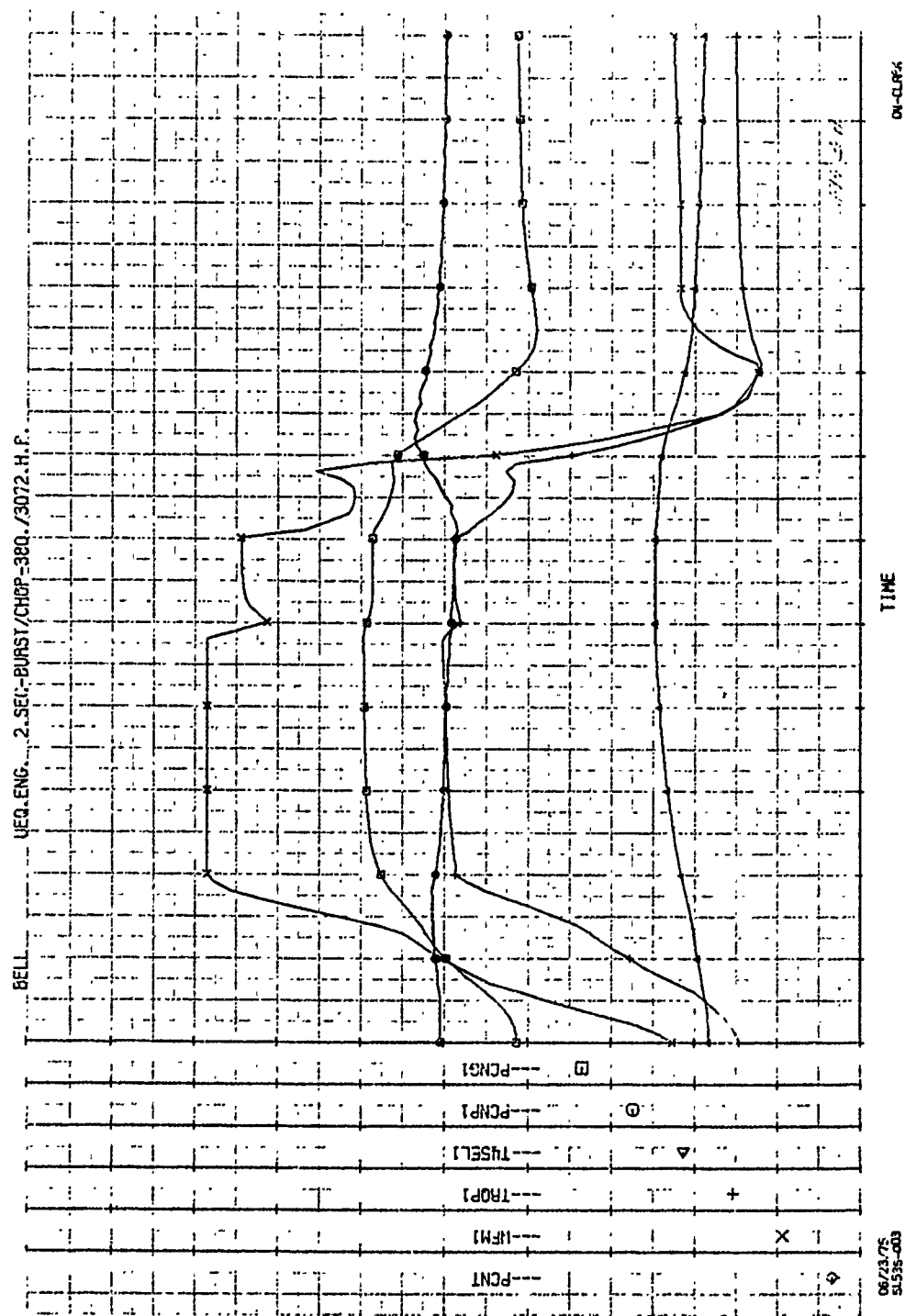
Figure 3A.

ATTACHMENT 1 TO APPENDIX K
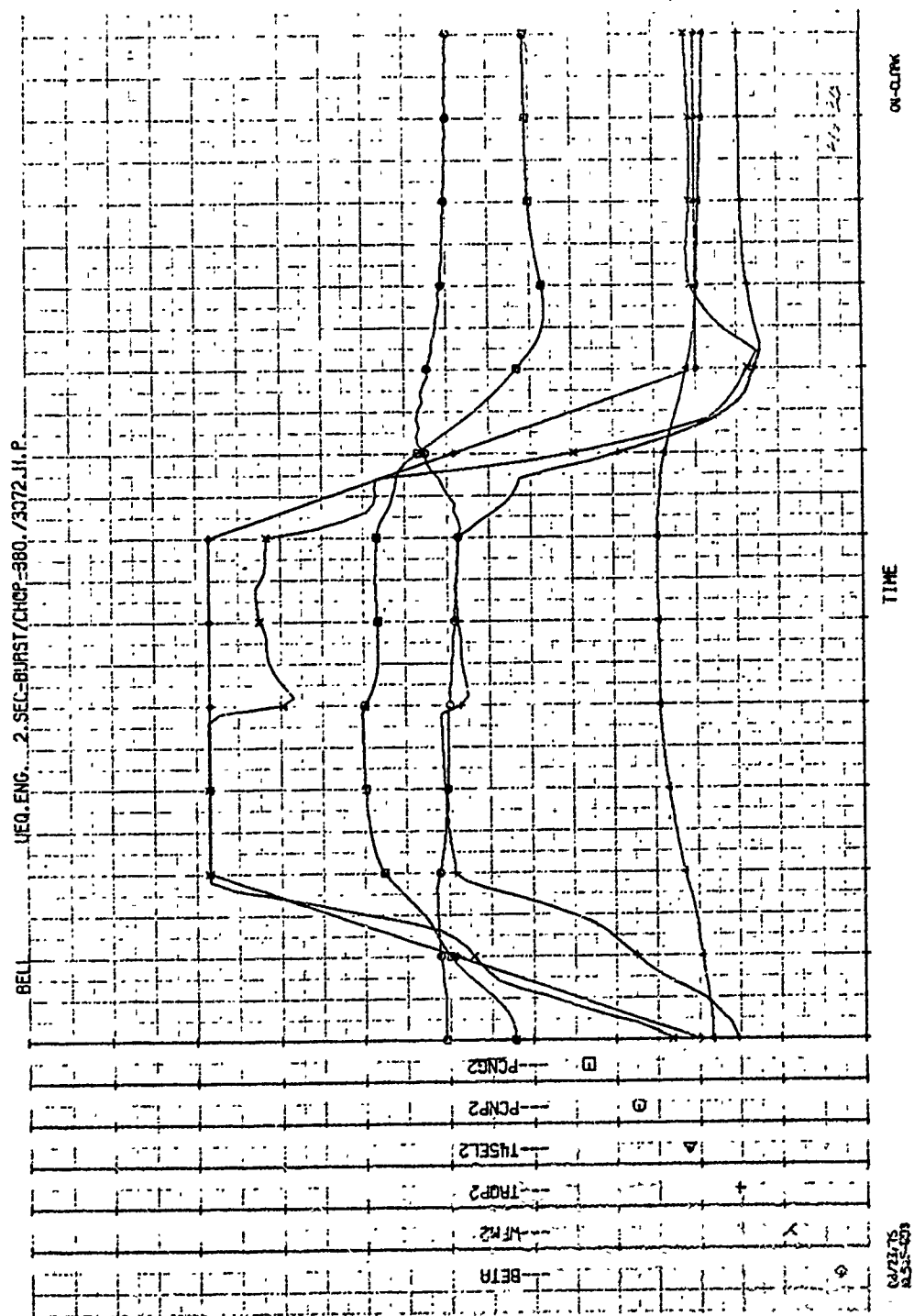
Figure 3B.
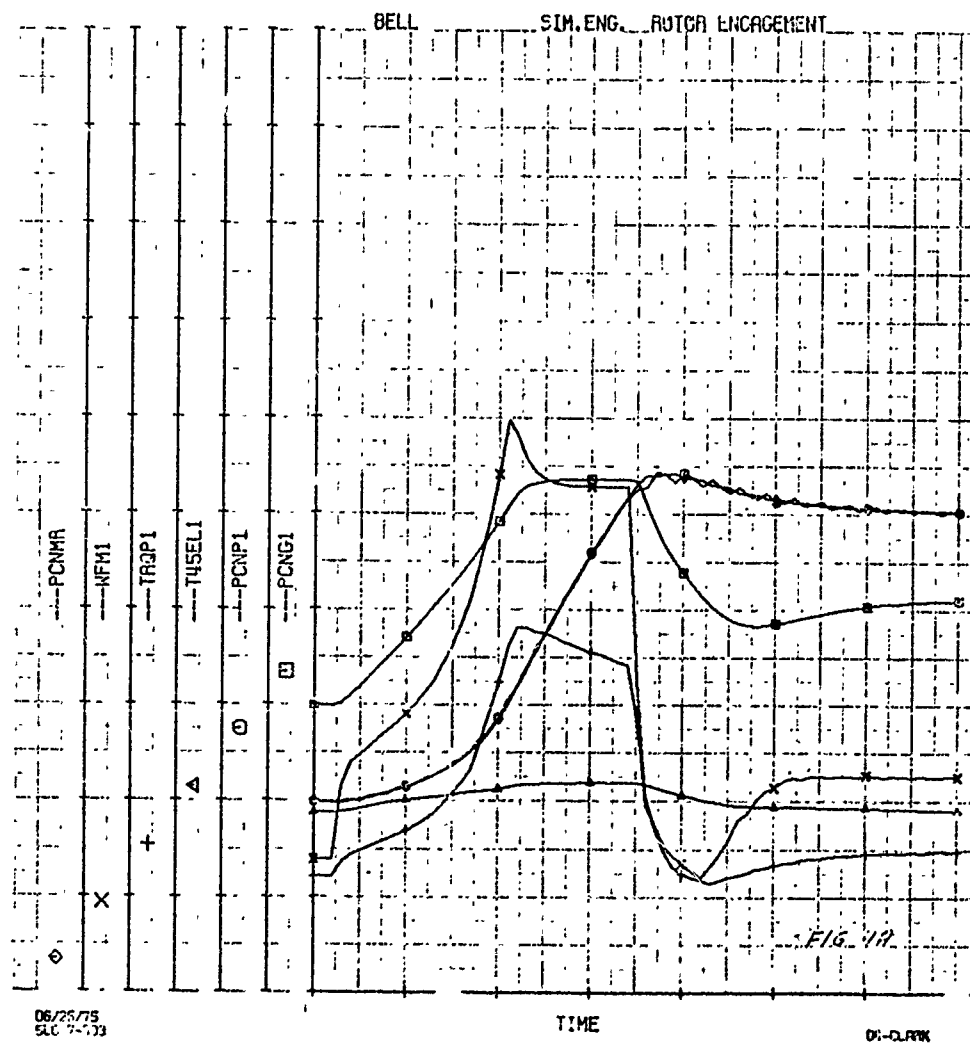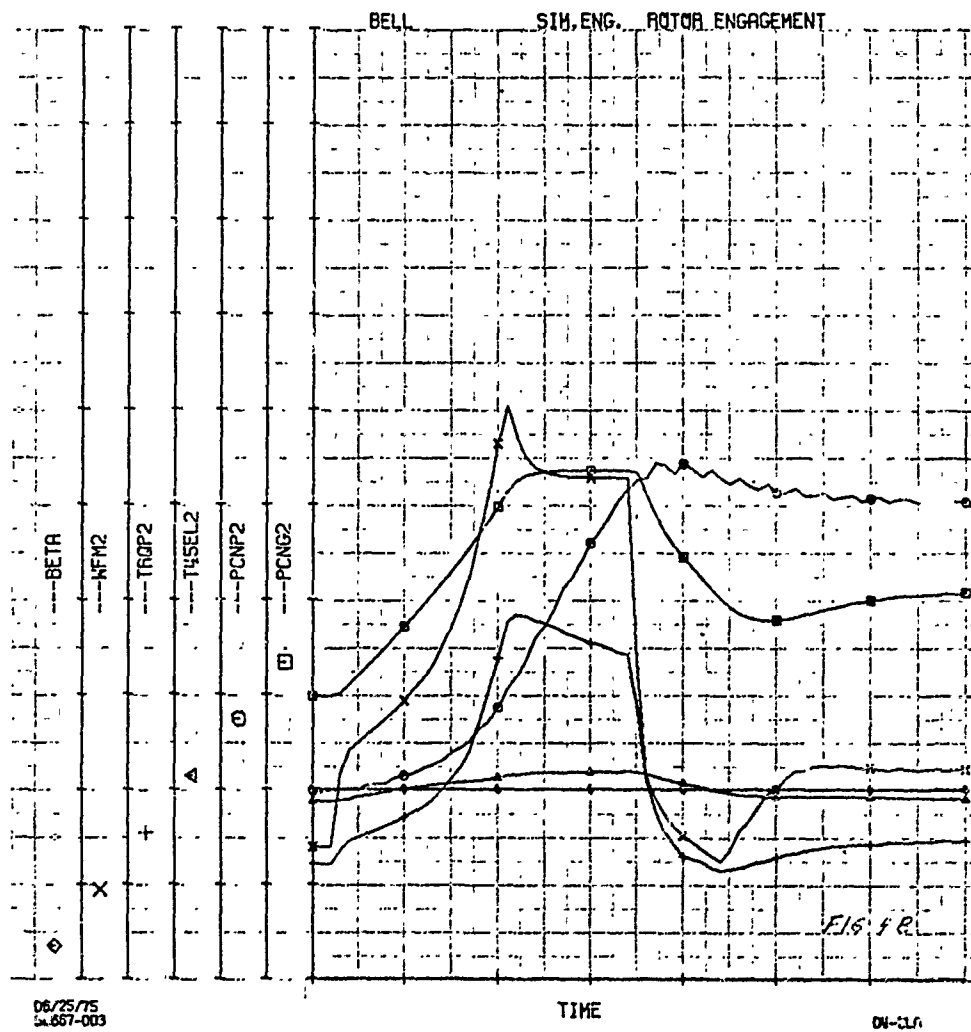
Figure 4A.

Figure 4B.

132

Figure 5A.

Figure 5B.

134

Figure 6A.

Figure 6B.

136

ATTACHMENT 1 TO APPENDIX K

Figure 7A.

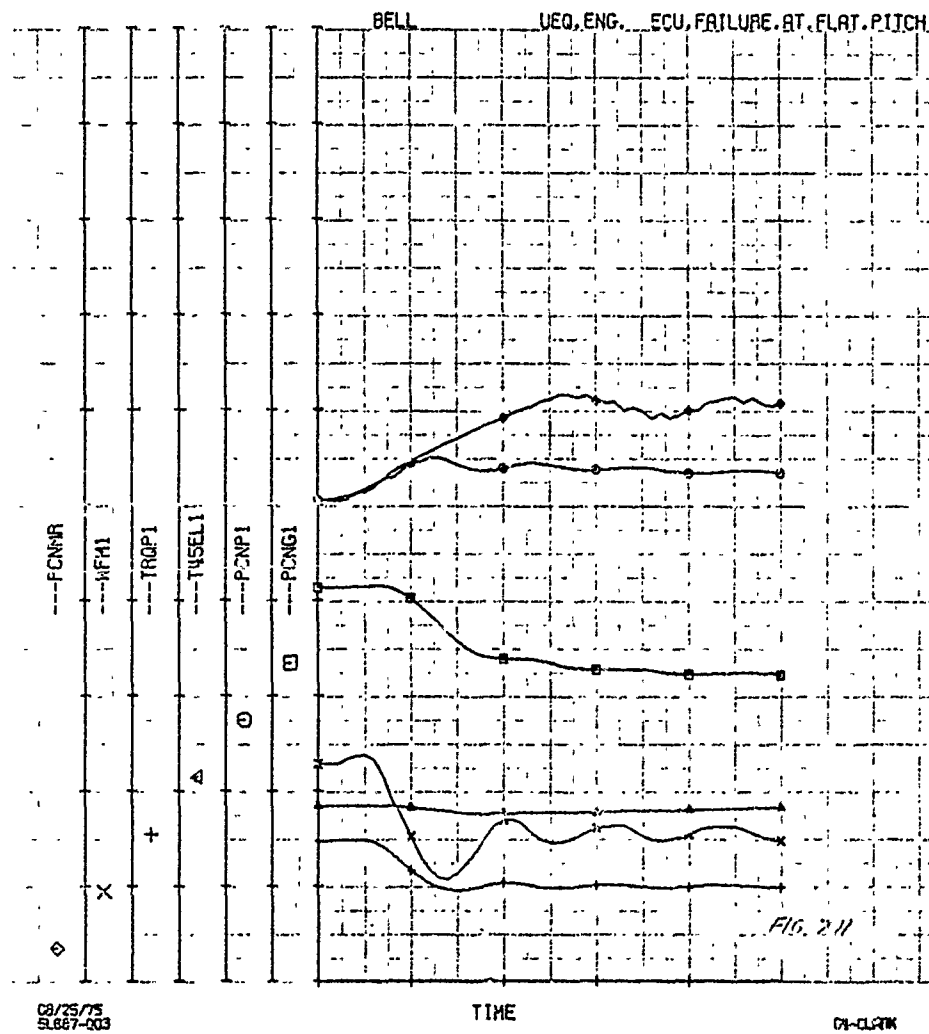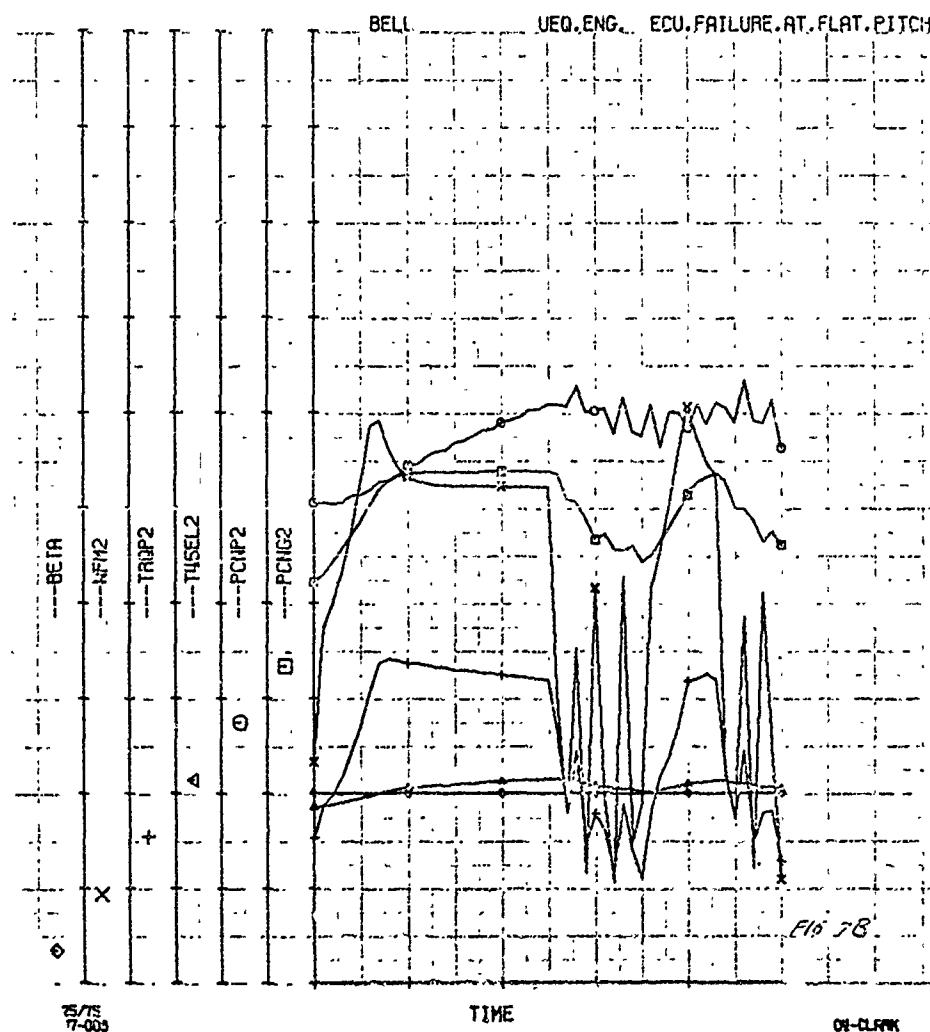Figure 7B.

Figure 8A.

Figure 8B.

Figure 9A.

Figure 9B.
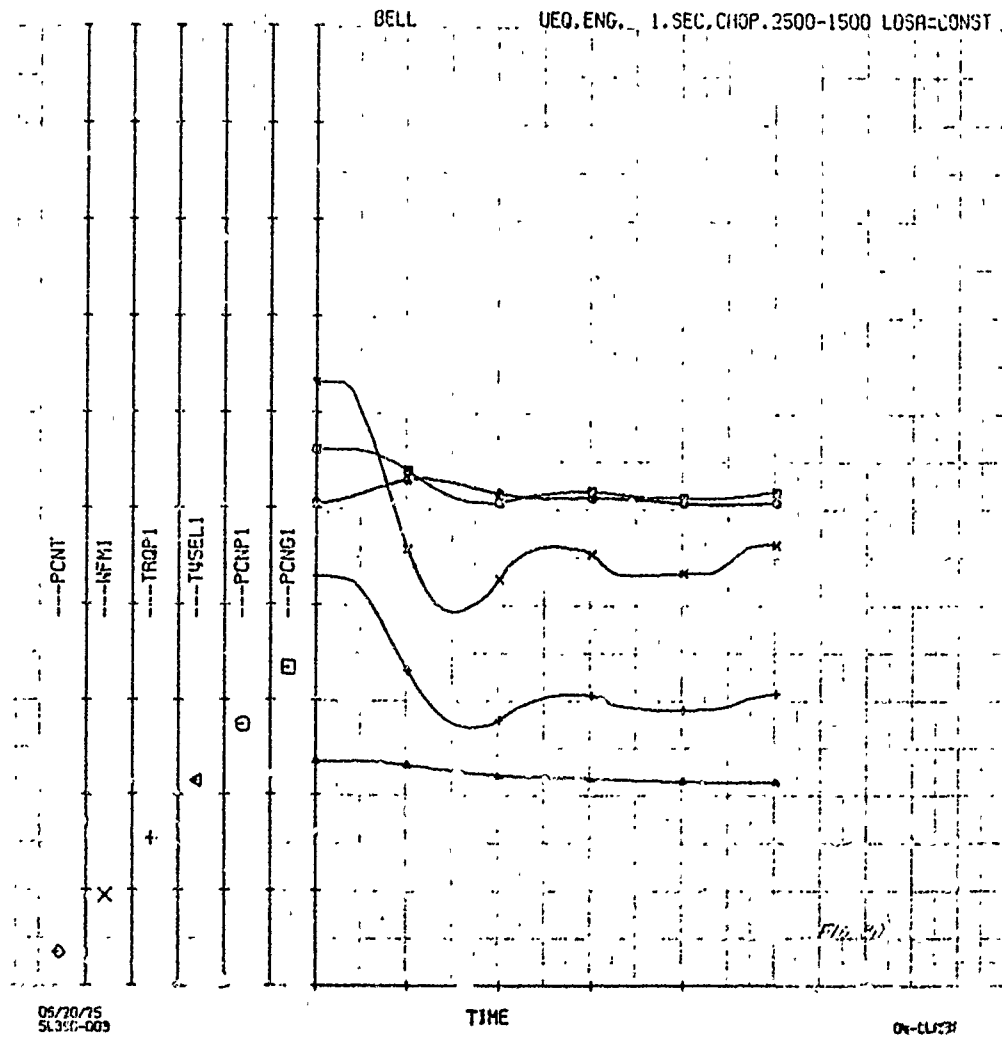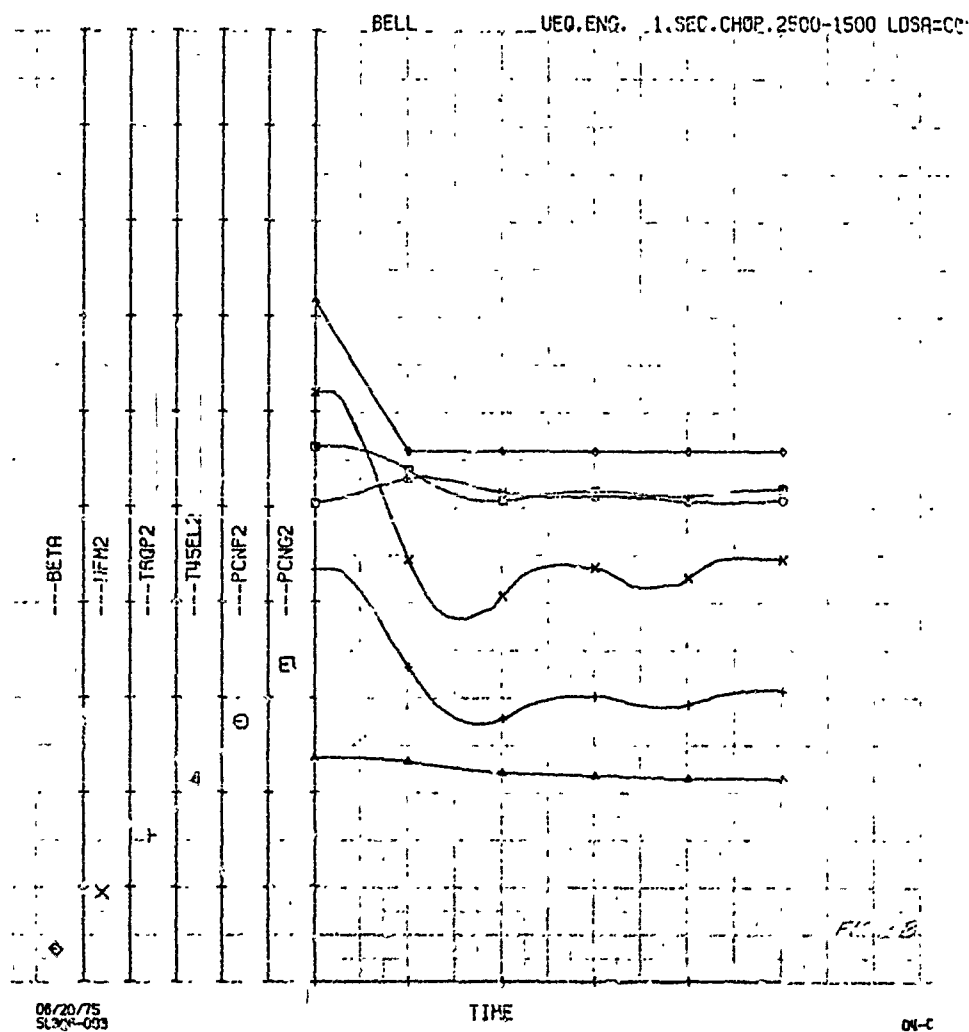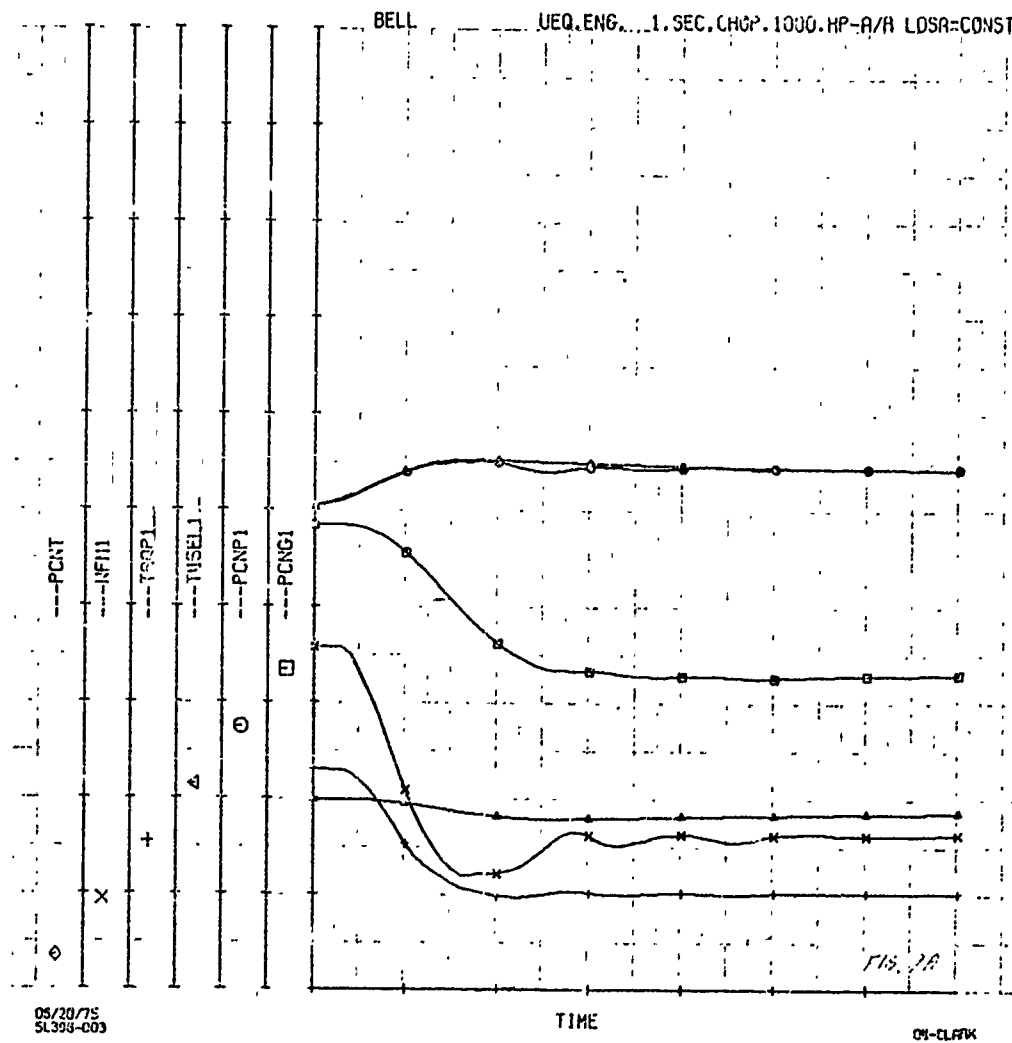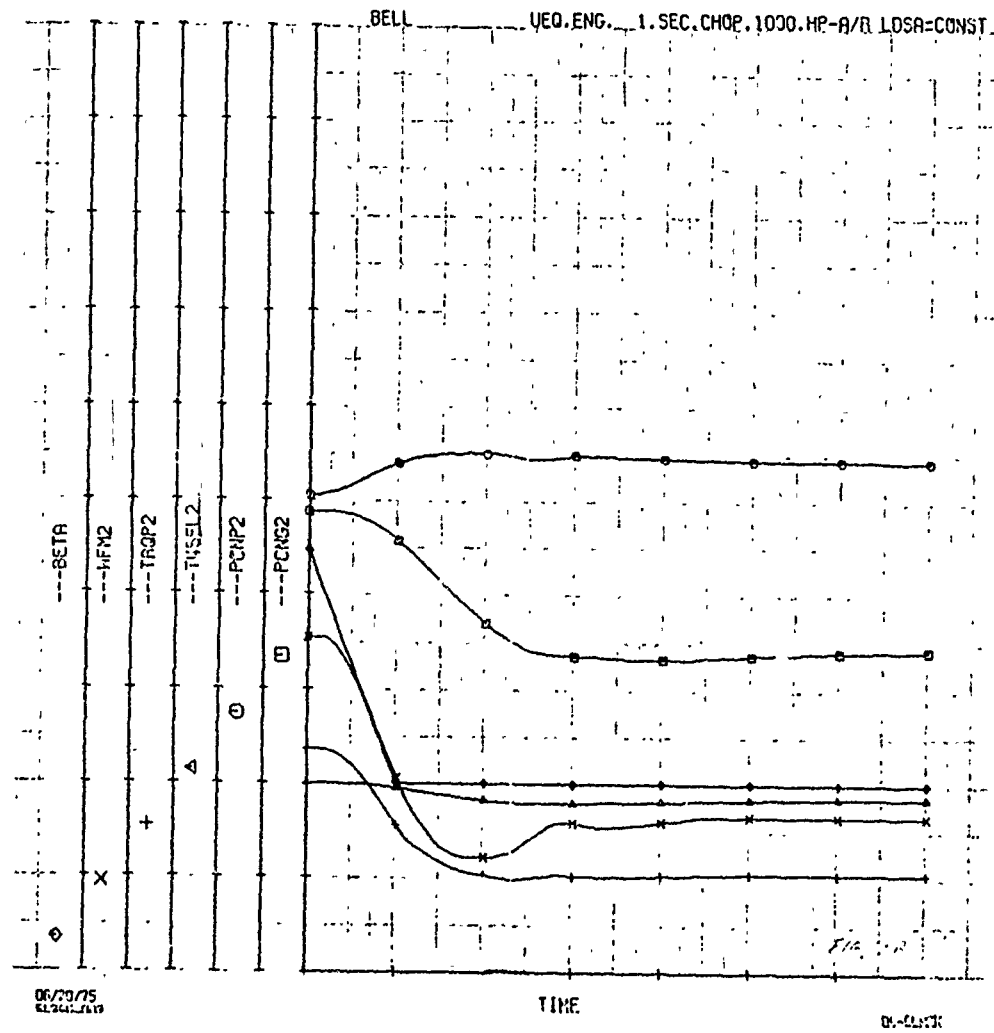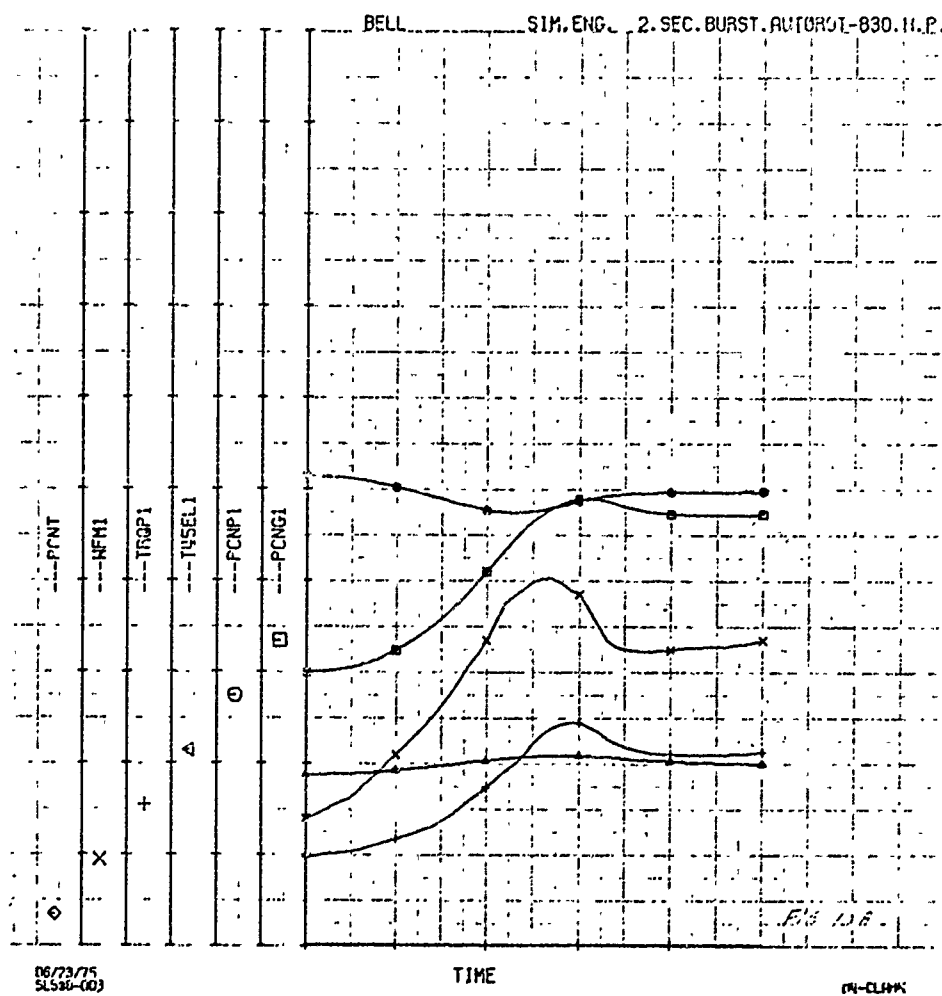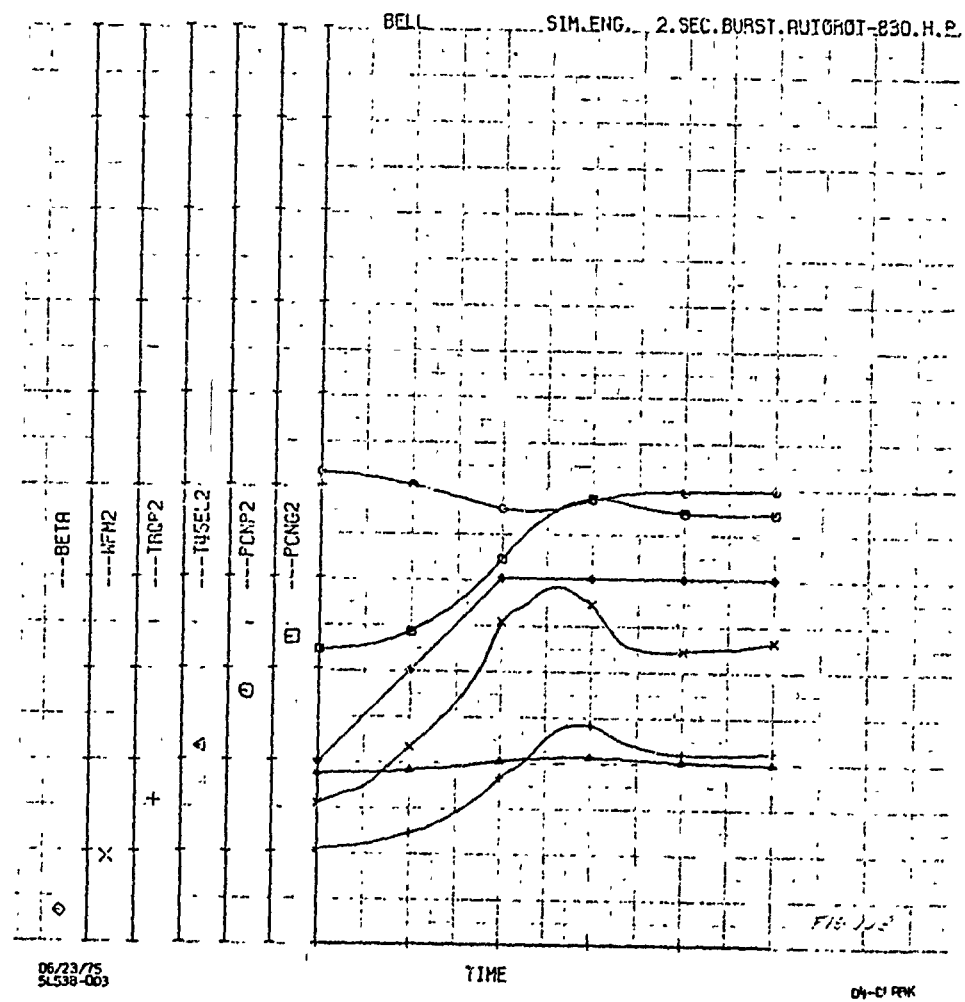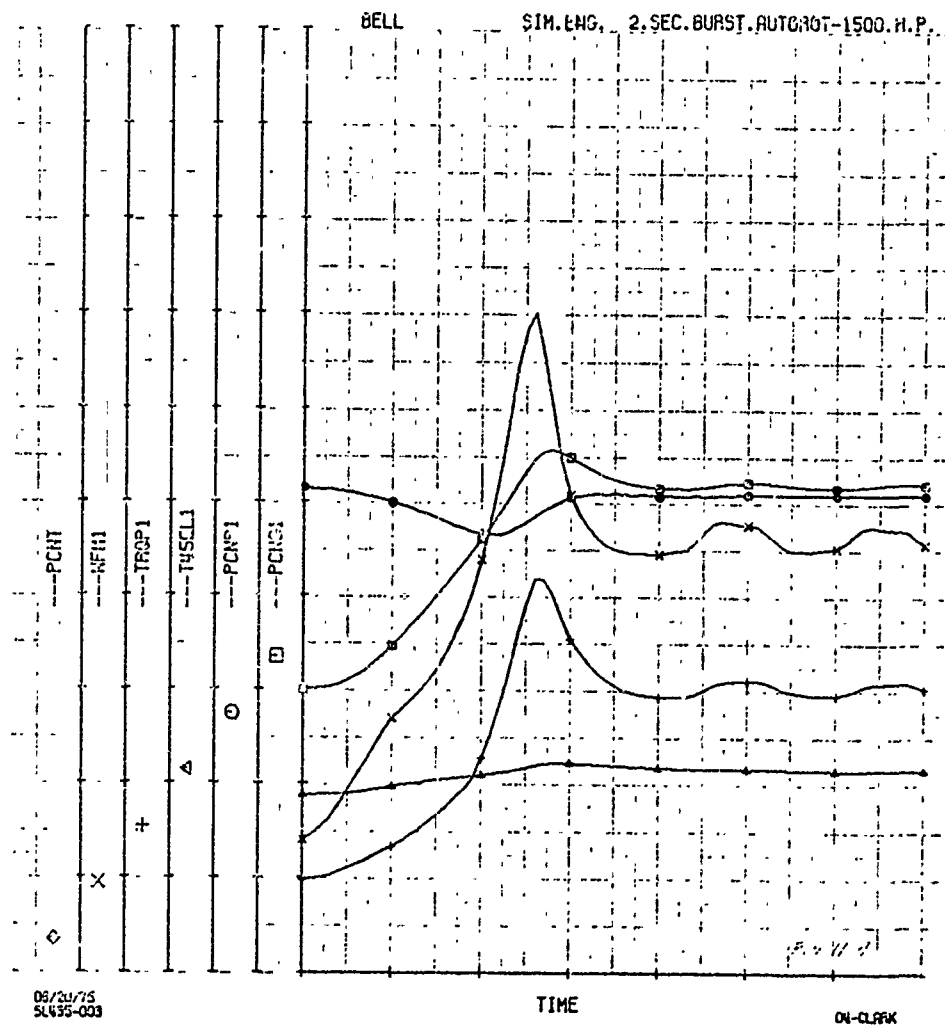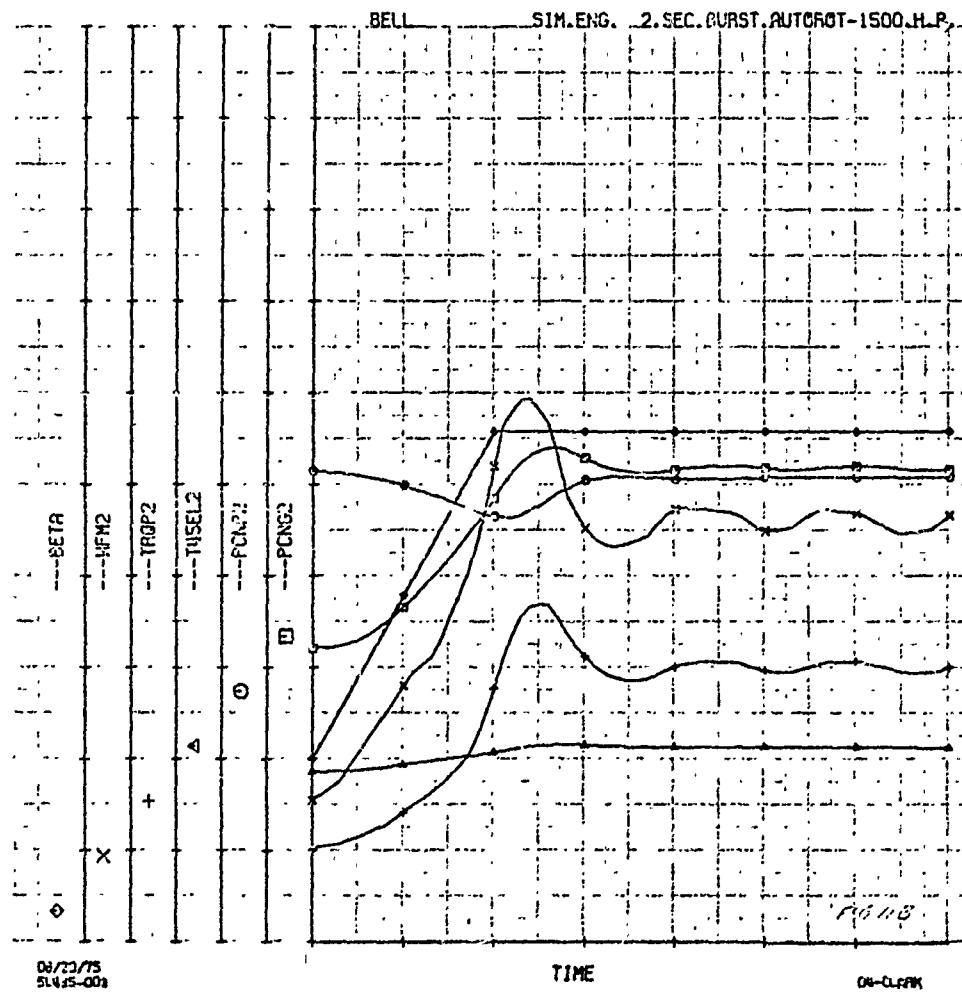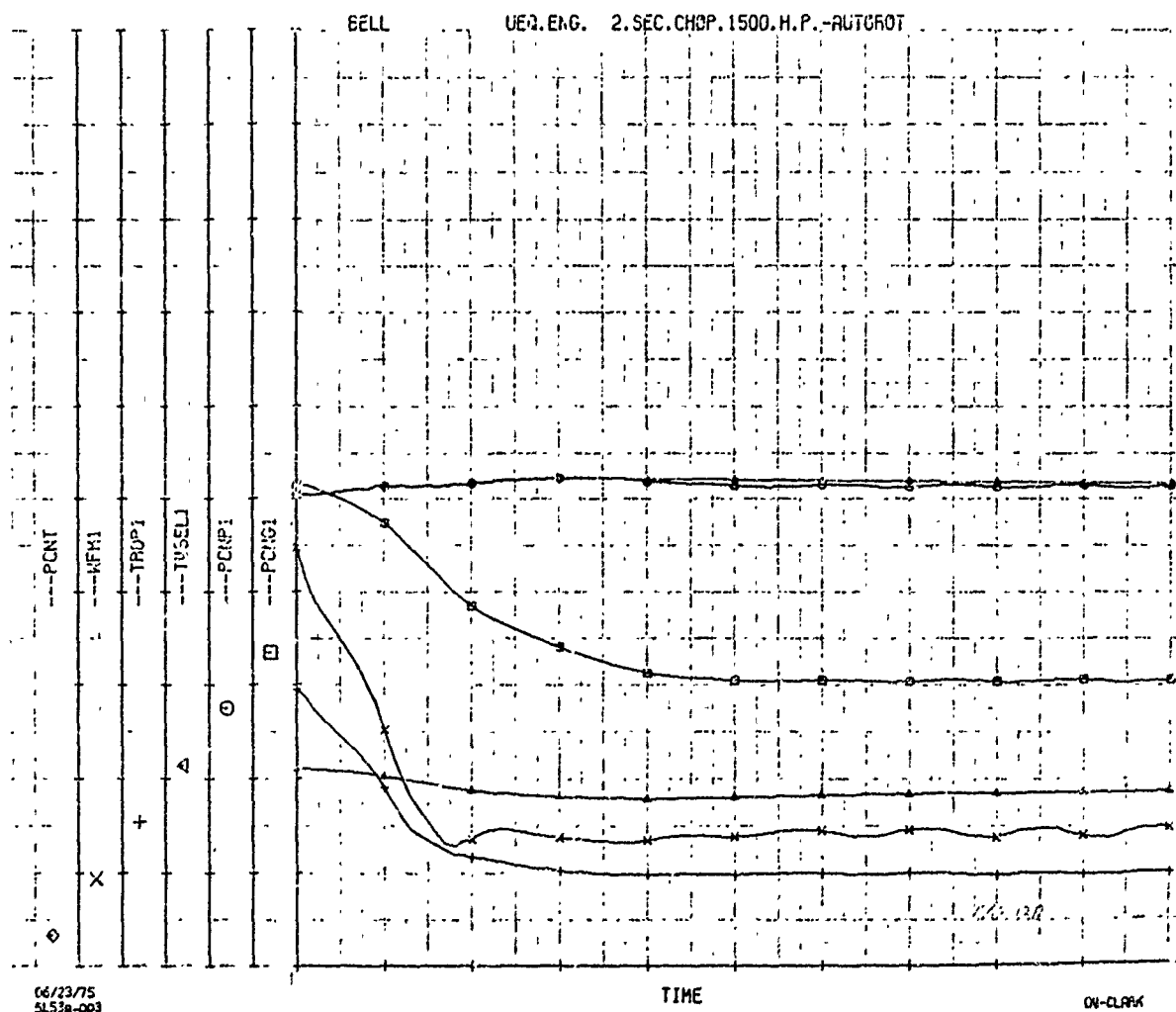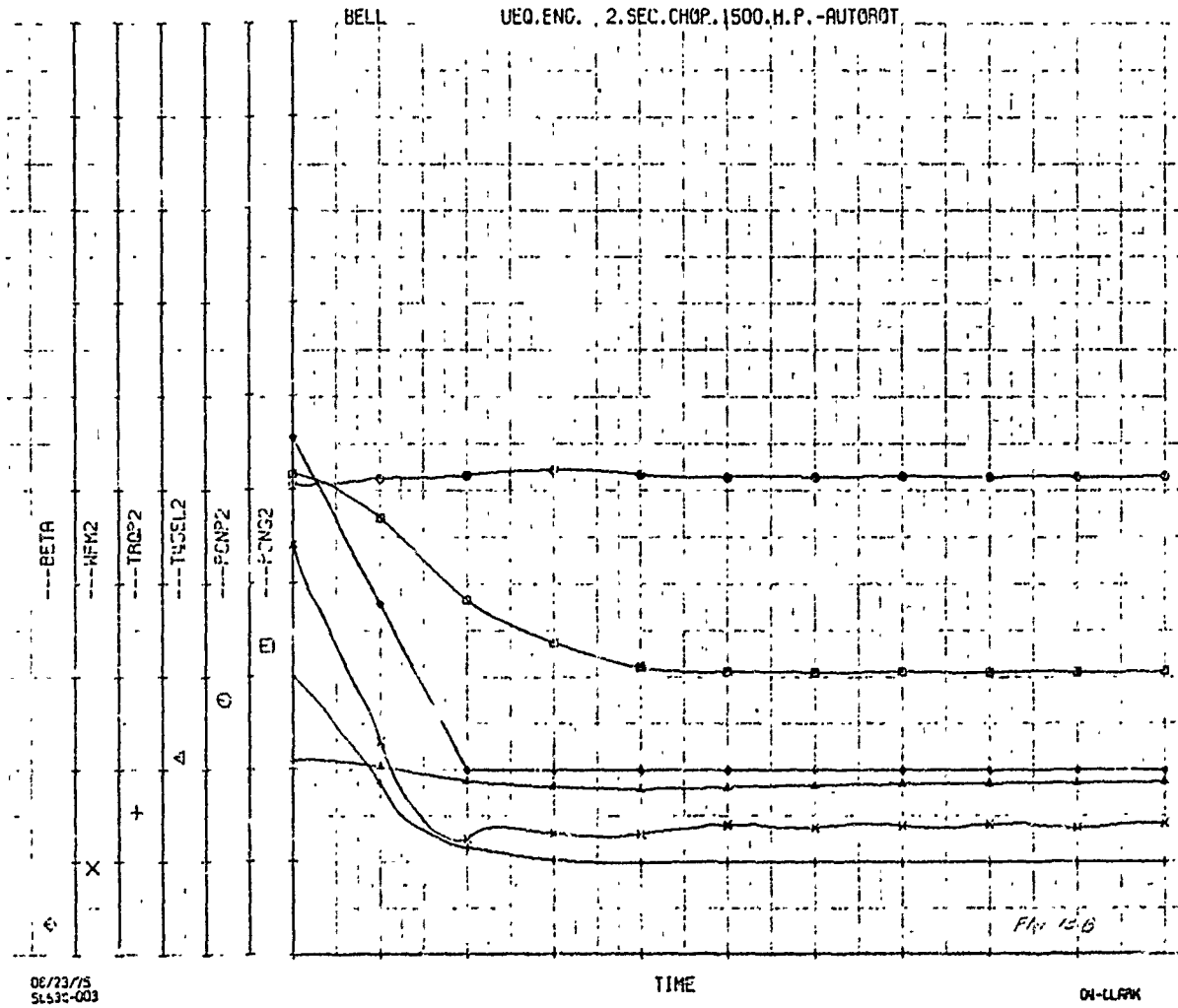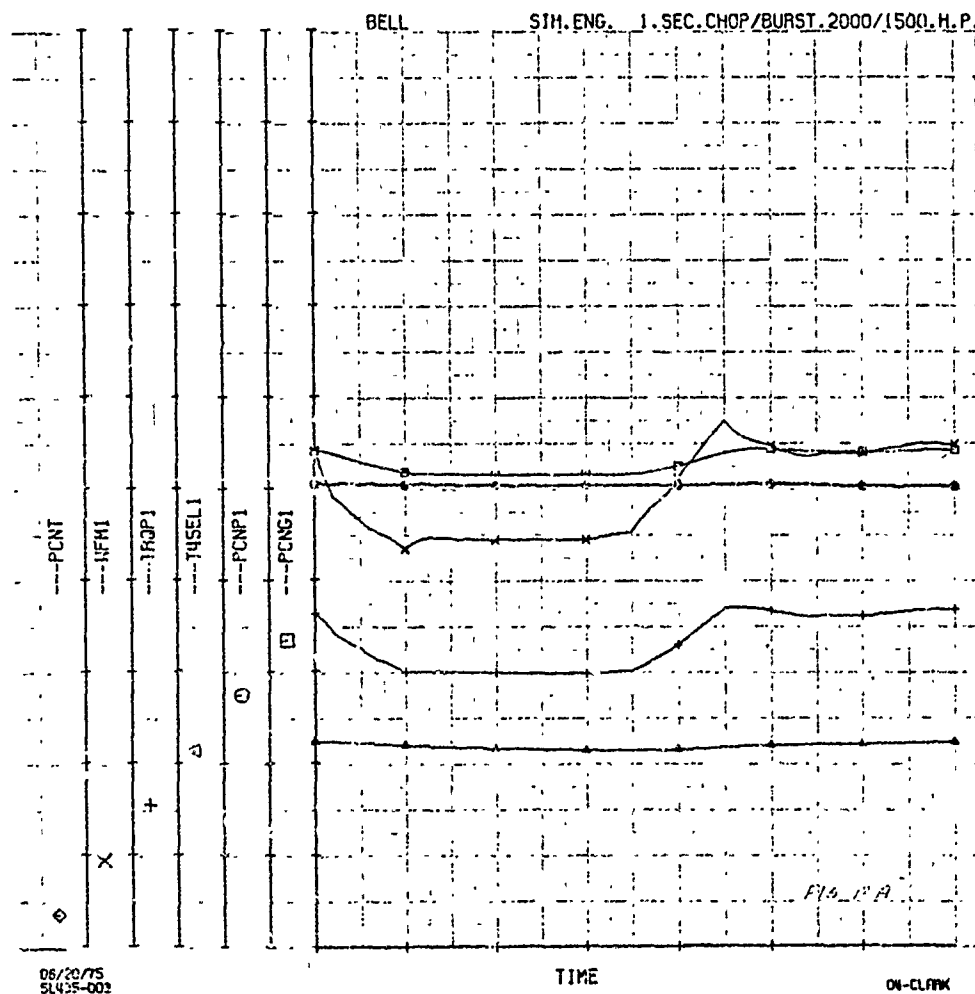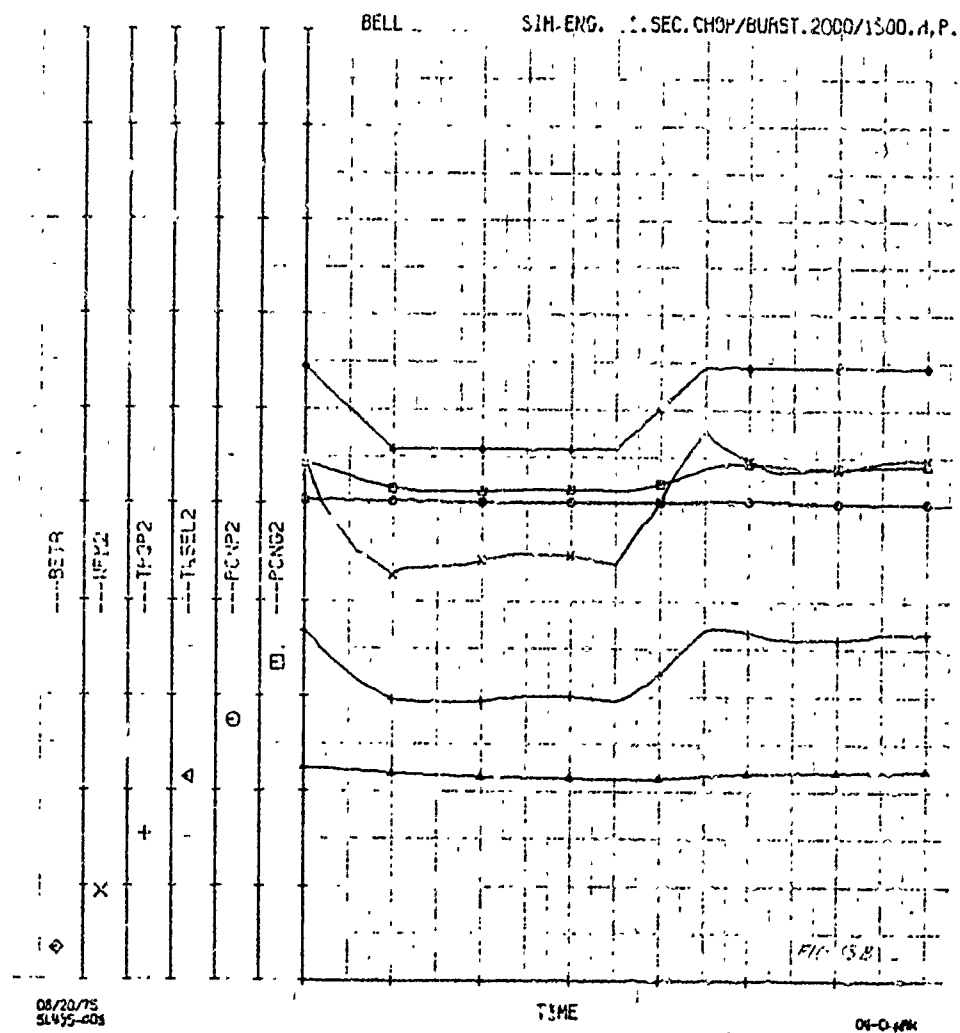
142
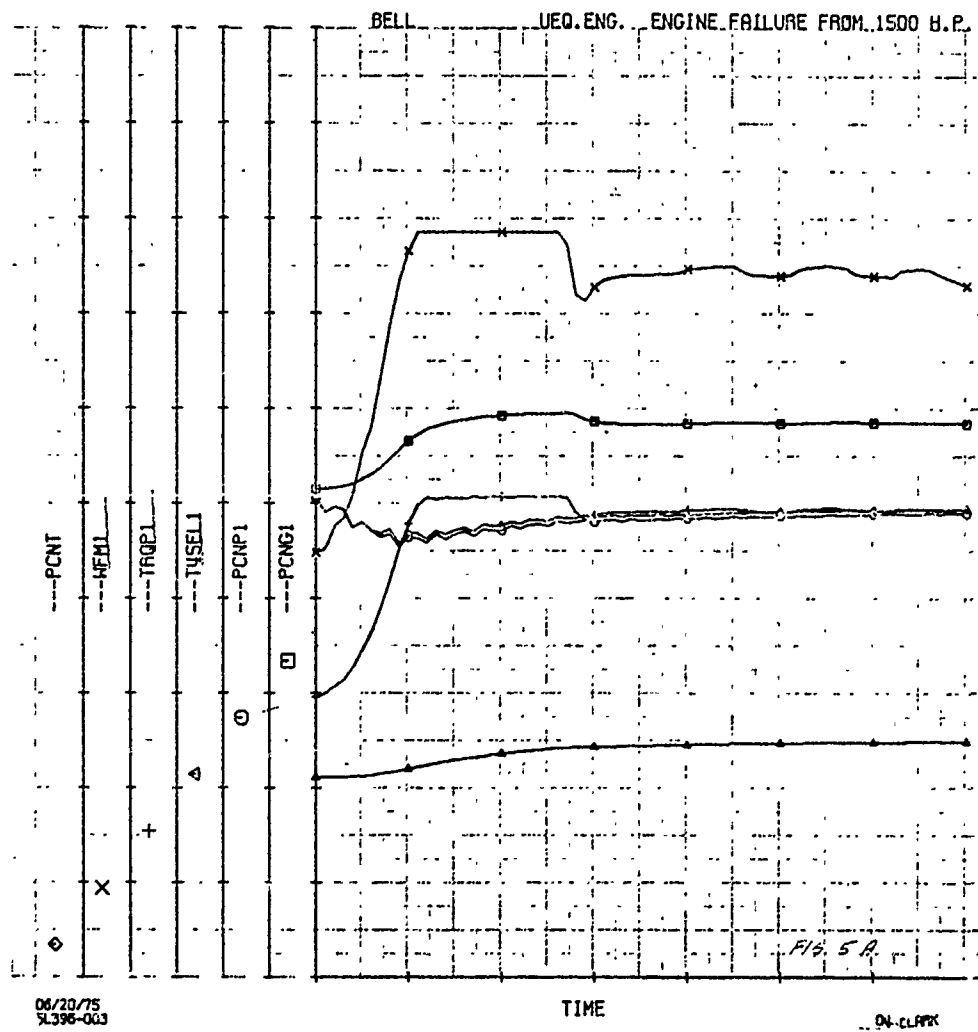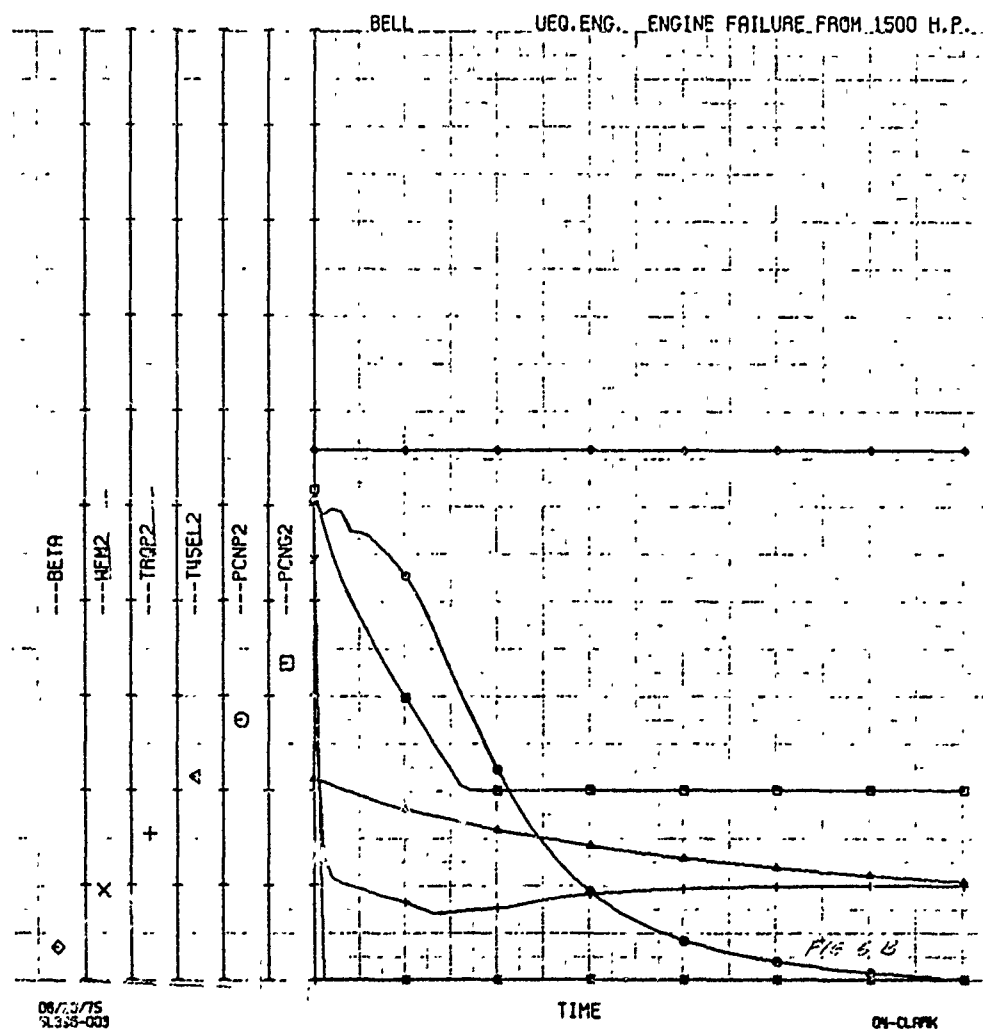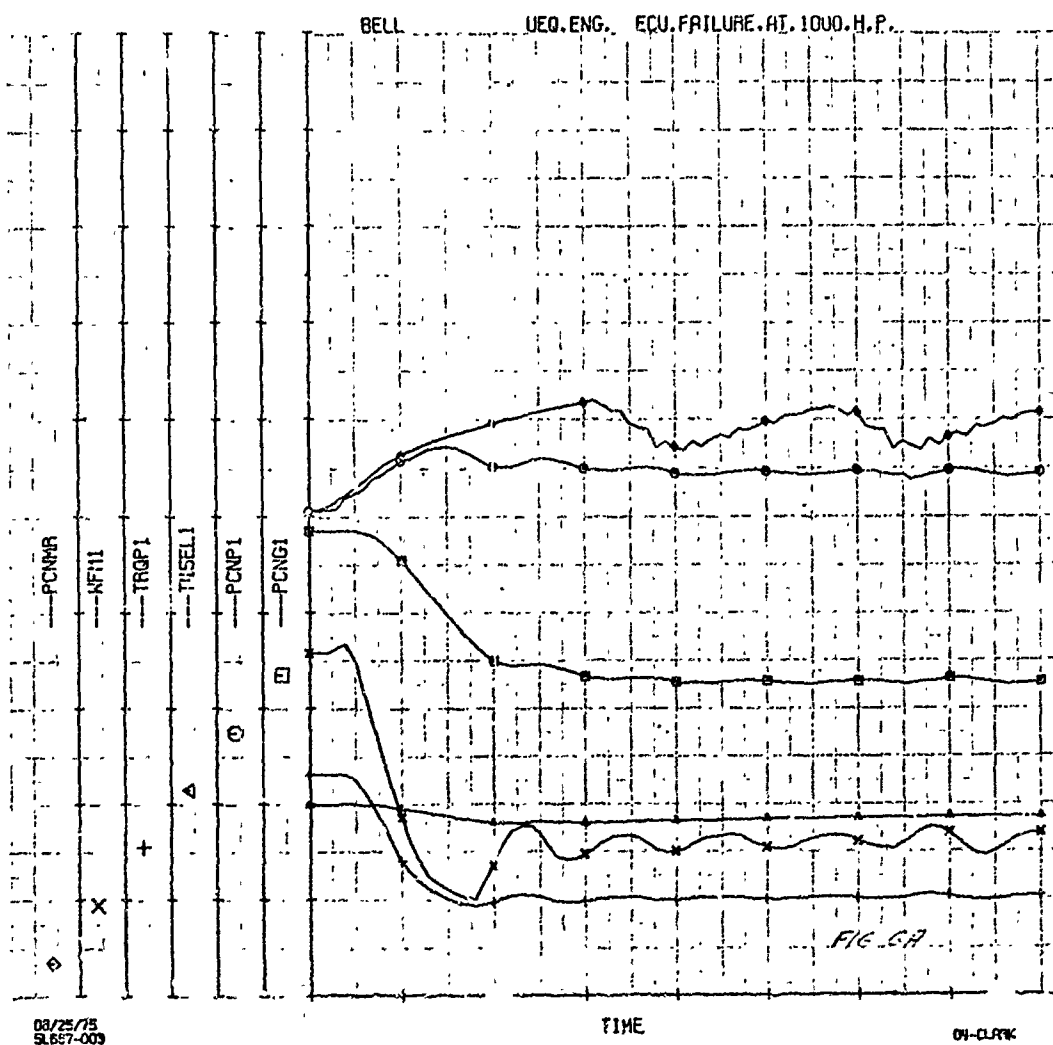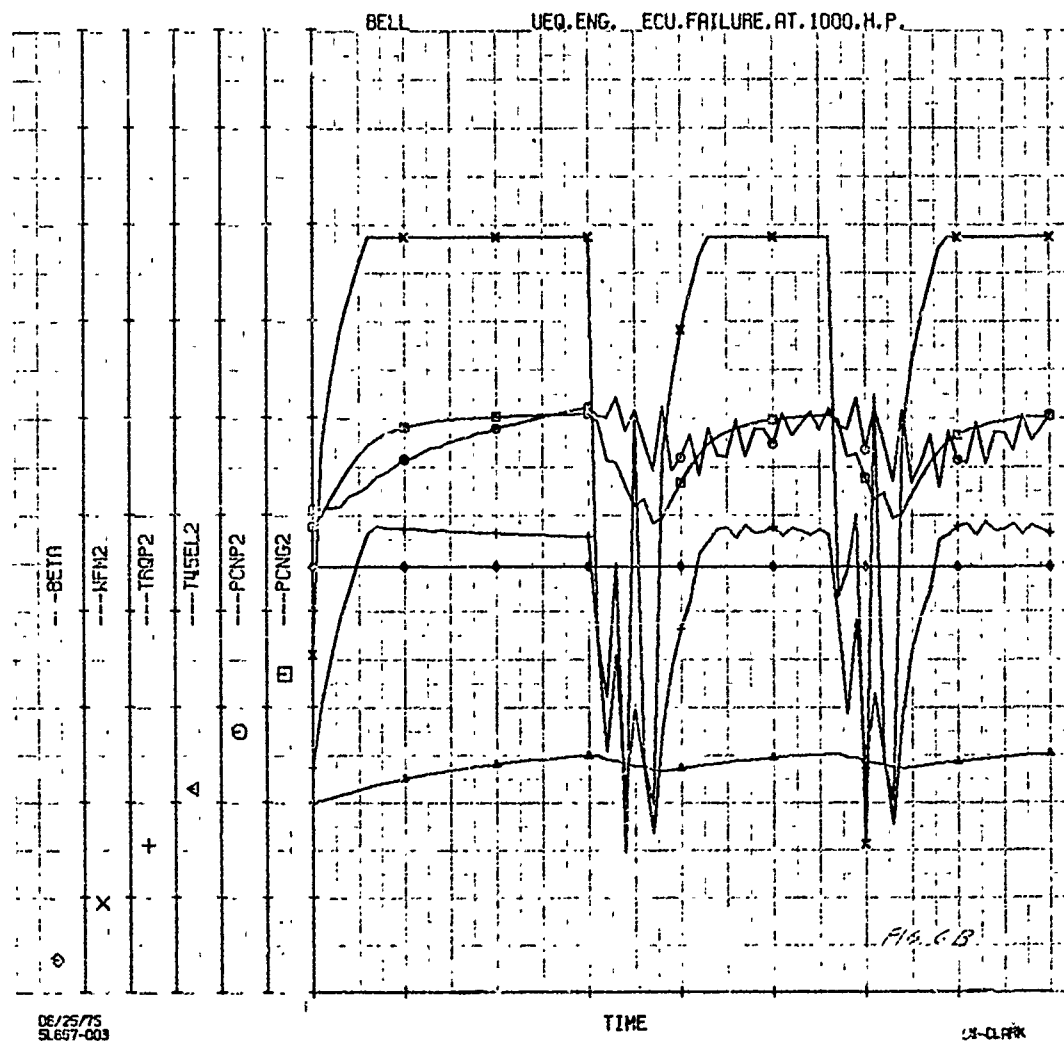
ATTACHMENT 1 TO APPENDIX K

Figure 10A.

ATTACHMENT 1 TO APPENDIX K

Figure 10B.

144

ATTACHMENT 1 TO APPENDIX K

Figure 11A.

145

Figure 11B.

ATTACHMENT 1 TO APPENDIX K

BELL   UEQ.ENG.   2.SEC.CHOP.1500.H.P.-AUTOROT

Figure 12A.

147

Figure 12B.

ATTACHMENT 1 TO APPENDIX K

Figure 13A.
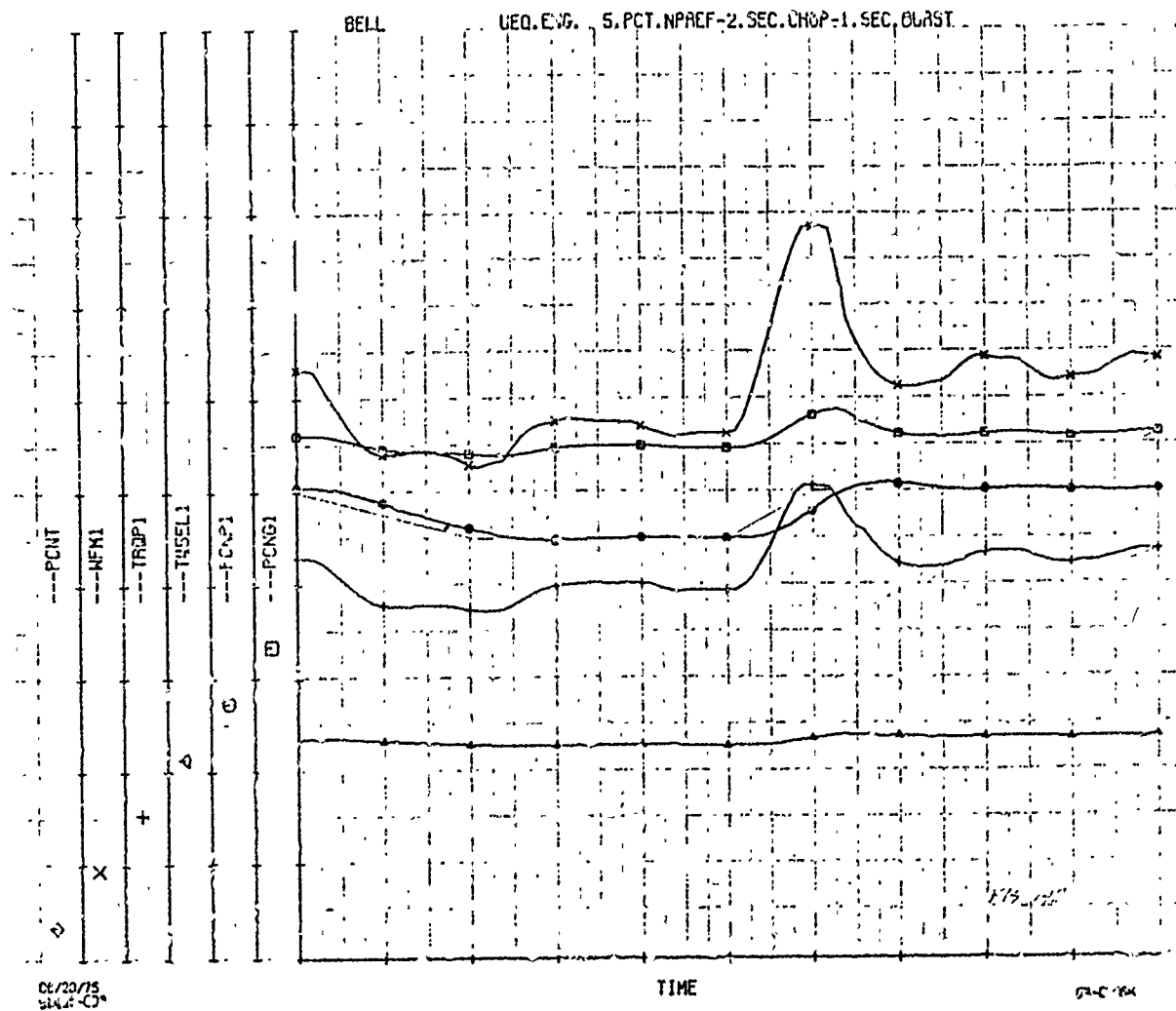
149
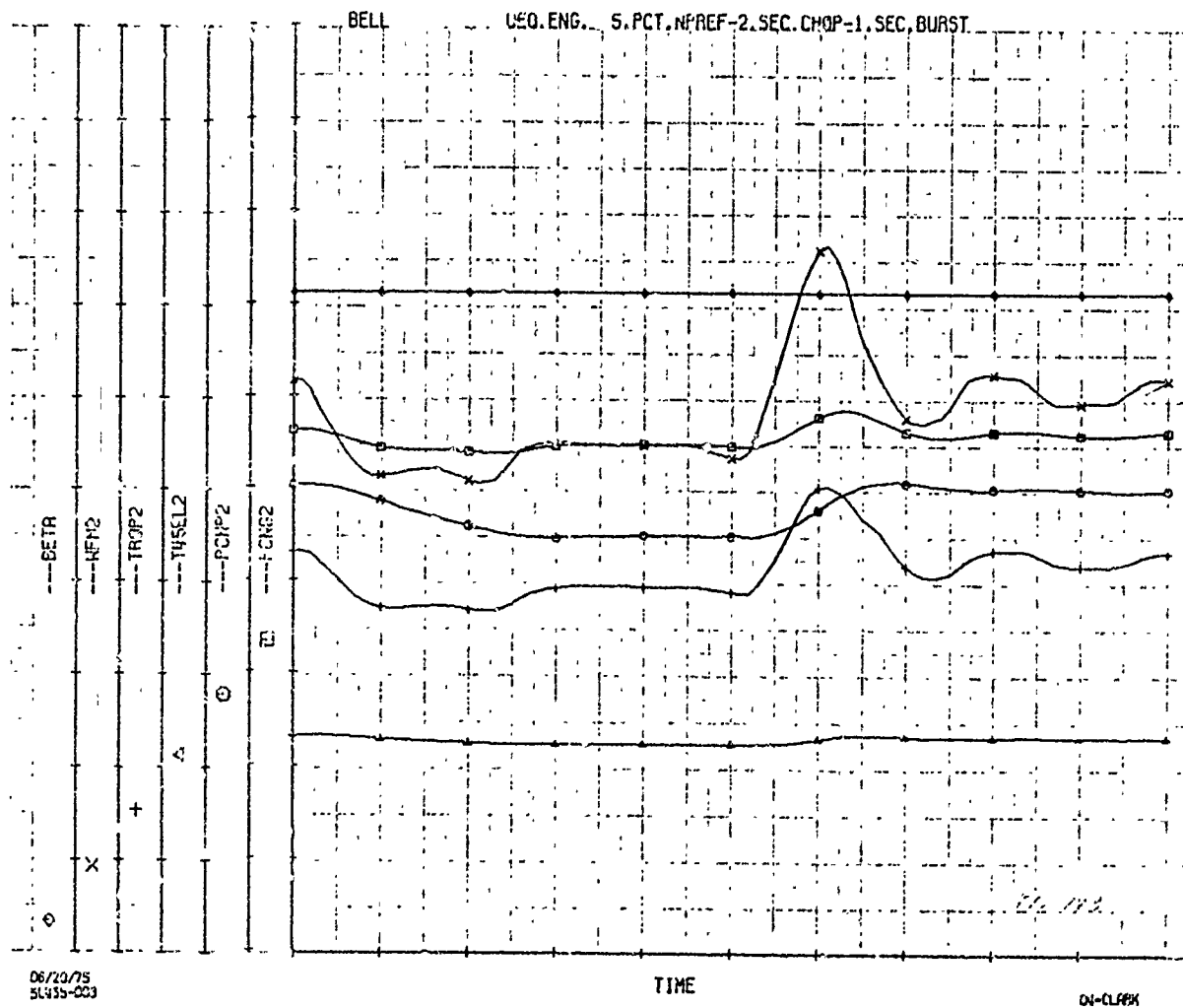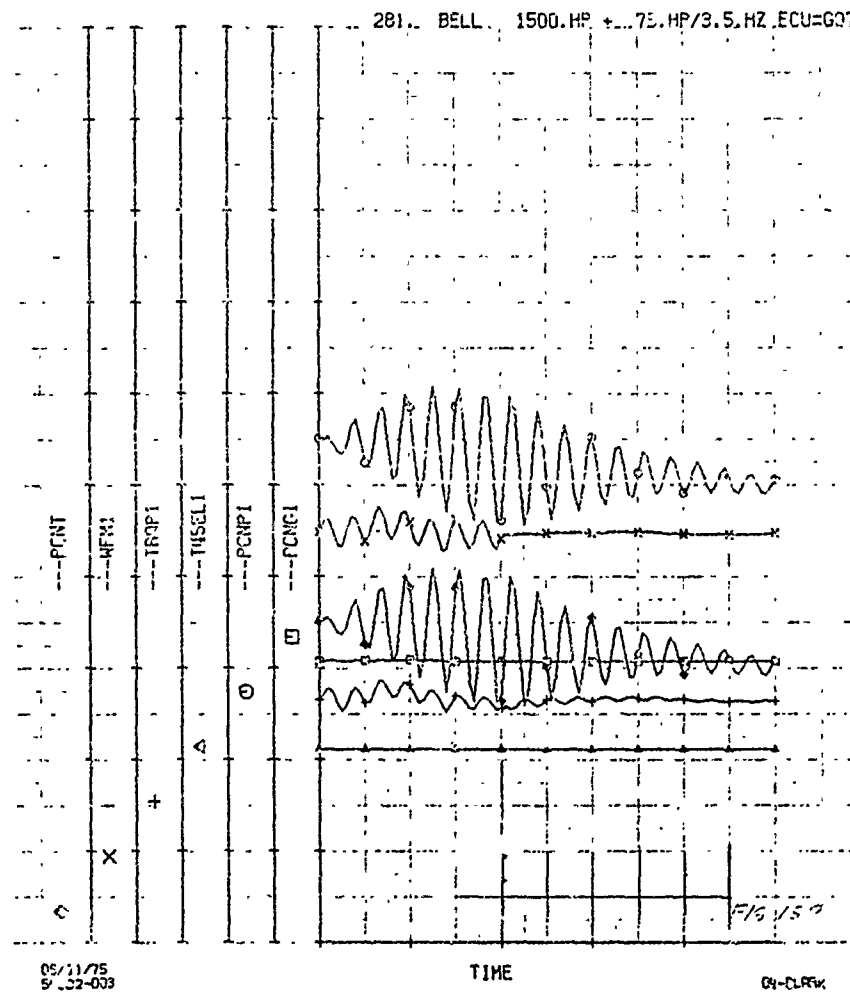
Figure 13B.

Figure 14A.

Figure 14B.
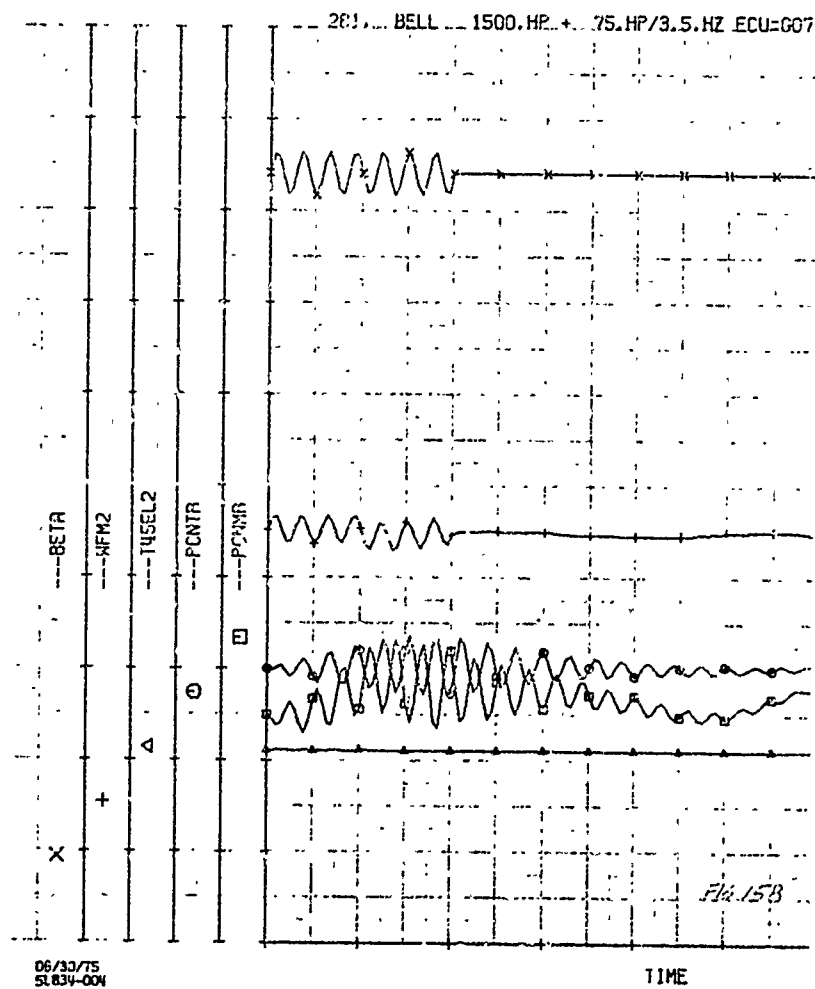
Figure 15A.

Figure 15B.

ATTACHMENT 2 TO APPENDIX K

1

YAH-63/T700/G09 ECU

TORSIONAL STABILITY AND

TRANSIENT RESPONSE ANALYSIS

INTRODUCTION

This report is prepared in response to the SSEB request for
additional clarification in the YAH-63 Propulsion Factor
Technical Negotiations with regard to the following:

Areas of Clarification

4. AAEFA test experienced:

    a. poor rotor speed control during maneuvering
        flight, and

    b. excessive transient rotor speed droop when
        rapid power application from minimum power
        conditions were conducted (i.e., quick stops).
        Should relate to T700 engine control improve-
        ments.

8. Torsional stability analysis per ADS-9A with T700 G09
    ECU necessary for evaluation. GE indicates previous
    design characteristics furnished Bell were to investi-
    gate transient droop, and not suitable for torsional
    stability analysis.

The analysis described herein was conducted by the BHT Structural
Dynamics Group and the Scientific and Technical Computing Group.
The discussions regarding design changes were coordinated with
the Power Plant Group.

Note: Figures 12 through 16 intentionally omitted. Informa-
tion proprietary to engine manufacturer.

155

ATTACHMENT 2 TO APPENDIX K

2

CONTROL HYSTERESIS AND 'STICTION'

The engine/airframe compatibility report, Reference 1, covering the tests conducted at BHT, concludes that:

> Significant N_2 droop occurred during rapid jump take-offs and during recoveries from autorotation to power...

which substantially agrees with the AAEFA test results, and recommended that:

> The fuel control/governor be evaluated in order to improve the droop characteristics.

It is BHT's understanding that the YAH-63 rotor speed droop is somewhat greater than other AVM's. Two areas which may affect this characteristic are:

1. the fuel control response characteristics, and

2. hysteresis or lost motion in the control linkage to the engine load demand spindle (LDS).

Since Item 1 is common to all AVM's, i.e., all are using the G07 controls during Phase 1 GCT, the control hysteresis was considered suspect and was, therefore, evaluated in detail. It was determined by measurement of LDS angle versus collective pitch that an amount of hysteresis, although small, did exist on Ship 22002 while that on Ship 22003A was significantly greater.

BHT has also reviewed the information supplied by Reference 2, included herein in Addendum I, which shows evidence of apparent 'stiction' in the LDS control system.

156

3

ANALYSIS

BHT conducted a nonlinear analysis of the YAH-63 helicopter with the preliminary T700 G09 ECU parameters provided by GE, Figure 1 and Table I.

The analysis evaluated the following:

1. The rotor speed transient droop characteristics for rapid power applications from minimum power conditions, such as might occur in quick stop maneuvers and evaluated the effect of hysteresis in the LDS versus collective pitch schedule. The droop of the G09 ECU was compared with the G07 ECU, Reference 3.

2. The torsional stability of the combined engine, rotor, drive system, and fuel control system.

The analysis was based on:

1. preliminary T700 G09 ECU parameters provided by GE,

2. YAH-63 drive system and rotor inertia parameters defined by the Phase 2 proposal and modified by all applicable EOC's and PDV's, and

3. LDS angle versus collective pitch angle hysteresis measured on Ships 22002 and 22003A.

The method of representing the LDS angle hysteresis is shown in Figure 2.

Note: Figures 1 and 2 and Table I intentionally omitted. Information proprietary to engine manufacturer.

RESULTS

Comparison of G07 and G09 Control Transient Droop Characteristics

For idealized control linkage (no hysteresis), the transient rotor speed droop of the preliminary G09 control was compared with that determined for the G07 control in Reference 3.

For these cases, the helicopter was trimmed and the rotor speed set at 100 percent rpm. Ramp inputs of duration from 1 to 5 seconds were applied originating at a collective setting for minimum power and leveling off at 50, 70, and 90 percent of the transmission limit power of 2791 horsepower.

For this baseline case, the schedule of LDS versus collective angle are as shown in Figure 3.

The results are shown in Figure 4. As can be seen, significant reductions in rotor speed droop, on the order of 2 percent for a 2 second ramp, are obtained.

Effect of Hysteresis

The hysteresis of the main rotor blade root collective angle versus LDS angle was measured on each the left and right engines on Ships S/N 22002 and S/N 22003A on 13 September 1976 at Edwards Air Force Base. These data are shown in Figure 5 for Ship 22002 and in Figure 6 for Ship 22003A. Note that for Ship 22003A, the hysteresis for both engines is on the order of 10 degrees LDS while Ship 22002 hysteresis for both engines is on the order of 3.5 degrees LDS angle.

The simulated hysteresis for Ship 22002 is shown in Figure 5 which, except for the extreme collective values, gives reasonable approximation. The simulated hysteresis for Ship 22003A is shown in Figure 6, which again gives a reasonable approximation.

For Ship 22002, the results of the hysteresis evaluation are shown in Figure 7 which compares the G09 ECU with idealized control linkage to that obtained with the simulated hysteresis.

The effect of this hysteresis loop moderately increases the droop by as much as 1.0 percent for a 2 second ramp time. For ramp times of 1 second or more, the trend was toward increased droop.

Figure 3. Baseline Collective vs LDS Relationship.

Figure 4.   Transient Droop Characteristics of
G07 and G09 ECU Controls with
Idealized Control Linkage.
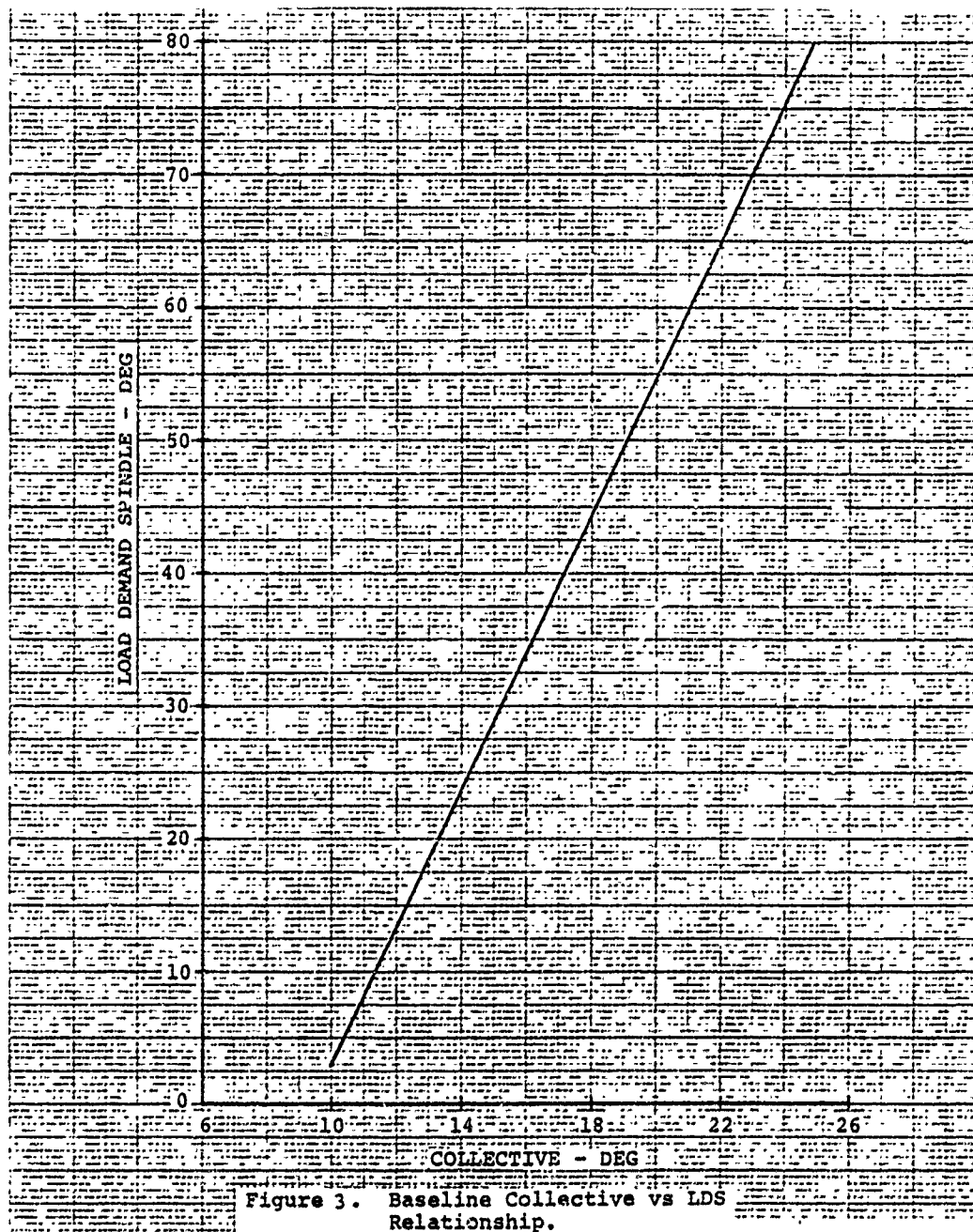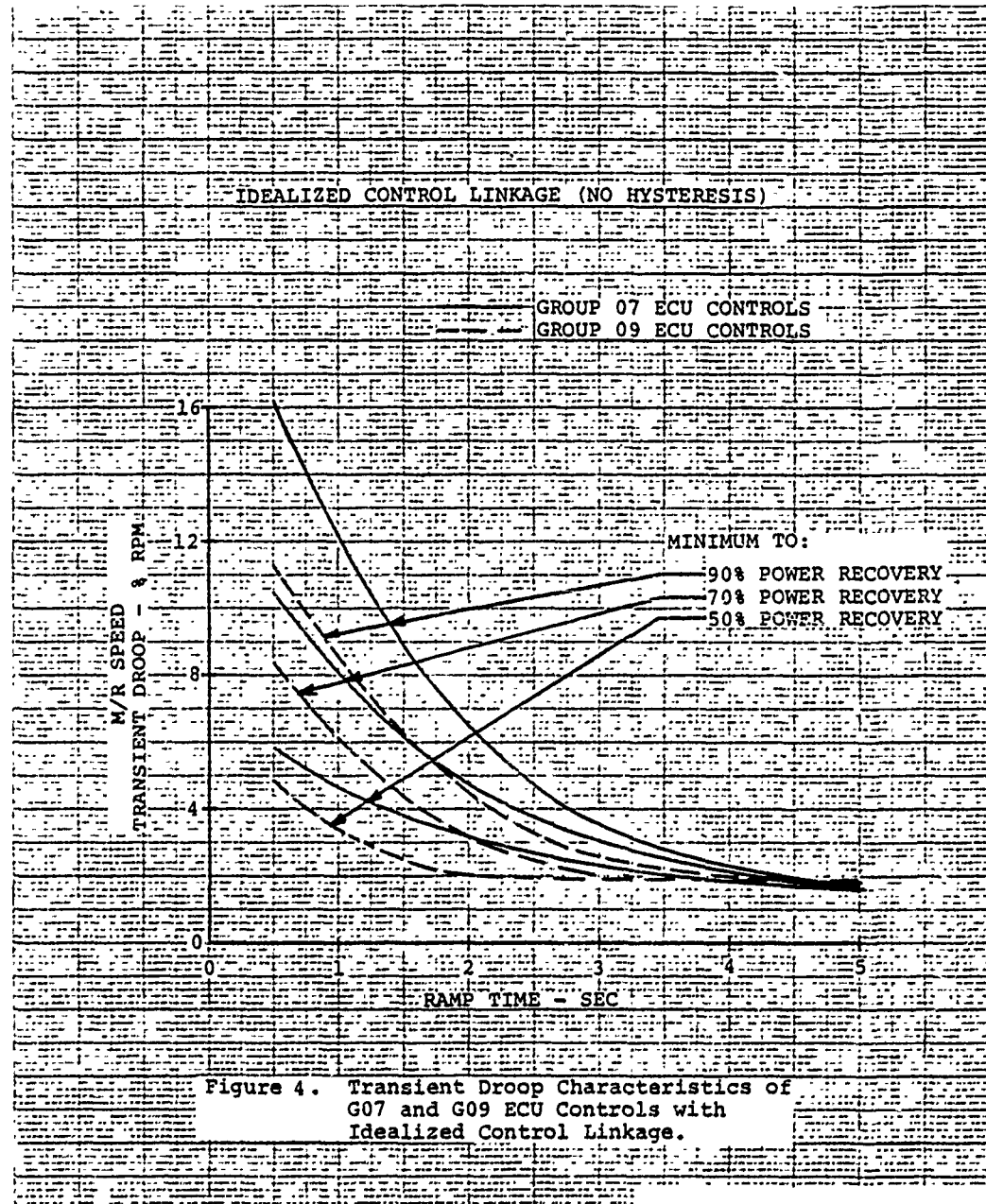
Figure 5. Ship #22002 Control Hysteresis.

Figure 6. Ship #22003A Control Hysteresis.

Figure 7. Hysteresis Effect on Droop Characteristics for Ship #22002.
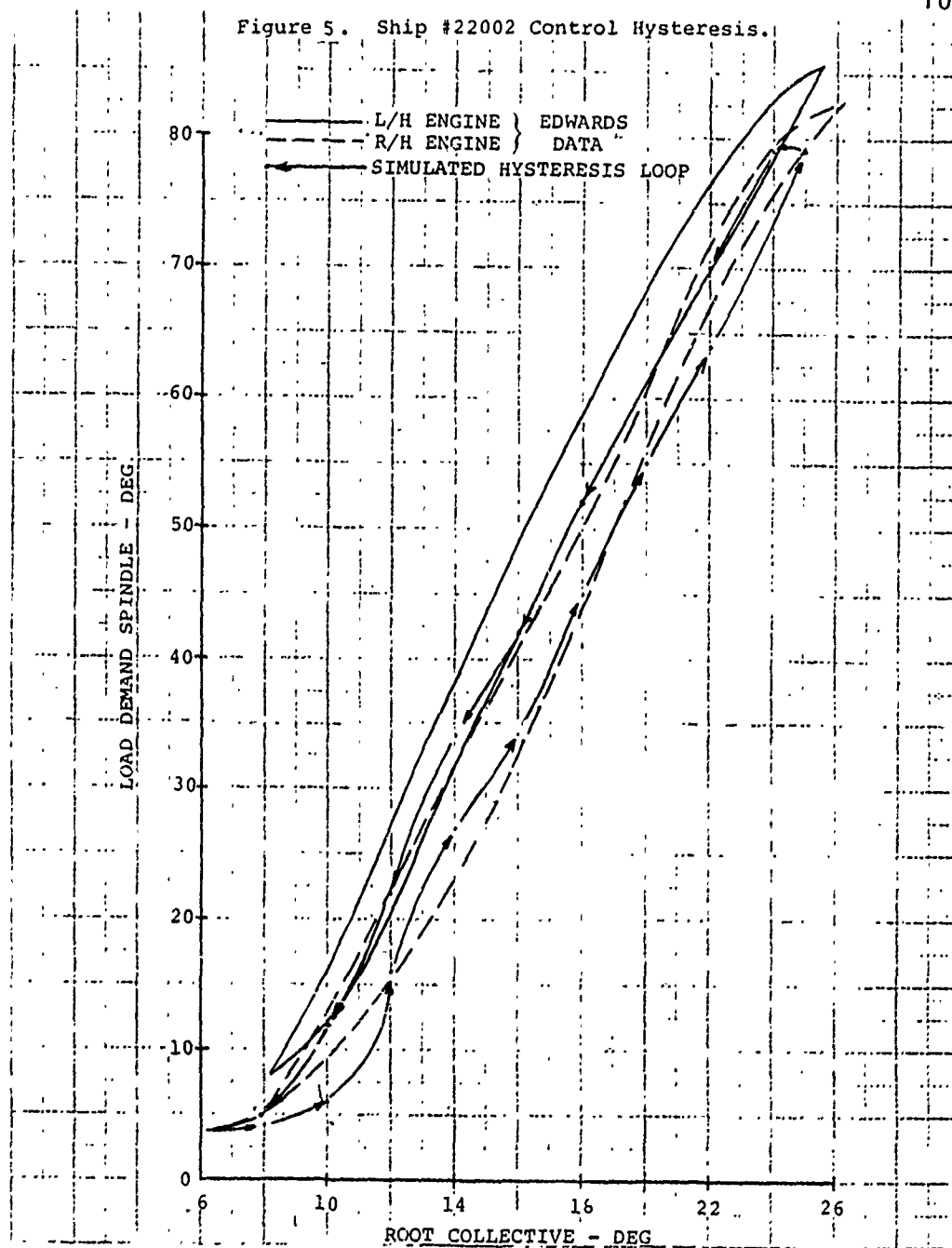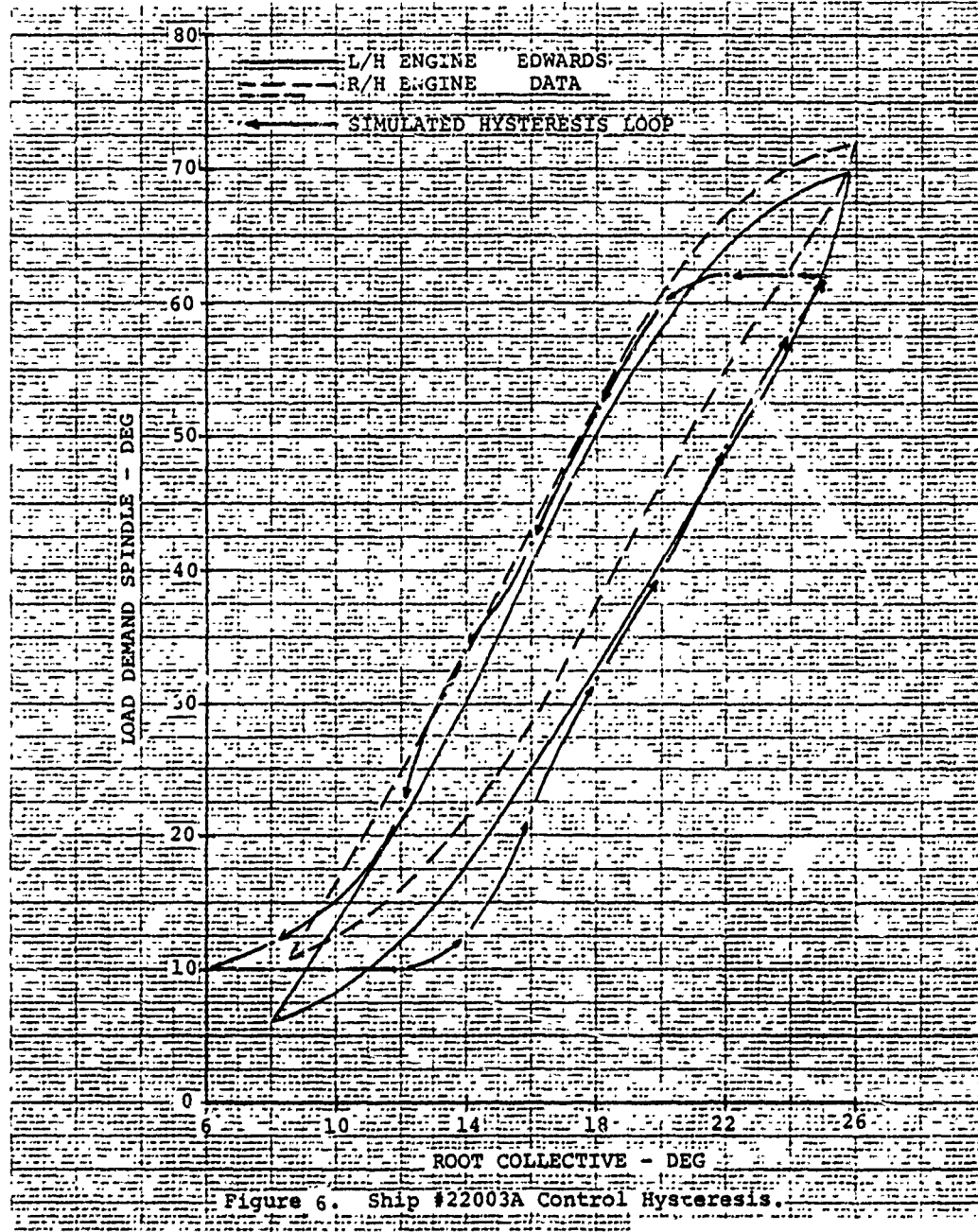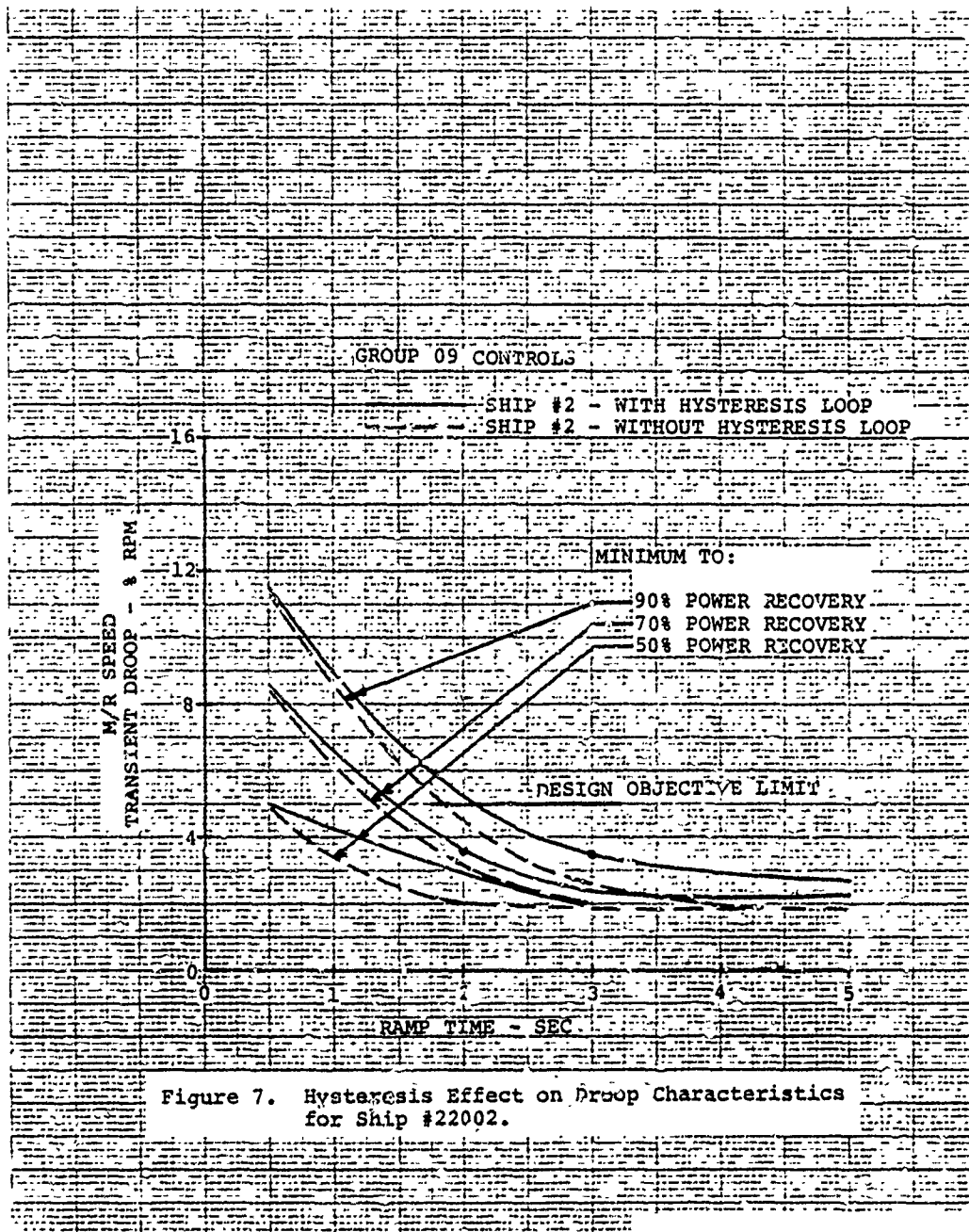
For Ship 22003A, the results of a similar evaluation are shown in Figure 8. The effect of this hysteresis loop significantly increases the droop values and these values are higher than those for Ship 22002. For example, in this case, the increase in droop due to hysteresis was on the order of 3.5 percent for a 2 second ramp time.

Experience has indicated that in addition to the droop magnitude, the duration of the droop beyond the normal rotor limits can affect the opinion of the pilots. Therefore, the duration of the droop below -5% was computed for various power recovery conditions considering the no-hysteresis, Ship 22002 hysteresis, and Ship 22003A hysteresis configurations. These results are tabulated in Table II. Generally, the duration of the droop below -5% is directly proportional to the power recovery and inversely proportional to the collective input ramp time.

The poor rotor speed control during maneuvering flight was observed to occur in the computer simulation, as shown in Figure 9. The steady state rotor speed set error for a specific collective setting increased with increasing LDS angle hysteresis. When collective maneuvers were executed, the speed set error from initiation to completion of the maneuver increased with increasing hysteresis.

A summary of the calculated rotor speed droop of Phase 1 aircraft with the G07 controls with that of the Phase 2 aircraft with the G09 controls and the engine control production design variance are compared in Figure 10. Data pertaining to the droop values for G07 ECU combined with the simulated Ship 22002 hysteresis and Ship 22003A hysteresis is discussed in a later section,

Torsional Stability of G09 ECU

The torsional stability of the preliminary G09 ECU control parameters were evaluated for a power sweep from 40 to 100 percent of transmission limit power. The results are shown in Table III and compared with the values obtained for the G07 controls, Reference 3.

The effect of the LDS angle hysteresis on stability was checked and found to be zero, as would be expected. However, it was noted that the magnitude of collective stick motion had to be increased to obtain the same magnitude of response.
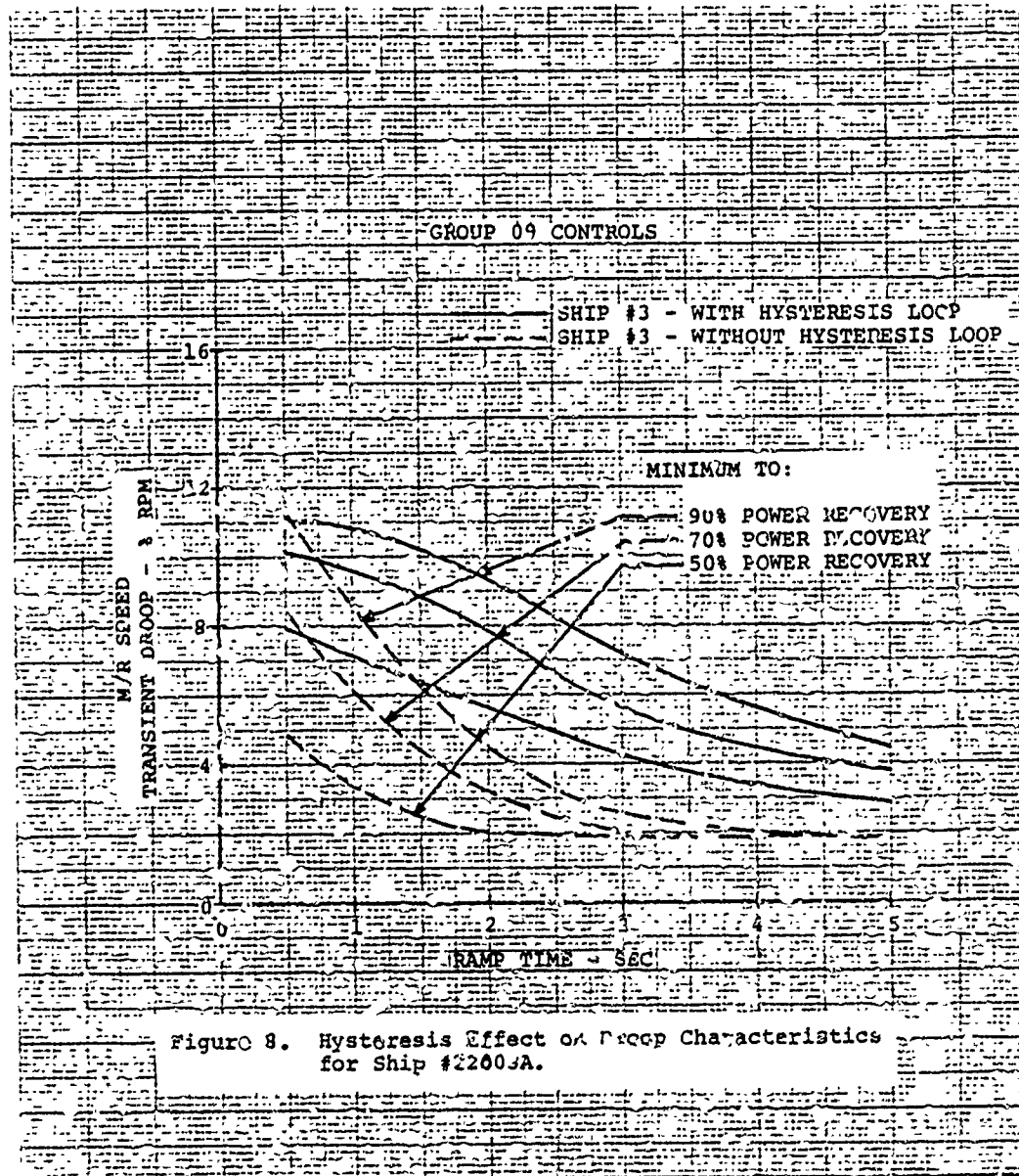
Figure 8. Hysteresis Effect on Droop Characteristics for Ship #2260JA.

TABLE II.   COMPARISON OF DURATION OF
ROTOR DROOP BELOW 95% N_R

RAMP TIME (SEC)	DURATION OF ROTOR SPEED BELOW 95% - SECONDS								
	50% Power Recovery Hysteresis			70% Power Recovery Hysteresis			90% Power Recovery Hysteresis		
	None	#3	#2	None	#3	#2	None	#3	#2
1	0	1.00	0	0.73	1.50	0.9	1.5	1.90	1.60
2	0	0.50	0	0	1.30	0	0	1.70	0.50
3	0	0	0	0	0.75	0.	0	1.30	0
4	0	0	0	0	0	0	0	0.70	0
5	0	0	0	0	0	0	0	0	0
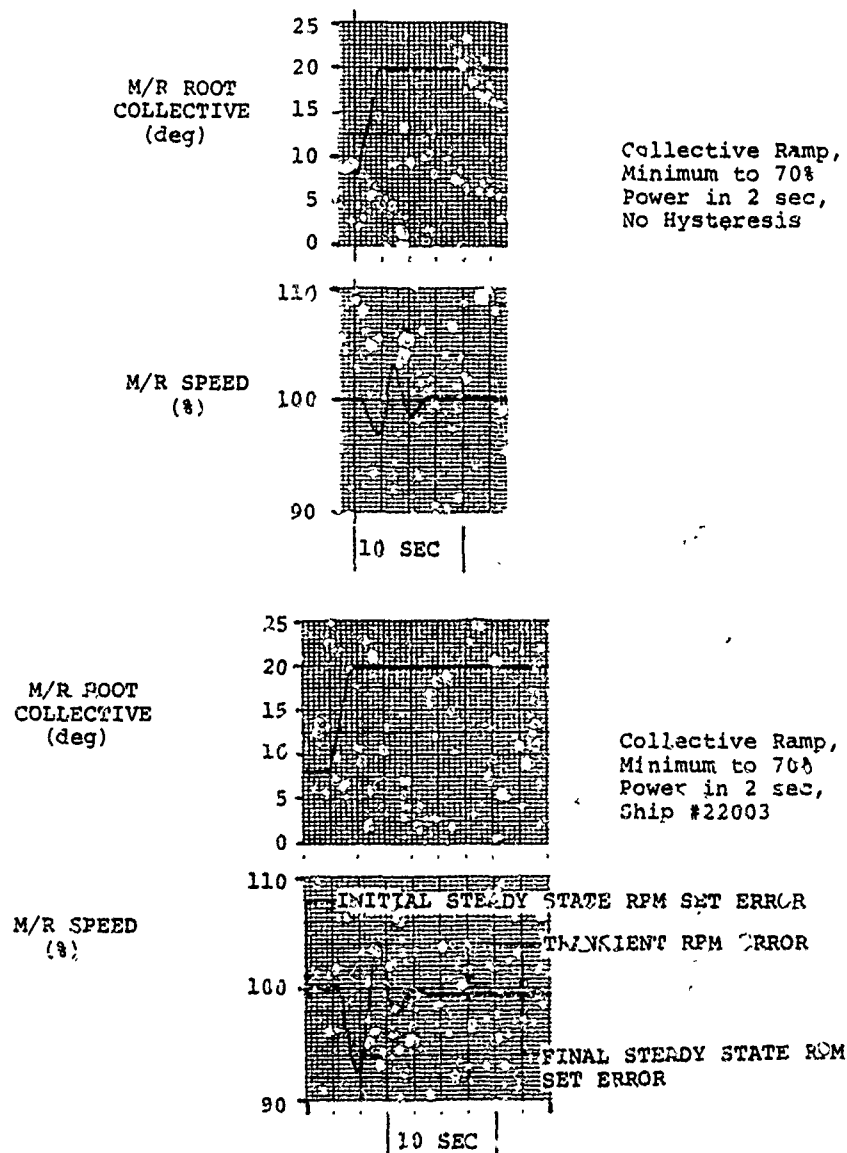
Figure 9. Collective Acceleration Traces Showing Rotor
Speed Error as a Function of Hysteresis.

167
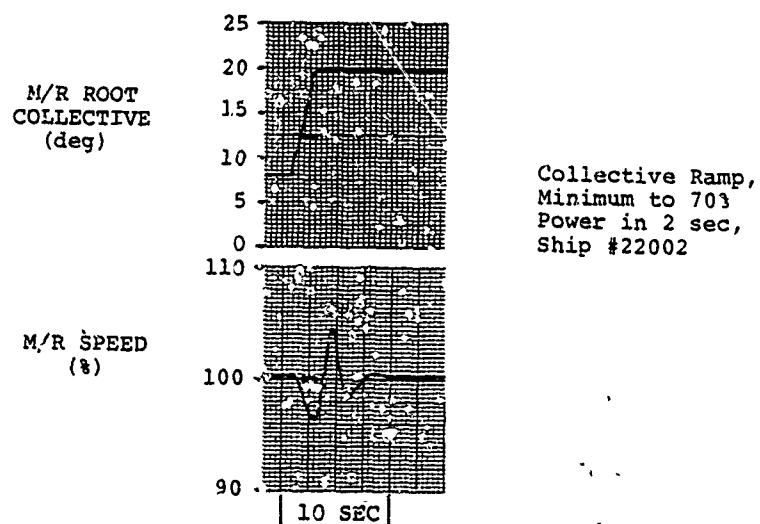
Figure 9. (continued)

ATTACHMENT 2 TO APPENDIX K

Figure 10. Comparison of Rotor Droop for Phase 1 and Phase 2 Airvehicles (2 Sec Ramp, Minimum to 90% Power)

PHASE 1 CONFIGURATION
(G07 ECU Control)

PHASE 2 CONFIGURATION
(G09 ECU and PDV 24AMA00-301)

HYSTERESIS
%
10
0

HYSTERESIS
%
3.5
0

HYSTERESIS
%
3.5
0

SHIP
22002

SHIP
22003

ALL SHIPS

15

10

5

0

Percent
Rotor Speed
Droop

169
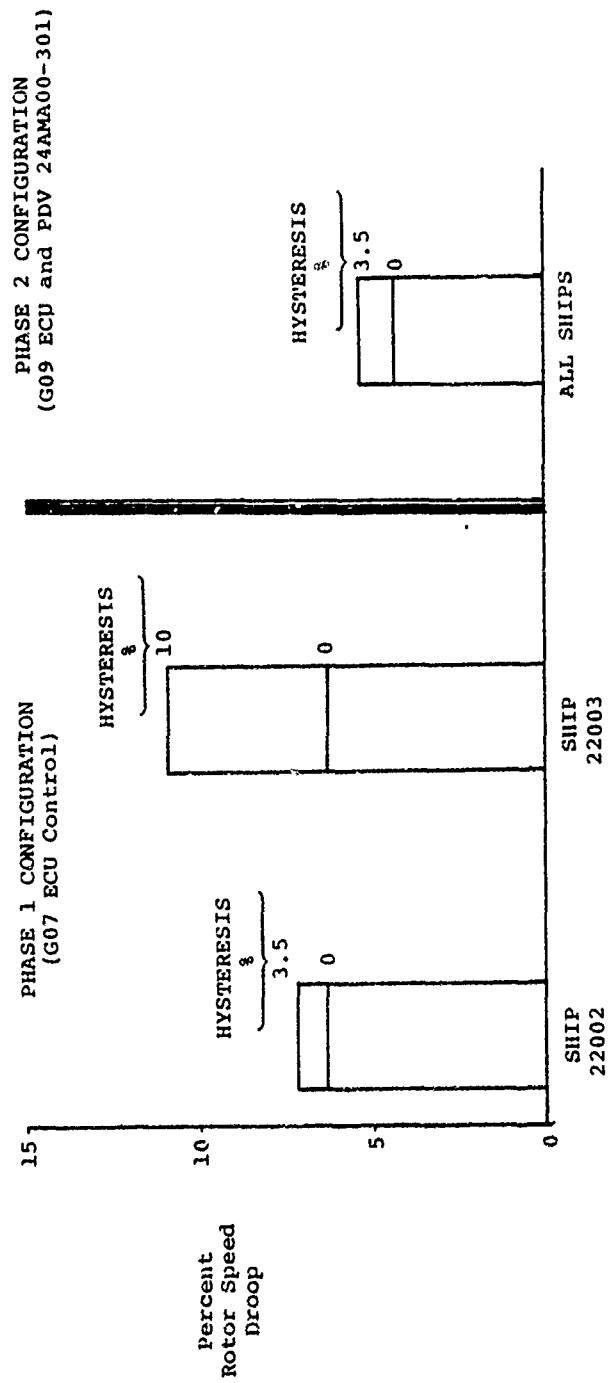
19

TABLE III.   TORSIONAL STABILITY OF
GROUP G09 ECU CONTROLS

Power Level %		Damping at the first torsional mode		
		No Hysteresis	Ship #22002 Hysteresis	Ship #22003A Hysteresis
20		2.303	2.158	1.982
40		2.032	2.058	1.954
60		2.002	1.967	1.918
80		1.985	1.973	1.905
100		1.952	1.995	1.823

ATTACHMENT 2 TO APPENDIX K

20

CORRELATION WITH GE ANALYSIS

A study was made of the rotor speed droop versus the LDS angle
hysteresis for a 2-second ramp from minimum to 2000 SHP.

These data are in good agreement in both magnitude and trend
with the results of a similar analysis conducted by GE using
the G07 controls, also shown in Figure 11. This figure shows
that for a reduction of hysteresis to 50% of that measured on
Ship 22002 a reduction in droop of 0.7% can be achieved for
this maneuver.

The traces supplied by GE are shown in Figures 12 through 16.

171

21

Figure 11. Comparison of BHT/G09 ECU with GE/G07 ECU Analyses
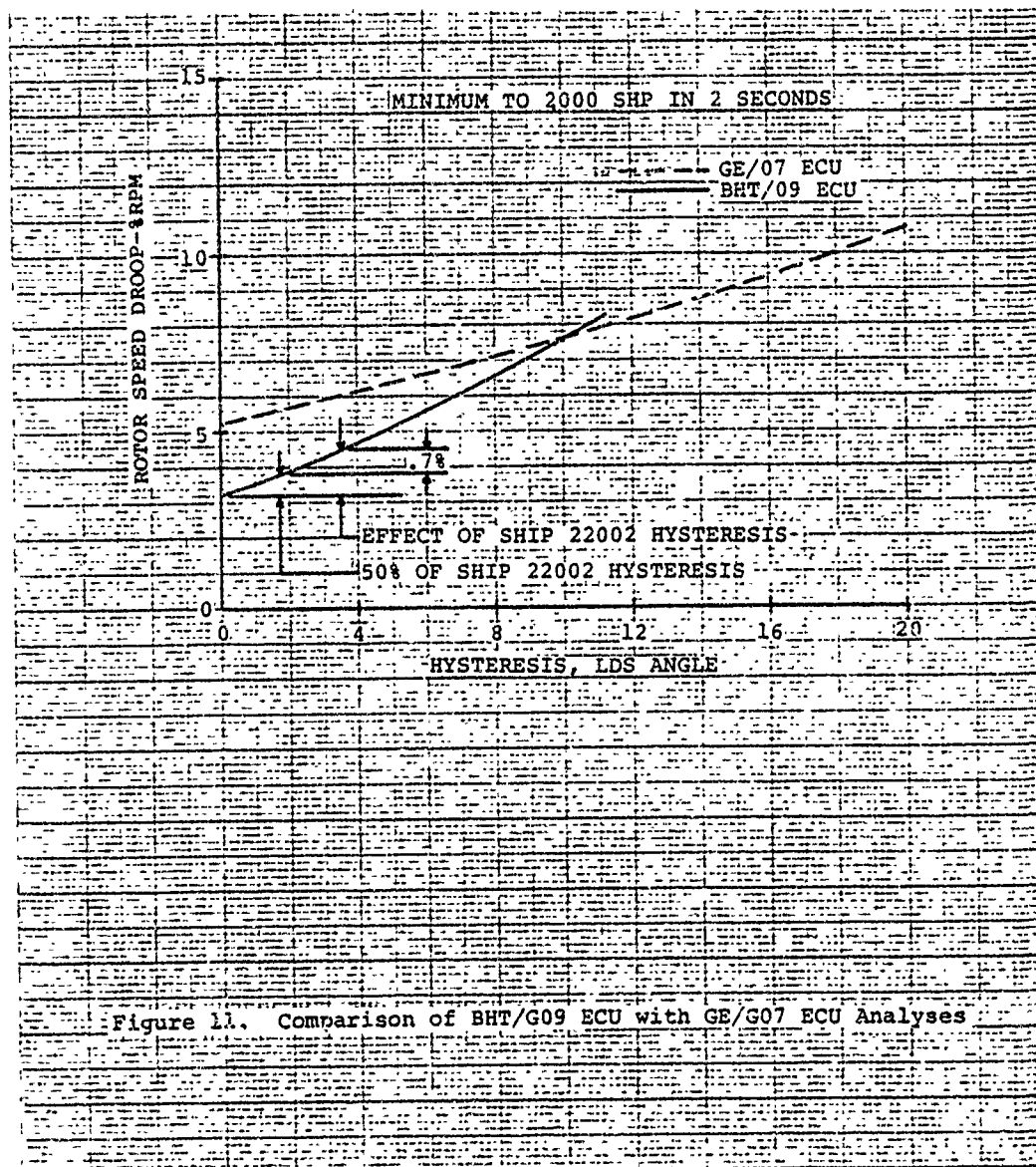
32

CORRELATION WITH AAEFA TEST RESULTS

To establish the effect of LDS angle hysteresis for Group 07 controls used on Ship 22002 and 22003 flown at AAEFA, a linear extrapolation analysis was conducted using incremental droop values for G09 ECU controls and LDS angle hysteresis. The analysis included the following:

1. Establish incremental droop due to hysteresis based on Figures 7 and 8 for Ships 22002 and 22003A.

2. Add this incremental droop to the droop values obtained from Reference 3 and establish droop values including hysteresis for G07 controls for Ships 22002 and 22003A.

These results are shown in Figure 17 and were used for constructing Phase 1 and Phase 2 droop estimates shown in Figure 10.

A study of the traces from Reference 2, found in Addendum I, show the collective motions to roughly approximate a ramp of from 1.5 to 2.0 seconds.

From Figure 17 (see shaded area), it is found that for collective ramps to 50 and 70 percent power in one-half second, the droop below 100 percent N_R varies from 8.0 to 10.0 percent, respectively, while for a two second ramp, the droop varies from 6.8 to 8.8 percent, respectively. The two traces obtained on Ship 22003A, from Reference 2, show a droop below 100 percent N_R of 8.2 and 8.8 percent for a recovery to approximately 55 percent of transmission power limit. (Note data points plotted on Figure 17.)

173
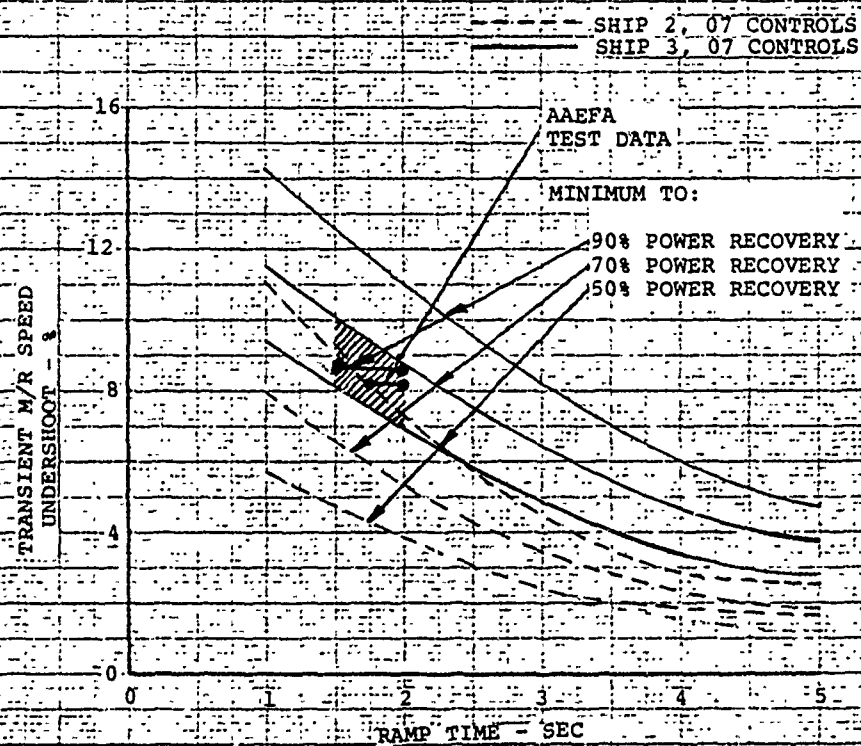
Figure 17.   Correlation of Droop Data of Extrapolated Group 07 Including Hysteresis with AAEFA Test Data

34

DESIGN OBJECTIVES

To clearly establish a design objective, previous experience on a number of BHT helicopters was reviewed and in particular, transient rotor speed droop conditions which were considered unacceptable. Emphasis was placed on AH-1 experience.

Additionally, the BHT YAH-63 project pilot was questioned as to what transient droop would be considered acceptable.

As a result of these actions, a design objective was established. This design objective included a maximum of 5 percent rotor speed droop (as shown in Figure 7) for

1. 2 second collective ramp from minimum to 2000 shp, and

2. 3 second collective ramp from minimum to 2500 shp.

35

PLAN OF ACTION

BHT Engineering has defined a number of alternate methods
by which the control hysteresis and 'stiction' can be
eliminated. After careful review of these, and an evalua-
tion in terms of cost, complexity, and reliability, a plan
of action was developed.

This action is

1. to execute the design changes shown on the applicable
    PDV, Addendum II, and

2. in the event that tests conducted in Phase 2 to critically
    evaluate these characteristics, with these PDV changes
    incorporated, do not result in a satisfactory solution,
    an alternate mechanical design will be made.

CONCLUSIONS

The following conclusions can be drawn:

1. The G09 ECU will substantially reduce the rotor speed droop
    from that obtained with the G07 controls.

2. The G09 ECU demonstrates torsional stability margins essen-
    tially the same as those obtained with the G07 controls.

3. For the G09 ECU, the hysteresis in LDS angle of the
    magnitude (10 degrees) measured on Ship 22003A substantially
    increases the rotor speed droop over the no-hysteresis case
    for ramp times of 2 seconds or more, while magnitudes on the
    order of 3.5 degrees as measured on Ship 22002 resulted in
    much less droop.

4. The analysis demonstrates that significant LDS angle
    hysteresis can account for the poor rotor speed control
    experienced during maneuvering flight.

5. The results of this analysis on the G09 ECU show similar
    results to those of similar and independent GE analysis on
    the G07 controls.

6. The results of this analysis are in substantial agreement
    with the AAEFA test data and demonstrate that the pilot
    comments relating to stability and controllability character-
    istics evaluated on Ship 22003A are probably not directly
    applicable to Ship 22002.

7. Potential solutions to the LDS angle hysteresis problem in-
    volving other than mechanical means result in increasing com-
    plexity and concern regarding reliability, while acceptable
    droop characteristics can be shown with small improvements in
    hysteresis which are achievable with mechanical systems.

8. The Phase 2 YAH-63 helicopter equipped with the T700/G09
    ECU and with the LDS angle hysteresis from Ship 22002
    is shown by analysis to give a 3.6 percent droop for a 2
    second ramp from minimum to 70 percent power and 3.5 per-
    cent droop for a 3 second ramp from minimum to 90 percent
    power (as shown in Figure 7). These values are well
    within the design objective limits. These droop values will
    be further reduced with improvements in LDS hysteresis in
    Phase 2.

ATTACHMENT 2 TO APPENDIX K

37

REFERENCES

1. BHT Report 409-993-008B, "Engine/Airframe Compatibility
    Survey and Demonstration for the YAH-63 Advanced Attack
    Helicopter."

2. Letter from U. S. Army Aviation Systems Command, St. Louis,
    Mo., DRSAV-PDAO, 0374-RF-0241, to Mr. Glenn Cordts, Bell
    Helicopter Textron, dated 28 October 1976.

3. BHT Report 409-909-031, "Torsional Compatibility Analysis
    of the YAH-63 Helicopter and GE-700 Engine with Group 07
    Controls."

ATTACHMENT 2 TO APPENDIX K

ADDENDUM I

EXCERPTS FROM ARMY LETTER DRSAV-PDAO, 0374-RF-0241

39

DEPARTMENT OF THE ARMY
HEADQUARTERS, US ARMY AVIATION SYSTEMS COMMAND
PO BOX 209, ST. LOUIS, MO 63166

DRSAV-PDAO

0374-RF-0241

2 8 OCT 1976

Mr. Glenn Cordts
Bell Helicopter Textron
PO Box 482
Fort Worth, TX 76101

Dear Mr. Cordts:

The following DTI test data, provided by AEFA, is forwarded herewith for
your information and evaluation.

    a.   Figure B-117 - Limits of Cyclic Control Travel

    b.   SCAS Authority

    c.   Figures B-118 thru B-124 - Control System Characteristics

    d.   Figures B-15 thru B-19, B-54 & B-55 - Control Positions in Trimmed
Forward Flight

    e.   Figures B-21 thru B-25 - Collective Fixed Static Longitudinal Stability

    f.   Figures B-26 thru B-30 - Static Lateral-Directional Stability

    g.   Figures B-38 thru B-41 - Low-Speed Forward & Rearward Flight

    h.   Figure B-128 - Lateral Acceleration

    i.   Figures B-59, B-79 thru B-84 - Maneuvering Stability

    j.   Figures B-125 - Vertical Displacement

    k.   Figures B-137 & B-138 - Vertical Displacement Time Histories

    l.   Figures B-130 thru B-132 - Summary of Controllability

40

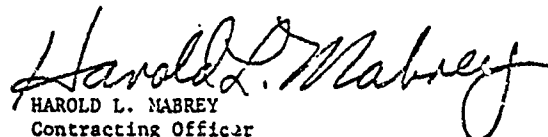DRSAV-PDAO   0374-RF-0241
Mr. Glenn Cordts

2 8 OCT 1976

   m. Figures B-85 thru B-88 - Longitudinal Control Response and
Sensitivity

   n. Figures B-89 thru B-92 - Lateral Control Response and Sensitivity

   o. Figures B-93 thru B-96, B-129 & B-136 · Directional Control
Response & Sensitivity

   p. Figures B-139 & B-140 - Longitudinal Short Period Response

   q. Figure B-141 - Longitudinal Long Period Response

   r. Figures B-133 thru B-135 ~ Engine Failure

   s. Figure B-143 - Quick Stop

The attached data will be used by the AAH SSEB as an aid in evaluating
the capabilities of your Phase 2 proposal, and will be adjusted as
appropriate to reflect proposed changes between your Phase 1 prototype
and Phase 2 design.

                Sincerely,

19 Incl   HAROLD L. MABREY
As stated   Contracting Officer

QUICK STOP

ENGINE RESPONSE
QUICK STOP MANEUVER
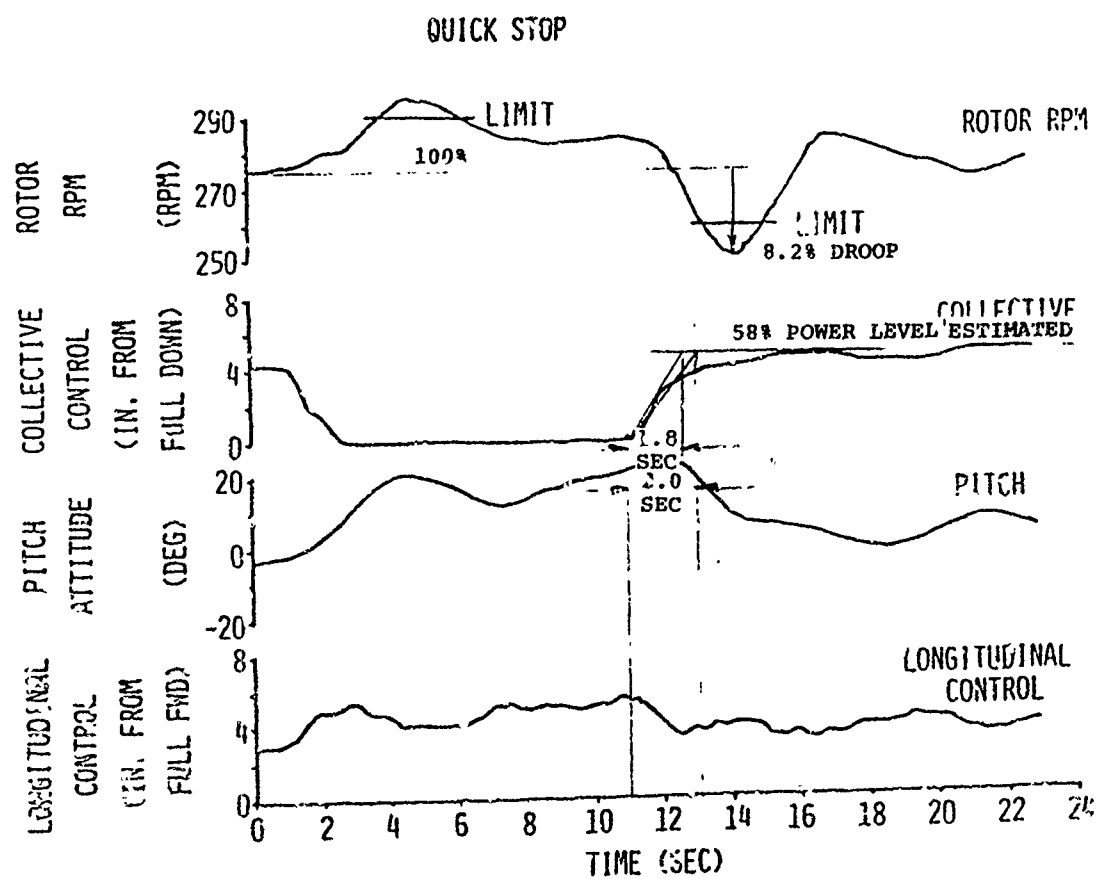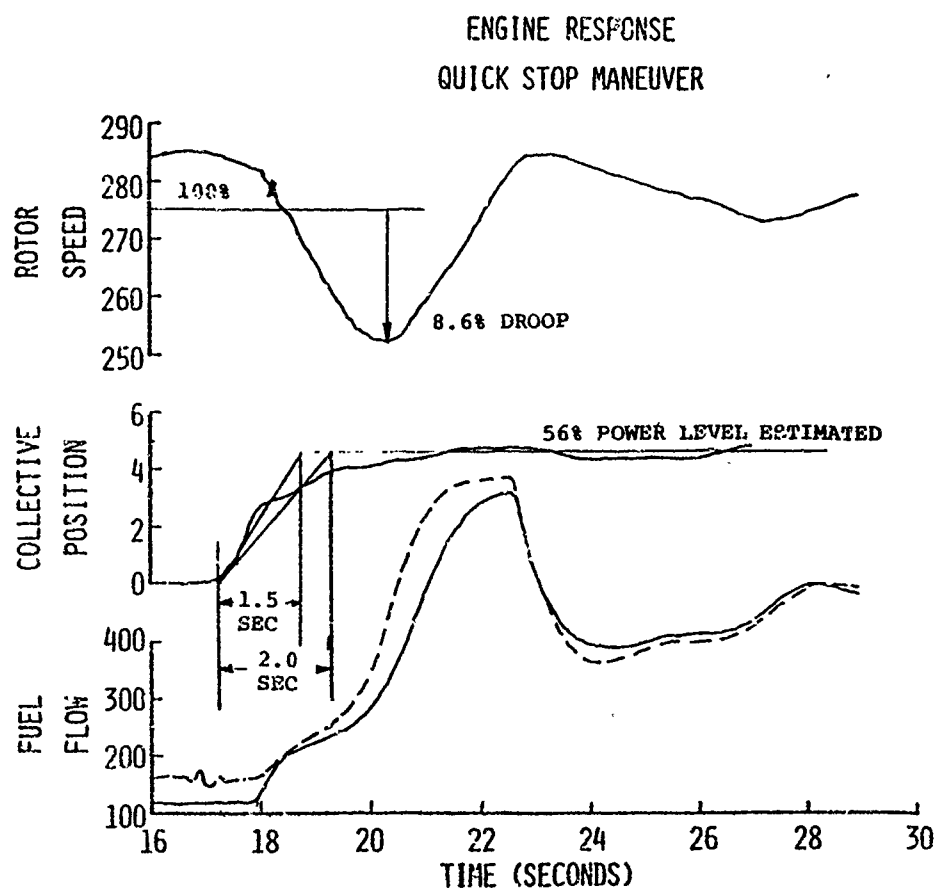
ENGINE RESPONSE

ENGINE RESPONSE
ECU LOCKOUT TEST

ADDENDUM II
PRODUCTION DESIGN VARIANCE
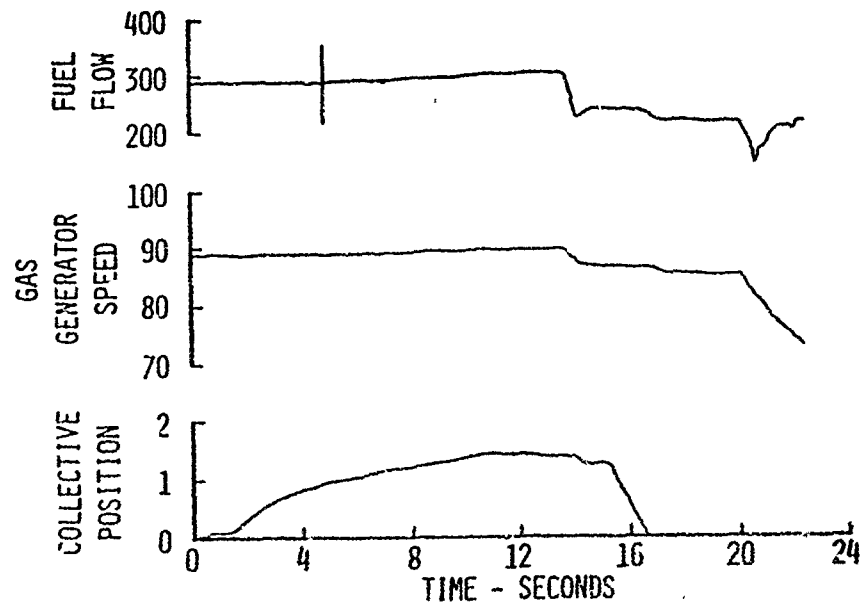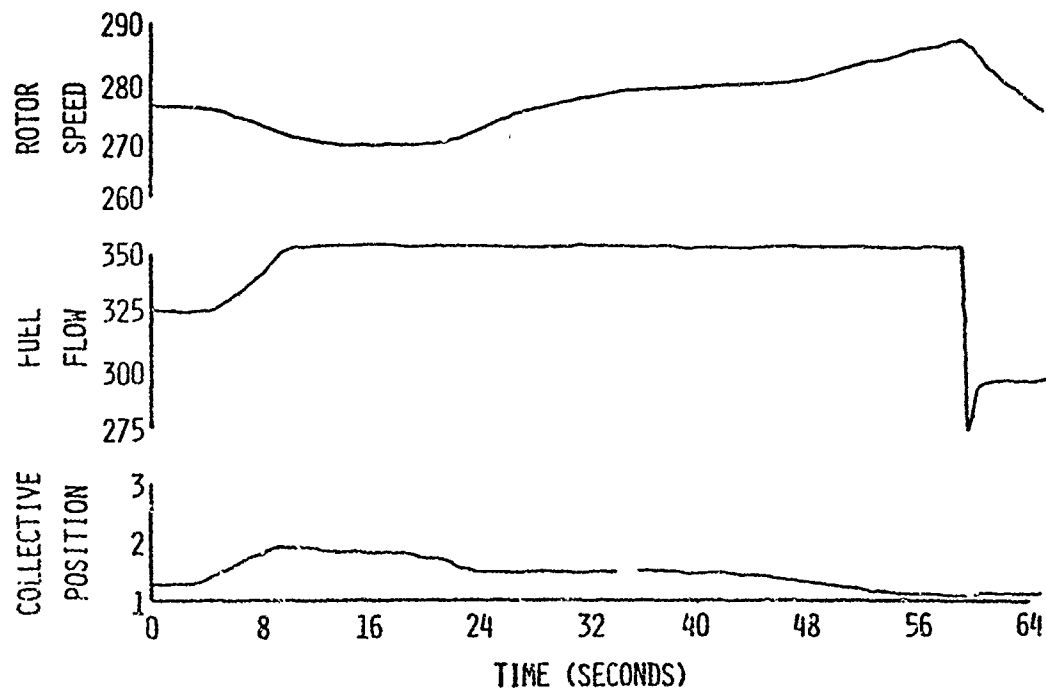
46

BELL HELICOPTER COMPANY Code Ident. No. 97499	**PRODUCTION DESIGN VARIANCE**		
DRAWING NUMBER 409-060-700	WBSE 24AMA00	P O A213	SERIAL NO 24AMA00-

DRAWING TITLE   CONTROL SYSTEM INSTALLATION~POWER PLANT

REASON FOR VARIANCE
    TO   REDUCE   HYSTERESIS

VARIANCE DESCRIPTION

    REVISE   JACKSHAFT, BULKHEAD AND CLAMPING

PRODUCT DESCRIPTION

(1) INCREASE STIFFNESS OF 409-060-702-1 JACKSHAFT ASSEMBLY.

(2) INCREASE STIFFNESS OF 409-030-510- BULKHEAD ASSEMBLY IN THE AREA OF SUPPORT FOR THE JACKSHAFT ASSEMBLY.

(3) REVISE CLAMPING SCHEME FOR CABLES.

(4) INVESTIGATE ALL BULKHEAD ATTACH POINTS FOR FRICTION, BINDING, ETC.

(5) INVESTIGATE FORCES REQ'D TO ACTUATE ENGINE MOUNTED FUEL CONTROLS.

(6) UPDATE INSTALLATION DRAWING TO AGREE WITH ABOVE CHANGES.

ESTIMATED ENGINEERING BUDGET DESIGN GROUP 200 HRS	PRODUCTION WEIGHT VARIANCE
STRESS _____ _____ CHECK _____	DEVELOPMENT _____
WEIGHTS_____ OTHER _____	PRODUCTION _____
TOTAL MANHOURS _____	VARIANCE _____

ORIGINATING GROUP POWER PLANT	GROUP ENGR	PROJ. ENGR
PREPARED BY A. BADGETT	WEIGHTS	

APPENDIX L

EXCESSIVE TORSIONAL LOADING OF THE DRIVE SYSTEM
DURING ENGINE OVERSPEED TRIPS

BHT, under Contract DAAJ01-73-C-0741(P40), developed a proto-
type Advanced Attack Helicopter, the YAH-63, powered by two
T700-GE-700 engines.

One feature of these engines is an electronic-mechanical
overspeed trip mechanism integral to each engine which pre-
vents excessive power turbine overspeeds in the event of an
electronic control unit (ECU), fuel control, or shafting
failure. When an overspeed trip occurs (at 111 percent N_p
per engine specification), the fuel flow is cut back until
power turbine speed reduces (to approximately 110 percent N_p),
at which time the overspeed trip resets and power turbine
speed can increase again as demanded.

To ensure that the overspeed trip device was functioning
properly, a check feature was provided. This feature as
incorporated in the helicopter consisted of two overspeed
trip test circuits (one for each engine) which were used during
the normal cockpit check procedure during ground run-up and
prior to flight. The initial BHT procedure for this check was
described as follows:

1. Test to be performed on single engine. If both
    engines are operating, only engine being tested to
    be providing power, other engine will have speed
    reduced to ground idle.

2. Operate Engine No. 1 at flat pitch rotor speed of
    102 percent. Then manually initiate the engine over-
    speed trip. Observe for several cycles of gas
    generator speed oscillation before releasing overspeed
    trip test circuit.

3. Repeat test with Engine No. 2.

Table L-1 lists seven instances of engine overspeed trips
encountered during BHT development of the YAH-63 where
sufficient data exists for documentation. Five of these
overspeed trips were intentional test conditions. The other
two overspeed trips occurred inadvertently, one during flight
and one during ground run. In all cases the engine overspeed
trip system functioned exactly as the engine manufacturer
intended. The most significant of these overspeed trip
instances have been summarized in the following figures.

186

Figure L-1 shows a single-engine overspeed trip sequence which occurred after a power recovery from autorotation. The ship was being flown from the gunner's station and a misrigging of the throttle linkage inadvertently caused the No. 2 engine ECU governor to go into the "lock-out" mode when the pilot engaged the engine throttles for the power recovery. This condition ultimately led to an Engine No. 2 overspeed trip. The pilot sensed the abnormal condition and took appropriate corrective action without endangering the flight.

Figure L-2 gives the sequence of a single-engine overspeed trip test showing how a multiple overspeed trip can cause amplification of drive system loads.

Figure L-3 shows amplification of drive system loads when both engines have multiple overspeed trips simultaneously.

Figure L-4 shows a single-engine overspeed trip sequence encountered during a twin-engine ground run at 110 percent N_p design test speed.

Figure L-5 shows the unstable characteristics of the drive system loads if an engine overspeed trip is allowed several cycles. Damaging loads were not attained in this test because of the initially low power setting of the engine. Note how each successive overspeed trip cycle amplifies the drive system load.

The single-cycle overspeed trip data show how the first two drive system torsional natural frequencies, 3.2 Hz and 6.2 Hz, are transiently excited as a result of the sudden power demand change. Each of these torsional natural frequencies exhibits desirable damping characteristics such that a single transient excitation response is normally short-lived. However, the frequency of switching of the overspeed trip system (on at 111 percent N_p, off at 110 percent N_p) for multiple overspeed trip cycles is such that the initial transient load does not have sufficient time to decay before the next transient excitation is encountered, thus resulting in more amplification for each successive overspeed trip cycle producing an unstable divergent condition.

Additionally, a GE analysis of an ECU failure is presented in Appendix K, Attachment 1, of this report. This analysis clearly shows the high transient torques which may be encountered during such an engine overspeed condition.

Based on the unstable characteristics of the drive system response as encountered during the multiple overspeed trip tests, and because of the high drive system transient loads

187

developed due to the sudden power demand changes, the overspeed
trip system checkout procedure should not require multiple
overspeed trip cycles. In order to keep the magnitudes of
the torsional oscillations to a minimum during checkout of the
overspeed trip system, in concurrence with recommended pro-
cedures by GE, the BHT operational check procedures were
modified to be:

1. To keep engine power at a minimum, test to be
    performed with both engines operating, equally
    sharing torque, driving the rotor at 102 percent
    flat pitch.

2. Engine No. 1 overspeed test circuit should be ener-
    gized and then broken as soon as a decrease is ob-
    served in N_G.

3. Ascertain that both engines have returned to equally
    sharing torque.

4. Repeat test with Engine No. 2.

This revised overspeed trip system checkout procedure proved
satisfactory in preventing excessive drive system loads
during the test and was used for the remainder of the
YAH-63 development program.

So long as the ECU governor is in normal operation, the only
condition which might realistically cause an engine overspeed
trip to occur at 111 percent N_P would be a sudden and drastic
loss of power required, such as an input driveshaft failure.
For this situation the overspeed trip will activate once to
cut back fuel flow, giving the ECU governor the extra response
time necessary to have fuel flow limited down by the time the
overspeed trip resets at 110 percent N_P, thus allowing the
engine to coast down to flight idle speed through normal ECU
governing for a zero power required condition.

In the event of an overpower condition resulting from an ECU
governor failure, or during ECU governor lock-out, the possi-
bility still exists for multiple overspeed trip cycles,
possibly resulting in damaging drive system torsional load
oscillations. However, in this case the pilot should observe
the high rotor rpm warning light on the console and be able
to take corrective action by backing off on the engine throttle,
thus alleviating the multiple overspeed trip cycling condition.
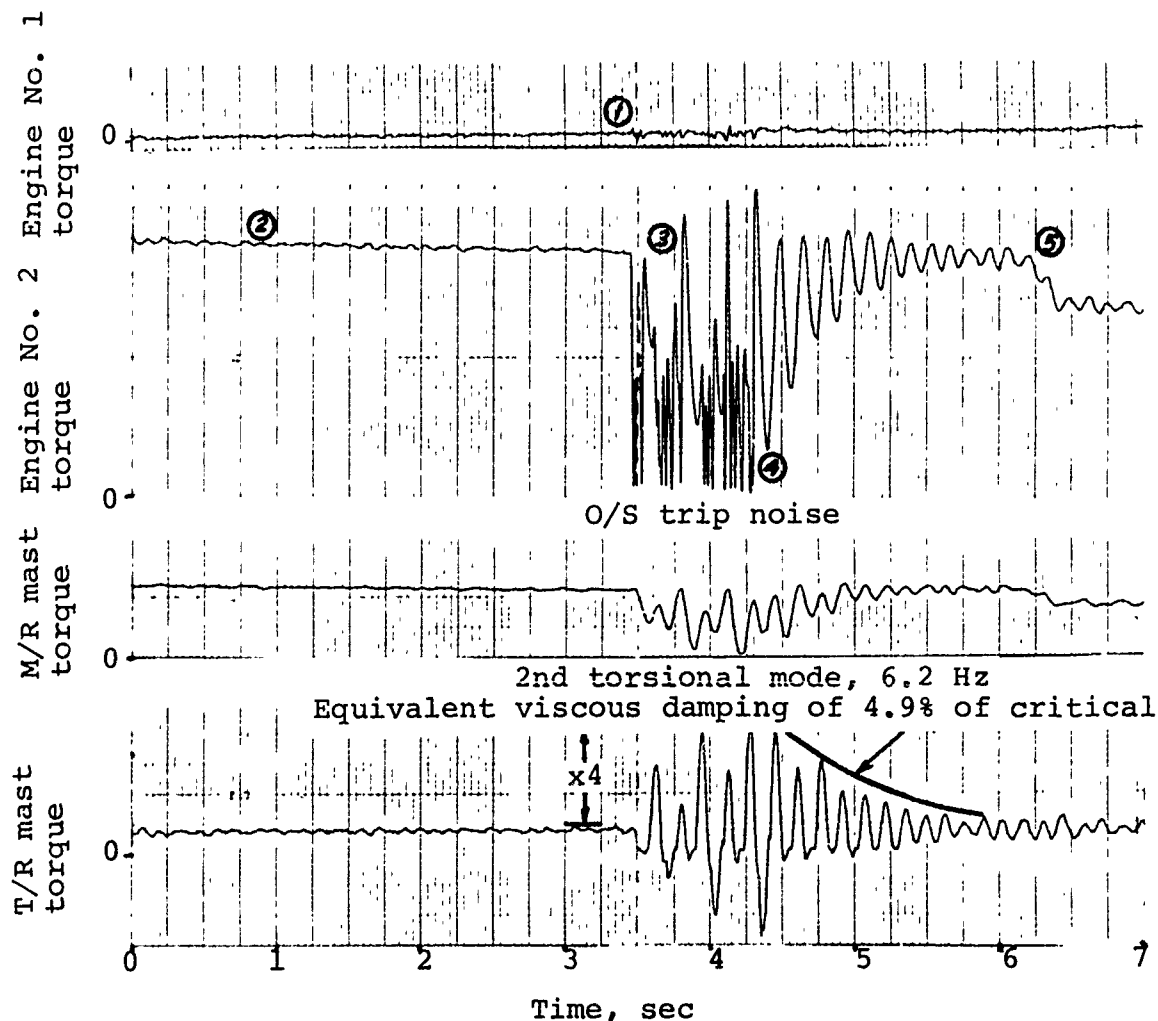
Although the overspeed trip system was acceptable for the
prototype testing of this aircraft, a production type installa-
tion should require more compatibility between the engine

188

overspeed trip system and the aircraft drive system to prevent
the possibility of multiple overspeed trip cycles causing
damaging drive system oscillatory torsional loading. This
condition might be made more stable by simply decreasing
the switching frequency (upper N_p to lower N_p limits) of the
overspeed trip system to allow additional time for each
transient condition to decay.

The YAH-63 program subsequently was contractually terminated
such that further investigations of the overspeed trip
system were never accomplished.

TABLE L-1. CHRONOLOGY OF DOCUMENTED ENGINE OVERSPEED TRIPS

Date	Fig. No.	Description	N_P at O/S Trip #1	O/S Trip #2	O/S Trip Cycles	Test Cond.
10-9-75	L-1	Engine #2 overspeed trip after power recovery from autorotation, had ECU in lock-out mode.	Flt. Idle	111%	1	No
10-28-75	L-2	Engine #2 overspeed trip test.	92%	102%	2	Yes
1-5-76	L-3	Twin-engine simultaneous overspeed trip test.	102%	102%	2	Yes
1-6-76	L-4	Engine #1 overspeed trip during twin-engine ground run at 110% N_P design test speed.	111%	110%	1	No
4-6-76		Engine #1 overspeed trip test.	102%	Off	1	Yes
4-6-76	L-5	Engine #1 overspeed trip test, at low power.	102%	Off	4	Yes
4-6-76		Engine #2 overspeed trip test.	102%	102%	1	Yes

190

Engine No. 1 torque

Engine No. 2 torque

M/R mast torque

T/R mast torque

O/S trip noise

2nd torsional mode, 6.2 Hz
Equivalent viscous damping of 4.9% of critical

x4

Time, sec

① Engine No.1 ECU governor senses that Engine No.2 is supplying all power requirements; therefore Engine No.1 N_p has been governed down to flight idle.

② Pilot is unaware that misrigging of throttle linkage has inadvertently put Engine No.2 in ECU lockout; that engine, now operating at full power, is providing sufficient power during autorotation power recovery.

③ After autorotation power recovery, power required is reduced, engine still operating at full power overspeeds, O/S trip activates at 111% N_p.

④ O/S trip resets at 110% N_p.

⑤ Pilot senses abnormal condition and is able to throttle back to maintain a stable flight condition before taking the appropriate corrective action which is to place Engine No.2 back into ECU governing.

Figure L-1. Single-engine overspeed trip after power recovery from autorotation.
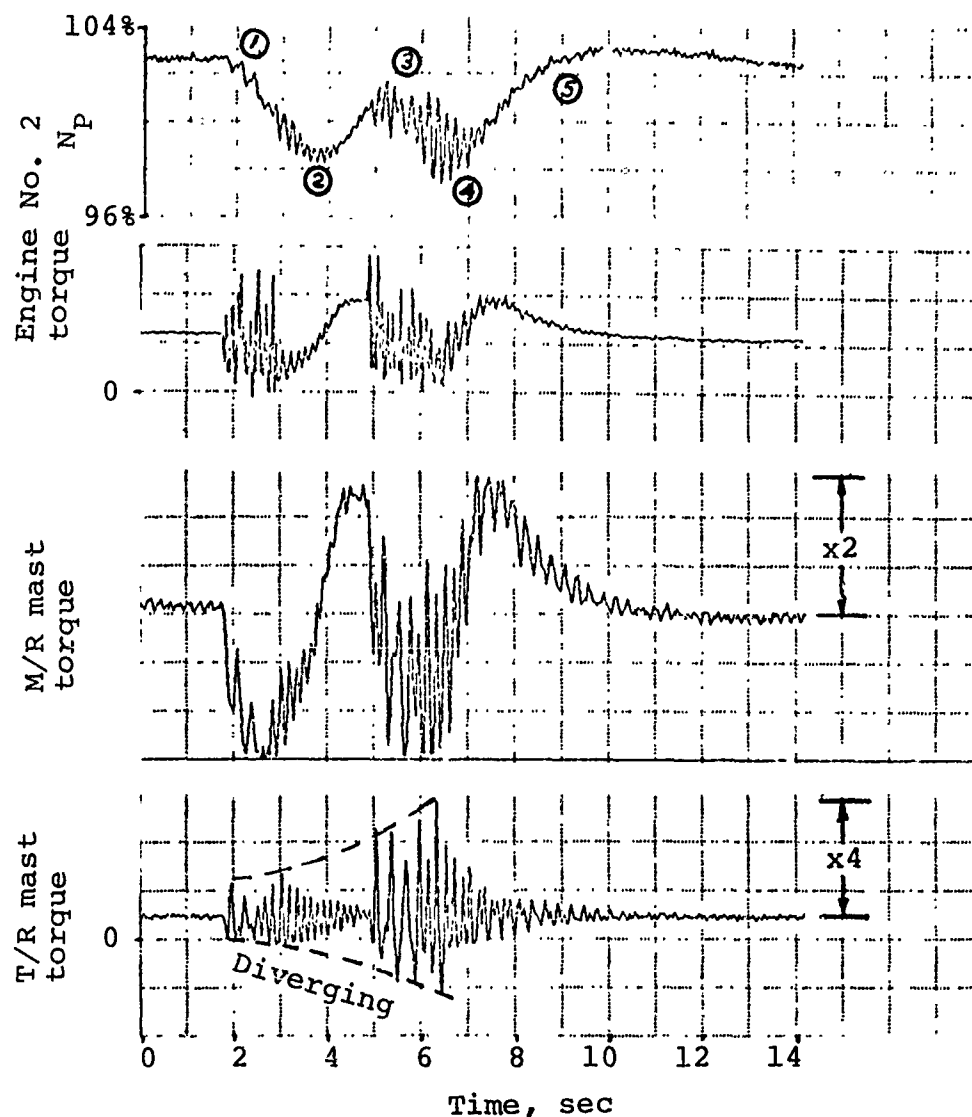
① Engine operating at 102% N_P when O/S trip test circuit is engaged by pilot which causes O/S trip activation. (With test circuit engaged, O/S trip activates above 100% N_p and resets at 99% N_P.)

② O/S trip resets at 99% N_p, ECU governor schedules more power to maintain the original 102% speed setting.

③ O/S trip activates again at 100% N_p.

④ O/S trip resets again at 99% N_p, ECU governor schedules more power to maintain the original 102% speed setting.

⑤ O/S trip test circuit released by pilot due to increasing tail rotor drive system loads resulting from second O/S trip cycle.

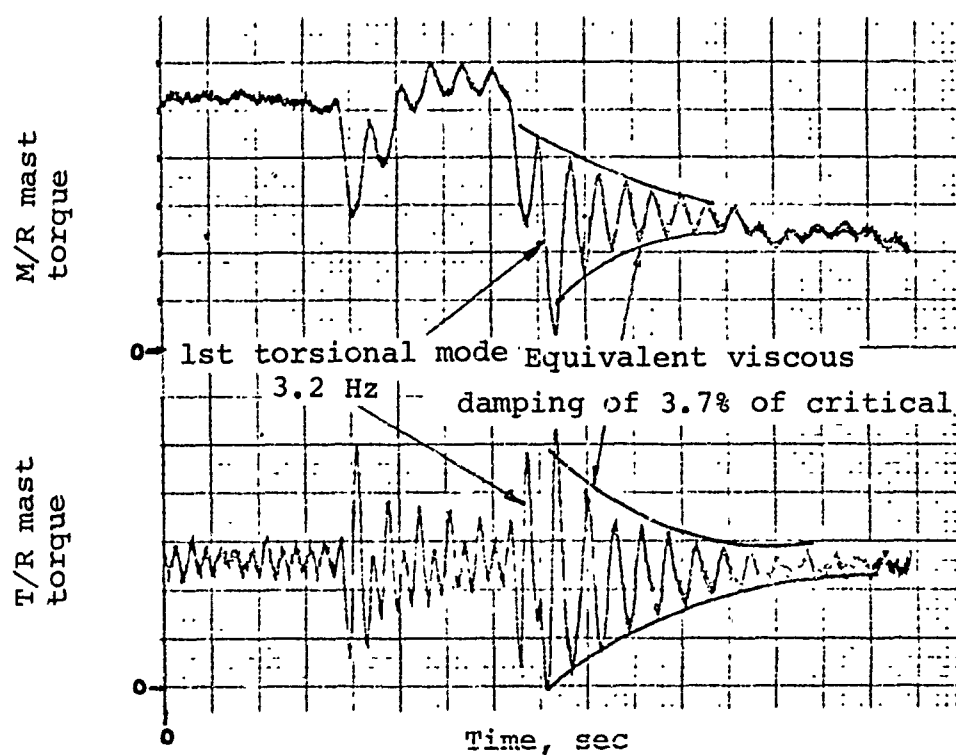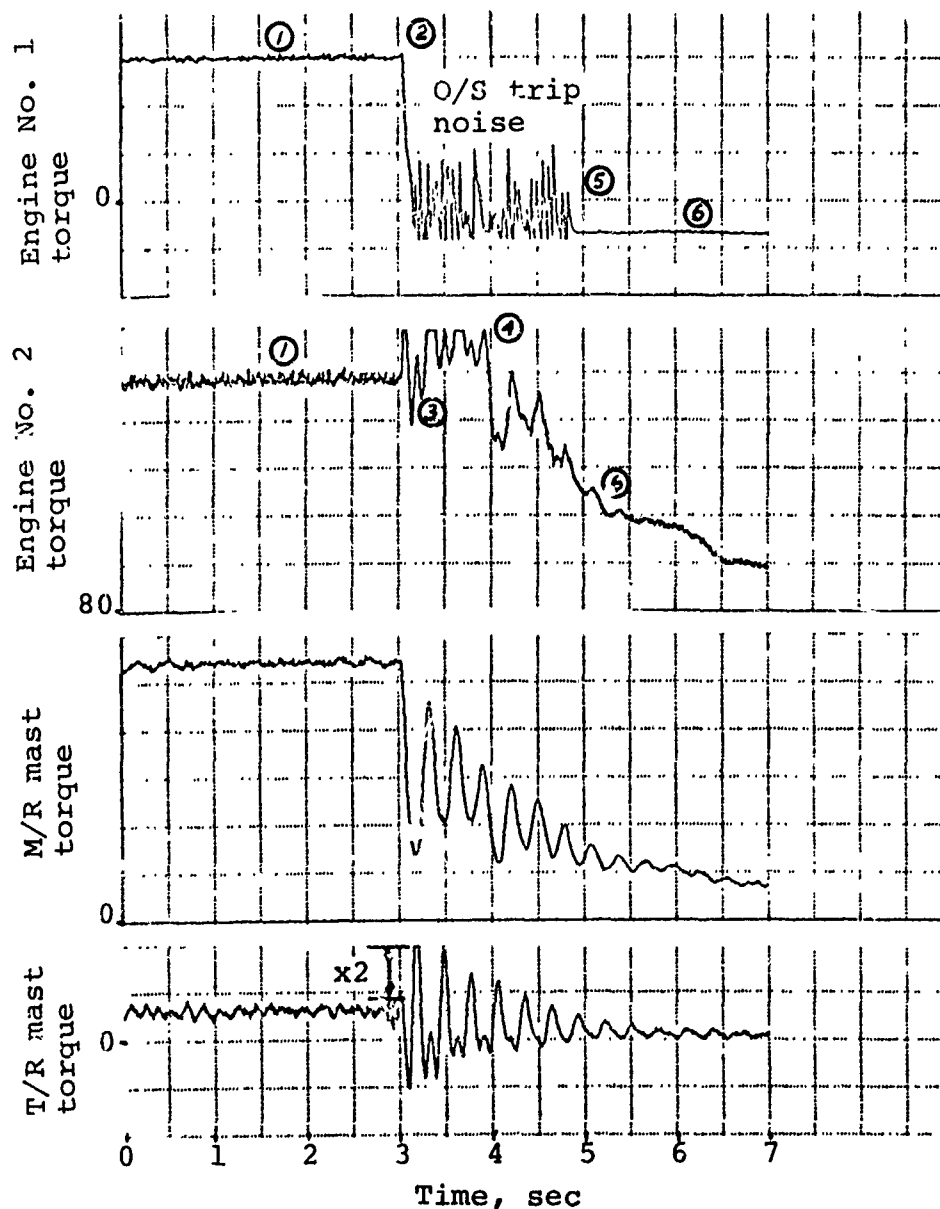Figure L-2. Single-engine overspeed trip test, two trip cycles.

Figure L-3. Twin-engine simultaneous overspeed trip test,
two trip cycles.

193

O/S trip
noise

①

②

⑤

⑥

Engine No. 1 torque

0

Engine No. 2 torque

①

④

③

⑤

80

M/R mast torque

0

T/R mast torque

x2

0

0   1   2   3   4   5   6   7

Time, sec

① Both engines, operating at 110% N_p design requirement, equally sharing power required.
② Engine No.1 O/S trip activates due to wind gust (wind gust provides additional lift-less power required, ECU governor response time from 110% N_p not fast enough to prevent the 111% O/S condition).
③ Engine No.2 ECU governor begins scheduling more power attempting to meet sudden additional torque requirement.
④ Pilot senses abnormal condition, begins throttling back both engines.
⑤ Engine No.1 O/S trip resets at 110% N_p.
⑥ Engine No.1 ECU governor senses that Engine No.2 is now supplying all power requirements; therefore Engine No.1 N_p continues to coast down, supplying no torque.

Figure L-4.   Single-engine overspeed trip encountered during twin-engine ground run.
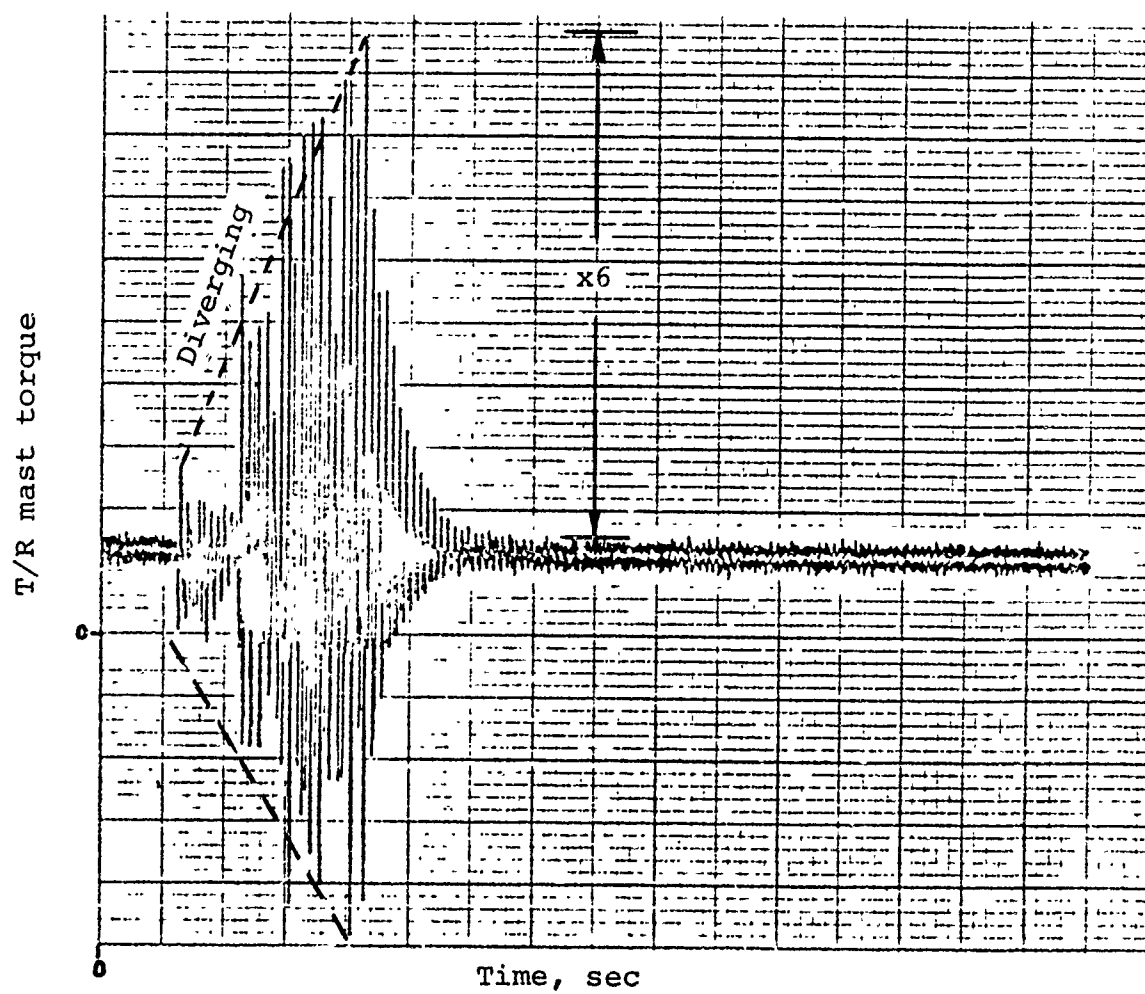
194

Figure L-5. Single-engine overspeed trip test, low power, four trip cycles.

195

APPENDIX M

HYDRAULIC SYSTEM NOISE

Description of Problem

In early production 214Bs, cabin noise was judged to be excessive. Noise data was taken in the cabin and the sources were identified with their characteristic frequencies. The measured spectrum shape is shown in Figure M-1. These data showed that both hydraulic systems were causing excessive noise, the upper pump generating noise at 832 Hz and the lower pump generating noise at 787 Hz. Discrete frequency tones at these frequencies and their harmonics caused a highly annoying cabin noise signature.

The hydraulic system noise was being transmitted to the cabin by the pressure oscillations (ripple) in the hydraulic lines. These oscillations were set up as each piston in the hydraulic pump passed the pressure port. Since the lines were clamped to the airframe structure, a sounding-board effect was set up, forming an efficient radiator for the hydraulic system noise.

Solutions Considered/Action Taken

To reduce the hydraulic system noise in the 214B cabin, several potential solutions were considered including standard soundproofing techniques, vibration isolation of the hydraulic lines, and modification of the hydraulic system to reduce the pressure oscillations.

Soundproofing

Extra soundproofing was added where possible, especially in the area of the cabin bulkheads near the clamping points of the hydraulic lines. However, this addition of soundproofing soon became prohibitive from a weight standpoint; also as soundproofing blankets became heavier and more bulky, the attachment, sealing, and handling problems became excessive. Figure M-2 shows 214B cabin noise level reduction as soundproofing was added. The point of diminishing returns was soon reached where the addition of substantial soundproofing weight produced little noise reduction. The noise levels of the other noise sources decreased with the extra soundproofing, but hydraulic system noise remained relatively unchanged, making it even more of a noticeable source.

Vibration Isolation

Isolation of the hydraulic lines from the cabin structure was considered but never implemented. It was judged that a new clamping arrangement at every line attachment point would be an excessive design effort. Limited action was taken in that the hydraulic reservoir was isolated from structure during tie-down testing of a Model 214 helicopter. No improvement in hydraulic system noise was noted.

Replace Hydraulic Pump

Consideration was given to installing a new hydraulic pump with random-spaced cylinders as a means of distributing the sound energy over a broad frequency range, rather than having a discrete tone. No off-the-shelf pump was found with this random spacing, although two pump manufacturers (Vickers and Abex) expressed opinions that such a pump could be built on a prototype basis. No action was taken.

Reduce Pressure Oscillations

A fourth, more successful approach to reducing the hydraulic system noise was to reduce the pressure pulsation in the hydraulic lines. BHT had recently completed a program to evaluate several devices designed to smooth hydraulic flow. One of these devices, the pulsation damper shown in Figure M-3, was installed in each of the hydraulic systems of the 214B, reducing the pressure ripple by a factor of 5. One pulsation damper was installed in the pressure line of each hydraulic system, upstream of any clamping points. The installation is shown in the sketch of Figure M-4 along with a trace of the pressure oscillation before and after installation. Hydraulic system noise was reduced because the pressure ripple had been reduced. Figure M-5 shows the noise data taken before and after the pulsation dampers were installed. A noise reduction of as much as 12 decibels was achieved in the hydraulic pump frequencies and their harmonics.

Adequacy of Solution

The solution was considered adequate, and the pulsation damper units are now being installed on production 214B and 212 helicopters to reduce cabin noise. Figure M-6 shows a prototype pulsation damper installed in a 212. The units weigh only about 2 pounds each, are relatively inexpensive, and require no maintenance. The reduction in cabin noise levels is deemed to be worth their installation.
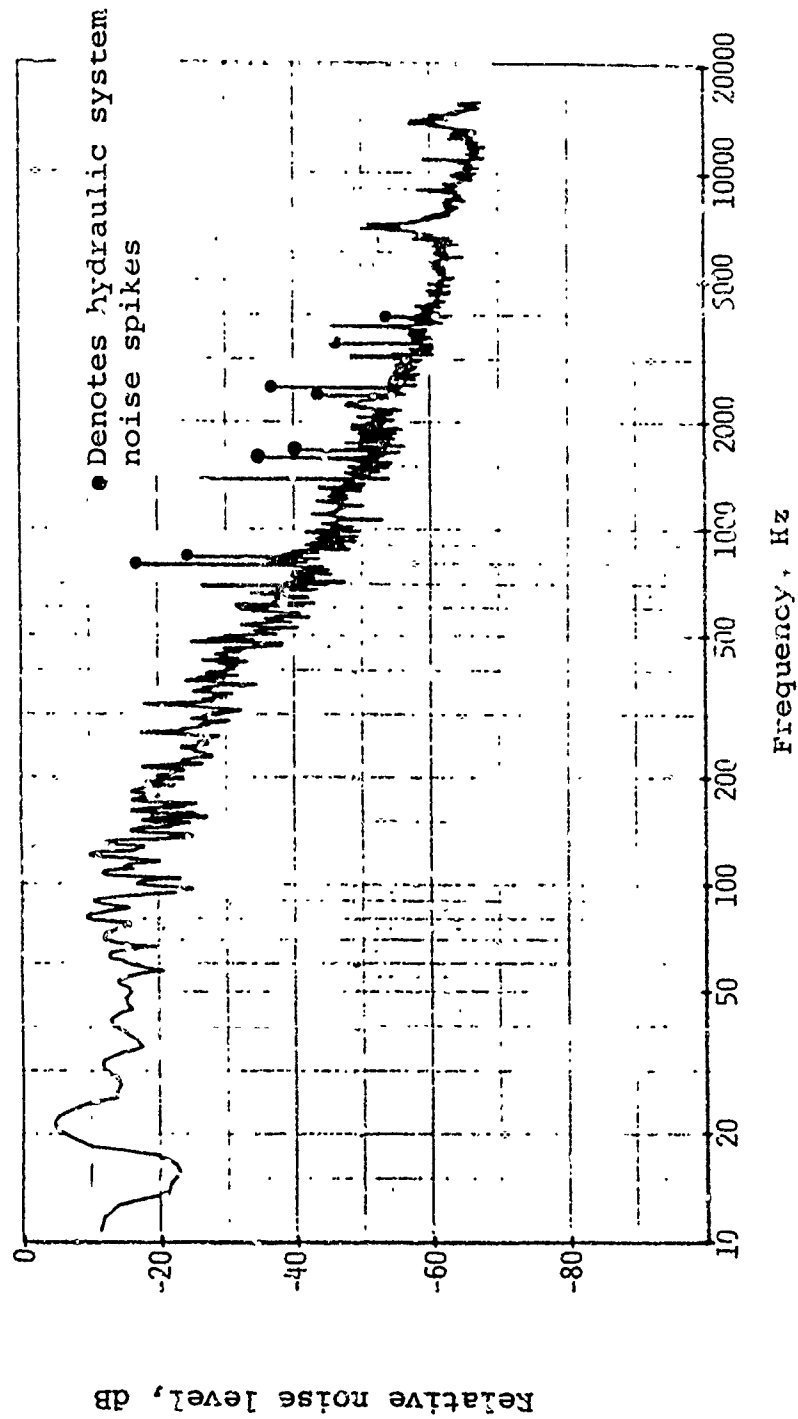
Figure M-1.   Cabin noise – standard hydraulic system before installation of pulsation damper.
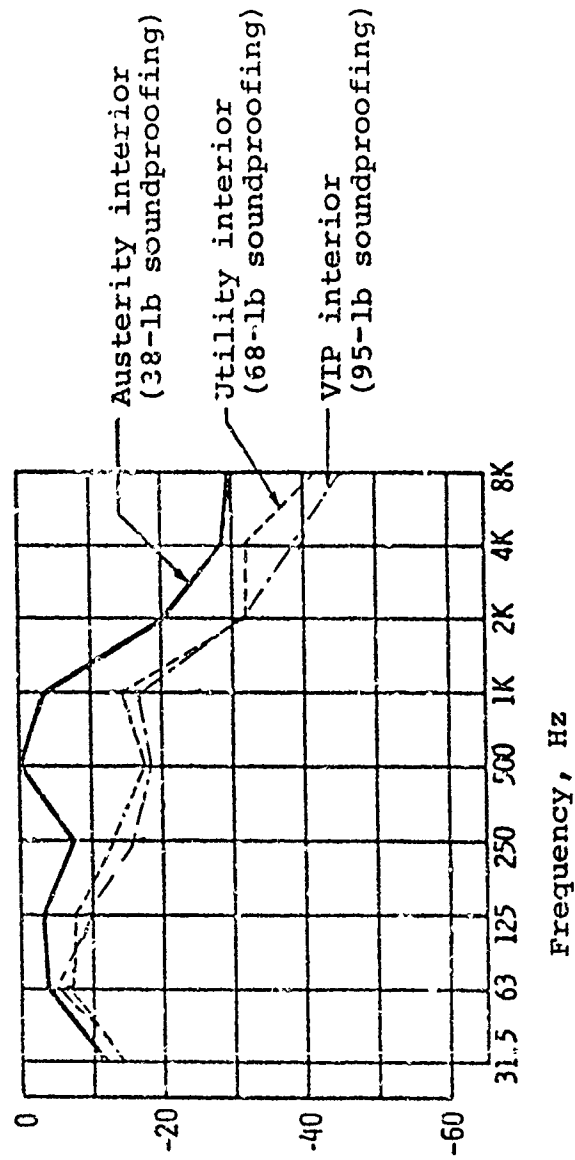
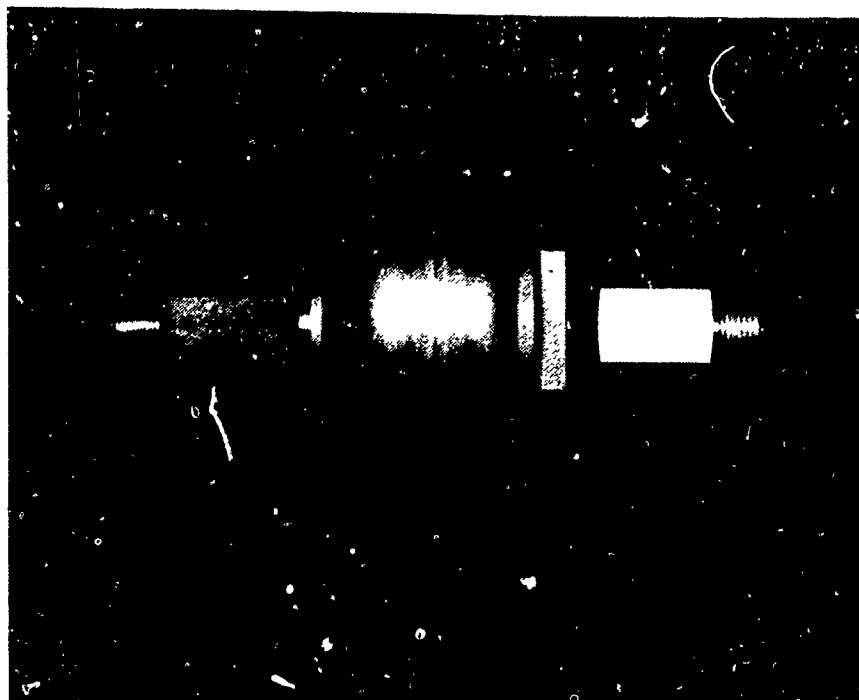Figure M-2. Effect of soundproofing weight upon cabin noise level.

199

Figure M-3.   Pulsation damper used in hydraulic
system noise reduction.

QUIET HYDRAULIC SYSTEM

Pulsation damper unit #1

Hydraulic pump #1
Hydraulic pump #2 Hydraulic line pressure ripple

Standard
system
(without
passive
volume
units)

Quiet
system
(with
passive
volume
units)

Reservoir/module
units (R/H and L/H)

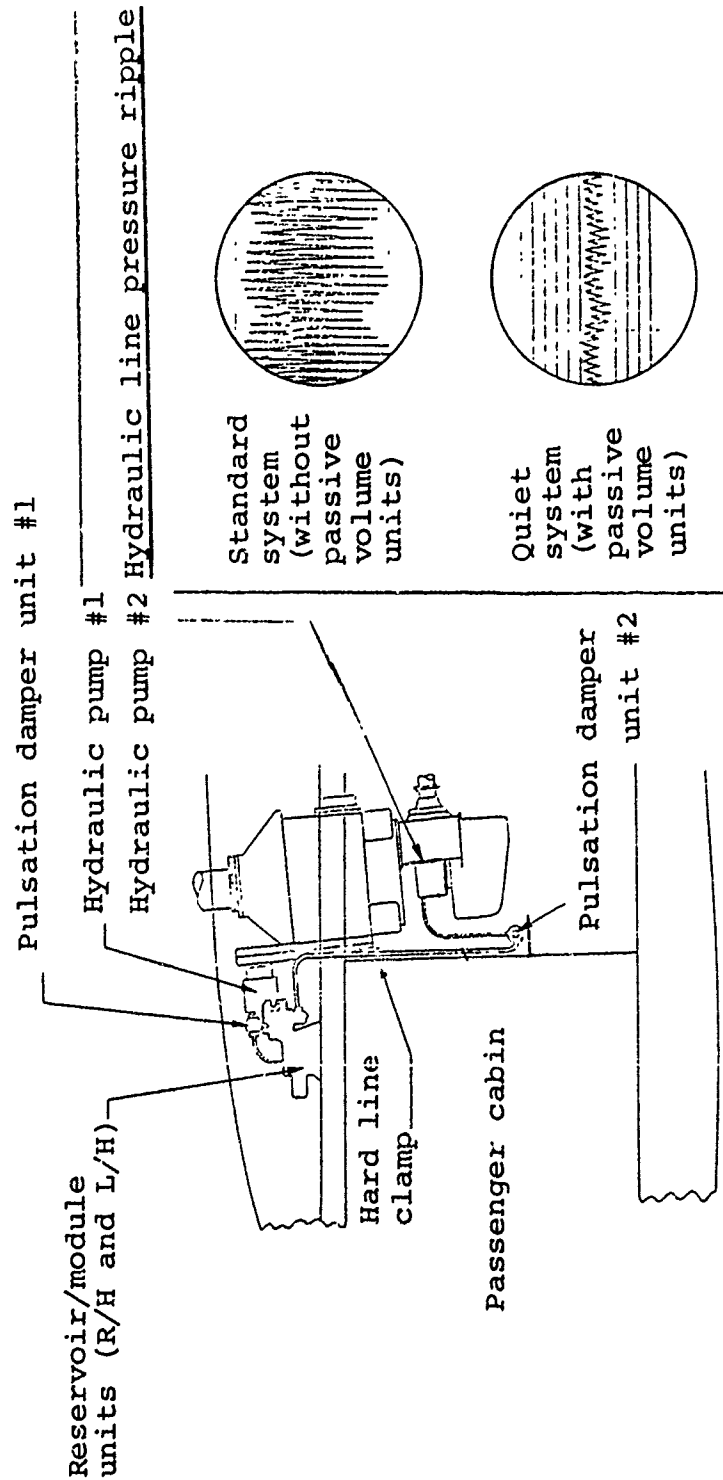Pulsation damper
unit #2

Hard line
clamp

Passenger cabin

Figure M-4.   Installation of pulsation dampers with
insert showing pressure ripple reduction.
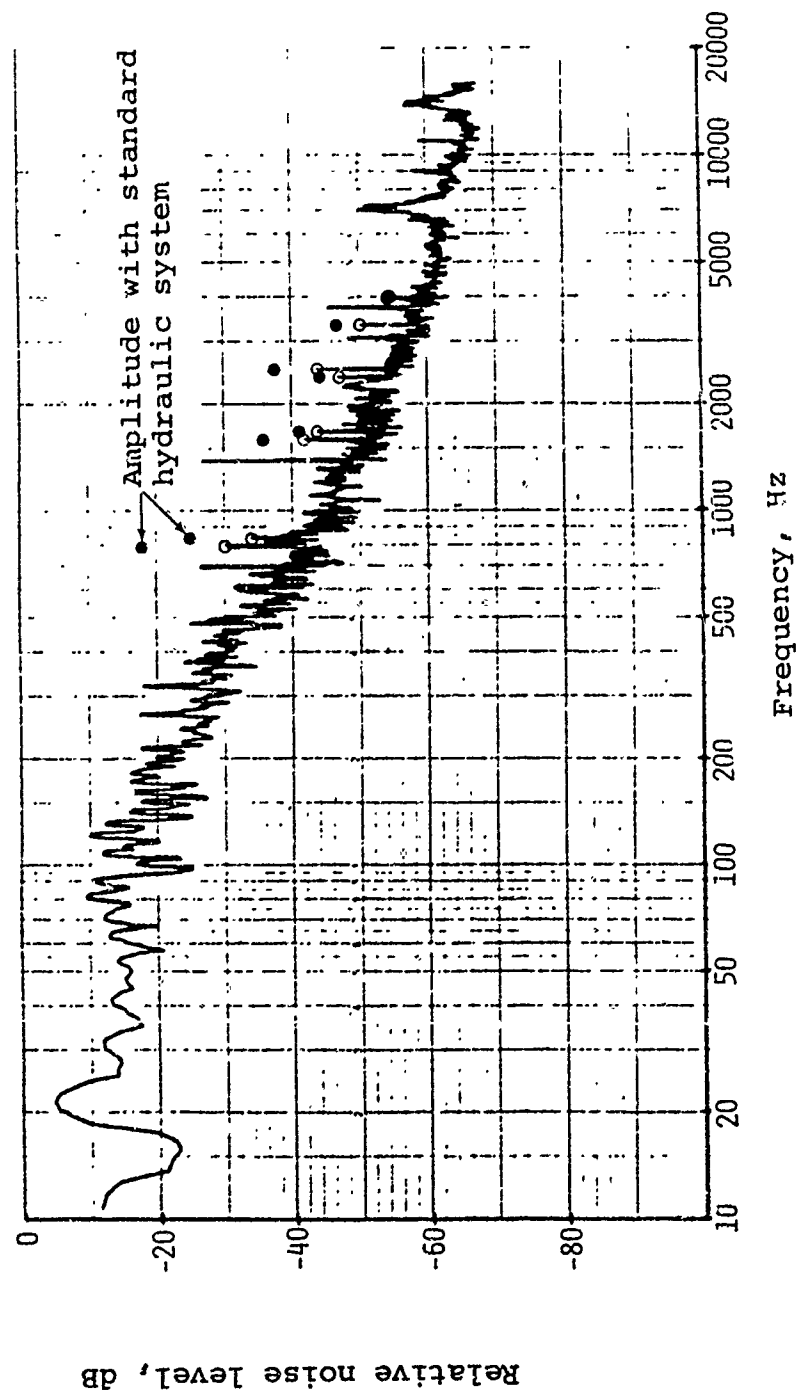
Figure M-5. Internal noise - quiet hydraulic system with pulsation damper installed.
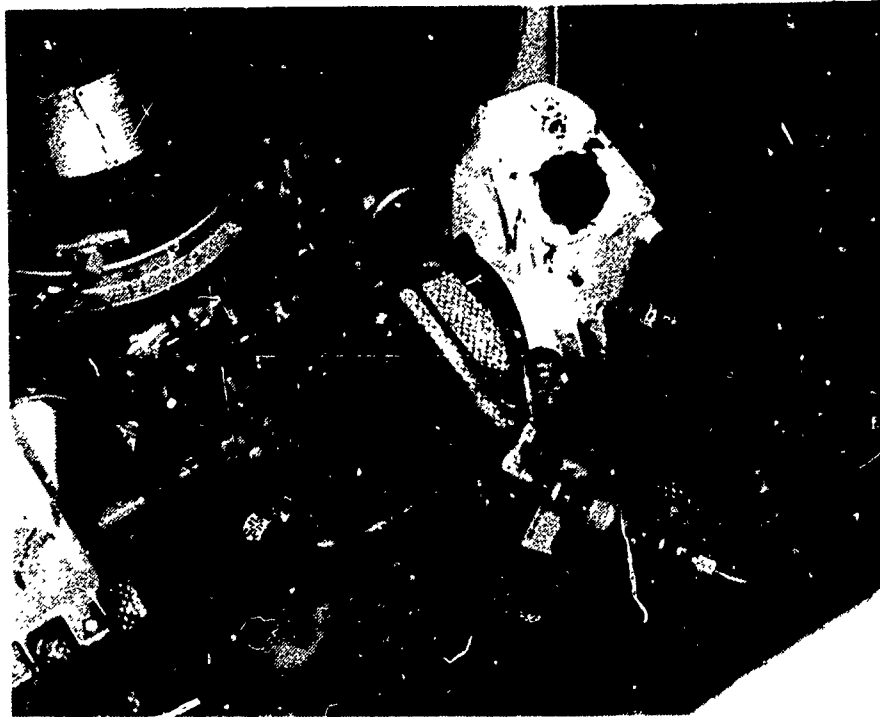
Figure M-6.   Prototype installation of pulsation
             damper on Model 212 helicopter.

11349-78